Applications of tropical geometry and cluster algebras to multi-particle scattering amplitudes

Dissertation

zur Erlangung des Doktorgrades
an der Fakultät für Mathematik,
Informatik und Naturwissenschaften

Fachbereich Physik
der Universität Hamburg

vorgelegt von

Niklas Johann Friedrich Henke

Hamburg
2022

Gutachter der Dissertation:	Dr. Georgios Papathanasiou Prof. Dr. Gleb Arutyunov
Zusammensetzung der Prüfungskommission:	Prof. Dr. Sven-Olaf Moch Dr. Georgios Papathanasiou Prof. Dr. Gleb Arutyunov Prof. Dr. Timo Weigand Prof. Dr. Kerstin Tackmann
Vorsitzender der Prüfungskommission:	Prof. Dr. Sven-Olaf Moch
Datum der Disputation:	12.07.2022
Vorsitzender Fach-Promotionsausschuss PHYSIK:	Prof. Dr. Wolfgang J. Parak
Leiter des Fachbereichs PHYSIK:	Prof. Dr. Günter H. W. Sigl
Dekan der Fakultät MIN:	Prof. Dr. Heinrich Graener

Abstract

Scattering amplitudes are key observables that describe the probability of possible outcomes in the interaction of fundamental particles. These interactions are investigated in particle colliders, where two beams of high-energy particles are collided. By comparing the measured distribution of scattering events to the predicted amplitudes, the underlying theory can be tested. Beyond bridging theory and experiment, amplitudes also show remarkably deep mathematical structures. Due to many hidden properties, they are often much simpler than might be expected from their conventional calculation in terms of Feynman diagrams. By uncovering these hidden properties of scattering amplitudes, many methods have been developed that allow a more direct calculation circumventing Feynman diagrams altogether.

This thesis is devoted to the study of two such structures that have recently emerged in the literature, cluster algebras and tropical Grassmannians, as well as their relation to each other. The main focus is on their application to $\mathcal{N} = 4$ super Yang-Mills theory, which is the simplest interacting gauge theory in four dimensions and a common testing ground for the development of novel methods. In this theory, it has been shown that the variables of cluster algebras associated to the Grassmannians $\mathrm{Gr}(4, n)$ encode the singularities, or more precisely letters of the amplitude symbol, of $n = 6, 7$ particle scattering and consequently allow the construction of these amplitudes via a bootstrap approach. However, for $n \geq 8$ particles, the cluster algebra contains infinitely many variables and thus lacks predictability. Furthermore, the rational variables of cluster algebras cannot account for singularities of so-called square-root type that have been observed in explicit calculations.

The main achievement of this work is a natural proposal that solves these obstructions and provides a finite set of singularities, also including those of square-root type, for any particle number. On the one hand, we show that the relation between the tropical Grassmannian $\mathrm{Tr}(4, n)$ and the cluster algebra of $\mathrm{Gr}(4, n)$ can be used to define a selection rule that selects a finite subset of the infinite set of cluster variables for $n \geq 8$. On the other hand, we show that the limits of certain infinite mutation sequences in these cluster algebras provide a way to access square-root symbol letters that have previously been found by alternative approaches. We explicitly apply our framework to the case of eight and nine-particle scattering and present a candidate alphabet for eight-particle scattering consisting of 272 rational and 18 square-root letters and for nine-particle scattering consisting of 3078 rational and 2349 square-root letters.

Finally, we also apply these methods to the amplitudes of generalised biadjoint scalar theory, which are defined via a generalisation of the scattering equations, and are essentially equal to the volume of the positive part of $\mathrm{Tr}(k, n)$. Our result gives the amplitude associated to $\mathrm{Tr}(3, 8)$ in a form containing a near-minimal amount of spurious poles.

Zusammenfassung

Streuamplituden sind grundlegende Observablen, welche die Wahrscheinlichkeiten möglicher Ausgänge von Interaktionen fundamentaler Teilchen beschreiben. Diese Interaktionen werden in Teilchenbeschleuniger untersucht, wo zwei hochenergetische Teilchenstrahlen miteinander kollidiert werden. Durch den Vergleich der gemessenen Distribution von Streuereignissen mit den vorhergesagten Amplituden lassen sich die zugrundeliegenden Theorien überprüfen. Streuamplituden bilden damit nicht nur eine Verbindung zwischen der theoretischen und der experimentellen Physik, sondern weisen zudem auch noch tiefgehende mathematische Strukturen auf. Aufgrund der Vielzahl an augenscheinlich versteckten Eigenschaften haben Streuamplituden häufig eine deutlich simplere Form als zunächst von der konventionellen Bestimmung über Feynmann-Diagramme erwartet werden kann. Durch das Aufdecken dieser versteckten Eigenschaften wurden in der Vergangenheit eine Vielzahl an Methoden entwickelt, die eine direkte Berechnung ohne die Verwendung von Feynmann-Diagrammen erlauben.

Diese Arbeit widmet sich dem Studium zweier solcher Strukturen, die vor Kurzem in der Literatur behandelt worden sind, Cluster-Algebren und tropische Graßmann- Mannigfaltigkeiten, sowie deren Verhältnis zueinander. Der Fokus liegt dabei im Wesentlichen auf deren Anwendung auf die $\mathcal{N} = 4$ supersymmetrische Yang-Mills Theorie, die einfachste interagierende Eichtheorie in vier Dimensionen. Für diese Theorie wurde gezeigt, dass die Variablen der Cluster-Algebren der Graßmann-Mannigfaltigkeiten $\mathrm{Gr}(4, n)$ die Singularitäten der Streuung von $n = 6, 7$ Teilchen beschreiben, was wiederrum die Konstruktion der Amplitude über ein Bootstrap-Verfahren ermöglicht. Für acht und mehr Teilchen enthält die Cluster-Algebra jedoch eine unendliche Anzahl an Variablen und weist somit keine Vorhersagbarkeit auf. Darüber hinaus können die per Definition rationalen Variablen der Cluster-Algebren nicht jene Singularitäten beschreiben, die Quadratwurzeln enthalten und in expliziten Berechnungen von Amplituden gefunden worden sind.

Der wesentliche Beitrag dieser Arbeit ist eine Methode, die diese Schwierigkeiten löst und eine endliche Anzahl an Singularitäten inklusive der Quadratwurzel-Singularitäten für eine beliebige Anzahl an Teilchen vorhersagt. Auf der einen Seite zeigen wir, dass das Verhältnis der tropischen Graßmann-Mannigfaltigkeiten $\mathrm{Tr}(4, n)$ zu den Cluster-Algebren von $\mathrm{Gr}(4, n)$ dazu benutzt werden kann eine Auswahlregel zu formulieren, die eine endliche Teilmenge der unendlichen Variablen für $n \geq 8$ auswählt. Auf der anderen Seite zeigen wir zudem, dass die Grenzwerte gewisser unendlicher Sequenzen an Mutationen in bestimmten Cluster-Algebren die beobachteten Quadratwurzel-Singularitäten beinhalten. Diese Methode wenden wir explizit auf die Streuung von acht und neun Teilchen an und bestimmen somit 272 rationale und 18 Quadratwurzel-Singularitäten für acht, sowie 3078 rationale und 2349 Quadratwurzel-Singularitäten für neun Teilchen.

Schlussendlich wenden wir diese Methoden zudem auf die Amplituden der sogenannten generalisierten bi-adjungierten Skalartheorie an und erhalten dadurch eine Form der Amplitude, die eine fast minimale Anzahl an nicht-physikalischen Singularitäten enthält.

Eidesstattliche Versicherung

Hiermit versichere ich an Eides statt, die vorliegende Dissertationsschrift selbst verfasst und keine anderen als die angegebenen Hilfsmittel und Quellen benutzt zu haben.

Hamburg, 31.05.2022

Niklas Henke

This thesis is based on the publications:

1. N. Henke, G. Papathanasiou, *How tropical are seven- and eight-particle amplitudes?*, *JHEP* **08** (2020) 005, [1912.08254].

2. N. Henke, G. Papathanasiou, *Singularities of eight- and nine-particle amplitudes from cluster algebras and tropical geometry*, *JHEP* **10** (2021) 007, [2106.01392].

Acknowledgments

I express my gratitude to my supervisor Dr. Georgios Papathanasiou for introducing me into the world of science, showing me fascinating mathematics and physics, guiding me along the way, and teaching me many valuable lessons that I will never forget. I also thank my family and those who have been close to my heart during the past years. Your support, confidence, and the time spent together has brought me here and has always been an invaluable part of my life. Finally, I also thank Prof. Dr. Volker Schomerus and the DESY for the opportunity they have offered me and the Studienstiftung des deutschen Volkes for making it possible.

Contents

1. Introduction and overview **1**

1.1. Introduction . . . 1

1.2. Overview . . . 6

2. Mathematical structure of amplitudes **9**

2.1. Mathematics of generic amplitudes . . . 9

2.1.1. Feynman integrals and their properties . . . 10

2.1.2. Multiple polylogarithms . . . 11

2.1.3. Algebraic structure and symbology . . . 13

2.2. Amplitudes and volumes . . . 16

2.2.1. Scattering equations and CHY formalism . . . 17

2.2.2. Amplitudes from volumes of dual associahedra . . . 19

2.2.3. Generalised biadjoint scalar theory . . . 22

2.3. Amplitudes of planar $\mathcal{N} = 4$ super Yang-Mills theory . . . 23

2.3.1. Planar $\mathcal{N} = 4$ super Yang-Mills theory . . . 23

2.3.2. Structure of amplitudes . . . 25

2.3.3. Kinematic space . . . 27

2.3.4. Loop amplitudes in planar $\mathcal{N} = 4$ super Yang-Mills theory . . . 34

2.3.5. Symbol bootstrap . . . 36

3. Amplitudes from cluster algebras **38**

3.1. Background . . . 38

3.1.1. A gentle introduction . . . 38

3.1.2. Cluster algebras with coefficients . . . 43

3.1.3. Convex geometry: polytopes and fans . . . 54

3.1.4. Cluster polytope & fan . . . 63

3.2. Cluster bootstrap . . . 66

3.2.1. Cluster adjacency . . . 69

3.2.2. Example: $\mathrm{Gr}(4, 6)$ and six-particle scattering . . . 70

3.2.3. Example: $\mathrm{Gr}(4, 7)$ and seven-particle scattering . . . 74

3.2.4. Beyond seven particles . . . 76

4. Finiteness from tropical geometry **78**

4.1. Tropical geometry . . . 79

4.1.1. Tropical varieties . . . 79

4.1.2. Web-parameterisation of $\widetilde{\mathrm{Gr}}_+(k, n)$ . . . 86

4.1.3. Fans of the totally positive tropical configuration space . . . 88

4.2. Tropical cluster bootstrap . . . 91

4.2.1. Triangulating tropical geometries . . . 91

4.2.2. Truncated cluster algebra . . . 93

4.3. Example: $\widetilde{\mathrm{pTr}}_+(4,7)$ and seven-particle scattering . . . 94
4.3.1. Truncated cluster algebra of $\mathrm{Gr}(4,7)$ . . . 95
4.3.2. Cluster adjacency of seven-particle amplitudes . . . 97
4.3.3. Weight-2 words in seven-particle amplitudes . . . 98

5. Non-rationality from infinite mutation sequences **100**
5.1. Continued fractions and square-roots . . . 101
5.2. Cluster-mutation periodicity . . . 102
5.3. Infinite mutation sequences of type $A_m^{(1)}$ . . . 103
5.4. Generalised cluster variables . . . 112

6. Applications and examples **114**
6.1. $\widetilde{\mathrm{Tr}}_+(3,8)$ and generalised biadjoint scalar amplitude . . . 115
6.1.1. Mutating and fusing cones . . . 116
6.1.2. Minimal triangulation . . . 117
6.1.3. Generalised biadjoint scalar amplitude . . . 118
6.2. $\widetilde{\mathrm{pTr}}_+(4,8)$ and eight-particle scattering . . . 120
6.2.1. Truncated $\mathrm{Gr}(4,8)$ cluster algebra . . . 120
6.2.2. Rational octagon alphabet . . . 123
6.2.3. Non-rational octagon alphabet . . . 126
6.2.4. Comparison with the scattering diagram approach . . . 129
6.3. $\widetilde{\mathrm{pTr}}_+(4,9)$ and nine-particle scattering . . . 134
6.3.1. Rational nonagon alphabet . . . 134
6.3.2. Non-rational nonagon alphabet . . . 137
6.4. Discussions and Outlook . . . 141
6.4.1. Extrapolating to arbitrary multiplicity . . . 142
6.4.2. Beyond $A_1^{(1)}$ singularities? . . . 143
6.4.3. Limitations of infinite mutation sequences and alternatives . . . 143
6.4.4. Outlook . . . 145

A. Proofs for mutation sequences of type $A_m^{(1)}$ **147**
A.1. Limit of γ_j . . . 147
A.2. The sink direction . . . 149

B. Non-rational alphabet of eight-particle scattering **152**

References **156**

List of Figures

1.1. Illustration of n-particle scattering . . . 2
1.2. Perturbative expansion in Feynman diagrams . . . 3
2.1. Feynman diagram of the scalar massless one-loop propagator . . . 9
2.2. Kinematic space $\mathcal{K}_4$ . . . 21
2.3. Examples of planar and non-planar graphs . . . 25
2.4. Kinematics in terms of momenta and dual variables . . . 29
2.5. Illustration of momentum twistors, momenta, and dual variables . . . 31
3.1. Initial quiver of $\mathrm{Gr}(2,5)$ cluster algebra . . . 39
3.2. Example for a quiver mutation . . . 40
3.3. Exchange graph of the A_2 cluster algebra . . . 42
3.4. Example of quiver mutation with frozen variables . . . 42
3.5. Modified example of quiver mutation with frozen variables . . . 43
3.6. 2-regular tree $\mathbb{T}_2$ . . . 48
3.7. Illustration of $\boldsymbol{g}$-vectors and cluster rays of the A_2 cluster algebra . . . 52
3.8. Example for the convex hull of a set of five points in $\mathbb{R}^2$ . . . 55
3.9. Example of a polytope defined as the intersection of half-spaces . . . 56
3.10. Examples for faces of a polytope . . . 57
3.11. Face lattice of the triangle . . . 58
3.12. Illustration of a cone obtained from three rays . . . 59
3.13. Construction of the normal fan of a polytope . . . 61
3.14. Examples of two fans obtained from hypersurface arrangmenets and their common refinement . . . 62
3.15. Example for fan triangulation . . . 63
3.16. Polytopal realisation of the A_2 cluster polytope, and its cluster fan . . . 65
3.17. Polytopal realisation of the A_3 cluster polytope, and its cluster fan . . . 66
3.18. Initial seeds of the $\mathrm{Gr}(4,n)$ cluster algebras . . . 68
3.19. Initial seed of the cluster algebra of $\mathrm{Gr}(4,6)$. . . . 70
3.20. Cluster polytope of the $\mathrm{Gr}(4,6)$ cluster algebra . . . 71
3.21. Initial seed of the cluster algebra of $\mathrm{Gr}(4,7)$. . . . 74
3.22. Initial seed of the cluster algebra of $\mathrm{Gr}(4,7)$ in terms of the homogenised cluster variables . . . 75
3.23. Cluster polytope of the $\mathrm{Gr}(4,7)$ cluster algebra . . . 75
4.1. Example of a tropical hypersurface . . . 82
4.2. Examdple of the positive region of a tropical variety . . . 84
4.3. Examples of web graphs . . . 87
4.4. Examples of non-intersecting paths in $\mathrm{Web}_{2,5}$ . . . 87
4.5. Collections of non-intersecting paths in Path $(3,5,6)$ of $\mathrm{Web}_{3,7}$ . . . 88
4.6. Fan $F_{2,5}$ of $\widetilde{\mathrm{Tr}}_+(2,5)$ . . . 90
4.7. Comparison of the cluster fan of the $\mathrm{Gr}(2,5)$ cluster algebra and the fan $F_{2,5}$ 91

4.8. Illustration of the triangulation of a simplicial cone 92
4.9. Examples of redundant triangulations of cones 92
4.10. Example of the fusion of cones along shared faces 93
5.1. Infinite mutation sequences in the $A_1^{(1)}$ cluster algebra 101
5.2. Clusters j and $j+1$ along the infinite mutation sequence in the $A_m^{(1)}$ cluster algebra 103
5.3. A triangulation of the annulus with two marked points on the outer and one marked point at the inner boundary 104
6.1. Example of a non-minimal triangulation of a non-simplicial cone 116
6.2. Example for the algorithm to triangulate a non-simplicial cone 118
6.3. Initial seed of the cluster algebra of $\mathrm{Gr}(4,8)$ 121
6.4. Principal part of an origin cluster in $\mathrm{Gr}(4,8)$ 128
6.5. Initial seed of the cluster algebra of $\mathrm{Gr}(4,9)$ 135
6.6. Example of an infinite cluster algebra 144
6.7. Fan of the cluster algebra with two nodes connected by three arrows 144
6.8. Example of a cluster in the truncated cluster algebra of $\mathrm{Gr}(4,9)$ containing nodes connected by three arrows 145
B.1. Initial seed of the cluster algebra of $\mathrm{Gr}(4,8)$ 152
B.2. Principal part of the origin cluster in $\mathrm{Gr}(4,8)$ utilized to find the square-root letters 153

List of Tables

3.1. Seeds of the A_2 cluster algebra 49
3.2. Variables, coefficient matrices, ray matrices, and $\boldsymbol{g}$-vectors of the A_2 cluster algebra 52
3.3. Comparison of the faces of a cluster algebra of rank r, its polytope and the cluster fan 65
3.4. Cluster adjacency of $\mathrm{Gr}(4,6)$ 72
4.1. Missing dimension-2 faces in $F_{4,7}$ compared to the E_6 cluster fan 96
4.2. Number of unordered pairs of distinct consecutive letters in the symbols of the seven-particle amplitudes at given loop level 97
4.3. Number of independent integrable weight-2 words appearing in the seven-particle amplitudes at given loop level 99
6.1. f-vectors of the full and truncated cluster polytope, and of $\widetilde{\mathrm{Tr}}_+(3,8)$ 117
6.2. Rational octagon alphabet, part 1 124
6.3. Rational octagon alphabet, part 2 125
6.4. Number of $\mathcal{A}$-variables of the truncated cluster algebra of $\mathrm{Gr}(4,9)$ 135

1. Introduction and overview

1.1. Introduction

Our current understanding of all known elementary particles and their fundamental interactions in nature is based on the *Standard Model*, which is a prime example of a *quantum field theory*, the physical framework combining quantum mechanics and special relativity. It consists of *Quantum Chromodynamics* (QCD), the theory governing the strong force, as well as the *Electroweak Theory*, which governs the electroweak force. The latter is the unification of *Quantum Electrodynamics* (QED) with the *weak interaction*. Experimentally, the Standard Model is tested in particle colliders such as the Large Hadron Collider (LHC). In this experiment, two beams of high-energy protons are collided while surrounding detectors measure their interaction. The thus obtained data is then compared to theoretic predictions of the Standard Model.

The key observables for this comparison are the *scattering amplitudes*, which describe the probability of the possible outcomes in the interaction of fundamental particles. In this way, amplitudes serve as a core object to not only falsify the physical theories but also to fix their free parameters and guide the search for new physics beyond the Standard Model. In addition, generic scattering amplitudes also exhibit remarkable mathematical structures ranging from number theory to geometry, see for example [1, 2]. Consequently, the study of scattering amplitudes interconnects pure mathematics, theoretical physics and phenomenology.

A plethora of highly significant results have been obtained from experiments such as the LHC. Among those is the widely publicised discovery of the Higgs boson in 2012 [3, 4], confirming the so-called Higgs mechanism discovered almost 50 years earlier [5–7]. On the other hand, results from the study of the mathematical structure of amplitudes have also provided crucial theoretical input for experiments, leading for example to improved methods of calculating QCD amplitudes [8] or much simplified expressions of the two-loop Higgs boson amplitude [9], to name only a few applications.

As discussed in many text books on quantum field theory, see eg. [10], the amplitude for the scattering of some initial state of n_i particles into a final state of n_f particles is formally defined in terms of the *S-matrix*, namely the evolution operator between the initial and final state of a scattering process, as

$$\mathcal{A}_{if} = \langle 1, \ldots, n_i \,|\, S \,|\, 1, \ldots, n_f \rangle \ , \tag{1.1}$$

whereas $\langle 1, \ldots, n_i|$ denotes the initial state at $t \to -\infty$ and $|1, \ldots, n_f\rangle$ the final state at $t \to \infty$. The experimentally observable probability density for this scattering is proportional to $|\mathcal{A}_{if}|^2$. Usually, the state of the particles is described in terms of their four-momentum and helicity, which essentially is the projection of the spin onto the direction of momentum. For our purposes, however, it is beneficial to instead adopt the convention where all particles are incoming with the outgoing particles having negative momentum. The setup we thus

consider is that of n particles labelled by $i = 1, \ldots, n$ with momenta p_i and helicities h_i, as is illustrated in figure 1.1.

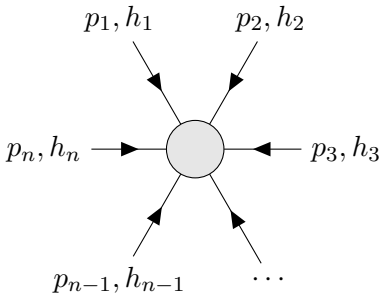

Figure 1.1: Illustration of the scattering setup of n particles with momenta p_i and helicity h_i for $i = 1, \ldots, n$.

By the Lehmann-Symanzik-Zimmermann reduction formula [11], a central result in quantum field theory, the amplitudes are essentially given by the renormalized Green functions – time-ordered correlation functions of the quantum fields describing the particles. For example, for n scalar fields $\Phi(k_i)$ with momenta k_i, which are the Fourier transformations of the space-time fields $\Phi(x_i)$, the momentum-space Green function is given by

$$G(k_1, \ldots, k_n) = \frac{\int d\Phi \, \Phi(k_1)\Phi(k_2)\cdots\Phi(k_n) \cdot \exp\left(i\mathcal{S}\left[\Phi\right]\right)}{\int d\Phi \, \exp\left(i\mathcal{S}\left[\Phi\right]\right)} \,, \tag{1.2}$$

whereas $d\Phi$ denotes the functional (or path integral) measure over all possible field configurations of the fundamental fields Φ and $\mathcal{S}$ is the *action* of the theory, a functional of the quantum fields. In four spacetime dimensions, it is usually given in terms of the *Lagrangian* $\mathcal{L}$ of the theory as

$$\mathcal{S}\left[\Phi\right] = \int d^4x \, \mathcal{L}\left[\Phi(x)\right] \,. \tag{1.3}$$

The Lagrangian, or the Lagrangian density to be precise, is a functional of the fields of the theory as well as their derivatives and describes their dynamics, for example by determining the classical equations of motion. For instance, the Lagrangian

$$\mathcal{L}\left[\Phi(x)\right] = \partial_\mu\Phi(x)\partial^\mu\Phi(x) - \frac{m^2}{2}\Phi^2(x) \,, \tag{1.4}$$

for a single scalar field $\Phi(x)$ describes a theory with a single scalar particle of mass m without any interactions. Many symmetries of the theory can be analysed on the level of the Lagrangian. Most importantly, the invariance of $\mathcal{L}$ under the action of the Poincaré group implies not only the compatibility of the theory and its amplitudes with special relativity but also energy and momentum conservation. Furthermore, if the Lagrangian is invariant under local transformations, that is transformations depending on the space-time point x, induced by a certain Lie group, the theory is said to be a *gauge theory*. For example, the Standard Model is a non-abelian gauge theory with symmetry group

$\mathrm{U}(1) \times \mathrm{SU}(2) \times \mathrm{SU}(3)$,[1] with $\mathrm{U}(1) \times \mathrm{SU}(2)$ corresponding to the gauge symmetry of the electroweak interaction, and $\mathrm{SU}(3)$ to the non-abelian gauge symmetry of QCD.

Finding closed-form expressions for the Green functions and ultimately amplitudes from the above formulas is prohibitively complicated for most of the physically interesting cases. For this reason, one usually writes the Lagrangian as

$$\mathcal{L} = \mathcal{L}_{\text{free}} + g\mathcal{L}_{\text{int}} \,, \tag{1.5}$$

whereas $\mathcal{L}_{\text{free}}$ describes the free part of the theory including the kinematic and mass terms such as for example those in eq. (1.4), $\mathcal{L}_{\text{int}}$ describes the interactions between the fields of the theory and g is the coupling constant encoding the strength of interaction. If the theory is weakly coupled, that is $g \ll 1$, we can expand the amplitudes as a perturbative series in g and calculate it term by term thus obtaining an approximate solution.

The conventional method to calculate this perturbative expansion works in terms of the so-called *Feynman diagrams*, which essentially correspond to graphical representations of the contributions to the scattering amplitude. Based on the Lagrangian of the theory, one derives the Feynman rules, which are the building blocks of all allowed diagrams. The perturbative expansion in the coupling constant g then essentially controls the number of loops that these diagrams can contain, which for this reason is often referred to as an expansion into loop order L. An example for this is illustrated in figure 1.2. Finally, by the Feynman rules we can associate a $4L$-fold integral to each diagram which corresponds to its contribution to the amplitude.

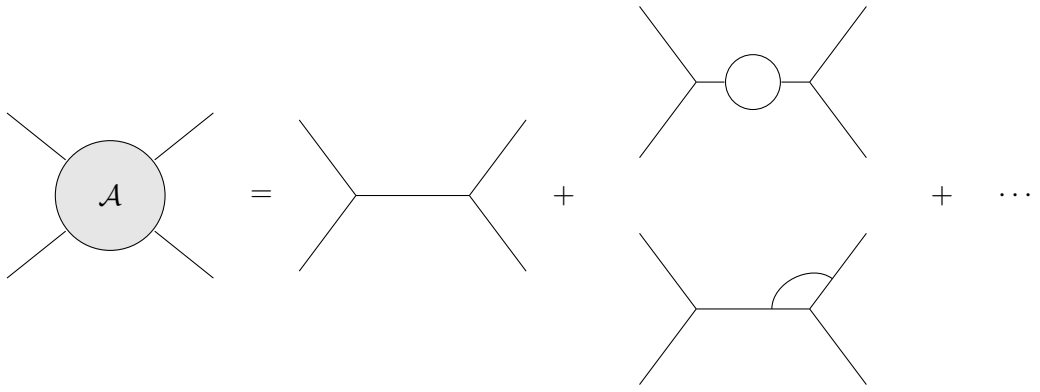

Figure 1.2: Examples of the terms in the perturbative expansion in Feynman diagrams of an amplitude of four-particle scattering at different loop numbers L.

However, beyond not capturing non-perturbative contributions such as solitons, the explicit calculation of amplitudes via Feynman diagrams becomes prohibitively complicated

[1] We remind the reader that $\mathrm{U}(n)$ denotes the group of unitary $n \times n$ matrices and $\mathrm{SU}(n)$ denotes the group of unitary $n \times n$ matrices with unit determinant.

for physically interesting cases that are studied in experiments such as the LHC. For example, already the tree-level contribution – the leading term without loops – to the amplitude of ten gluon scattering requires the calculation of millions of Feynman diagrams [12].

Furthermore, it was noted that the results of these calculations can often be expressed in a much simpler form than expected, sometimes involving only a few functions or even a single term. For instance, while the calculation requires to solve and sum up a large amount of Feynman integrals, the resulting tree-level term of the scattering amplitude of n massless gluons in the maximally helicity violating (MHV) configuration, where $n-2$ particles have helicity $+1$ and two have helicity -1, is essentially given by the Parke-Taylor factor [13]

$$\mathcal{A}_n^{\text{MHV}}\left(1^+,\ldots,i^-,\ldots,j^-,\ldots,n^+\right) = \frac{\langle ij\rangle^4}{\langle 12\rangle\langle 23\rangle\cdots\langle n1\rangle}\,, \tag{1.6}$$

up to prefactors enforcing the conservation of momentum. The kinematic variables $\langle ij\rangle$ will be explained in section 2.3.3, however the compactness of the final expression points to the large amount of redundancies in Feynman diagrams. Individual diagrams often result in physically impossible final states or introduce spurious poles that cancel out when summing over all contributing integrals. Furthermore, while the final amplitude itself has to be consistent with the symmetries of the theory, such as the invariance under gauge transformations, this is not the case for individual diagrams.

For these reasons, alternative methods have been developed that circumvent the calculation of Feynman diagrams altogether and instead attempt to construct amplitudes directly from the properties of the underlying physical theories. This initiative goes back decades with attempts to calculate the S-matrix based on its expected analytic structure and other physical constraints [14].

In more recent advances, the study of poles of tree-level gluon amplitudes has led to the Britto-Cachazo-Feng-Witten (BCFW) recursion [15–18], which relates amplitudes of n gluons to those of lower particle number. Similarly, based on unitarity, the condition that the physical state is evolved by a unitary operator, and the so-called collinear limits, unitarity cuts of Feynman integrals [19] allow to construct an ansatz for the amplitude. Furthermore, the scattering equations or Cachazo-He-Yuang (CHY) formalism [20–22] connect the space of kinematics to that of points on $\mathbb{CP}^1$, the space of complex lines through the origin in $\mathbb{C}^2$, and result in expressions for tree-level amplitudes in Yang-Mills and gravity theories in arbitrary spacetime dimension. Finally, remarkable geometric interpretations of amplitudes such as the amplituhedron [2] have been proposed that allow to derive amplitudes and their fundamental properties such as unitarity from an abstract geometric object alone.

Many of these advances were first made in the setting of $\mathcal{N}=4$ super Yang-Mills theory, the simplest interacting gauge theory in four dimensions. Similarly, we focus on this theory and especially its so-called planar limit. It is obtained by taking the rank of the gauge group N to infinity while keeping the square of the Yang-Mills coupling constant, g_{YM}^2, times N constant and has the advantage that only planar Feynman diagrams contribute to the amplitudes. This theory, which is structurally similar to QCD, is often used to explore and develop new methods as it allows to recognize some of the underlying intricate

mathematical structures more easily, which in some cases were also successfully transferred to theories more closely aligned to nature, see for example [8, 9].

For the remainder of this section, we review some of these mathematical structures that lay the foundation for the work presented in this thesis. One of the most powerful examples of such structures is the space of functions which describe the amplitudes. Explicit results as well as general arguments [23][2] suggest that the functions which describe the (appropriately normalised [25–28]) $\mathcal{N} = 4$ pSYM amplitudes in the maximally helicity violating or next-to-MHV configurations are restricted to the class of *multiple polylogarithms* (MPLs), a class of functions well-established in the mathematics literature [29–31], which can be represented as iterated integrals over rational integration kernels.

As is reviewed for example in [9], the space of multiple polylogarithms carries the structure of a so-called *Hopf algebra*, which can be used to simplify expressions involving such functions. Specifically, it allows us to recursively construct the map $\mathcal{S}$ as

$$\mathcal{S}\left[F_w\right] = \sum_{\phi_\alpha} \mathcal{S}\left[F^{\phi_\alpha}_{w-1}\right] \otimes \ln \phi_\alpha \,, \tag{1.7}$$

which maps a MPL F_w of weight w to its *symbol* [32], a w-fold tensor product of logarithms of the *letters* ϕ_α. The letters are rational functions in the kinematic parameters that encode the branch-cut and singularity structure of the function. The virtue of the symbol is that, with the tensor product being multilinear, calculations become much simpler, allowing for example to prove functional relations between multiple polylogarithms. The union of all the letters is called the *symbol alphabet* and is the starting point of the so-called *cluster bootstrap*, see [33, 34] for recent reviews.

Whereas in theory the symbol alphabet and the entire amplitude can be computed directly via Feynman diagrams [35, 36], this method becomes unwieldy very quickly with increasing loop number. Instead of directly computing the amplitudes, the cluster bootstrap attempts to first obtain the alphabet of the amplitude's symbol by some alternative way. Utilizing the observation that an L-loop (N)MHV amplitude is given by a weight $2L$ MPL, the space of all weight $2L$ symbols is then constructed from the alphabet. After fixing the amplitude's symbol from this space using consistency and physical constraints, the symbol can be integrated to obtain the actual function.

A key insight for this boostrap program is the observation that the letters of n-particle scattering are cluster $\mathcal{A}$-variables of the *cluster algebra* associated to the Grassmannian $\mathrm{Gr}(4, n)$ [37], following the emergence of these structures at the level of the integrand [23, 38]. Due to the dual conformal symmetry of the theory [39–43], a certain quotient of the Grassmannian – the *configuration space* $\widetilde{\mathrm{Gr}}(4, n)$ of n points in complex projective space $\mathbb{P}^3$ – corresponds to the space of kinematics of n-particle scattering, which can be conveniently described in terms of momentum twistor variables [44].

In cluster algebras the $\mathcal{A}$-variables are organized in overlapping sets, the *clusters*, which are connected by an operation called *mutation*. Starting from an initial cluster, the cluster algebra and thus all of its $\mathcal{A}$-variables are constructed by performing all possible mutations.

[2] See however also [24] for certain subtleties.

In this way, the cluster algebra allows to obtain the amplitude's symbol alphabet and thus ultimately its symbol.

This boostrap program has been successfully applied to the six-particle amplitude with up to seven loops [28, 45–53] (see also [54] for some more recent higher-loop results in its codimension-1 double-scaling limit) and for the seven-particle amplitude with up to four loops [55–58]. For many years however, two major obstructions prevented expanding the program to higher multiplicity. First of all, the relevant cluster algebras become infinite for $n \geq 8$, that is they contain infinitely many variables. Whereas it is possible that with increasing loop numbers ever more relevant discontinuities of the amplitude and thus new letters appear, it is believed that the amplitude requires only a finite number of letters, in line with finite number of its Landau singularities [59], as obtained by the amplituhedron [2, 60]. Furthermore, cluster variables are always rational functions (in momentum twistor variables), whereas also square-root letters are required to describe all amplitudes, as is for example the case for the eight-particle two-loop NMHV amplitude [61].

Hope for overcoming this obstacle has recently been raised thanks to yet another intriguing connection, between scattering amplitudes and the geometry of *tropical Grassmannians* $\mathrm{Tr}(k,n)$ [62], or more accurately *tropical configuration spaces* $\widetilde{\mathrm{Tr}}(k,n)$. This connection has first been established in the context of tree-level amplitudes in a generalised biadjoint scalar theory [63, 64]. These arise as an extension of the aforementioned CHY formulation [21, 22] of the corresponing amplitudes in usual (cubic) biadjoint scalar theory as an integral over $\mathbb{P}^1$, to an integral over $\mathbb{P}^{k-1}$. Other aspects of these amplitudes have been studied more recently in [65–68].

Building on the geometric picture for amplitudes in the $k = 2$ case [69], it was elucidated in [70] that the (canonically ordered) generalised biadjoint scalar amplitude is equal to the volume of a region of $\widetilde{\mathrm{Tr}}(k,n)$, which we shall denote as the *totally positive tropical configuration space*[3] $\widetilde{\mathrm{Tr}}_+(k,n)$ [71]. In [70], it was also pointed out that cluster algebras provide triangulations of $\widetilde{\mathrm{Tr}}_+(k,n)$, and that the nature of infinities of the former can be interpreted as an infinitely redundant decomposition of the finite volume of the latter into smaller simplices. Therefore a possible way to cure the infinities is to prevent these redundant triangulations, which in essence picks out a particular finite subset of the variables of the cluster algebra.

1.2. Overview

In this thesis, we further study cluster algebras of the Grassmannians $\mathrm{Gr}(k,n)$, the tropical configuration spaces $\widetilde{\mathrm{Tr}}(k,n)$, and in how far their relation can be applied to scattering amplitudes of both, generalised scalar biadjoint theory and planar $\mathcal{N} = 4$ super Yang-Mills theory. In the latter case, our main advance is a proposal for an algorithm that solves the long-standing obstructions preventing the application of the cluster bootstrap to eight and more particles, as described in the previous section. This work is organised as follows.

[3] In the literature, $\widetilde{\mathrm{Tr}}_+(k,n)$ is often also called totally positive tropical Grassmannian by abuse of notation.

First, we begin in chapter 2 with a general review of the mathematical structure of amplitudes. This includes an introduction to the mathematics of generic amplitudes to highlight the type of questions and methods that can be used to study generic amplitudes as well as a review of the multiple polylogarithms and their algebraic structure, that is often sufficient to describe amplitudes. As some of the methods we develop in here also have applications to the amplitudes of generalised biadjoint scalar theory, we also review this theory and in particular how its amplitudes are related to certain geometric structures. Finally, we end the chapter with a review of $\mathcal{N} = 4$ super Yang-Mills theory and its planar limit thus introducing the main theory of interest to this thesis.

In chapter 3, we turn our focus to one of the central mathematical structures of planar $\mathcal{N} = 4$ super Yang-Mills amplitudes studied in this thesis, the so-called cluster algebras. We begin with a gentle introduction to the topic and review the notion of cluster algebras as it is commonly used in the physics literature. Next, we dive deeper into the mathematical foundations of cluster algebras and discuss the framework of so-called coefficients, which becomes useful in the later chapters, and also allows us to introduce the cluster polytope and fan, two geometric structures associated to cluster algebras. Finally, we review the cluster bootstrap for scattering amplitudes of six and seven particles, for which the relevant cluster algebras are finite, that is they predict a finite set of singularities.

Next, we introduce tropical geometry in chapter 4. After a general review on the topic, we discuss the very interesting relation between finite cluster algebras and tropical geometries, namely that the former triangulates the latter. Pushing this analogy to the infinite case allows us to reverse the argument and formulate a selection rule that selects a finite subset of the infinite cluster variables. As a first consistency check, we apply this concept of a *truncated cluster algebra* to the scattering of six and seven particles. While we demonstrate that the cluster algebras truncated by the *totally positive tropical configuration spaces* $\widetilde{\mathrm{Tr}}_+(4,6)$ and $\widetilde{\mathrm{Tr}}_+(4,7)$, respectively, are consistent with the results from the conventional cluster bootstrap, we find that a certain *partial tropicalisation* best describes the adjacency conditions present in seven-particle MHV amplitudes.

In chapter 5, we move on to address the second obstruction, namely the appearance of square-root letters which cannot be described by the rational cluster variables themselves. For this purpose, we study so-called *infinite mutation sequences* in the cluster algebras of $\mathrm{Gr}(4,n)$. These sequences correspond to infinite sequences of clusters related by mutation with ever new cluster variables and arise in cluster algebras obeying a certain periodicity condition. Remarkably, we find that the limits of these sequences can be used to define *generalised cluster variables* which do contain square roots and are thus a natural candidate for the non-rational letters known to appear in the scattering of eight and more particles. In order to construct these letters, we develop and present the general solution of a large class of infinite mutation sequences in affine cluster algebras.

Finally, in chapter 6 we apply the methods we have developed in the preceding chapters to a variety of cases to obtain explicit results. First, we apply them to the amplitudes of generalised biadjoint scalar amplitude and obtain an expression with a near-minimal amount of spurious poles in section 6.1. Next, we move on to study $\widetilde{\mathrm{Tr}}_+(4,8)$ and the eight-particle amplitude of planar $\mathcal{N} = 4$ super Yang-Mills theory in section 6.2. There, we

obtain a finite set of 272 cluster variables, which is expected to contain the rational symbol letters of the eight-particle MHV amplitude as well as 18 non-rational letters, which are in agreement with results obtained from similar and other approaches [61, 72]. As a cross-check, we also compare our method to the closely related *scattering diagram* approach [73] and find that they agree, with the only exception being the two cyclically inequivalent realisations of the four-mass box square-root formed by eight massless legs, see e.g. [74]. Given this almost complete overlap between the two methods, we next move on to apply our results to the nine-particle amplitude in section 6.3. There, we find a collection of 3,078 rational and 2,349 square-root letters expected to appear in the nine-particle amplitude. As a nontrivial check of our proposal, we confirm that it also contains the alphabet of the 2-loop NMHV nine-particle amplitude, whose symbol was recently computed in [75]. Finally, we conclude in section 6.4, discuss some of the limitations of our approach and point to future directions of research.

2. Mathematical structure of amplitudes

With amplitudes as the main object of interest in this thesis, we devote this chapter to study their general mathematical structure. While some things can be said for any amplitude arising from Feynman integrals, as is reviewed in section 2.1, we will quickly consider specific theories. More precisely, in section 2.2 we review how amplitudes can be obtained as the volume of certain geometries in the context of generalised biadjoint scalar theories and in section 2.3 we finally turn to planar $\mathcal{N} = 4$ super Yang-Mills theory and discuss the general structure of its amplitudes.

2.1. Mathematics of generic amplitudes

When computing the amplitude of some scattering process, the standard approach is to use perturbation theory and expand the amplitude into a sum of Feynman diagrams with a fixed number of loops at each term. To each of these diagrams we associate an integral contributing to the overall amplitude. Consider for example the simple scalar massless one-loop propagator depicted in fig. 2.1.

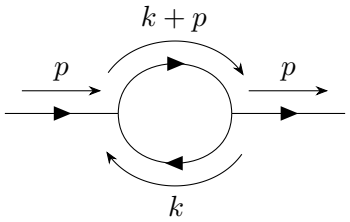

Figure 2.1: Feynman diagram of the scalar massless one-loop propagator.

Considering this diagram in D spacetime dimensions, we can use the Feynman rules to obtain the associated integral. In this case, the integral is simply solved so that we obtain the contribution of this diagram to the amplitude as

$$I(p^2) = \int \frac{d^D k}{i\pi^{D/2}} \frac{1}{k^2 \, (k+p)^2} = p^{D-4} \frac{\Gamma(\frac{D}{2}-1)^2 \Gamma(2-\frac{D}{2})}{\Gamma(D-2)} \,. \tag{2.1}$$

To compute physical amplitudes, we want to specify $D = 4$. However, since the Γ-function is divergent at negative integer values, we have to regulate the above integral. One approach is to use dimensional regularization by slightly perturbing the dimension to $D = D_0 - 2\epsilon$ and expanding the resulting function in a Laurent series in ϵ. This leads to

$$e^{\gamma_E \epsilon} \cdot I(p^2) = \frac{1}{\epsilon} + 2 - \log(-p^2) + \epsilon \left[\frac{1}{2} \log^2(-p^2) - 2 \log(-p^2) - \frac{1}{2} \zeta_2 + 4 \right] + \mathcal{O}(\epsilon^2) \,, \tag{2.2}$$

whereas ζ_n denotes the Riemann ζ function at integer values n, also called zeta values, with $\zeta_2 = \pi^2/6$ and γ_E is the Euler-Mascheroni constant, which appears as an overall factor in this result.

Considering this result, one might ask in how far this generalises to other amplitudes as well. Whereas it can be shown that the general Feynman integral I is a meromorphic function of ϵ, one might ask what kind of numbers and functions can appear as coefficients of its Laurent series in ϵ and what kind of properties they obey. In the above example, we have seen the appearance of logarithms and transcendental functions such as the zeta values. Can arbitrarily complex functions appear? What about trigonometric functions or exponentials? In the remainder of this section, following [1, 9], we review in how far these questions can be answered in general and introduce the main functions of interest for this thesis, the *multiple polylogarithms*.

2.1.1. Feynman integrals and their properties

We consider a generic Feynman graph with L loops, N propagators with momenta q_i and masses $m_i \geq 0$ for $1 \leq i \leq N$, and E external momenta p_i for $1 \leq i \leq E$. The associated integral is of the form

$$I = \int \left(\prod_{j=1}^{L} e^{\gamma_E \epsilon} \frac{d^D k_j}{i\pi^{D/2}} \right) \frac{\mathcal{N}\left(\{p_i, k_j\}\right)}{\left(q_1^2 - m_1^2\right)^{\nu_1} \cdots \left(q_N^2 - m_N^2\right)^{\nu_N}} , \tag{2.3}$$

whereas $\nu_i \in \mathbb{Z}$ and $\mathcal{N}$ is some polynomial in terms of Lorentz invariants formed out of the external and loop momenta p_i and k_j, respectively. By enforcing momentum conservation, the propagator momenta q_i can be expressed in terms of the external and loop momenta.

In dimensional regularisation, we consider the above integral in $D = D_0 - 2\epsilon$ spacetime dimensions such that I will be a function of ϵ. It can be shown that this function is meromorphic and hence at most has poles in the complex ϵ-plane and no branch cuts. Consequently, we expand the integral in the Laurent series

$$I = \sum_{\substack{k \in \mathbb{Z} \\ k \geq k_0}} \epsilon^k I_k \, , \tag{2.4}$$

for some $k_0 \in \mathbb{Z}$. Keeping the external momentum fixed for now, we ask what kind of numbers can appear as the coefficients I_k. In the above example, eq. (2.2), we have seen coefficients I_k consisting of integers, logarithms and multi zeta values. How can we classify these types of numbers?

First of all, we define the *algebraic numbers* over $\mathbb{Q}$, denoted by $\bar{\mathbb{Q}}$, as all complex numbers which are given as the root of some polynomial with rational coefficients. This immediately implies that $\mathbb{Q} \subset \bar{\mathbb{Q}}$. A complex number that is not algebraic, is called *transcendental*. Similarly, a function is algebraic if it is the root of a polynomial whose coefficients are rational functions. An example for an algebraic number is the n-th root $\sqrt[n]{q}$ of a rational number $q \in \mathbb{Q}$, which can be obtained from $p(z) = z^n - q$. Similarly, the function $(x, y) \to \sqrt{x + y}$ is algebraic, since it is the root of $p(z) = z^2 - (x + y) \cdot z^0$.

Since it can be shown that ζ_2 and $\log q$ for any $q \in \mathbb{Q}$ are transcendental, the set of algebraic numbers is too narrow to describe the coefficients of generic Feynman integrals. We hence introduce the set of periods $\mathbb{P}$ as all complex numbers, whose real and imaginary part can be obtained as an integral of an algebraic function with algebraic coefficients, over a domain defined by polynomial inequalities with algebraic coefficients [76]. Since for any $q \in \bar{\mathbb{Q}}$ we can write $q = \int_D dx$ with the domain $D = \{0 \leq x \leq q\}$ we have $\bar{\mathbb{Q}} \subset \mathbb{P}$ and obtain the inclusion

$$\mathbb{Q} \subset \bar{\mathbb{Q}} \subset \mathbb{P} \subset \mathbb{C}\,. \tag{2.5}$$

Besides the algebraic numbers, there are many examples for complex numbers which are periods. For our purposes, the following two examples are the most significant.

Example 2.1. Similar to expressing the algebraic numbers as integrals, we can easily show that the logarithm of any algebraic number $q \in \bar{\mathbb{Q}}$ is a period, by writing

$$\log q = \int_1^q \frac{dx}{x}\,. \tag{2.6}$$

Note that for some transcendental numbers the logarithm is not a period, as is conjectured for example for $\log \pi$.

Example 2.2. Another class of periods are given by the multi zeta values ζ_n. For example, consider ζ_2, which, using the integral representation of the Riemann zeta function, can be expressed as

$$\zeta_2 = \int_0^\infty \frac{x}{e^x - 1} dx = -\int_0^1 \frac{\ln(1-u)}{u} du = \int_{0\leq v\leq u\leq 1} \frac{du\, dv}{u(1-v)}\,, \tag{2.7}$$

demonstrating that $\zeta_2 \in \mathbb{P}$.

These two examples demonstrate that all the numbers appearing in the coefficients of the expansion in eq. (2.2) are periods.[1] Fascinatingly, this observation applies to generic Feynman integral, as expressed by the following theorem.

Theorem 2.3 (Bogner-Weinzierl [77])**.** *If all kinematic invariants $p_i \cdot p_j$ are negative or zero, all masses m_i are positive or zero, and all ratios of invariants and masses are algebraic, the coefficients I_k of the Laurent series of a Feynman integral I, eq. (2.3), are periods.*

2.1.2. Multiple polylogarithms

Whereas the class of periods offers a generalised description of the types of numbers that can appear as the coefficients of the Laurent expansion of generic Feynman integrals, we can further specify the functions, in terms of the external kinematic data, that we expect to appear. In fact, eq. (2.7) already suggests to consider the *dilogarithm*, which is defined as

$$\mathrm{Li}_2(z) = -\int_0^z \frac{\ln(1-u)}{u} du\,, \tag{2.8}$$

[1] Note that for this to be the case, the introduction of the factor $\exp(\gamma_E \epsilon)$ was necessary to remove the Euler-Mascheroni constant, which is conjectured to not be a period, from the final expansion.

and is related to the multi zeta values by $\zeta_2 = \mathrm{Li}_2(1)$.

Whereas it has been known for a some time that the general one-loop one-, two-, three- and four-point functions can be expressed in terms of the dilogarithm [78], more recent arguments [23] have shown that a large class of amplitudes of planar $\mathcal{N} = 4$ super Yang-Mills theory are a generalisation thereof, the so-called multiple polylogarithms (MPLs). In fact, all amplitudes that are of interest to this thesis are in this class of functions, so that we from now on entirely focus on MPLs, which are defined as follows.

Definition 2.4 (Multiple polylogarithm [29, 79])**.** Given w complex constants $a_i \in \mathbb{C}$, the multiple polylogarithm of weight w is recursively defined as the iterated integral

$$I_w\left(a_0; a_1, \ldots, a_w; a_{w+1}\right) = \int_{a_0}^{a_{w+1}} I_{w-1}\left(a_0; a_1 \ldots, a_{w-1}; t\right) \frac{dt}{t - a_w}\,, \tag{2.9}$$

whereas $I_{w-1}\left(a_0; a_1 \ldots, a_{w-1}; t\right)$ is a multiple polylogarithm of weight $w-1$ and the multiple polylogarithm of weight 0 is $I_0(z) = 1$.

From the definition, eq. (2.9), one can immediately see that the multiple polylogarithms are singular for $z = a_w$. Assuming that the $a_i \neq 0$, they are multivalued analytic functions with a complicated branch cut structure. While for algebraic arguments the multiple polylogarithms are certainly periods, it is not known whether they are transcendental. We will nonetheless assume this in the remainder of this thesis. In a more precise treatment, one can work with the *motivic* version of these iterated integrals, for which the following constructions are well-defined [29, 30].

In the physics literature, another definition for the multiple polylogarithms is more common. Denoted by G_w, they are related to eq. (2.9) by

$$G_n\left(a_w, \ldots, a_1; z\right) = I_w\left(0; a_1, \ldots, a_w; z\right)\,. \tag{2.10}$$

In fact, these two different notions of polylogarithms are completely equivalent, since it can be shown that any I_w can be expressed in terms of the G_w.

Before turning to the properties of these functions, we first consider some basic examples of multiple polylogarithms.

Example 2.5. The simplest example of a multiple polylogarithm is the ordinary logarithm. In particular, for any $w \geq 0$ and $a \in \mathbb{C}^*$ we have

$$I_w(a, \ldots, a; z) = \frac{1}{w!} \log^w\left(1 - \frac{z}{a}\right)\,, \tag{2.11}$$

as can be easily demonstrated by induction.

Example 2.6. In another example, the MPLs also generalise a class of functions called *classical polylogarithms*, which includes the dilogarithm Li_2. They can be recursively defined for $w \geq 2$ by

$$\mathrm{Li}_w = \int_0^z \mathrm{Li}_{w-1}(t) \frac{dt}{t}\,, \tag{2.12}$$

and for $w = 1$ by $\mathrm{Li}_1(z) = -\log(1 - z)$.

2.1.3. Algebraic structure and symbology

In order to study analytic properties such as singularities or branch cuts of the amplitudes computed from Feynman integrals in terms of multiple polylogarithms, it is beneficial to obtain the simplest possible expression, since individual terms might have spurious poles that cancel in the overall result. Usually, many different and equivalent expressions are possible due to functional relations. Consider for example the very well known property of the logarithm

$$\log(ab) = \log(a) + \log(b)\,. \tag{2.13}$$

In fact, all other functional relations of the logarithm can be derived from this one. For the more general dilogarithm, there are many more relations, such as [80]

$$\mathrm{Li}_2(z) + \mathrm{Li}_2(-z) - \frac{1}{2}\,\mathrm{Li}_2(z^2) = 0\,, \tag{2.14}$$

$$\mathrm{Li}_2(z) + \mathrm{Li}_2(1-z) + \log(z)\log(1-z) = \zeta_2\,. \tag{2.15}$$

One might then wonder how to find and classify all functional relations for general multiple polylogarithms. First, by noting that $\zeta_2 = \mathrm{Li}_2(1)$ and that $\ln(z)\ln(1-z)$ is an MPL of weight 2, we observe that all relations in eqs. (2.13)–(2.15) only include MPLs of the same weight. Together with the assumption of transcendentality, this leads to the following conjecture.

Conjecture 2.7. *The multiple polylogarithms are transcendental functions and only satisfy functional relations among the same weight.*

Assuming this conjecture, which we will do throughout this thesis, allows us to grade the vector space (over $\mathbb{Q}$) spanned by all multiple polylogarithms $\mathcal{A}$ by weight and write it as the direct sum

$$\mathcal{A} = \bigoplus_{w=0}^{\infty} \mathcal{A}_w\,, \tag{2.16}$$

whereas $\mathcal{A}_w$ denotes the space spanned by all multiple polylogarithms of weight w and $\mathcal{A}_0 = \mathbb{Q}$. Since the product of two MPLs of weight w_1 and w_2, respectively, is a MPL of weight $w_1 + w_2$, $\mathcal{A}$ is a graded algebra.

Furthermore, in [30] it is shown that this space can be equipped with a *coproduct*.[2] Loosely speaking, the coproduct decomposes an element of $\mathcal{A}$ into smaller pieces as

$$\Delta : \mathcal{A}_w \to \bigoplus_{p+q=w} \mathcal{A}_p \otimes \mathcal{A}_q\,, \tag{2.17}$$

while satisfying coassociativity $(\Delta \otimes \mathrm{id})\Delta = \Delta(\Delta \otimes \mathrm{id})$, whereas id denotes the identity, and being compatible with the usual multiplication $\Delta(a \cdot b) = \Delta(a) \cdot \Delta(b)$. We denote the components of the coproduct by $\Delta_{p,q}$, which refers to the part of the coproduct that lies in $\mathcal{A}_p \otimes \mathcal{A}_q$. In this way, we can also write the action of Δ on $\mathcal{A}_w$ as

$$\Delta = \sum_{p+q=w} \Delta_{p,q}\,. \tag{2.18}$$

[2] Consequently, the vector space of multiple polylogarithms is a Hopf algebra, since it also is equipped with an antipode map.

The interested reader is referred to [9] for more details on this construction. In the case of multiple polylogarithms, the coproduct can be defined as

$$\Delta\left(I_w\left(a_0;a_1,\ldots,a_w;a_{w+1}\right)\right) = \sum_{0=i_1<\cdots<i_{k+1}=w} I_k\left(a_0;a_{i_1},\ldots,a_{i_k};a_{w+1}\right)\otimes\left[\prod_{p=1}^{k} I_{i_{p+1}-i_p-1}\left(a_{i_p};a_{i_p+1},\ldots,a_{i_{p+1}-1};a_{p+1}\right)\right]. \tag{2.19}$$

While this equation is somewhat abstract, there is a more pictorial way to obtain the coproduct of generic multiple polylogarithms in terms of the combinatorial properties of a rooted decorated polygon associated to the MPL [81], see also [1]. Note that for these definitions to be well-defined, we have to work modulo $i\pi$ [31] and change the coproduct to

$$\Delta : \mathcal{A}_w \to \bigoplus_{p+q=w} \mathcal{A}_p \otimes \mathcal{A}_q^{\pi}\,, \tag{2.20}$$

whereas $\mathcal{A}_q^{\pi}$ denotes the space of weight q MPLs modulo $i\pi$. We can take care of this technicality by simply setting all terms to zero that contain a factor of $i\pi$ anywhere except in the first position of the tensor product.

Example 2.8. The logarithm is a multiple polylogarithm of weight one. Applying the coproduct to it, we get

$$\Delta\left(\log(z)\right) = \log(z)\otimes 1 + 1\otimes\log(z)\,. \tag{2.21}$$

In fact applying the coproduct to any MPL I, the result will always include $I\otimes 1 + 1\otimes I$. An element of $\mathcal{A}$, such as $\log z$, that only consists of this part is called *primitive*.

Example 2.9. In a non-trivial example, we consider the dilogarithm. Expanding the logarithm in the integral of eq. (2.8) in a similar way as we did in eq. (2.7), we see that $\mathrm{Li}_2(z) = -I(0;1,0;z)$. Applying eq. (2.19), we obtain its coproduct as

$$\Delta\left(\mathrm{Li}_2(z)\right) = \mathrm{Li}_2(z)\otimes 1 + 1\otimes\mathrm{Li}_2(z) + \mathrm{Li}_1(z)\otimes\log(z)\,. \tag{2.22}$$

Note that $\mathrm{Li}_1(z) = -\log(1-z)$ and hence a multiple polylogarithm of weight one. If we specify eq. (2.22) to $z=1$, we obtain the coproduct of ζ_2 as

$$\Delta\left(\zeta_2\right) = \zeta_2\otimes 1\,, \tag{2.23}$$

whereas the second term of eq. (2.22) evaluates to zero due to working modulo $i\pi$ and the third term vanishes due to the logarithm.

From the general definition as well as the previous examples, we have seen that the coproduct splits up a multiple polylogarithm of weight w into MPLs of smaller weights. We can use this and repeatedly apply the coproduct to fully decompose a MPL. Since the coproduct obeys coassociativity, that is it satisfies $(\Delta\otimes\mathrm{id})\Delta = \Delta(\Delta\otimes\mathrm{id})$, the result of

repeatedly applying the coproduct does not depend on the position to which we apply it. In this way, we can define

$$\mathcal{A}_w \xrightarrow{\Delta} \bigoplus_{p+q=w} \mathcal{A}_p \otimes \mathcal{A}_q^\pi \xrightarrow{\Delta\otimes\mathrm{id}} \bigoplus_{p+q+r=w} \mathcal{A}_p \otimes \mathcal{A}_q^\pi \otimes \mathcal{A}_r^\pi \xrightarrow{\Delta\otimes\mathrm{id}\otimes\mathrm{id}} \cdots \tag{2.24}$$

Similar to before, at each level we define the individual components of the coproduct by $\Delta_{p,q,r,\ldots}$. Since these indices always have to sum to w, after applying the coproduct $w-1$ times, the result will contain the component $\Delta_{1,\ldots,1}$. With this in place, we can define the *symbol* map.

Definition 2.10. The symbol maps a multiple polylogarithm of weight w to a w-fold tensor product of weight-1 polylogarithms via

$$\mathcal{S} : \mathcal{A}_w \to [\mathcal{A}_1^\pi]^{\otimes n} \,, \quad I_w \mapsto \Delta_{1,\ldots,1}\left(I_w\right) \mod i\pi \,, \tag{2.25}$$

where we now put all factors of $i\pi$ to zero.

Example 2.11. Continuing the example from above, we can immediately read off the symbol of the dilogarithm from eq. (2.22) to be

$$\mathcal{S}\left[\mathrm{Li}_2(z)\right] = -\log(1-z)\otimes\log(z)\,. \tag{2.26}$$

Evaluating this at $z=1$ shows that $\mathcal{S}\left[\zeta_2\right]=0$, which is true for all zeta values (and their generalisation, the multi zeta values).

Remark 2.12. Note that not any w-fold tensor product of weight-1 polylogarithms can appear as the symbol of some weight w multiple polylogarithm. Given a w-fold tensor product of weight-1 polylogarithms φ_{i_j},

$$S = \sum_{i_1,\ldots,i_w} \varphi_{i_1}\otimes\cdots\otimes\varphi_{i_w} \,, \tag{2.27}$$

it is the symbol of some weight-w polylogarithm if and only if

$$\sum_{i_1,\ldots,i_w} d\log\varphi_{i_j}\wedge d\log\varphi_{i_{j+1}}\varphi_{i_1}\otimes\cdots\varphi_{i_{j-1}}\otimes\varphi_{i_{j+2}}\otimes\cdots\otimes\varphi_{i_w} = 0\,, \tag{2.28}$$

for all $j=1,\ldots w-2$, as was demonstrated in [82].

Symbols have first been introduced into the physics literature in the context of functional equations of the two-loop six-particle maximally helicity violating remainder function in $\mathcal{N}=4$ super Yang-Mills theory [32] using the following construction. Similar to the weight of MPLs, we can associate a transcendentality degree $k\in\mathbb{N}$ to any transcendental functions $F_k(x_1,\ldots,x_n)$ of some variables $x_1,\ldots,x_n$. If this function satisfies

$$dF_k = \sum_{\phi_\alpha} F_{k-1}^{\phi_\alpha} d\log\phi_\alpha \,, \tag{2.29}$$

for ϕ_α rational functions in the variables x_i and $F_{k-1}^{\phi_\alpha}$ transcendental functions of weight $k-1$, we can recursively define its symbol as

$$\mathcal{S}\left[F_k\right] = \sum_{\phi_\alpha} \mathcal{S}\left[F_{k-1}^{\phi_\alpha}\right] \otimes \log \phi_\alpha \,. \tag{2.30}$$

Using the integral representation of (2.9), it can be shown that for generic arguments $a_i \neq a_j \neq 0$, the multiple polylogarithms indeed satisfy the differential equation [29]

$$\begin{aligned} &dI_n\left(a_0; a_1, \ldots, a_n; a_{n+1}\right) = \\ &\quad \sum_{i=1}^{n} I_{n-1}\left(a_0; a_1, \ldots, \hat{a}_i, \ldots, a_n; a_{n+1}\right) d\log\left(\frac{a_{i+1}-a_i}{a_{i-1}-a_i}\right) , \end{aligned} \tag{2.31}$$

whereas $\hat{a}_i$ denotes omission of the argument a_i. In fact, the recursive definition of the symbol via eq. (2.30) is equivalent to that of eq. (2.25). Since the entries of the symbol are always logarithms of rational functions ϕ_α, we usually drop the log in the notation of the symbol and only write the *letter* ϕ_α.

Facilitating this notation, we can use the additivity of the logarithm, eq. (2.13), to follow that any symbol obeys

$$\cdots \otimes \phi_\alpha \cdot \phi_\beta \otimes \cdots = \cdots \otimes \phi_\alpha \otimes \cdots + \cdots \otimes \phi_\beta \otimes \cdots \,, \tag{2.32}$$

$$\cdots \otimes (\phi)^n \otimes \cdots = n\left(\cdots \otimes \phi \otimes \cdots\right) . \tag{2.33}$$

Finally, since we are considering all entries of the tensor product modulo $i\pi$, the symbol vanishes whenever any of its entries is proportional to ρ for any $\rho^n = 1$. This implies that the symbol map has a non-trivial kernel.

To summarise, we have started with the question of how to find functional relations among multiple polylogarithms. This has lead us to the definition of the symbol, which decomposes polylogarithms into their building blocks, the letters. The upside of this is that due to the relations eqs. (2.32) and (2.33), simplifying expressions is much easier with symbols than with the actual functions. For this reason, one approach is to first convert a possible relation between MPLs into its symbol, perform some computations and than find an MPL whose symbol is given by the result of these computations. When doing so, one has to account for the fact that the symbol map has a non-trivial kernel. The remaining ambiguities can often be fixed by making use of known explicit values of the function.

In the remainder of this thesis, we will make use of a similar approach. In order to compute an amplitude, we use other information to first fix its symbol. Having found an appropriate multiple polylogarithm with that symbol, one can then try to fix the remaining constants by making use of physical constraints.

2.2. Amplitudes and volumes

In the previous section, we have seen how one can use abstract mathematics to derive properties of generic amplitudes. While planar $\mathcal{N} = 4$ super Yang-Mills theory will be

the main object of interest of this thesis, we first take a look at another theory and the mathematical methods that can be applied to obtain its amplitudes. Discussing the so-called generalised biadjoint scalar theory allows us to introduce and have a first look at how geometries enable the computation of amplitudes.

2.2.1. Scattering equations and CHY formalism

Consider the scattering of n massless particles with momenta p_i in D spacetime dimensions. The Mandelstam invariants s_{ij} are defined as

$$s_{ij} = (p_i + p_j)^2 \equiv 2p_i \cdot p_j \,. \tag{2.34}$$

Scattering equations were introduced in [20, 21] to connect the kinematic space spanned by these Mandelstam invariants to the configuration space of n points in $\mathbb{CP}^1$. As reviewed above, this space can be constructed as the quotient of the Grassmannian $\mathrm{Gr}(2,n)$ by the torus action $(\mathbb{C}^*)^{n-1}$. To construct such a map, we introduce the potential function

$$\mathcal{S}_2 = \sum_{1\leq i\leq j\leq n} s_{ij} \log\left[i\,j\right] \,, \tag{2.35}$$

whereas $(i\ j)$ denotes the $\mathrm{SL}\,(2,\mathbb{C})$-invariant combination of the homogeneous variables σ_i, σ_j of points i and j on $\mathbb{CP}^1$, respectively, defined by

$$\left[i\,j\right] = \det \begin{pmatrix} \sigma_{i,1} & \sigma_{j,1} \\ \sigma_{i,2} & \sigma_{j,2} \end{pmatrix} \,. \tag{2.36}$$

For the potential function to be well-defined, it needs to be compatible with the projective equivalence relation $\sigma_k \sim t_k \sigma_k$ for any $t_a \in \mathbb{C}^*$ and all points k. Due to momentum conservation, the Mandelstam variables satisfy

$$\sum_{\substack{j=1 \\ j\neq i}}^{n} s_{ij} = 0 \quad \forall i \,, \tag{2.37}$$

assuring that $\mathcal{S}$ actually is invariant under the torus action. Consequently, we may choose inhomogeneous coordinates x_i on $\mathbb{CP}^1$ and replace $[i\,j]$ by

$$\left[i\,j\right] = \det \begin{pmatrix} 1 & 1 \\ x_i & x_j \end{pmatrix} \equiv x_j - x_i \,. \tag{2.38}$$

To map the Mandelstam variables to points in $\mathbb{CP}^1$, we consider the critical points of the potential function, which are found by

$$\frac{\partial \mathcal{S}_2}{\partial x_i} = \sum_{\substack{j=1 \\ j\neq i}}^{n} \frac{s_{ij}}{x_i - x_j} = 0 \quad \forall i \,. \tag{2.39}$$

These are known as the scattering equations and are the cornerstone to the so-called Cachazo-He-Yuan (CHY) formalism [21], which allows to write down very compact formulas for the complete tree-level S-matrix of certain theories in arbitrary spacetime dimension.

The simplest example, which is also the most relevant to this thesis, is that of a massless scalar field ϕ in the adjoint representation of the product of two color groups $U(N)\times U(\tilde{N})$, the biadjoint scalar theory, with Lagrangian

$$\mathcal{L} = \frac{1}{2}\left(\partial_\mu \phi^{ab}\right)\left(\partial^\mu \phi^{ab}\right) - \lambda f_{abc}\tilde{f}_{a'b'c'}\phi^{aa'}\phi^{bb'}\phi^{cc'}\,, \tag{2.40}$$

whereas f and $\tilde{f}$ are the structure constants of the two color groups. As demonstrated in [22], the double-partial amplitudes of this theory, which, after color decomposition, form the building blocks of the tree-level S-matrix, are given by

$$m_n^{(2)}(\alpha|\beta) = \int \frac{\prod_{i=1}^n dx_i}{\mathrm{vol}\left(\mathrm{SL}(2,\mathbb{C})\right)} \prod_{i=1}^n \delta\left(\frac{\partial \mathcal{S}_2}{\partial x_i}\right) \mathrm{PT}^{(2)}(\alpha)\,\mathrm{PT}^{(2)}(\beta)\,, \tag{2.41}$$

whereas $\alpha,\beta \in S_n/\mathbb{Z}_n$ are two orderings with S_n the symmetric group of n elements and the Parke-Taylor factors $\mathrm{PT}^{(2)}$ are defined as

$$\mathrm{PT}^{(2)}(\alpha) = \frac{1}{(x_{\alpha(1)}-x_{\alpha(2)})(x_{\alpha(2)}-x_{\alpha(3)})\cdots(x_{\alpha(n)}-x_{\alpha(1)})}\,. \tag{2.42}$$

As can be seen from eq. (2.41), the integral localizes on the solutions of the scattering equations, eq. (2.39). To make use of this property, we first discuss the Jacobian matrix associated to the system of scattering equations following [22, 63]. It is a symmetric $n\times n$ matrix whose components Φ_{ij} are given by $\partial^2\mathcal{S}_2/\partial x_i\partial x_j$. Since this matrix has non-maximal rank and hence vanishing determinant, we introduce the reduced determinant

$$\det{}'\Phi = \frac{\det \Phi^{ijk}_{pqr}}{V_{ijk}V_{pqr}}\,, \tag{2.43}$$

whereas Φ^{ijk}_{pqr} is the matrix obtained from Φ by deleting rows i,j,k and columns p,q,r and $V_{ijk} = (x_i-x_j)(x_j-x_k)(x_k-x_i)$. Using this determinant, the integral of eq. (2.41) can be equivalently evaluated such that we obtain

$$m_n^{(2)}(\alpha|\beta) = \sum_{I=1}^{(n-3)!}\left(\frac{1}{\det{}'\Phi}\,\mathrm{PT}^{(2)}(\alpha)\,\mathrm{PT}^{(2)}(\beta)\right)\Big|_{x_i=x_i^{(I)}}\,, \tag{2.44}$$

whereas the sum goes over the solutions $x_i^{(I)}$ of the scattering equations. It can be shown that in this case, due to the $\mathrm{SL}(2,\mathbb{C})$ invariance, there are $(n-3)!$ solutions for generic kinematics [20].

Example 2.13. As an example, consider the unit ordering, $\alpha=\beta=(12\cdots n)$. For $n=4$, there are 6 Mandelstam variables of which 2 can be chosen as independent variables due to momentum conservation, eq. (2.37). Selecting s_{12} and s_{23}, it can be shown that the biadjoint scalar amplitude is given by [63]

$$m_4^{(2)}(1234|1234) = \frac{1}{s_{12}} + \frac{1}{s_{23}}\,. \tag{2.45}$$

For $n = 5$, there are 10 unique Mandelstam variables, out of which 5 can be chosen as independent after momentum conservation. In this case, the biadjoint scalar amplitude is given by [63]

$$m_5^{(2)}(12345|12345) = \frac{1}{s_{12}s_{34}} + \frac{1}{s_{23}s_{45}} + \frac{1}{s_{34}s_{51}} + \frac{1}{s_{45}s_{12}} + \frac{1}{s_{51}s_{23}}\,. \tag{2.46}$$

In general, the biadjoint scalar amplitude will be of the form of eqs. (2.45) and (2.46). It was shown in [22] that the function $m_n^2(\alpha|\beta)$ computes the sum of all trivalent scalar diagrams compatible with the α- and β-ordering. In this way, the amplitude will always be a sum of inverse products of Mandelstam variables.

2.2.2. Amplitudes from volumes of dual associahedra

While the formula for the amplitude of biadjoint scalar ϕ^3 theory, eq. (2.44), is already remarkably simple, we will now see that it equivalently can be expressed in terms of a geometric object. In the Arkani-Hamed–Bai–He–Yan (ABHY) construction [69], the amplitude can be obtained from the volume of the (dual of the) *associahedron*, a $(n-3)$-dimensional polytope. In the later parts of this thesis, we will encounter generalisations of these polytopes, which play an important role in the computation of amplitudes of planar $\mathcal{N} = 4$ SYM theory.

We begin with the Mandelstam variables s_{ij}, which, after using momentum conservation, eq. (2.37), span the *kinematic space* $\mathcal{K}_n$ of n canonically ordered massless momenta p_i for $i = 1, \ldots, n$. This space is of dimension

$$\dim \mathcal{K}_n = \binom{n}{2} - n = \frac{n(n-3)}{2}\,. \tag{2.47}$$

Note that if the spacetime dimension is $D < n-1$, there are further constraints on the Mandelstam variables, so-called Gram determinant conditions, that lower the dimensionality of this space. These Gram determinant conditions arise due to the fact that in D dimensions, at most D vectors can be linearly independent simultaneously. For simplicity, we will always assume that D is sufficiently large.

Next, we define the planar variables $X_{i,j}$ in terms of the generalized Mandelstam variables $s_{i,i+1,\ldots,j-1}$ for any pair of indices $1 \le i < j \le n$ as

$$X_{ij} = s_{i,i+1,\ldots,j-1} = (p_i + p_{i+1} + \cdots + p_{j-1})^2\,, \tag{2.48}$$

which are manifestly invariant under cyclic permutation of the indices. Note that $X_{ii} \equiv 0$, $X_{i,i+1} = p_i^2$ and $X_{1n} = (p_1 + \cdots + p_{n-1})^2 = (-p_n)^2$ vanish trivially and that indices are always considered modulo n. The two-particle Mandelstam variables s_{ij} can be expanded in terms of the planar variables as

$$s_{ij} = X_{i,j+1} + X_{i+1,j} - X_{ij} - X_{i+1,j+1}\,, \tag{2.49}$$

In fact, from this identity it follows that the non-vanishing planar variables also form a basis for the kinematic space, since they span this space and there exist as many as the dimension of $\mathcal{K}_n$.

Using the planar variables, we define the positive region Δ_n in kinematic space $\mathcal{K}_n$ by imposing

$$X_{ij} \geq 0 \quad \text{for all} \quad 1 \leq j < j \leq n\,. \tag{2.50}$$

Note that since $X_{i,i+1}$ and X_{1n} vanish trivially, they do not contribute to these inequalities. Next, we further restrict to a $(n-3)$-dimensional subspace $\mathcal{H}_n \subset \mathcal{K}_n$ by imposing

$$s_{ij} = -c_{ij} \quad \text{for all} \quad 1 \leq i < j \leq n-1 \quad \text{with} \quad i \neq j+1\,, \tag{2.51}$$

for positive constants c_{ij}. The dimension of $\mathcal{H}_n$ can be seen by counting the number of independent variables and constraints. Finally, we obtain the *associahedron* $\mathcal{A}_n$ of dimension $n-3$ as the polytope

$$\mathcal{A}_n = \mathcal{H}_n \cap \Delta_n\,. \tag{2.52}$$

Example 2.14. Consider the simplest example for $n = 4$. As already discussed above, we can choose s_{12} and s_{23} as independent Mandelstam variables spanning the kinematic space $\mathcal{K}_4$. From eq. (2.49), we see that $\mathcal{K}_4$ is equivalently spanned by $X_{13} = s_{12}$ and $X_{24} = s_{23}$, which are the only non-vanishing planar variables for this case. The positive region is hence given by

$$\Delta_4 = \left\{(X_{13}\,, X_{24}) \;\middle|\; X_{13} \geq 0\,, X_{24} \geq 0\right\}\,. \tag{2.53}$$

From eq. (2.51), we see that the subspace $\mathcal{H}_4$ is given in terms of one positive constant c_{13} by $s_{13} = -c_{13}$. Using eq. (2.49), we hence conclude that

$$\mathcal{H}_4 = \left\{(X_{13}\,, X_{24}) \;\middle|\; X_{24} = c_{13} - X_{13}\right\}\,. \tag{2.54}$$

Consequently, as is also illustrated in fig. 2.2, the associahedron $\mathcal{A}_4$ is the 1-dimensional polytope defined by

$$\mathcal{A}_4 \equiv \mathcal{H}_4 \cap \Delta_4 = \left\{(X, c_{13} - X) \;\middle|\; 0 \leq X \leq c_{13}\right\}\,, \tag{2.55}$$

with two vertices and one 1-dimensional facet.

To see how the associahedron is related to the amplitudes of biadjoint scalar ϕ^3 theory, we first look at how its volume is defined. Without going too much into detail, the concept of *positive geometry* was introduced in [83] as a real, closed geometry $\mathcal{P}$ with a unique, complex, top-dimensional differential form, the *canonical form* $\Omega(\mathcal{P})$, such that the boundaries $\partial\mathcal{P}$ are positive geometries themselves. The defining property of the canonical form is that it has only logarithmic singularities on the boundaries of $\mathcal{P}$ with the residue given by the canonical form of that boundary.

Example 2.15. Continuing our example of the associahedron $\mathcal{A}_4$, which is a positive geometry, the canonical form is given by

$$\Omega(\mathcal{A}_4) = d\log X - d\log(X - c_{13}) \tag{2.56}$$

This form has logarithmic singularities at $X = 0$ and $X = c_{13}$, which are the boundaries of $\mathcal{A}_4$. The residues at these points are $+1$ and -1, respectively, which, by definition, correspond to the canonical forms of the point with the sign reflecting different orientations.

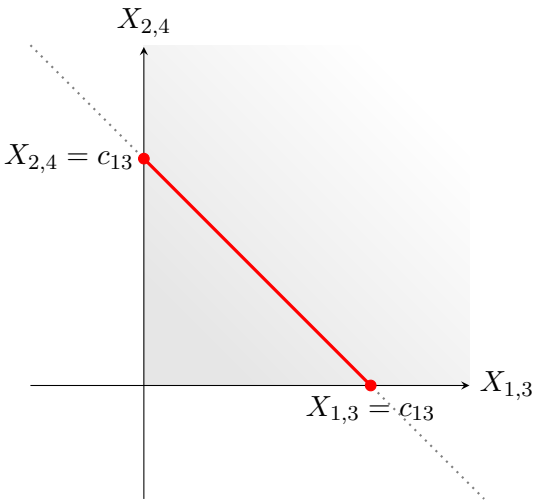

Figure 2.2: The figure shows the kinematic space $\mathcal{K}_4$ with Δ_4 highlighted by the shaded area, $\mathcal{H}_4$ by the dotted gray line and $\mathcal{A}_4$ by the red line.

Splitting off the measure of $\Omega(\mathcal{P})$, eg. $d^{n-3}X$ in the case of associahedra, we obtain the *canonical rational function* $\underline{\Omega}(\mathcal{P})$. As is discussed in [83], this function has the interpretation of the volume of the *dual* of $\mathcal{P}$. Roughly speaking, in the case that $\mathcal{P}$ is a polytope of dimension d, its dual is obtained as the convex hull of the normal vectors to its facets. In the dual, each dimension-k face corresponds to a dimension-$(d-k)$ face of $\mathcal{P}$.

Example 2.16. Concluding our previous example, we see that the canonical rational function of $\mathcal{A}_4$ is given by

$$\underline{\Omega}(\mathcal{A}_4) = \frac{1}{X} + \frac{1}{c_{13} - X}\,. \tag{2.57}$$

Since we considered the kinematic space to be spanned by X_{13}, X_{24} and by construction have that $X_{13} = x$ and $X_{24} = c_{13} - X_{13}$ and furthermore $X_{13} = s_{12}$ and $X_{24} = s_{23}$, we can conclude

$$\underline{\Omega}(\mathcal{A}_4) = \frac{1}{s_{12}} + \frac{1}{s_{23}}\,, \tag{2.58}$$

which exactly corresponds to the biadjoint scalar amplitude $m_4^{(2)}$ for the canonical ordering, eq. (2.45).

The remarkable result of the example for $n = 4$, in which we expressed the biadjoint scalar ϕ^3 amplitude of $n = 4$ particles as the volume of the dual of the associahedron $\mathcal{A}_4$, generalizes to any n. In a concise way, the statement is

$$m_n^{(2)}(12\cdots n|12\cdots n) = \mathrm{Vol}(\mathcal{A}_n^*) \equiv \underline{\Omega}(\mathcal{A}_n)\,, \tag{2.59}$$

whereas $\mathcal{A}_n^*$ denotes the dual of the $(n-3)$-dimensional associahedron. As is demonstrated in [69], one can also do a similar construction for any orderings $\alpha, \beta \in S_n/\mathbb{Z}_n$.

2.2.3. Generalised biadjoint scalar theory

In the previous sections we have seen two alternative approaches to compute the amplitudes of biadjoint scalar ϕ^3 theory. In the first approach, as reviewed in section 2.2.1, we studied scattering equations connecting the kinematic space with the configuration space of n points in $\mathbb{CP}^1$. Ultimately, this allowed us to express the amplitude as a sum over the solutions to the scattering equations, eq. (2.44). In section 2.2.2 we have seen that the amplitude can alternatively be expressed as the volume of the associahedron, eq. (2.59).

In [63], the authors discuss a generalisation of the scattering equations to points on $\mathbb{CP}^{k-1}$ for any $k \geq 2$. We consider the generalised Mandelstam invariants $s_{i_1,\ldots,i_k}$, defined by

$$s_{i_1,\ldots,i_k} = (p_{i_1} + \cdots + p_{i_k})^2 \,, \tag{2.60}$$

and map them to the configuration space of n points in $\mathbb{CP}^{k-1}$, which similar to before can be constructed as the quotient of the Grassmannian $\mathrm{Gr}(k,n)$ by the torus action $(\mathbb{C}^*)^{n-1}$. To obtain this map, we introduce the generalised potential function

$$\mathcal{S}_k = \sum_{1\leq i_1<i_2<\cdots<i_k\leq n} s_{i_1,\ldots,i_k} \log\left[i_1 \cdots i_k\right] . \tag{2.61}$$

The generalisation of the now $\mathrm{SL}\,(k,\mathbb{C})$-invariant functions of the homogeneous variables σ_{i_j} of points i_j on $\mathbb{CP}^{k-1}$ is naturally defined by

$$\left[i_1 \cdots i_k\right] = \det \begin{pmatrix} \sigma_{i_1,1} & \cdots & \sigma_{i_k,1} \\ \vdots & & \vdots \\ \sigma_{i_1,k} & \cdots & \sigma_{i_k,k} \end{pmatrix} . \tag{2.62}$$

As before, for the generalised potential function, eq. (2.61), to be well-defined, it must be invariant under the scaling of each point. This is achieved by the $k > 2$ equivalent of massless momentum conservation,

$$\sum_{\substack{i_2,\ldots,i_k=1 \\ i_a\neq i_b}}^{n} s_{i_1,\ldots,i_k} = 0 \quad \forall i_1 \,. \tag{2.63}$$

The scattering equations for the more general case of points in $\mathbb{CP}^{k-1}$ are then, similar to before, given by the critical points of the potential function. In terms of inhomogeneous coordinates $x_i^{(a)}$ of the point i on $\mathbb{CP}^{k-1}$ these are given by

$$\frac{\partial \mathcal{S}_k}{\partial x_i^{(a)}} = 0 \quad \forall a, i \,. \tag{2.64}$$

While in the case of $k > 2$ no generalisation of the scalar ϕ^3 Lagrangian of eq. (2.40) has been identified so far, we can nonetheless consider the natural analog of the double-partial amplitde $m_n^{(2)}$, eq. (2.41), given by

$$m_n^{(k)}\left(\alpha|\beta\right) := \int \frac{\prod_{i=1}^{n}\prod_{a=1}^{k-1} dx_i^{(a)}}{\mathrm{vol}\left(\mathrm{SL}\,(k,\mathbb{C})\right)} \prod_{i=1}^{n}\prod_{a=1}^{k-1} \delta\left(\frac{\partial \mathcal{S}_k}{\partial x_i^{(a)}}\right) \mathrm{PT}^{(k)}\left(\alpha\right) \mathrm{PT}^{(k)}\left(\beta\right) , \tag{2.65}$$

whereas similar to before, the factor vol $(\mathrm{SL}(k,\mathbb{C}))$ indicates that for the integral to be well-defined we need to fix the $\mathrm{SL}(k,\mathbb{C})$-invariance and the generalised Parke-Taylor factors are

$$\mathrm{PT}^{(k)}(12\cdots n) = \frac{1}{[1\,2\,\cdots\,k]\,[2\,3\,\cdots\,k+1]\cdots[n\,1\,\cdots\,k-1]}\,. \tag{2.66}$$

Finally, we take the integral of eq. (2.65), which again will localise on the solutions of the scattering equations, as the definition for the amplitudes of a *generalised biadjoint scalar theory*. Since these theories do not originate from a Lagrangian, whose existence is currently unknown, they are an example of so-called *non-Lagrangian* theories.

To sum up, by considering biadjoint scalar ϕ^3 theory, we have seen an example of how amplitudes can be computed in different ways. While the approach via scattering equations resulted in a compact analytical equation, eq. (2.44), the consideration of the associahedron led to an expression relating the amplitude to the volume of a geometric object, eq. (2.59). It is the latter concept which is a central motif of this work, and we will see in the later chapters how *tropical geometry* results in a generalisation of the associahedron allowing to also express the generalised biadjoint scalar amplitudes for $k>2$ as volumes, see in particular section 6.1. Furthermore, it also solves long-standing challenges in the computation of loop amplitudes of $\mathcal{N}=4$ pSYM with eight and more particles, see in particular section 4.2 and sections 6.2 and 6.3.

2.3. Amplitudes of planar $\mathcal{N}=4$ super Yang-Mills theory

Whereas the methods we develop in this work also have applications to other theories, such as the generalised biadjoint scalar theories reviewed in section 2.2, the central theory of interest is the so-called planar limit of $\mathcal{N}=4$ supersymmetric Yang-Mills theory. In this section, we briefly summarize its structure and introduce the concepts that form the foundation of the work presented in the remainder of this thesis. Note that from now on we restrict to $D=4$ spacetime dimensions

2.3.1. Planar $\mathcal{N}=4$ super Yang-Mills theory

The simplest interacting gauge theory in $D=4$ spacetime dimensions is the maximally supersymmetric or $\mathcal{N}=4$ super Yang-Mills theory (SYM), first described in [84, 85]. Due to the maximal amount of symmetries, it has been successfully used to make significant progress in the understanding of amplitudes and their structure, see eg. [8, 9].

The theory can be constructed by starting with a ten-dimensional $\mathcal{N}=1$ supersymmetric Yang-Mills theory on ten-dimensional Minkowski space, see eg. [84, 86]. When performing a dimensional reduction to four-dimensional Minkowski space, we are left with a field content of one gauge field A_μ with $\mu=1,\ldots,4$ a spacetime index, six real scalar fields ϕ_{AB} with $A,B=1,\ldots,4$ antisymmetric $\mathrm{SU}(4)$ indices, and four Weyl fermions $\bar{\psi}^{\dot{\alpha}A}$ as well as four anti-fermions $\psi_{\alpha A}$ with $\alpha,\dot{\alpha}=1,2$ spinor indices. The Lagrangian $\mathcal{L}$ of the theory is given by [84, 86]

$$\mathcal{L} = \mathrm{tr}\left(-\frac{1}{4}F_{\mu\nu}F^{\mu\nu} - \frac{1}{2}(D_\mu\phi_{AB})(D^\mu\phi^{AB}) + i\bar{\psi}^A_{\dot{\alpha}}\sigma^{\dot{\alpha}\alpha}_\mu D^\mu\psi_{\alpha A}\right.$$

$$- g_{YM}\left(\psi_A^\alpha[\phi^{AB},\psi_{\alpha B}] - \bar{\psi}_{\dot{\alpha}}^A[\phi_{AB},\bar{\psi}^{\dot{\alpha}B}]\right) + \frac{g_{YM}^2}{4}[\phi_{AB},\phi_{CD}][\phi^{AB},\phi^{CD}]\Bigg), \quad (2.67)$$

whereas $\sigma_\mu^{\dot{\alpha}\alpha}$ denotes the Pauli matrices, $F_{\mu\nu} = \partial_\mu A_\nu - \partial_\nu A_\mu - ig_{YM}[A_\mu, A_\nu]$ is the field-strength tensor, $D_\mu \Psi = \partial_\mu \Psi - ig_{YM}[A_\mu, \Psi]$ is the covariant derivative in the adjoint representation, and g_{YM} is the dimensionless gauge coupling constant. All fields are massless and transform in the adjoint representation of the gauge group $\mathrm{SU}(N)$ such that the gauge coupling g_{YM} as well as the rank N of the gauge group – the number of colors – are the free parameters of this theory.

The Lagrangian is symmetric under the action of the *superconformal symmetry* group $\mathrm{PSU}(2,2|4)$, see eg. [87] or [88, 89] for a pedagogical review. This supergroup consists of a bosonic part given by $\mathrm{SU}(2,2) \times \mathrm{SU}(4)$ as well as a fermionic part. The associated Lie superalgebra is a $\mathbb{Z}_2$-graded algebra, that is the usual commutator is replaced by a graded commutator, which acts on two fermionic elements as an anticommutator and on a bosonic with any other element as a commutator.

The subgroup $\mathrm{SU}(2,2)$ – the subgroup of $\mathrm{SL}(4,\mathbb{C})$ preserving a Hermitian quadratic form with two positive and two negative signs – corresponds to *conformal* symmetry. It is generated by translations, Lorentz transformations, dilatations as well as special conformal transformations. Conformal symmetry is an extension to the Poincaré group and, roughly speaking, relates different scales of the theory to each other. Consequently, a conformal field theory is scale invariant and its observables such as the correlation functions are much simplified, see eg. [90] for an introduction to conformal field theories.

The superconformal symmetry group further consists of the internal R-symmetry group $\mathrm{SU}(4) \cong \mathrm{SO}(6)$, which transforms the scalar fields and fermions among themselves. This symmetry can be interpreted as rotations of the six dimensions that are compactified in the construction of the theory from a field theory in ten-dimensional Minkowski space.

Finally, the superconformal symmetry group also contains a fermionic part generating the *supersymmetry* transformations. Supersymmetry is the only possible extension to the Poincaré group besides internal symmetries that is allowed under the Coleman-Mandula theorem [91] and its extensions [92]. The $\mathcal{N} = 4$ generators of this symmetry mix the bosonic and fermionic field content of the theory with each other such that for each fermion we have a bosonic superpartner and vice versa.

Remarkably, the theory not only has a large amount of symmetries but is also closely related to string theory. As the prime example of *AdS/CFT-correspondence*, $\mathcal{N} = 4$ SYM is conjectured to be dual to type IIB superstring theory on a $\mathrm{AdS}_5 \times S^5$ background [93, 94]. In this correspondence, the string coupling constant is proportional to g_{YM}^2 whereas the radius of curvature of the background space is proportional to $(g_{YM}^2 N)^{1/4}$. Due to this relation, the duality is very difficult to verify, since the gauge theory is weakly coupled for $g_{YM} \ll 1$ whereas the string theory reduces to supergravity only for large curvature radii.

However, further simplifications occur in the *planar limit* [95], which is obtained by taking the number of colors, that is the rank of the gauge group, $N \to \infty$ and the gauge coupling $g_{YM} \to 0$ while keeping the *'t Hooft coupling* $\lambda = g_{YM}^2 N$ constant. In this limit the string theory becomes free, whereas the gauge theory becomes *planar*, that is only

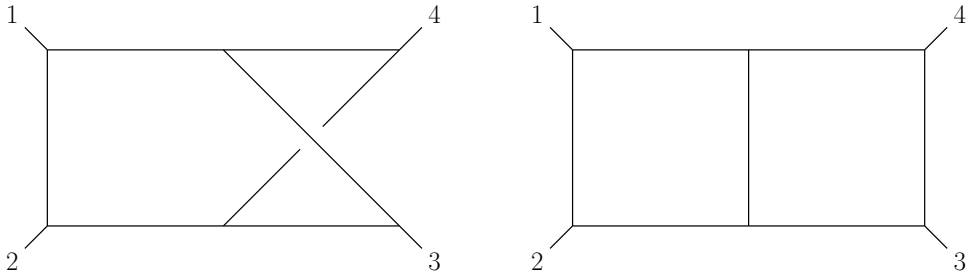

(a) Non-planar graph (b) Planar graph

Figure 2.3: Examples of a (a) non-planar and (b) planar graph. The non-planar graph on the left cannot be embedded on the plane, since it cannot be drawn without the lines going to 3 and 4 intersecting each other. In contrast, all edges in the planar graph only intersect at the vertices.

planar diagrams contribute to the amplitude. This can be seen by noting that in the limit of infinite colors, the amplitudes obtained from a Feynman graph of genus g scale like N^{2-2g}. Consequently, only the contributions of diagrams with $g = 0$ survive. In this sense, a Feynman diagram is planar if it can be drawn on the plane without intersecting lines, see figure 2.3 for some examples.

While the perturbative regimes are still incompatible in the planar limit since planar $\mathcal{N} = 4$ SYM is weakly coupled for small values of λ and thus small curvature radii of the string background, this limit makes present a property of the theory referred to as *integrability*. This phenomenon is typically encountered in two-dimensional theories and is characterised by a very high number of conserved quantities allowing to exactly solve the system. Remarkably, it is also present in planar $\mathcal{N} = 4$ SYM, where it can be interpreted as another, hidden symmetry and has lead to immense progress towards an exact solution of the theory [96].

2.3.2. Structure of amplitudes

Having discussed the basic structure and symmetries of planar $\mathcal{N} = 4$ super Yang-Mills theory, we now turn to its amplitudes. We have already seen that in the planar limit only planar diagrams contribute to the amplitude, which significantly simplifies its computation. Further simplifications are possible by organising the dependence of the amplitudes on the remaining quantum numbers, which are color, helicities, and momenta.

Consequently, in this section we consider color and helicity and how they can be used to decompose amplitudes of planar $\mathcal{N} = 4$ super Yang-Mills theory. Furthermore, this allows to discuss further symmetries that these amplitudes exhibit. The constructions of this subsection lay the foundation for the discussion of loop amplitudes in section 2.3.4.

Color decomposition

We begin by briefly commenting on color decomposition in the planar limit. For more details, see eg. the reviews [97, 98]. Consider a generic gauge theory with coupling constant

g_c and gauge group SU(N), which is generated by T^a for the color index $a = 1, \ldots, N^2 - 1$. The L-loop scattering amplitude of n gluons can be decomposed as [98, 99]

$$\mathcal{A}_n^{(L)} = g_c^{n-2} \left(g_c^2 N\right)^L \left[\sum_{\sigma \in S_n/\mathbb{Z}_n} \mathrm{tr}\left(T^{a_{\sigma(1)}} \cdots T^{a_{\sigma(n)}}\right) A_n^{(L)}\left(\sigma(1^{h_1}), \ldots, \sigma(n^{h_n})\right) + \mathcal{O}\left(\frac{1}{N}\right) \right], \tag{2.68}$$

whereas $h_i = \pm 1$ denotes the helicity of the i-th gluon, and the sum runs over all inequivalent permutations $\sigma \in S_n/\mathbb{Z}_n$ given by all permutations S_n, the symmetric group of n elements, modulo all cyclic permutations $\mathbb{Z}_n$ due to the cyclicity of the trace. In this decomposition, we have stripped off all color factors such that only kinematic information remains in the *partial amplitude* $A_n^{(L)}\left(\sigma(1^{h_1}), \ldots, \sigma(n^{h_n})\right)$. This amplitude is *color-ordered* since it only receives contributions from Feynman diagrams with the external gluons ordered according to the cyclic ordering σ.

In the planar limit, as can be seen from eq. (2.68), the first term, containing only a single trace, dominates and is the only one to survive. Consequently, in the remainder of this thesis we always refer to the partial, color-ordered amplitude $A_n^{(L)}$ when discussing loop amplitudes of planar $\mathcal{N} = 4$ SYM theory.

Superamplitude and helicity decomposition

Having seen that the partial amplitude allows for neatly organising the color-dependence of the amplitude, we now turn to the dependence on helicity and further decompositions of the amplitude. First, the superconformal symmetry of the theory can be represented by an on-shell superfield, which contains the entire on-shell particle content of the theory and is given by [100]

$$\Phi = G^+ + \eta^A \Gamma_A + \frac{1}{2!}\eta^A \eta^B S_{AB} + \frac{1}{3!}\eta^A \eta^B \eta^C \epsilon_{ABCD} \bar{\Gamma}^D + \frac{1}{4!}\eta^A \eta^B \eta^C \eta^D \epsilon_{ABCD} G^- , \tag{2.69}$$

whereas η^A are fermionic parameters which transform in the fundamental representation of SU(4), $G^\pm$ are gluons with helicity ± 1, Γ_A and $\bar{\Gamma}^A$ are fermions with helicity $\pm 1/2$, and S_{AB} are scalars with helicity 0, respectively. This superfield has (generalised) helicity 1, as can be seen from eq. (2.69) by noting that η has helicity $1/2$.

Correspondingly, we describe the simultaneous scattering of all on-shell states of the theory in terms of a color-ordered *superamplitude* $\mathcal{A}_n(\Phi_1, \ldots, \Phi_n)$. Due to the R-symmetry invariance of the theory, this amplitude can be expanded in the SU(4)-invariants formed out of multiples of four fermionic parameters η as

$$\mathcal{A}_n = \mathcal{A}_{n,0} + \mathcal{A}_{n,1} + \cdots + \mathcal{A}_{n,n-4} , \tag{2.70}$$

whereas $\mathcal{A}_{n,k}$ is of degree $4k + 8$ in the fermionic parameters. Terms with $k < 0$ do not contribute since invariance under supersymmetry transformations implies the appearance of a fermionic supermomentum conserving delta-function which is of degree 8 in the fermionic parameters. As can be seen from eq. (2.69), the first term $\mathcal{A}_{n,0}$ contains the MHV gluon amplitude, that is the scattering of n gluons where all but two gluons have positive helicity. Similarly, the term $\mathcal{A}_{n,k}$ corresponds to the N^kMHV configuration with $k+2$ negative and $n - k - 2$ positive helicity gluons.

Discrete symmetries

Before we conclude this section, let us briefly comment on discrete symmetries of the amplitude. Due to the cyclicity of the trace, any color-ordered gauge theory amplitude is invariant under cyclic permutations acting on the particle index as $i \to i+1$,[3] as can be seen eg. for the n gluon amplitude in eq. (2.68). Since all fields of (planar) $\mathcal{N}=4$ SYM transform in the adjoint representation of the color group, the superamplitude $\mathcal{A}_n$ is invariant under these cyclic shifts as well. Furthermore, it can be shown that the individual amplitudes that make up the superamplitude transform into each other under the reflections $i \to n+1-i$, see eg. [101, 102]. Taken together, these transformations generate the *dihedral group* D_n, which is a discrete symmetry group of order $2n$. Consequently, the superamplitude is invariant under this *dihedral symmetry*.

Furthermore, while the entire superamplitude is invariant under spacetime *parity transformations* $x_\mu \to -x_\mu$ with the Lorentz index $\mu = 1, \dots, 3$ ranging over the spatial dimensions, the helicity degree k is mapped to $n-4-k$. Consequently, only few individual amplitudes such as $\mathcal{A}_{6,1}$ or $\mathcal{A}_{8,2}$ are parity invariant by themselves. On the other hand, this allows to only compute amplitudes of helicity degree $k \leq \lfloor (n-4)/2 \rfloor$, since the remaining helicity configurations can be obtained via parity transformation.

2.3.3. Kinematic space

Having organised the amplitude in terms of color and helicity, we turn to its kinematic dependence in this section. In general, we consider the scattering of n ordered massless particles with momenta p_i for $i = 1, \dots, n$. Consequently, the amplitudes are functions of these external on-shell momenta. However, due to the on-shell condition $p_i^2 = 0$, these momenta only have three degrees of freedom. Furthermore, momentum conservation as well as the action of other symmetries make the parameterisation of the kinematics in terms of the momenta p_i less optimal. For this reason, we review more suitable parameterisations and discuss the space of kinematics of n particle scattering in planar $\mathcal{N}=4$ super Yang-Mills theory.

Before we begin with the discussion, let us briefly discuss the complexification of Minkowski space. It is obtained by allowing spacetime coordinates and momenta to assume complex values, that is by analytically continuing the functions depending on them. The complexification allows to better understand eg. amplitudes by studying their analytic properties as functions of complex variables. To obtain the physical quantities, we have to later impose reality conditions that select the real slice of the complex space that corresponds to the original real spacetime. In the remainder of this thesis, we will usually assume the momenta to have complex values and not consider the reality conditions.

Spinor-helicity variables

Let us first consider the on-shell condition, which is given by $p_i^2 = 0$ for all massless particles $i = 1, \dots, n$. One approach to trivialise this constraint is to pass to the so-called *spinor-helicity variables*. Originally, they have been introduced for the calculation of QED

[3] As always, the particle indices are understood modulo n, that is we identify $i+n \sim i$.

and QCD amplitudes [103–105] and often allow for much simpler analytic expressions of massless scattering amplitudes, see also the review in [106]. The helicity spinors are constructed by first projecting the momenta with the Pauli matrices $\sigma^{\mu}_{\alpha\dot{\beta}} = (\mathbf{1}, \boldsymbol{\sigma})$ to obtain

$$(p_i)_{\alpha\dot{\beta}} := (p_i)_\mu \sigma^{\mu}_{\alpha\dot{\beta}} = \begin{pmatrix} p_0 + p_3 & p_1 - ip_2 \\ p_1 + ip_2 & p_0 - p_3 \end{pmatrix} . \tag{2.71}$$

In terms of this matrix, the on-shell condition reduces to $\det((p_i)_{\alpha\dot{\beta}}) = (p_i)_\mu (p_i)^\mu = 0$. Consequently, the matrix is of rank at most 1 and can be decomposed into a row times a column vector. We thus write

$$(p_i)_{\alpha\dot{\beta}} = (\lambda_i)_\alpha (\tilde{\lambda}_i)_{\dot{\beta}} , \tag{2.72}$$

whereas the *helicity spinors* $\lambda_i, \tilde{\lambda}_i$ are Weyl spinors transforming in the $(0, 1/2)$ and $(1/2, 0)$ representations of the Lorentz group, respectively. This equation defines the helicity spinors only up to the rescaling

$$\left(\lambda, \tilde{\lambda}\right) \sim \left(t\lambda, t^{-1}\tilde{\lambda}\right) , \tag{2.73}$$

for any $t \in \mathbb{C}^*$, which corresponds to little group transformations which in the case of massless momenta is given by the two-dimensional Euclidean group. To construct Lorentz invariant quantities, we contract the helicity spinors with the fully antisymmetric tensors $\epsilon^{\alpha\beta}$ and $\epsilon^{\dot{\alpha}\dot{\beta}}$ and introduce the *spinor brackets* as

$$\langle ij \rangle \equiv \langle \lambda_i \lambda_j \rangle := \epsilon^{\alpha\beta} (\lambda_i)_\alpha (\lambda_j)_\beta , \tag{2.74}$$

$$[ij] \equiv [\tilde{\lambda}_i \tilde{\lambda}_j] := \epsilon^{\dot{\alpha}\dot{\beta}} (\tilde{\lambda}_i)_{\dot{\alpha}} (\tilde{\lambda}_j)_{\dot{\beta}} . \tag{2.75}$$

Note that we use the fully antisymmetric tensors to lower and raise the spinor indices, such that eg. the first equation could also be written as $(\lambda_i)_\alpha (\lambda_j)^\alpha$.

Remarkably, the spinor helicity variables allow for much simplified expressions for massless scattering amplitudes. Consider for example the scattering of n massless gluons. The tree-level MHV amplitude is given by the Parke-Taylor factor [13]

$$A_n^{\text{MHV}}\left(1^+, \ldots, i^-, \ldots, j^-, \ldots, n^+\right) = \delta^{(4)}\left(\sum_{i=1}^{n} \lambda_{i\alpha} \tilde{\lambda}_{i\dot{\alpha}}\right) \frac{\langle ij \rangle^4}{\langle 12 \rangle \langle 23 \rangle \cdots \langle n1 \rangle} , \tag{2.76}$$

whereas the delta function enforces momentum conservation, as can be seen from eq. (2.72).

Dual variables and dual conformal symmetry

Similar to how the spinor-helicity variables trivialise the on-shell condition, we can alternatively choose a parameterisation that trivialises momentum conservation. We begin by considering the scattering of n ordered massless particles with momenta p_i, for which the momentum conservation is given by

$$\sum_{i=1}^{n} p_i = 0 . \tag{2.77}$$

This constraint is automatically satisfied when passing to the dual variables x_i for $i = 1, \ldots, n$, which are, similar to the planar variables introduced in sec. 2.2, defined as

$$x_i - x_{i+1} = p_i \,, \tag{2.78}$$

whereas the indices are understood to be cyclic, that is $i+n \sim i$. Instead of parameterising the amplitudes in terms of the momenta p_i, the kinematics can alternatively be described in terms of the dual variables x_i. Since the massless on-shell condition implies that $(x_i - x_{i+1})^2 = 0$, the dual variables are the vertices of a light-like polygon, as depicted in fig. 2.4. Finally, they are related to the generalised Mandelstam invariants via

$$s_{i,i+1,\ldots,j-1} = (p_i + p_{i+1} + \cdots + p_{j-1})^2 = x_{ij}^2 \,, \tag{2.79}$$

whereas we have introduced the shorthand notation $x_{ij}^2 = (x_i - x_j)^2$.

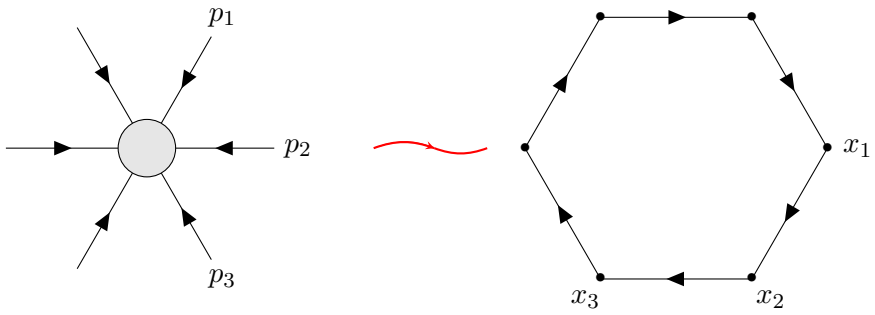

Figure 2.4: A depiction of the kinematics of the amplitude in terms of the momenta $p_1, \ldots, p_n$ on the left as well as the dual variables $x_1, \ldots, x_n$ on the right.

While the dual variables have the advantage of implicitly solving the momentum conservation constraint, such that it does no longer have to be enforced explicitly, they also make the *dual conformal symmetry* of the theory manifest. This symmetry, which does not appear on the level of the Lagrangian, is essentially given by the conformal symmetry group $\mathrm{SO}(2,4) \simeq \mathrm{SU}(2,2)$ acting on the dual variables x_i. It was first discovered in the setting of the Wilson loop / amplitude equivalence [107], which is naturally understood when considering the kinematics in terms of the light-like polygon defined by the dual variables, as well as in perturbative calculations of four and five gluon scattering [39, 40, 108]. Furthermore, in [109] it was extended to a dual superconformal symmetry of the entire superamplitude, and has been proven to hold for all tree-level amplitudes [110], whereas it is broken by infrared divergences in loop amplitudes, see also the review in [111].

The dual conformal symmetry group $\mathrm{SU}(2,2)$ can be obtained from the Poincaré group by adding the discrete conformal inversion transformation. First contracting the dual variables with the Pauli matrices to obtain $(x_i)_{\alpha\dot{\beta}} = (x_i)_\mu \sigma^\mu_{\alpha\dot{\beta}}$, they transform under conformal inversion as

$$I\left[(x_i)_{\alpha\dot{\beta}}\right] = \frac{(x_i)_{\beta\dot{\alpha}}}{x_i^2} \,. \tag{2.80}$$

Furthermore, it can be shown that the distances x_{ij}^2, which are invariant under transformations of the Poincaré group, transform covariantly under conformal inversion as [109]

$$I\left[x_{ij}^2\right] = \frac{x_{ij}^2}{x_i^2 x_j^2}\,. \tag{2.81}$$

Consequently, a natural choice for dual conformally invariant quantities, which can be used to parameterise the kinematics of n particle scattering, is given by the *conformal cross ratios* defined as

$$u_{ij} = \frac{x_{i,j+1}^2 x_{i+1,j}^2}{x_{ij}^2 x_{i+1,j+1}^2}\,. \tag{2.82}$$

Out of these $n(n-5)/2$ distinct cross ratios, one can choose an algebraically independent subset and express the remaining variables in terms of the independent ones with the help of Gram determinants.

Momentum twistors

We have seen that the dual variables trivialise the momentum conservation condition and make the dual conformal symmetry of the theory manifest. In this way, a dual conformally invariant combination of dual variables, such as the cross ratios, eq. (2.82), could be used to parameterise the kinematics of n particle scattering. Alternatively, the amplitude could be parameterised in terms of the helicity spinors, eq. (2.72), which trivially satisfy the on-shell condition $p_i^2 = 0$. It turns out that by using the so-called *momentum twistors* [44], we can trivialise both of these constraints simultaneously, see also the review in [112].

In standard twistor theory introduced by Penrose [113], null rays in spacetime are connected to an auxiliary complex space, the twistor space, and vice versa. Similarly, we start the construction of momentum twistors by defining another set of Weyl spinors via the *incidence relation*

$$(\mu_i)_{\dot\alpha} = (x_i)_{\beta\dot\alpha}(\lambda_i)^\beta\,, \tag{2.83}$$

whereas $(x_i)_{\alpha\dot\beta}$ is the projection of the dual variable x_i with the Pauli matrices.

Next, we define the momentum twistors $Z_i = (\lambda_i, \mu_i)$ for $i = 1, \ldots, n$. Since the helicity spinors are defined only up to a rescaling, so are the momentum twistors, that is

$$Z_i \sim t \cdot Z_i\,, \tag{2.84}$$

for any $t \in \mathbb{C}^*$. Consequently, momentum twistors can also be considered as vectors of the complex projective space $\mathbb{CP}^3$.

To understand the relation of momentum twistors to spacetime, first note that by contracting eq. (2.72) with $(\lambda_i)^\alpha$ and observing that $(p_i)_{\alpha\dot\alpha}(\lambda_i)^\alpha = \epsilon^{\alpha\beta}(\lambda_i)_\alpha(\lambda_i)_\beta(\tilde\lambda_i)_{\dot\alpha} = 0$ we can also write the incidence relation, eq. (2.83), as

$$(\mu_i)_{\dot\beta} = (x_i)_{\alpha\dot\beta}(\lambda_i)^\alpha = (x_{i+1})_{\alpha\dot\beta}(\lambda_i)^\alpha\,. \tag{2.85}$$

For this reason, x_i and x_{i+1} are called incident to Z_i and are both required to define the momentum twistor. Consequently, the momentum twistor Z_i can be associated to the null

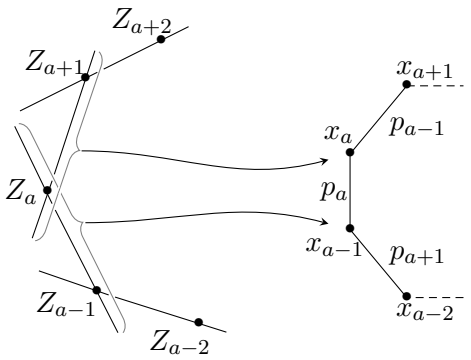

Figure 2.5: Illustration of the relation of the momentum twistors $Z_1, \ldots, Z_n$, the dual variables $x_1, \ldots, x_n$, and the momenta $p_1, \ldots, p_n$.

line separating x_i and x_{i+1}, or equivalently the null momentum p_i, whereas the line between Z_i and Z_{i-1} can be associated to the point x_i, see also fig. 2.5. The inverted relation can be checked to be

$$(x_i)_{\alpha\dot{\beta}} = \frac{(\lambda_{i-1})_\alpha(\mu_i)_{\dot{\beta}} - (\lambda_i)_\alpha(\mu_{i-1})_{\dot{\beta}}}{\langle\lambda_{i-1}\lambda_i\rangle} \,. \tag{2.86}$$

Using this relation between the dual variables x_i and the momentum twistors $Z_i = (\lambda_i, \mu_i)$, which originally were parameterised in terms of x_i, x_{i+1} and λ_i via eq. (2.85), we can instead parameterise the kinematics of n particle scattering in terms of the Z_i. Consequently, since the momenta parameterised in terms of the dual variables x_i trivially satisfy momentum conservation, they also will when parameterised in terms of momentum twistors via the relation (2.86).

In the previous section we have seen that dual conformal symmetry naturally acts on the dual variables x_i via the conformal group $\mathrm{SU}(2,2)$. The only non-trivial transformation of this group is the conformal inversion, whose action on the dual variables is given by eq. (2.80). Similarly, in [109] its action on the helicity spinors λ_i was formulated as[4]

$$I\left[(\lambda_i)^\alpha\right] = (x_i)^{\dot{\alpha}\beta}(\lambda_i)_\beta \,. \tag{2.87}$$

Noting that by construction we have $(x_i)_{\alpha\dot{\beta}}(x_i)^{\dot{\beta}\gamma} = x_i^2\delta_\alpha^\gamma$, we can use eqs. (2.87), (2.80) and (2.83) to show that the components of the momentum twistor $Z_i = ((\lambda_i)^\alpha, (\mu_i)_{\dot{\alpha}})$ transform linearly under conformal inversion as

$$I\left[(\lambda_i)^\alpha\right] = (\mu_i)^{\dot{\alpha}} \,, \quad I\left[(\mu_i)_{\dot{\alpha}}\right] = (\lambda_i)_\alpha \,. \tag{2.88}$$

With the remaining (ie. Lorentz) transformations of the conformal group $\mathrm{SU}(2,2)$ being straightforward, this demonstrates that the dual conformal symmetry takes a particularly simple, that is linear form when acting on the momentum twistors. As is discussed in eg. [115–117], this shows that the momentum twistors transform in the fundamental representation of $\mathrm{SU}(2,2)$.

[4]Note that compared to [109], we have chosen a different conformal weight factor for λ_i, as was also done for example in [114].

As discussed at the beginning of this section, it is usually beneficial to work with complexified momenta. The complexification of the conformal group is given by $\mathrm{SL}(4,\mathbb{C})$ of which $\mathrm{SU}(2,2)$ is the real form that corresponds to the $(+,-,-,-)$-signature of ordinary spacetime, see eg. the discussion in [118]. By the same argument as above, the momentum twistors transform in the fundamental representation of the complexified conformal group. Consequently, we can construct the basic $\mathrm{SL}(4,\mathbb{C})$-invariants as

$$\langle ijkl\rangle = \epsilon_{ABCD} Z_i^A Z_j^B Z_k^C Z_l^D \equiv \det\left(Z_i Z_j Z_k Z_l\right) , \tag{2.89}$$

whereas A denotes the $\mathrm{SL}(4,\mathbb{C})$ index of the momentum twistor Z_i. Note that this bracket vanishes whenever at least two of the indices are identical, since the corresponding matrix is singular such that the determinant vanishes.

Using these four-brackets, we can write the Mandelstam invariants $s_{i,i+1,\dots,j-1}$ or equivalently the Lorentz invariant separation x_{ij}^2 of the points x_i and x_j in terms of the momentum twistors as

$$x_{ij}^2 = \frac{\langle i-1\, i\, j-1\, j\rangle}{\langle \lambda_{i-1}\lambda_i\rangle \langle \lambda_{j-1}\lambda_j\rangle} , \tag{2.90}$$

as can be seen by using eq. (2.86) to compute $x_{ij}^2 \equiv (x_i - x_j)_{\alpha\dot\beta}(x_i - x_j)^{\dot\beta\alpha}$. With this result, it is straightforward to see that the dual variables x_i parameterised in terms of momentum twistors via eq. (2.86) satisfy

$$x_{i,i+1}^2 = 0 , \tag{2.91}$$

implying that the on-shell condition $p_i^2 = x_{i,i+1}^2 = 0$ is trivially satisified!

In fact, the four-bracket map defined by eq. (2.89) is not well-defined due to the projective nature of the momentum twistors.[5] However, we can immediately see that the dual conformally invariant cross ratios of eq. (2.82) can be written entirely in terms of the four-brackets as

$$u_{ij} = \frac{\langle i-1\, i\, j\, j+1\rangle \langle i\, i+1\, j-1\, j\rangle}{\langle i-1\, i\, j-1\, j\rangle \langle i\, i+1\, j\, j+1\rangle} , \tag{2.92}$$

and are thus well-defined invariants under the action of $\mathrm{SL}(4,\mathbb{C})$, since each momentum twistor Z_i appears with the same multiplicity in both the numerator and denominator.

Finally, let us remark that strictly speaking we would also have to consider the fermionic parameters η^A of which the superamplitude $\mathcal{A}_n$ also is a function. In fact, the previous constructions of the dual variables x_i as well as the momentum twistors Z_i do have a fermionic analogue and the kinematics of the superamplitude can be described in terms of the momentum twistors Z_i as well as the momentum supertwistors $\mathcal{Z}_i$. For our purposes, however, it is sufficient to only consider the bosonic variables.

[5] In the same vein, scalar transformations with unit determinant, denoted as $\mathrm{SZ}(4,\mathbb{C}) \subset \mathrm{SL}(4,\mathbb{C})$ and identified with the roots of unity, act trivially on the momentum twistors, mapping an equivalency class of vectors $Z \sim t\cdot Z$ to itself. For that reason, the complexified conformal group is strictly speaking given by the induced action of $\mathrm{SL}(4,\mathbb{C})$ on the projective space $\mathbb{CP}^3$, or explicitly by the complex projective special linear group $\mathrm{PSL}(4,\mathbb{C}) = \mathrm{SL}(4,\mathbb{C})/\mathrm{SZ}(4,\mathbb{C})$. Note that in this case, we can identify $\mathrm{PSL}(4,\mathbb{C}) \simeq \mathrm{PGL}(4,\mathbb{C}) = \mathrm{GL}(4,\mathbb{C})/\mathrm{Z}(4,\mathbb{C})$, with $\mathrm{Z}(4,\mathbb{C})$ being scalar transformations on $\mathbb{C}^4$ identified with the non-zero complex numbers, since roughly speaking we can take the modulus of the scalar transformation to normalize the determinant of the $\mathrm{GL}(4,\mathbb{C})$ transformation, leaving only the roots of unity in the quotient. For simplicity, we will nonetheless continue the discussion in terms of $\mathrm{SL}(4,\mathbb{C})$.

Kinematic space of momentum twistors

Having seen that momentum twistors $Z_1, \ldots, Z_n \in \mathbb{CP}^3$ trivially satisfy the momentum conservation as well as massless on-shell constraints and hence are unconstrained variables themselves, they are very well suited to be used as variables to parameterise the kinematics of n particle scattering amplitudes in planar $\mathcal{N}=4$ super Yang-Mills theory. Consequently, the space of all such kinematic configurations, or *kinematic space*, is the configuration space $\mathrm{Conf}_n\left(\mathbb{P}^3\right)$, the space of n ordered points in $\mathbb{CP}^3$ up to the action of $\mathrm{SL}(4,\mathbb{C})$, and is of dimension $3n-15$. Note that these points are ordered since the association of momentum twistors and dual variables relies on an ordering of the variables.

This kinematic space is closely related to the *Grassmannian* $\mathrm{Gr}(k,n)$, which can be defined as the space of k-dimensional planes passing through the origin inside an n-dimensional space. Since a k-plane can be specified by a basis of k vectors that span it, $\mathrm{Gr}(k,n)$ may be equivalently described as the space of $k\times n$ matrices, modulo $\mathrm{GL}(k)$ transformations that correspond to a change of basis. On the other hand, an element of the configuration space is given by n momentum twistors up to the action of $\mathrm{SL}(4,\mathbb{C})$. These n twistors, considered as vectors of $\mathbb{C}^4$, form a $4\times n$ matrix up to the action of $\mathrm{SL}(4,\mathbb{C}) \simeq \mathrm{GL}(4,\mathbb{C})/\mathbb{C}^*$ as well as independent rescaling of the n columns, that is the action of $(\mathbb{C}^*)^n$. Equivalently, the quotient by the diagonal component $\mathbb{C}^*_{\mathrm{diag}} \subset (\mathbb{C}^*)^n$ can be taken care of by taking the quotient with $\mathrm{GL}(4,\mathbb{C})$ instead of $\mathrm{SL}(4,\mathbb{C})$. This roughly sketched argument can be made precise and it can be shown that there exists an isomorphism [118]

$$\mathrm{Conf}_n\left(\mathbb{P}^3\right) \simeq \mathrm{Gr}(4,n)/\left(\mathbb{C}^*\right)^{n-1} =: \widetilde{\mathrm{Gr}}(4,n)\,, \tag{2.93}$$

whereas we have introduced the notation $\widetilde{\mathrm{Gr}}(4,n)$ for the kinematic space. In this picture, the four-brackets defined for momentum-twistors in eq. (2.89), are the minors of the matrix spanned by the Z_i. These are also known as the *Plücker variables* $p_{i_1\ldots i_k}$ of the Grassmannian, which are defined as the determinants made out of the columns $i_1,\ldots,i_k$ of the aforementioned $k\times n$ matrix. If we restrict the Plücker variables $p_{i_1\ldots i_k}$ for all ordered sequence $1\le i_1<\cdots<i_k\le n$ to real, positive values, we obtain the positive region of the Grassmannian. The *totally positive configuration space*, denoted by $\widetilde{\mathrm{Gr}}_+(k,n)$, is defined in a similar way.

For our purposes, a formulation of $\mathrm{Gr}(k,n)$ as the variety attached to a polynomial ideal will be more convenient. We thus consider the ring $\mathbb{Z}[p]$ of integer coefficient polynomials in the Plücker variables $p_{i_1\ldots i_k}$ for $1\le i_1<\cdots<i_k\le n$. From here on we denote the number of distinct Plücker variables of $\mathrm{Gr}(k,n)$ as

$$D = \binom{n}{k}\,. \tag{2.94}$$

Due to their nature as determinants, which are not all independent, Plücker variables will thus obey algebraic relations known as the Plücker relations. For any two ordered sequences $1\le i_1<i_2<\cdots<i_{k-1}\le n$ and $1\le j_1<\cdots<j_{k+1}\le n$ they are given by

$$\sum_{r=1}^{k+1}(-1)^r p_{i_1\ldots i_{k-1}j_r} p_{j_1\ldots\hat{j}_r\ldots j_{k+1}} = 0\,, \tag{2.95}$$

where $j_1, \ldots, \hat{j}_r, \ldots j_{k+1}$ denotes the sequence $j_1, \ldots, j_{k+1}$ with the term j_l omitted. These homogeneous polynomials form the Plücker ideal $I_{k,n}$ in $\mathbb{Z}[p]$. The projective variety of this ideal, that is the set of zeros of these polynomials quotiented by global rescalings of the Plücker variables, $p_{i_1 \ldots i_k} \to t \cdot p_{i_1 \ldots i_k}$ with $t \in \mathbb{C}^*$, can be identified with the Grassmannian $\mathrm{Gr}(k,n)$. The dimension of this space is $k(n-k)$.

Note that the Plücker relations are not only invariant under global rescaling but also under the local scaling

$$p_{i_1 \ldots i_k} \to t_{i_1} \ldots t_{i_k} p_{i_1 \ldots i_k} \,, \text{ for } t_1, \ldots, t_n \in \mathbb{C}^* \,. \tag{2.96}$$

If we further quotient the Grassmannian by this local scaling, we obtain the generalisation of the above configuration space as

$$\widetilde{\mathrm{Gr}}(k,n) \equiv \mathrm{Gr}(k,n) / (\mathbb{C}^*)^{n-1} = \mathrm{Conf}_n\left(\mathbb{P}^{k-1}\right) \,, \tag{2.97}$$

which is of dimension

$$d = (k-1)(n-k-1) \,. \tag{2.98}$$

To summarise, in this section we have reviewed different parameterisations of n particle scattering amplitudes in planar $\mathcal{N}=4$ super Yang-Mills theory. Since the external momenta $p_1, \ldots, p_n$ are constrained by momentum conservation and on-shell conditions, they are not the ideal variables. Instead, we have seen that momentum twistors $Z_1, \ldots, Z_n$ trivially satisfy all these constraints and are hence used to parameterise the kinematics. Consequently, the space of all kinematic configurations is described by the configuration space of n ordered points in $\mathbb{CP}^3$, which is equivalently described by the Grassmannian $\mathrm{Gr}(4,n)$ quotiened by the torus action $(\mathbb{C}^*)^{n-1}$. In later sections, see chapters 3 and 4, we will see that parameterising the kinematics in terms of this space allows to use some of its intricate properties in order to compute scattering amplitudes.

2.3.4. Loop amplitudes in planar $\mathcal{N}=4$ super Yang-Mills theory

In the previous sections we have seen that the kinematics of the n-particle color-ordered superamplitude $\mathcal{A}_n$ can be described in terms of momentum twistors such that the space of kinmeatics is the quotient of the Grassmannian $\mathrm{Gr}(4,n)$ by the torus action $(\mathbb{C}^*)^{n-1}$. These variables have the advantage that they are unconstrained since on-shell conditions and momentum conservation are trivially satisfied. Furthermore, these variables made the hidden dual conformal symmetry of the theory manifest.

This symmetry, however, is broken by infrared divergences, which essentially arise at the cusps of the null polygon in the dual space depicted in fig. 2.4. These infrared divergences result from loop corrections to the amplitude and require regularisation. One common procedure for this is *dimensional regularisation* where the amplitudes are computed in $D = 4 - 2\epsilon$ dimensions and then expanded into a power series in ϵ.

In fact, as we will review now, we can factor out a universal infrared-divergent part of the amplitude leaving a finite, normalized factor to focus on. As is the case for different renormalisation schemes in any gauge theory, this normalisation is not unique since one can always add certain finite terms to the normalisation factor. One well-established choice for

the normalisation of amplitudes of planar $\mathcal{N}=4$ SYM is the *BDS ansatz*. In [25], Bern, Dixon, and Smirnov conjectured an ansatz for planar MHV n-particle amplitudes as[6]

$$\mathcal{A}_n^{\text{BDS}} \equiv \frac{\mathcal{A}_n^{\text{MHV}}}{\mathcal{A}_n^{(0)}} = \exp\left[\sum_{L=1}^{\infty} g^{2L}\left(\frac{f^{(L)}(\epsilon)}{2}A_n^{(1)}(L\epsilon) + C^{(L)}\right)\right] . \tag{2.99}$$

In this ansatz, $g^2 = \lambda/16\pi^2$ is the 't Hooft coupling, $A_n^{(1)}$ is the one-loop MHV gluon amplitude first computed in [19], $\mathcal{A}_n^{(0)}$ the tree-level contribution, $C^{(L)}$ are transcendental constants, and $f^{(L)}$ corresponds to the $\mathcal{O}(g^{2L})$ term of the Taylor series expansion around $g=0$ of the function $f(\epsilon) = \frac{1}{2}\Gamma_{\text{cusp}} + \mathcal{O}(\epsilon)$, with Γ_{cusp} the planar cusp anomalous dimension,

$$\frac{1}{4}\Gamma_{\text{cusp}} = g^2 - 2\zeta_2 g^4 + \mathcal{O}(g^6) , \tag{2.100}$$

which is known to all loop orders [120].

While the BDS ansatz was verified to hold for $n=4$ particles with up to five loops [121–123] and $n=5$ particles with up to three loops [25, 124, 125], it requires a finite correction starting at $n=6$ particles [126, 127]. Consequently, the planar MHV amplitude for $n>5$ particles is given by

$$\mathcal{A}_n^{\text{MHV}} = \mathcal{A}_n^{(0)}\mathcal{A}_n^{\text{BDS}}\exp\left(R_n\right) , \tag{2.101}$$

whereas the *remainder function* R_n is finite and dual conformally invariant, see eg. [39]. The latter property implies that it depends on the $3(n-5)$ algebraically independent dual conformally invariant cross ratios, which do not exist for $n \leq 5$.

The BDS ansatz of eq. (2.101) nicely captures the infrared divergences of the MHV amplitude $\mathcal{A}_n^{\text{MHV}}$ in terms of the divergences of the one-loop MHV gluon amplitude $A_n^{(1)}$. As is described eg. in [111], the IR divergence is in fact universal for any N^kMHV amplitude, such that we can use the factor $\mathcal{A}_n^{\text{BDS}}$ defined by eq. (2.101) to normalise the amplitude and factor out the divergent part for any k.

However, this one-loop amplitude also depends on three-particle Mandelstam invariants s_{ijk} causing the BDS ansatz as well as the remainder function to not obey the *Steinmann relations* separately, even though their product, that is the entire amplitude, does. The Steinmann relations [128–130] place constraints on consecutive discontinuities of the amplitude, with the generalisation to multiple discontinuities being referred to as extended Steinmann relations [53]. For loop amplitudes, these conditions are given by

$$\text{Disc}_{s_{j,j+1,j+2}}\left(\text{Disc}_{s_{i,i+1,i+2}} A\right) = 0 , \quad \text{for } j = i \pm 1, i \pm 2 . \tag{2.102}$$

Since the Steinmann conditions allow for a powerful analytic bootstrap programme, see eg. [51, 56] or the review [33], it is highly beneficial to use the remaining freedom in the normalisation in a way that the individual parts obey these constraints. Whenever n is not a multiple of 4, this can be achieved with the *BDS-like ansatz*. As first considered

[6] Note that our conventions differ from the original formulation, as we eg. chose a different coupling constant, and are the same as those used in [119].

at strong coupling in [26, 27], there exists a unique infrared finite and dual conformally invariant function Y_n such that the modified ansatz given by

$$\mathcal{A}_n^{\text{BDS-like}} = \mathcal{A}_n^{\text{BDS}} \exp\left(\frac{\Gamma_{\text{cusp}}}{4} Y_n\right) \tag{2.103}$$

only depends on the two-particle Mandelstam invariants such that both, the normalisation factor $\mathcal{A}_n^{\text{BDS-like}}$ as well as the normalised amplitude, obey the Steinmann conditions. Using this ansatz, we define the normalised amplitude $\mathcal{E}_n$ as

$$\mathcal{E}_n := \frac{\mathcal{A}_n}{\mathcal{A}_n^{(0)} \mathcal{A}_n^{\text{BDS-like}}} \,. \tag{2.104}$$

The BDS-like normalised amplitude is a function of the momentum twistors Z_i (and supertwistors $\mathcal{Z}_i$) only and can, like the superamplitude in eq. (2.70), be expanded by its degree in the fermionic variables as

$$\mathcal{E}_n = \mathcal{E}_{n,0} + \mathcal{E}_{n,1} + \cdots + \mathcal{E}_{n,n-4} \,, \tag{2.105}$$

whereas again $\mathcal{E}_{n,k}$ corresponds to the N^kMHV helicity configuration. Using eq. (2.101), it is easy to see that the BDS-like normalised MHV amplitude is given by

$$\mathcal{E}_n^{\text{MHV}} \equiv \mathcal{E}_{n,0} = \exp\left(R_n - \frac{\Gamma_{\text{cusp}}}{4} Y_n\right) \,, \tag{2.106}$$

in terms of the finite remainder function R_n.

2.3.5. Symbol bootstrap

To summarize, we have started this section with a review of $\mathcal{N} = 4$ super Yang-Mills theory and its planar limit. After collecting the entire on-shell particle content of the theory in an on-shell superfield, we have constructed the superamplitude that describes the simultaneous scattering of all on-shell states. Decomposing this in terms of the different ways to attach color to the external particles and splitting of the generators of the color group, we are left with the color-ordered superamplitude of n particles $\mathcal{A}_n$. This amplitude can be expanded by N^kMHV degree in terms of $\mathcal{A}_{n,k}$ for $k = 0, \ldots, n-4$, corresponding to the helicity configuration where all but $k+2$ particles have positive helicity.

The amplitude $\mathcal{A}_{n,k}$ still depends on the kinematic data of the scattering process. As we have reviewed, symmetries such as the dual conformal symmetry and constraints such as momentum conservation cause the momenta $p_1, \ldots, p_n$ to be constrained variables. Instead, it is beneficial to parameterise the kinematic setup in terms of the momentum twistors $Z_1, \ldots, Z_n \in \mathbb{CP}^3$, which transform in the fundamental representation of $\text{SL}(4, \mathbb{C})$, corresponding to the action of dual conformal symmetry. Consequently, the kinematic variables are chosen to be the $\text{SL}(4, \mathbb{C})$-invariants $\langle ijkl \rangle$, the Plücker variables, or strictly speaking projectively invariant ratios thereof. It can be shown that therefore, the space of kinematics is the configuration space of n points in $\mathbb{CP}^3$, which has dimension $3n - 15$.

Finally, we have discussed that we can choose a universal IR divergent factor to normalise the amplitude, such that we are left with a finite, renormalized quantity. Using the so-called BDS-like ansatz, we have defined the normalised amplitude $\mathcal{E}_{n,k}$ in eqs. (2.104) and (2.105).

Remarkably, while more complicated functions are certainly known to appear in generic quantum field theories at two loops [131] and beyond, explicit calculations as well as general arguments on the level of the integrand, see eg. [132], suggest that the functions which describe the BDS-like normalised MHV and NMHV amplitudes are restricted to the class of multiple polylogarithms.[7] More precisely, it is conjectured that the function of the L-loop MHV or NMHV amplitude of n particles is given by a MPL of weight $2L$.

Based on this conjecture, we can consequently employ the mathematical structure of the multiple polylogarithms and compute the symbol of the amplitude as the symbol of its function. Since the symbol describes the analytic structure of the function, it is closely related to the physical information encoded in the amplitude, as it eg. diverges whenever a particle goes on-shell. Whereas in theory the alphabet of the amplitude, that is the collection of all letters appearing in the symbol, can be calculated via Feynman diagrams [35, 36] or symmetry-related computations [133, 134], these explicit methods become unwieldy very quickly with increasing loop number.

In fact, we can turn this principle around and make use of a powerful boostrap programme, as has been similarly done in the past in the analytic S-matrix bootstrap [14]. Without ever resorting to Feynman diagrams or other explicit calculations, we can instead start with the knowledge of the analytic structure of the amplitude as encoded by its symbol. Given a candidate or conjecture for the alphabet, we can construct the space of all possible weight-$2L$ symbols, that is the space of all $2L$-fold tensor products over the alphabet.[8] Using physical constraints, such as the Steinmann relations of eq. (2.102), which on the level of the symbol are constraints on the appearance of consecutive pairs of letters, constraints on which letters can appear in the first [135] or last [56, 133] entry of the symbol, or certain kinematic limits [136–155], one can reduce the space of all symbols and uniquely fix the symbol of the amplitude.

A key insight for this boostrap programme is the observation that the letters of n-particle scattering are cluster $\mathcal{A}$-variables of the *cluster algebra* associated to the Grassmannian $\mathrm{Gr}(4, n)$ [37], following the emergence of these structures at the level of the integrand [23, 38]. In cluster algebras, see section 3 or [156–159] for more details, the $\mathcal{A}$-variables are organized in overlapping sets, the *clusters*, which are connected by an operation called *mutation*. Starting from an initial cluster, the cluster algebra and thus all of its $\mathcal{A}$-variables are constructed by performing all possible mutations. In this way, the cluster algebra allows to obtain the amplitude's symbol alphabet and thus ultimately its symbol.

This *cluster boostrap* programme has been successfully applied to the six-particle amplitude with up to seven loops [28, 45–53] (see also [54] for some more recent higher-loop results in its codimension-1 double-scaling limit) and for the seven-particle amplitude with up to four loops [55–58]. These specific applications of the cluster bootstrap will be reviewed in more detail in sections 3.2.2 and 3.2.3, respectively.

[7] However, see also [24] for certain subtleties.

[8] Since not every w-fold tensor product of letters actually is the symbol of a weight-w MPL, we have to impose the *integrability condition*, see remark 2.12.

3. Amplitudes from cluster algebras

We have concluded the previous chapter with the insight that the so-called *cluster algebras* are a crucial input for the symbol bootstrap programme. In particular, we briefly reviewed how the set of variables associated to the cluster algebra of the Grassmannian $\mathrm{Gr}(4,n)$ are conjectured to form the alphabet of n-particle scattering in planar $\mathcal{N}=4$ super Yang-Mills theory. For this reason, in the first part of this chapter we review the theory of cluster algebras and introduce their definition, basic properties and geometric descriptions. In the second part of this chapter, we apply the general theory of cluster algebras to $\mathcal{N}=4$ super Yang-Mills theory and review explicit results obtained for six- and seven-particle scattering.

3.1. Background

Before turning to the more elaborate mathematical theory of *cluster algebras with coefficients*, we begin this chapter with a gentle introduction into cluster algebras associated to the Grassmannians $\mathrm{Gr}(k,n)$, which are closely related to the space of kinematics of $\mathcal{N}=4$ pSYM amplitudes, see section 2.3.3. Beyond this relevance for the physical applications in this work, the Grassmannian cluster algebras also serve as a nice example to demonstrate the framework of unfrozen and frozen variables, as is commonly used in physics literature [118].

While this introduction will mostly be focused on exhibiting the main properties of cluster algebras by discussing some examples, we will exhibit a more rigorous review of cluster algebras in section 3.1.2. In there, the framework of so-called cluster algebras with coefficients is discussed. While completely equivalent to the description in terms of frozen and unfrozen variables, this language is much better suited for the discussion of infinite mutation sequences in chapter 5.

3.1.1. A gentle introduction

As was demonstrated in [160], the coordinate ring of the Grassmannian $\mathrm{Gr}(k,n)$ naturally carries the structure of a *cluster algebra* of rank $d=(k-1)(n-k-1)$. A cluster algebra of rank d, as first described in [156–159], consists of the so-called $\mathcal{A}$-variables – rational functions in d arguments – which are organised in overlapping sets of d variables, the *clusters*. Each cluster consists of d such variables $\boldsymbol{a}=(a_1,\ldots,a_d)$ as well as m frozen variables $\boldsymbol{a}^{(f)}=(a_{d+1},\ldots,a_{d+m})$. Note that the variables $a_1,\ldots,a_d$ are sometimes referred to as unfrozen variables.

Furthermore, to each cluster we associate an adjacency matrix B, a $(d+m)\times(d+m)$ antisymmetrisable matrix encoding the connection among the variables within the cluster, whose components are denoted by b_{ij}. If the adjacency matrix is antisymmetric, we can equivalently represent the cluster by a quiver – a directed graph with multiple arrows between vertices – where nodes correspond to cluster variables, and the absolute value

and sign of the entries of B corresponds to the number of arrows between nodes and their direction, respectively.[1] To be precise, the components b_{ij} of the adjacency matrix are related to the quiver via

$$b_{ij} = \#\,\text{arrows} \quad i \to j\,. \tag{3.1}$$

Note that frozen nodes are never connected to each other[2] and that due to the antisymmetric property of the adjacency matrix, such that $b_{ii} = 0$, the quiver does not contain 1-cycles. Finally, the full data of the cluster and thus the cluster itself is denoted by $(\boldsymbol{a}, \boldsymbol{a}^{(f)}, B)$.

Example 3.1 (Cluster of $\mathrm{Gr}(2,5)$)**.** Consider the cluster algebra of $\mathrm{Gr}(2,5)$, which is of rank $d = 2$ and contains $m = 5$ frozen variables. Its defining cluster contains the $\mathcal{A}$-variables

$$a_1 = \langle 13\rangle\,, \quad a_2 = \langle 14\rangle\,, \tag{3.2}$$

$$a_3 = \langle 12\rangle\,, \quad a_4 = \langle 23\rangle\,, \quad a_5 = \langle 34\rangle\,, \quad a_6 = \langle 45\rangle\,, \quad a_7 = \langle 15\rangle\,, \tag{3.3}$$

which are all Plücker variables. The 7×7 adjacency matrix of the cluster is given by

$$B = \begin{pmatrix} 0 & 1 & -1 & 1 & -1 & 0 & 0 \\ -1 & 0 & 0 & 0 & 1 & -1 & 1 \\ 1 & 0 & 0 & 0 & 0 & 0 & 0 \\ -1 & 0 & 0 & 0 & 0 & 0 & 0 \\ 1 & -1 & 0 & 0 & 0 & 0 & 0 \\ 0 & 1 & 0 & 0 & 0 & 0 & 0 \\ 0 & -1 & 0 & 0 & 0 & 0 & 0 \end{pmatrix}. \tag{3.4}$$

As one can immediately see, this adjacency matrix is antisymmetric, such that it can be represented by a quiver, which is depicted in fig. 3.1.

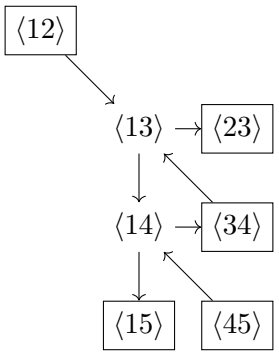

Figure 3.1: Quiver of the initial cluster of the cluster algebra of $\mathrm{Gr}(2,5)$. The nodes $\langle 13\rangle$ and $\langle 14\rangle$ correspond to the $\mathcal{A}$-variables of the cluster, which in this case are Plücker variables. The frozen variables are highlighted by the rectangles.

[1] Even if the adjacency matrix is not antisymmetric, it can be represented by a generalised quiver, so-called valued quivers, see also [161].

[2] For this reason, the information contained in the adjacency matrix can actually be expressed by a $(d+m) \times d$ antisymmetrisable matrix, since the $m \times m$ bottom right part of the $(d+m) \times (d+m)$ matrix B is trivially zero.

The clusters within the cluster algebra are related by a birational transformation, the *mutation* $\mu_j : (\boldsymbol{a}, \boldsymbol{a}^{(f)}, B) \mapsto (\boldsymbol{a}', \boldsymbol{a}^{(f)}, B')$ for $j = 1, \ldots, d$. In this way, mutating a cluster $(\boldsymbol{a}, \boldsymbol{a}^{(f)}, B)$ along the j-th variable, we obtain the new cluster $(\boldsymbol{a}', \boldsymbol{a}^{(f)}, B')$. The adjacency matrix B' is related to the previous adjacency matrix B by

$$b'_{il} = \begin{cases} -b_{il} & \text{for } i = j \text{ or } l = j \\ b_{il} + [-b_{ij}]_+ \, b_{jl} + b_{ij} \, [b_{jl}]_+ & \text{otherwise} \end{cases} , \tag{3.5}$$

whereas we use $[x]_+ = \max(0, x)$. Similarly, if the adjacency matrix is antisymmetric, we can equivalently describe a mutation rule for the associated quiver as

1. For each path $i \to j \to k$ add an arrow $i \to k$.
2. Delete 2-cycles, that is remove arrows if there exist the paths $i \to k$ and $k \to i$.
3. Reverse all arrows connected to node j.

When mutating a cluster at the variable a_j, this variable is replaced with a mutated version a'_j whereas the remaining cluster variables a_i for $i \neq j$ remain unchanged. The mutated variable is given by

$$a'_j = a_j^{-1} \left(\prod_{i=1}^{d+m} a_i^{[b_{ij}]_+} + \prod_{i=1}^{d+m} a_i^{[-b_{ij}]_+} \right) . \tag{3.6}$$

Note that the frozen variables are never mutated – hence their name – and consequently are the same for each cluster in the cluster algebra. Furthermore, it can easily be demonstrated that mutation is an involution, such that applying the same mutation twice results in the initial cluster.

Example 3.2 (Mutation in $\mathrm{Gr}(2,5)$)**.** Continuing our example from before, we can mutate the quiver of fig. 3.1 for example at the node of $a_2 = \langle 14 \rangle$. As described in general above, this results in another cluster $(\boldsymbol{a}', \boldsymbol{a}^{(f)}, B')$ with a mutated quiver and a new variable a'_2. The mutated quiver is depicted in fig. 3.2.

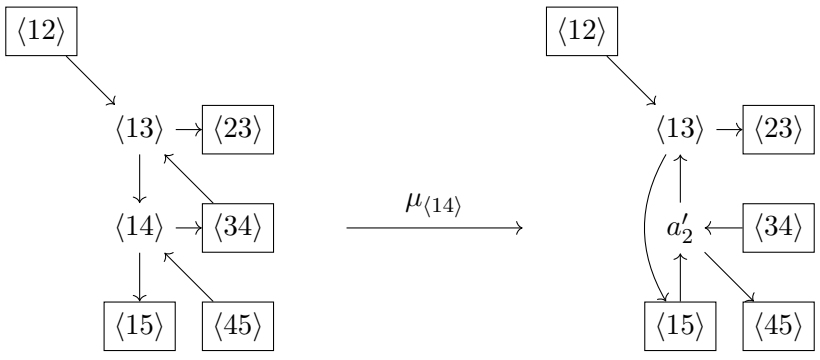

Figure 3.2: Mutation of the quiver on the left at the node of $a_2 = \langle 14 \rangle$. In the mutated quiver on the right, the mutation results in a new variable a'_2.

The mutated adjacency matrix can be read off from the mutated quiver on the right hand

side of fig. 3.2. Applying the mutation rule of eq. (3.6), we obtain the mutated cluster variable a' as

$$a_2' = \frac{\langle 13\rangle \langle 45\rangle + \langle 15\rangle \langle 34\rangle}{\langle 14\rangle} \,. \tag{3.7}$$

In general, a mutated cluster variable is a rational function of the variables of the cluster that is mutated. In this case, however, we can make use of the Plücker relations, see eg. 2.95, such as

$$\langle 13\rangle \langle 45\rangle - \langle 14\rangle \langle 35\rangle + \langle 15\rangle \langle 34\rangle = 0 \,, \tag{3.8}$$

to obtain the simplified expression

$$a_2' = \langle 35\rangle \ . \tag{3.9}$$

As we will see later on, we can often use the Plücker relations to simplify the cluster variables of Grassmannian cluster algebras to polynomials of some set of Plücker variables.

Using mutation, we can start at some cluster, the so-called *initial cluster* or *seed*, and perform all possible mutations to generate all clusters as well as the cluster algebra itself. For *finite cluster algebras*, which consist of a finite number of cluster $\mathcal{A}$-variables and clusters, this process terminates after a finite number of mutations, after which mutation only generates variables and clusters that we have already encountered. In contrast to this, *infinite cluster algebras* consist of an infinite number of $\mathcal{A}$-variables and clusters, so that we can always find a mutation that generates a new variable and/or cluster. Similarly, if a cluster algebra consists of finitely many inequivalent quivers, whereas quivers are considered equivalent if they are the same up to a relabelling of the vertices, it is said to be of *finite mutation type*. Note that all finite cluster algebras are also of finite mutation type.

The clusters within a cluster algebra can be arranged into an undirected graph, the *exchange graph* of the cluster algebra. The vertices of this graph are the clusters, which are connected by an edge if there exists a mutation relating the two clusters. By construction, the vertices of the exchange graph are d-valent, that is there are always exactly d edges attached to each vertex, since there is one mutation per $\mathcal{A}$-variable in the cluster.

As was shown in [157], the finite cluster algebras can be classified in terms of the Cartan-Killing classification of semisimple Lie algebras. If the *principal part* – the subquiver that consists of the vertices of the unfrozen $\mathcal{A}$-variables – of some cluster of a cluster algebra is equivalent to a Dynkin diagram, the cluster algebra is said to be of that Dynkin type and is finite.

Example 3.3 (A_2 cluster algebra)**.** From fig. 3.1 we can immediately identify the principal part as the subquiver $\langle 13\rangle \to \langle 14\rangle$. Consequently, the cluster algebra of $\mathrm{Gr}(2,5)$ is of A_2 Dynkin type. Since this is a finite cluster algebra, we can compute all of its clusters and cluster variables. For simplicity, we do this for the A_2 cluster algebra without frozen variables, which can be obtained from that of $\mathrm{Gr}(2,5)$ by setting all frozen variables to one. The exchange graph of the cluster algebra is depicted in fig. 3.3.
By using the mutation relation, eq. (3.6), we can compute all cluster $\mathcal{A}$-variables in terms of the variables a_1, a_2 of the initial cluster. They are given by

$$a_3 = \frac{1+a_2}{a_1} \,, \quad a_4 = \frac{1+a_1+a_2}{a_1 a_2} \,, \quad a_5 = \frac{1+a_1}{a_2} \,. \tag{3.10}$$

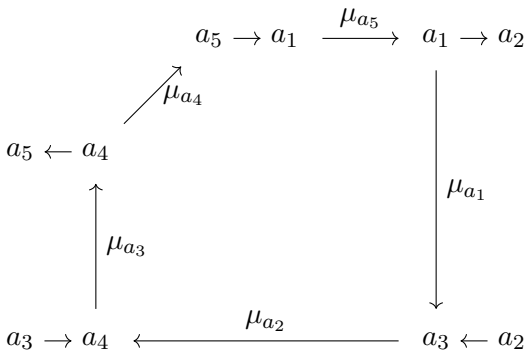

Figure 3.3: Exchange graph of the A_2 cluster algebra. Note that the actual exchange graph is undirected and that the arrows in this graph are only illustrative of the mutations used to generate the entire cluster algebra.

Note that the way we have arranged the exchange graph of the A_2 cluster algebra is suggestive of the geometric structures of cluster algebras that we will discuss in section 3.1.4.

Finally, we also introduce another set of variables defined on the cluster algebra. To every unfrozen node and thus $\mathcal{A}$-variable in a cluster we further associate the so-called cluster $\mathcal{X}$-variable of Fock and Goncharov [162], which is defined as

$$x_i = \prod_{l=1}^{d+n} a_l^{b_{li}} \,. \tag{3.11}$$

For example, in the initial quiver of the $\mathrm{Gr}(2,5)$ cluster algebra, we get the two $\mathcal{X}$-variables

$$x_1 = \frac{\langle 12\rangle \langle 34\rangle}{\langle 14\rangle \langle 23\rangle} \,, \quad x_2 = \frac{\langle 13\rangle \langle 45\rangle}{\langle 15\rangle \langle 34\rangle} \,, \tag{3.12}$$

attached to the nodes of the two $\mathcal{A}$-variables $a_1 = \langle 13\rangle$ and $a_2 = \langle 24\rangle$, respectively.

Remark 3.4. While this framework of cluster algebras with frozen variables is intuitive and the natural language to describe cluster algebras of Grassmannians, it has some disadvantages for the application to infinite mutation sequences, which are discussed in chapter 5. For example, consider a mutation of the A_2 cluster algebra with two frozen variables f_1, f_2 as depicted in figure 3.4.

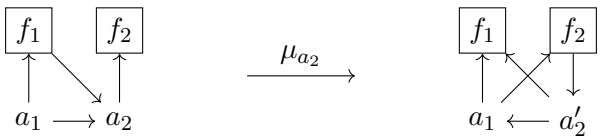

Figure 3.4: Example of mutating a A_2 cluster algebra with frozen variables f_1, f_2 on the node of a_2.

With the mutation rule, eq. (3.6), it can easily be demonstrated that the mutated variable

is given by

$$a_2' = \frac{f_1 a_1 + f_2}{a_2} \,. \tag{3.13}$$

While the frozen variables do not change under mutation and in this way take somewhat of a spectator role, they very significantly influence the precise functional form of the mutated variable. Consider for example a slight modification of the above example, depicted in fig. 3.5.

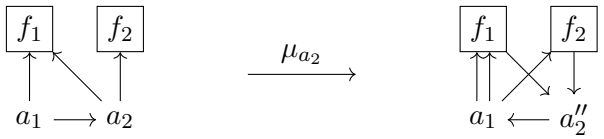

Figure 3.5: Modified example of mutating a A_2 cluster algebra with frozen variables f_1, f_2 on the node of a_2.

The mutated variable a_2'' is now given by

$$a_2'' = \frac{a_1 + f_1 f_2}{a_2} \,. \tag{3.14}$$

Whereas this dependence on the choice of frozen variables appears by construction, it does complicate the study of *cluster subalgeras*. In the obvious way, a cluster subalgebra is defined as the cluster algebra obtained by restricting mutation in some cluster of a cluster algebra to a subset of $\mathcal{A}$-variables, see eg. [163]. In this embedding, the $\mathcal{A}$-variables not contained in the cluster subalgebra effectively behave like frozen variables for the subalgebra, as they are never mutated.

Consequently, it is very difficult to use the properties, eg. the functional form of the cluster variables, of some cluster algebra appearing as a subalgebra in a higher-rank cluster algebra, since the functional form depends on the frozen variables and thus on the embedding. Using instead the language of cluster algebras with coefficients, where frozen and unfrozen variables are put on an equal level, avoids these problems, as we will see in section 3.1.2.

3.1.2. Cluster algebras with coefficients

In the mathematics literature, there is another equivalent description of cluster algebras using the so-called *coefficients* [159]. As we will detail momentarily, in this formalism all frozen variables connected to a given $\mathcal{A}$-variable are grouped into a single coefficient, which also changes under mutation and is associated to the $\mathcal{A}$-variable. The main advantage of cluster algebras with general coefficients is that they can be constructed once, and then specialized to *any* particular choice of frozen variables at the very end. This allows for a unified treatment of what would be several distinct computations in the language of frozen variables, and it will be crucial in obtaining the singularities of eight- and nine-particle amplitudes, as described in chapter 5 as well as sections 6.2 and 6.3, in essentially one go.

Closely following the original reference [159], we now review the theory of cluster algebras with coefficients, albeit skipping some of the mathematical rigour in favour of applications

and examples, as well as with a focus on cluster algebras of *geometric type*. Before we can define the eponymous coefficients though, we introduce the *cluster-tropical semifield*. Note that we consider a semifield as a multiplicative abelian group together with an addition that is commutative, associative, and distributive but in contrast to a field does not have an inverse.

Definition 3.5 (Cluster-tropical semifield)**.** Given a multiplicative abelian group $\mathrm{Tr}(u_j : j \in J)$ freely generated[3] by the elements u_j labelled by the set $j \in J$, we define the cluster-tropical addition $\hat{\oplus}$ in this group by

$$\prod_j u_j^{a_j} \,\hat{\oplus}\, \prod_l u_l^{b_l} = \prod_j u_j^{\min(a_j, b_j)} \,. \tag{3.15}$$

The group, equipped with multiplication and the cluster-tropical addition, forms the *cluster-tropical semifield* $(\mathrm{Tr}(u_j : j \in J), \hat{\oplus}, \cdot)$.

Example 3.6. Consider for example the cluster-tropical semifield $(\mathrm{Tr}(u_1, u_2), \hat{\oplus}, \cdot)$. The cluster-tropical addition is defined so that it selects the minimum exponent of each generator u_j, that is we for example have that

$$\left(u_1^{-2} u_2\right) \,\hat{\oplus}\, \left(u_2^{-1}\right) = u_1^{-2} \cdot u_2^{-1} \,, \tag{3.16}$$

since $1 = (u_1)^0$.

Next, we define a cluster algebra of rank r in terms of some cluster-tropical semifield $\mathbb{P}$,[4] whose elements are the coefficients. The *group ring* $\mathbb{QP}$, which is also required for the following definition, can be considered as the set of formal linear combinations of the elements of $\mathbb{Q}$ and $\mathbb{P}$. To construct a cluster algebra, we begin, as before, by defining its clusters or *labelled seeds*.

Definition 3.7 (Labelled seed)**.** Given a cluster-tropical semifield $\mathbb{P} = \mathrm{Tr}(u_1, \ldots, u_m)$ and the field $\mathcal{F}$ of rational functions in r variables with coefficients in $\mathbb{QP}$, the *ambient field*, a *labelled seed* in $\mathcal{F}$ is a triple $\Sigma = (\boldsymbol{a}, \boldsymbol{y}, B)$, whereas

- $\boldsymbol{a} = (a_1, \ldots, a_r)$ is an r-tuple of elements of $\mathcal{F}$, the $\mathcal{A}$-variables or cluster variables, that are algebraically independent over $\mathbb{QP}$ and generate the field $\mathcal{F}$, that is we can write $\mathcal{F} = \mathbb{QP}(a_1, \ldots, a_r)$,
- $\boldsymbol{y} = (y_1, \ldots, y_r)$ is an r-tuple of elements of $\mathbb{P}$, the coefficients, and
- $B = (b_{ij})$ is an integer $r \times r$, skew-symmetrisable matrix.

Note that sometimes only the variables $\boldsymbol{a}$ are referred to as a *cluster*, whereas the triple $(\boldsymbol{a}, \boldsymbol{y}, B)$ is a labelled seed. Wherever the notation does not cause confusion, we refer to the full data of the labelled seed as a cluster instead. The triple $(\boldsymbol{a}, \boldsymbol{y}, B)$ up to simultaneous permutations of the components of $\boldsymbol{x}$ and $\boldsymbol{y}$ and the rows and columns of B is also referred to as the *unlabelled seed*.

[3] Roughly speaking, freely generated means that the set $\{u_j : j \in J\}$ can be considered as a multiplicative basis for the abelian group.

[4] Since we focus on cluster algebras of geometric type, this semifield is of cluster-tropical type. For general cluster algebras, this restriction is lifted and the cluster algebra is defined in terms of any semifield.

Remark 3.8. Note that in the mathematics literature, the $\mathcal{A}$-variables are usually denoted by $\boldsymbol{x} = (x_1, \ldots, x_r)$. To connect to the more common notation of the physics literature, we denote the $\mathcal{A}$-variables instead by $\boldsymbol{a} = (a_1, \ldots, a_r)$ and use $\boldsymbol{x}$ for the $\mathcal{X}$-variables.

Due to the restriction to cluster algebras of geometric type, we can directly connect this abstract definition of labelled seeds to cluster algebras with frozen variables. In this way, throughout this section we also establish the equivalence of the two perspectives on cluster algebras.

Remark 3.9 (Labelled seeds and clusters with frozen variables)**.** Consider a cluster in a cluster algebra of rank r with $\mathcal{A}$-variables $a_1, \ldots, a_r$, frozen variables $a_{r+1}, \ldots, a_{r+m}$, and adjacency matrix $\tilde{B}$, a $(r+m) \times (r+m)$ skew-symmetrisable integer matrix. Taking the cluster-tropical semifield $\mathbb{P}$ to be the group generated by the frozen variables, that is $\mathbb{P} = \mathrm{Tr}(a_{r+1}, \ldots, a_{r+m})$, we define the coefficients for $j = 1, \ldots, r$ as

$$y_j = \prod_{i=r+1}^{r+m} a_i^{b_{ij}}\,, \tag{3.17}$$

which, being Laurent monomials in the frozen variables, are indeed elements of $\mathbb{P}$. Restricting the adjacency matrix $\tilde{B}$ to the principal part B, that is the $r \times r$ component describing the connectivity of the r $\mathcal{A}$-variables, the triple $((a_1, \ldots, a_r), (y_1, \ldots, y_m), B)$ indeed forms a labelled seed as defined above.

Conversely, eq. (3.17) could also be used as a definition to extend the $r \times r$ adjacency matrix of a labelled seed to the full $(r+m) \times (r+m)$ adjacency matrix of a cluster with the frozen variables obtained from the generators of the cluster-tropical semifield. In this way, labelled seeds are fully equivalent to clusters with frozen variables.

In the special case that a cluster algebra of rank r has r frozen variables $(a_{r+1}, \ldots, a_{2r})$ such that there exists a cluster for which $a_{r+j} = y_j$, it is said to have *principal coefficients.*

As can already be seen from eq. (3.17), the coefficients are closely related to the $\mathcal{X}$-variables of Fock and Goncharov [162], x_i with $i = 1, \ldots, r$. In the language of cluster algebras with coefficients, they are defined as follows.

Definition 3.10 ($\mathcal{X}$-variables)**.** Given a labelled seed $(\boldsymbol{a}, \boldsymbol{y}, B)$ with r $\mathcal{A}$-variables, we define the $\mathcal{X}$-variables as

$$x_j = \prod_{i=1}^{r} a_i^{b_{ij}} \cdot y_j\,, \tag{3.18}$$

for each $j = 1, \ldots, r$. This definition is equivalent to the previous definition in eq. (3.11), as can be easily seen by using eq. (3.17).

As before, we can mutate labelled seeds on one of the $\mathcal{A}$-variables to obtain another cluster with mutated variables, coefficients and adjacency matrix. The mutation rules are now defined as follows.

Definition 3.11 (Seed mutation)**.** Consider a labelled seed $(\boldsymbol{a}, \boldsymbol{y}, B)$ in $\mathcal{F}$. The *seed mutation* μ_j in the direction $j = 1, \ldots, r$ transforms the seed into the mutated seed $\mu_j(\boldsymbol{a}, \boldsymbol{y}, B) = (\boldsymbol{a}', \boldsymbol{y}', B)$, whereas

- the $\mathcal{A}$-variables $\boldsymbol{a}'$ are given by $a'_i = a_i$ for $i \neq j$ and $a'_j \in \mathcal{F}$ is given by

$$a'_j = \frac{y_j \prod_{i=1}^r a_i^{[b_{ij}]_+} + \prod_{i=1}^r a_i^{[-b_{ij}]_+}}{a_j \left(1 \hat{\oplus} y_j\right)}\,, \tag{3.19}$$

  whereas as before $[x]_+ = \max(0, x)$,

- the coefficients $y'_1, \ldots, y'_r \in \mathbb{P}$ are given by

$$y'_i = \begin{cases} y_j^{-1} & \text{if } i = j\,, \\ y_i y_j^{[b_{ji}]_+} \left(1 \hat{\oplus} y_j\right)^{-b_{ji}} & \text{if } i \neq j\,, \end{cases} \tag{3.20}$$

- and the mutated adjacency matrix is given as before, eq. (3.5), by

$$b'_{il} = \begin{cases} -b_{il} & \text{for } i = j \text{ or } l = j\,, \\ b_{il} + [-b_{ij}]_+ \, b_{jl} + b_{ij} \, [b_{jl}]_+ & \text{otherwise}\,. \end{cases} \tag{3.21}$$

Remark 3.12. Note that the definition of the $\mathcal{X}$-variables, eq. (3.18), and the mutation rule for the coefficients, eq. (3.20), induce an analogous mutation rule for the former. Considering the mutation of a labelled seed, $\mu_k(\boldsymbol{a}, \boldsymbol{y}, B) = (\boldsymbol{a}', \boldsymbol{y}', B)$, it can be shown [159] that the $\mathcal{X}$-variables $(x'_1, \ldots, x'_r)$ of the mutated seed are given by

$$x'_i = \begin{cases} x_j^{-1} & \text{if } i = j\,, \\ x_i x_j^{[b_{ji}]_+} \left(1 + x_j\right)^{-b_{ji}} & \text{if } i \neq j\,, \end{cases} \tag{3.22}$$

in terms of the $\mathcal{X}$-variables $(x_1, \ldots, x_r)$ of the original seed.

Again, this prescription is completely equivalent to the formulation of cluster algebras with frozen variables, especially the mutation relation eq. (3.6), as can be seen by continuing our example from above.

Remark 3.13 (Equivalence to mutation of clusters with frozen variables)**.** Consider the same cluster with $\mathcal{A}$-variables $(a_1, \ldots, a_r)$ and frozen variables $(a_{r+1}, \ldots, a_{r+m})$ and the associated labelled seed $(\boldsymbol{a}, \boldsymbol{y}, B)$ as above. Mutating the seed in some direction $j = 1, \ldots, r$, we get the mutated seed with the mutated variable a'_j given by eq. (3.19). Using the relation of the coefficient y_j to the frozen variables, eq. (3.17), we see that

$$1 \hat{\oplus} y_j = 1 \hat{\oplus} \prod_{i=r+1}^{r+m} a_i^{b_{ij}} = \prod_{i=r+1}^{r+m} a_i^{\min(0, b_{ij})} = \prod_{i=r+1}^{r+m} a_i^{-[-b_{ij}]_+}\,, \tag{3.23}$$

which can be inserted back into the mutation relation of eq. (3.19) to obtain

$$a'_j = a_j^{-1} \left(\prod_{i=r+1}^{r+m} a_i^{b_{ij} + [-b_{ij}]_+} \prod_{i=1}^{r} a_i^{[b_{ij}]_+} + \prod_{i=1}^{r+m} a_i^{[-b_{ij}]_+} \right)\,. \tag{3.24}$$

Noting that $x = [x]_+ - [-x]_+$, this is indeed the same relation as the original mutation relation of eq. (3.6).

It remains to verify that the mutated coefficients y'_i obtained from eq. (3.20) are the same as the ones associated to the mutated cluster with frozen variables via eq. (3.17). First, for $i = j$, we can use the mutation rule $b'_{li} = -b_{li}$ to write

$$\prod_{l=r+1}^{r+m} a_l^{b'_{lj}} = \left(\prod_{l=r+1}^{r+m} a_l^{b_{lj}} \right)^{-1} = y_j^{-1} = y'_j \tag{3.25}$$

Next, for $i \neq j$, the mutation rule similarly results in

$$\prod_{l=r+1}^{r+m} a_l^{b'_{li}} = \left(\prod_{l=r+1}^{r+m} a_l^{b_{li}} \right) \left(\prod_{l=r+1}^{r+m} a_l^{[-b_{lj}]_+} \right)^{b_{ji}} \left(\prod_{i=r+1}^{r+m} a_i^{b_{lj}} \right)^{[b_{ji}]_+} = y_i y_j^{[b_{ji}]_+} \left(1 \hat{\oplus} y_j\right)^{-b_{ji}} = y'_i \,, \tag{3.26}$$

whereas the second equality can be seen from noting that $[-b_{lj}]_+ = -\min(0, b_{lj})$ such that we can express the second monomial in terms of a cluster-tropical sum.

As we have done in the previous, more gentle introduction to cluster algebras, sec. 3.1.1, once we have defined clusters and their mutation, we can construct the entire cluster algebra by performing all possible mutations to generate all clusters. This can be formalised by first introducing the *r-regular tree* $\mathbb{T}_r$.

Definition 3.14 (r-regular tree)**.** A *r-regular tree* $\mathbb{T}_r$ is an infinite connected acyclic undirected graph, that is an infinite undirected graph in which any two vertices are connected by exactly one path, with r edges at each vertex, which we label by the numbers $1, \ldots, r$. We write $t \overset{j}{\to} t'$ if the vertices $t, t' \in \mathbb{T}_r$ are connected by an edge labelled by j.

The r-regular trees, which very closely resemble the exchange graph of a cluster algebra we have seen in the previous section, can be used in the obvious way to label the clusters in a cluster algebra by its vertices and mutation by its edges. Indeed, this leads to the concept of a *cluster pattern*.

Definition 3.15 (Cluster pattern)**.** Given a r-regular tree $\mathbb{T}_r$, a *cluster pattern* of rank r is the assignment of a labelled seed $\Sigma_t = (\boldsymbol{a}_t, \boldsymbol{y}_t, B_t)$ to each vertex $t \in \mathbb{T}_r$, so that for every edge $t \overset{j}{\to} t'$ between two vertices $t, t' \in \mathbb{T}_r$ we have

$$\mu_j(\boldsymbol{a}_t, \boldsymbol{y}_t, B_t) = (\boldsymbol{a}_{t'}, \boldsymbol{y}_{t'}, B_{t'}) \,, \tag{3.27}$$

that is the labelled seed $\Sigma_{t'}$ is obtained from Σ_t by mutation along j.

In this way, a cluster pattern is uniquely defined by specifying any of its labelled seeds, with the other seeds arising from mutation. We refer to this seed as the *initial seed* or initial cluster and assign it to the vertex $t_0 \in \mathbb{T}_r$.

Remark 3.16. Note that we from now on label the clusters or labelled seeds of a cluster algebra by subscript t, which is understood to be a vertex $t \in \mathbb{T}_r$. Specifically, the variables and coefficients of a cluster are denoted by $a_{i;t}$, $x_{i;t}$ and $y_{i;t}$, respectively, with the first index

i denoting the position within the cluster and the second index t denoting the label of the cluster. Similarly, the components of the adjacency matrix of a cluster are denoted by $b_{ij;t}$. When the notation does not cause confusion, we will sometimes drop the label t or denote the components of the initial seed by 0 instead of t_0. Finally, we write $t \xrightarrow{j} t'$ to denote the mutation of the seed Σ_t along direction j resulting in the seed $\Sigma_{t'}$.

Before continuing with the formal discussion, let us first demonstrate the previous abstract definitions with a concrete example. To do so, we consider the simple rank-2 cluster algebra of A_2 Dynkin type, which we have already seen in the previous example 3.3.

Example 3.17 (A_2 cluster pattern)**.** For $r = 2$, the r-regular tree $\mathbb{T}_2$ is an infinite chain and is depicted in fig. 3.6.

$$\cdots \overset{1}{\text{———}} t_{-1} \overset{2}{\text{———}} t_0 \overset{1}{\text{———}} t_1 \overset{2}{\text{———}} t_2 \overset{1}{\text{———}} \cdots$$

Figure 3.6: The 2-regular tree $\mathbb{T}_2$.

To obtain the A_2 cluster pattern, we choose the initial seed $((a_{1;0}, a_{2;0}), (y_{1;0}, y_{2;0}), B_0)$ at t_0 with the adjacency matrix

$$B_0 = \begin{pmatrix} 0 & 1 \\ -1 & 0 \end{pmatrix} . \tag{3.28}$$

The seed Σ_{t_1}, for example, can then be constructed by mutating Σ_0 in the direction 1, with the mutated adjacency matrix given by $B_{t_1} = B_0^T$ and the mutated variables given by

$$a_{1;1} = \frac{y_{1;0}a_{2;0} + 1}{a_{1;0}(1 \hat{\oplus} y_{1;0})} , \quad a_{2;1} = a_{2;0} , \qquad y_{1;1} = y_{1;0}^{-1} , \quad y_{2;1} = y_{2;0}(1 \hat{\oplus} y_{1;0}) . \tag{3.29}$$

Continuing in this way along the chain in the right direction, we can obtain all seeds Σ_t as a function of the initial seed. They are given in table 3.1 for t_i with $i = 0, \ldots, 5$.

As we have already seen in example 3.3, the A_2 cluster algebra is finite and consists of 5 clusters. Indeed, as can be seen from table 3.1, Σ_{t_5} is in fact equivalent to Σ_{t_0} up to interchanging the indices 1 and 2. In this way, the A_2 cluster pattern continues with the obvious periodicity, that is with the first five seeds $\Sigma_0, \ldots, \Sigma_4$ repeating. In the obvious way, this kind of identification leads us to the formal definition of a cluster algebra with coefficients below.

Finally, with the concept of a cluster pattern, all components are in place to give a formal definition of a cluster algebra, see also [159].

Definition 3.18 (Cluster algebra)**.** Given a cluster pattern of rank r, we denote the union of the $\mathcal{A}$-variables of all seeds in the pattern by

$$\mathcal{A} = \bigcup_{t \in \mathbb{T}_r} \boldsymbol{a}_t \equiv \{a_{i;t} : t \in \mathbb{T}_r , \, i = 1, \ldots, r\} . \tag{3.30}$$

t	B_t	$\boldsymbol{y}_t$		$\boldsymbol{a}_t$	
t_0	$\begin{pmatrix} 0 & 1 \\ -1 & 0 \end{pmatrix}$	y_1	y_2	a_1	a_2
t_1	$\begin{pmatrix} 0 & -1 \\ 1 & 0 \end{pmatrix}$	$\frac{1}{y_1}$	$\frac{y_1 y_2}{1 \hat{\oplus} y_1}$	$\frac{y_1 + a_2}{a_1(1 \hat{\oplus} y_1)}$	a_2
t_2	$\begin{pmatrix} 0 & 1 \\ -1 & 0 \end{pmatrix}$	$\frac{y_2}{1 \hat{\oplus} y_1 \hat{\oplus} y_1 y_2}$	$\frac{1 \hat{\oplus} y_1}{y_1 y_2}$	$\frac{y_1 + a_2}{a_1(1 \hat{\oplus} y_1)}$	$\frac{y_1 + a_2 + a_1 y_1 y_2}{a_1 a_2(1 \hat{\oplus} y_1 \hat{\oplus} y_1 y_2)}$
t_3	$\begin{pmatrix} 0 & -1 \\ 1 & 0 \end{pmatrix}$	$\frac{1 \hat{\oplus} y_1 \hat{\oplus} y_1 y_2}{y_2}$	$\frac{1}{y_1(1 \hat{\oplus} y_2)}$	$\frac{1 + a_1 y_2}{a_2(1 \hat{\oplus} y_2)}$	$\frac{y_1 + a_2 + a_1 y_1 y_2}{a_1 a_2(1 \hat{\oplus} y_1 \hat{\oplus} y_1 y_2)}$
t_4	$\begin{pmatrix} 0 & 1 \\ -1 & 0 \end{pmatrix}$	$\frac{1}{y_2}$	$y_1(1 \hat{\oplus} y_2)$	$\frac{1 + a_1 y_2}{a_2(1 \hat{\oplus} y_2)}$	a_1
t_5	$\begin{pmatrix} 0 & -1 \\ 1 & 0 \end{pmatrix}$	y_2	y_1	a_2	a_1

Table 3.1: Seeds Σ_{t_i} for $i = 0, \ldots, 5$ in terms of the variables $(a_1, a_2) \equiv (a_{1;0}, a_{2;0})$ and coefficients $(y_1, y_2) \equiv (y_{1;0}, y_{2;0})$ of the initial seed Σ_0.

The *cluster algebra* $\mathscr{A}$ associated to the cluster pattern is the $\mathbb{ZP}$-subalgebra of the ambient field $\mathcal{F}$ generated by the cluster variables, that is $\mathscr{A} = \mathbb{ZP}[\mathcal{X}]$.[5] Since we can construct the entire cluster algebra from any seed $\Sigma = (\boldsymbol{a}, \boldsymbol{y}, B)$, we also write $\mathscr{A} = \mathscr{A}(\boldsymbol{a}, \boldsymbol{y}, B)$.

We have seen in the previous example that the cluster pattern is an infinite graph where equivalent labelled seeds appear multiple or infinitely many times. If we take the obvious quotient by the equivalence relation $\Sigma_t \sim \Sigma_{t'}$ for labelled seeds Σ_t and $\Sigma_{t'}$ that are equivalent up to simultaneous permutations of the components of $\boldsymbol{a}$ and $\boldsymbol{y}$ as well as the rows and columns B, that is whenever the labelled seeds describe the same (unlabelled) seed, we obtain the *exchange graph*.

Definition 3.19 (Exchange graph)**.** Given a cluster pattern and the associated cluster algebra of rank r, we define the *exchange graph* of the cluster algebra as the finite or infinite r-regular undirected graph[6] whose vertices are the seeds of the cluster algebra and whose edges connect any two seeds that are related to each other by a single mutation.

Example 3.20 (A_2 cluster algebra)**.** We have seen in the previous example that the A_2 cluster pattern consists of five inequivalent seeds. Consequently, as we have also already seen before in example 3.3, the associated A_2 cluster algebra consists of five clusters with five cluster variables. Furthermore, by quotiening the tree $\mathbb{T}_2$, see fig. 3.6, by the identification of equivalent seeds, in this case $\Sigma_{t_i} \sim \Sigma_{t_{i+5}}$, we obtain the A_2 exchange graph that is depicted in fig. 3.3.

[5] Note that this notation means that the cluster algebra is the algebra of polynomials in the cluster variables with coefficients taken from $\mathbb{ZP}$, which itself can be considered as formal linear combinations of integers and coefficients $y \in \mathbb{P}$.

[6] Note that a r-regular graph is a graph with exactly r edges attached to each vertex.

Another advantage of considering cluster algebras with coefficients instead of frozen variables is that it makes the *separation principle* manifest. Using eq. (3.18) to express $y_{j;t}$ in terms of the $\mathcal{A}$- and $\mathcal{X}$-variables of the cluster t, we can rewrite the mutation rule (3.19) as

$$a_{j;t'} = (a_{j;t})^{-1} \prod_{i=1}^{r} a_{i;t}^{[-b_{ij;t}]_+} \cdot \frac{1 + x_{j;t}}{1 \hat{\oplus} y_{j;t}} \,. \tag{3.31}$$

The consequence of this factored form of the mutation relation is that, in the cases relevant to this article, any $\mathcal{A}$-variable can be written in the following factored way, see also [159, Corollary 6.2].

Proposition 3.21 (Separation principle)**.** *Given a cluster algebra $\mathscr{A}(\boldsymbol{a}_0, \boldsymbol{y}_0, B_0)$ of rank r, an arbitrary cluster variable $a_{l;t}$ can be written in terms of the initial seed as*

$$a_{l;t} = \prod_{i=1}^{r} (a_{i;0})^{g_i} \cdot \frac{F_{l;t}\left(x_{1;0}, \ldots, x_{r;0}\right)}{F_{l;t}|_{\mathbb{P}}\left(y_{1;0}, \ldots, y_{r;0}\right)} \,, \tag{3.32}$$

for some $g_1, \ldots, g_r \in \mathbb{Z}$ and whereas $F_{l;t}$ is a polynomial of the initial $\mathcal{X}$-variables and $F_{l;t}|_{\mathbb{P}}$ denotes the function obtained by replacing addition with cluster-tropical addition and $\mathcal{X}$-variables by coefficients.

Definition 3.22 ($\boldsymbol{g}$-vector)**.** By the means of the separation principle, eq. (3.32), we can associate a unique integer vector

$$\boldsymbol{g}_a = (g_1^{(a)}, \ldots, g_r^{(a)}) \in \mathbb{Z}^r \,, \tag{3.33}$$

the *$\boldsymbol{g}$-vector*, to each $\mathcal{A}$-variable. Its components $g_i^{(a)}$ correspond to the exponents of the initial $\mathcal{A}$-variables when writing the $\mathcal{A}$-variable a in the factored form of eq. (3.32).

As is outlined in e.g. [159], we can use the mutation rules, eqs. (3.19)–(3.22), to also obtain a mutation rule for the $\boldsymbol{g}$-vector associated to an $\mathcal{A}$-variable. However, for our purposes it is better to work with a modified version thereof. In order to more closely align the vectors associated to the $\mathcal{A}$-variables to the rays of the totally positive tropical configuration space, which will become relevant in chapter 4, we use a modified mutation rule, see also [70, 164]. To construct this relation, we first attach a coefficient matrix C to each cluster. While its definition appears ad-hoc, the coefficient matrix has a close relation to the cluster algebra, as is discussed in remark 3.26.

Definition 3.23 (Coefficient matrix)**.** Given a cluster algebra of rank r with initial seed labelled by t_0, we attach the *coefficient matrix* $C_{t_0} = \mathbf{1}_r$, whereas $\mathbf{1}_r$ is the $r \times r$ identity matrix, to the initial seed. In the remaining clusters of the cluster algebra, the coefficient matrix is defined recursively via a mutation rule. For the mutation $t \xrightarrow{j} t'$ it is given by

$$c_{il;t'} = \begin{cases} -c_{il;t} & \text{if } l = j \,, \\ c_{il;t} - [c_{ij;t}]_+ b_{jl;t} + c_{ij;t}[b_{jl;t}]_+ & \text{otherwise} \,, \end{cases} \tag{3.34}$$

in terms of the components $c_{il;t}$ of the original coefficient matrix C_t as well as $b_{il;t}$ of the adjacency matrix B_t.

Similar to the $\boldsymbol{g}$-vectors, we next associate a *cluster ray* to each $\mathcal{A}$-variable in the cluster algebra.[7] Collecting the cluster rays of all variables in a cluster as the columns of the ray matrix G, we can recursively define the cluster rays as follows.

Definition 3.24 (Cluster rays)**.** Similar to the coefficient matrix, we attach the *ray matrix* $R_{t_0} = \mathbf{1}_r$ to the initial seed Σ_0 in a cluster algebra of rank r. The ray matrices of the other clusters are recursively defined via a mutation rule, which for $t \overset{j}{\to} t'$ is given by

$$\rho_{il;t'} = \begin{cases} \rho_{il;t} & \text{if } l \neq j\,, \\ -\rho_{il;t} + \sum_{m=1}^{r} \left(\rho_{im;t}[-b_{mj;t}]_+ + b_{im;0}[c_{mj;t}]_+\right) & \text{otherwise}\,, \end{cases} \tag{3.35}$$

in terms of the components $\rho_{il;t}$ of the original ray matrix R_t, $c_{il;t}$ of the original coefficient matrix C_t, $b_{il;t}$ of the original adjacency matrix B_t, as well as the components $b_{il;0}$ of the adjacency matrix B_{t_0} of the initial seed. The *cluster ray* associated to the cluster variable $a_{l;t}$ is the half-line emanating from the origin in the direction of $\boldsymbol{\rho}_{l;t} = (\rho_{1l;t}, \ldots, \rho_{rl;t})$, the l-th column of the ray matrix R_t.

We can visualise these abstract definitions by continuing our simple, 2-dimensional cluster algebra of type A_2 and compute both, its $\boldsymbol{g}$-vectors as well as cluster rays.

Example 3.25 (A_2 cluster algebra)**.** From the adjacency matrix B_0 of the initial seed of the A_2 cluster algebra, see eq. (3.28), we can read off the $\mathcal{X}$-variables of the initial cluster to be

$$x_1 = (a_2)^{-1} y_1\,, \quad x_2 = a_1 y_2\,, \tag{3.36}$$

whereas we have again dropped the label t_0 for the initial variables. Using these relations, we can rewrite the cluster variables in the separated form of eq. (3.32) and thus read off the $\boldsymbol{g}$-vectors. Similarly, we can use the mutation rules of eqs. (3.34) and (3.35) to obtain the cluster rays. The results are collected in table 3.2.

Note that the last seed Σ_{t_5} again is equivalent to the initial seed by interchanging the cluster variables a_1 and a_2, while simultaneously interchanging the corresponding rows and columns in the adjacency matrix. In contrast to the adjacency matrix, whose components b_{ij} describe the connection of variables i to j, the l-th column of the coefficient and ray matrix, respectively, describe properties of the cluster variable l. Consequently, the equivalence to the initial seed holds when interchanging the columns only of the coefficient and ray matrix.

To compare the $\boldsymbol{g}$-vectors more directly to the cluster rays, we illustrate both of them in fig. 3.7. In this figure, the positive span of any two $\boldsymbol{g}$-vectors or rays that appear together in a seed is labelled by that seed. Fascinatingly, it turns out that this splits up the entire $\mathbb{R}^2$ into surfaces that are uniquely labelled by a seed of the cluster algebra. This will be further investigated in the following sections.

[7] Strictly speaking, we associate a vector to each variable. The cluster ray is then the half-line emanating from the origin and pointing in the direction of this vector.

t	B_t	$\boldsymbol{a}_t$	$\boldsymbol{g}_t$	C_t	R_t
t_0	$\begin{pmatrix} 0 & 1 \\ -1 & 0 \end{pmatrix}$	$a_1 \quad a_2$	$\begin{pmatrix} 1 \\ 0 \end{pmatrix} \begin{pmatrix} 0 \\ 1 \end{pmatrix}$	$\begin{pmatrix} 1 & 0 \\ 0 & 1 \end{pmatrix}$	$\begin{pmatrix} 1 & 0 \\ 0 & 1 \end{pmatrix}$
t_1	$\begin{pmatrix} 0 & -1 \\ 1 & 0 \end{pmatrix}$	$\frac{a_2}{a_1}\frac{1+x_1}{1 \hat{\oplus} y_1} \quad a_2$	$\begin{pmatrix} -1 \\ 1 \end{pmatrix} \begin{pmatrix} 0 \\ 1 \end{pmatrix}$	$\begin{pmatrix} -1 & 0 \\ 0 & 1 \end{pmatrix}$	$\begin{pmatrix} -1 & 0 \\ 0 & 1 \end{pmatrix}$
t_2	$\begin{pmatrix} 0 & 1 \\ -1 & 0 \end{pmatrix}$	$\frac{a_2}{a_1}\frac{1+x_1}{1 \hat{\oplus} y_1} \quad \frac{1}{a_1}\frac{1+x_1+x_1x_2}{1 \hat{\oplus} y_1 \hat{\oplus} y_1y_2}$	$\begin{pmatrix} -1 \\ 1 \end{pmatrix} \begin{pmatrix} -1 \\ 0 \end{pmatrix}$	$\begin{pmatrix} -1 & 0 \\ 0 & -1 \end{pmatrix}$	$\begin{pmatrix} -1 & 0 \\ 0 & -1 \end{pmatrix}$
t_3	$\begin{pmatrix} 0 & -1 \\ 1 & 0 \end{pmatrix}$	$\frac{1}{a_2}\frac{1+x_2}{1 \hat{\oplus} y_2} \quad \frac{1}{a_1}\frac{1+x_1+x_1x_2}{1 \hat{\oplus} y_1 \hat{\oplus} y_1y_2}$	$\begin{pmatrix} 0 \\ -1 \end{pmatrix} \begin{pmatrix} -1 \\ 0 \end{pmatrix}$	$\begin{pmatrix} 1 & -1 \\ 0 & -1 \end{pmatrix}$	$\begin{pmatrix} 1 & 0 \\ -1 & -1 \end{pmatrix}$
t_4	$\begin{pmatrix} 0 & 1 \\ -1 & 0 \end{pmatrix}$	$\frac{1}{a_2}\frac{1+x_2}{1 \hat{\oplus} y_2} \quad a_1$	$\begin{pmatrix} 0 \\ -1 \end{pmatrix} \begin{pmatrix} 1 \\ 0 \end{pmatrix}$	$\begin{pmatrix} 0 & 1 \\ -1 & 1 \end{pmatrix}$	$\begin{pmatrix} 1 & 1 \\ -1 & 0 \end{pmatrix}$
t_5	$\begin{pmatrix} 0 & -1 \\ 1 & 0 \end{pmatrix}$	$a_2 \quad a_1$	$\begin{pmatrix} 0 \\ 1 \end{pmatrix} \begin{pmatrix} 1 \\ 0 \end{pmatrix}$	$\begin{pmatrix} 0 & 1 \\ 1 & 0 \end{pmatrix}$	$\begin{pmatrix} 0 & 1 \\ 1 & 0 \end{pmatrix}$

Table 3.2: Cluster variables $\boldsymbol{a}_t$, coefficient matrix C_t, ray matrix R_t and $\boldsymbol{g}$-vectors $\boldsymbol{g}_{l;t}$ for the seeds in the A_2 cluster algebra. The cluster rays $\boldsymbol{\rho}_{l;t}$ correspond to the columns of the ray matrix R_t.

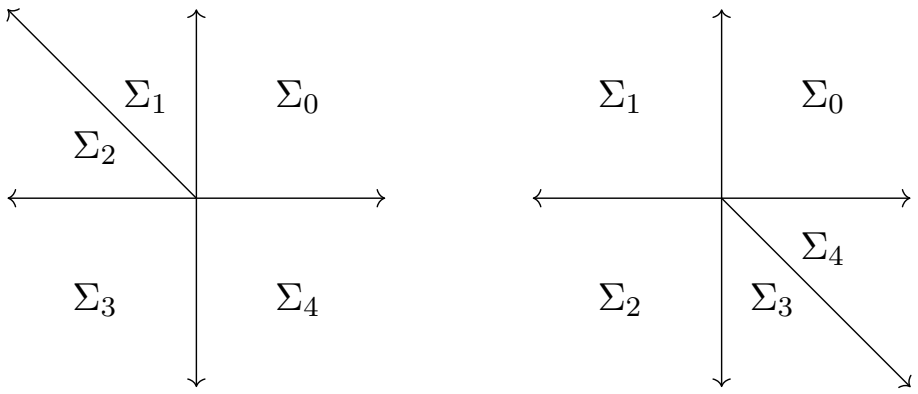

(a) $\boldsymbol{g}$-vectors (b) cluster rays

Figure 3.7: Illustration of the (a) $\boldsymbol{g}$-vectors and (b) cluster rays of the A_2 cluster algebra. The rays split up the plane $\mathbb{R}^2$ into five surfaces, which are labelled by the seed Σ_t that contains the two rays that form the border of the surface. For simplicity, we write Σ_i instead of Σ_{t_i}.

Remark 3.26. Note that the ad-hoc definition of the cluster rays via the mutation relation of eq. (3.35) can in fact be obtained from the cluster algebra itself, as was also done for example in [73]. Consider a cluster algebra $\mathscr{A} = \mathscr{A}(\boldsymbol{a}_0, \boldsymbol{y}_0, B_0)$ with ambient field $\mathcal{F}$ and cluster-tropical semifield $\mathbb{P}$. The *dual* $\mathscr{A}^\vee$ of this cluster algebra is defined as the cluster

algebra with the same ambient field and cluster-tropical semifield obtained by flipping the arrows of the initial quiver, that is $\mathscr{A}^\vee = \mathscr{A}(\boldsymbol{a}_0^\vee, \boldsymbol{y}_0^\vee, -B_0)$, whereas $\boldsymbol{a}_0^\vee = \boldsymbol{a}_0$ and $\boldsymbol{y}^\vee = \big((y_1)^{-1}, \dots, (y_r)^{-1}\big)$, and again we drop the label t_0 for the variables of the initial seed.

As was shown in [159] for the case of principal coefficients, the cluster variables of the dual cluster algebra are the same as those of the original cluster algebra, that is $\mathcal{A}^\vee = \mathcal{A}$. However, when expressing the cluster variables in the factorised form of eq. (3.32) with respect to the dual coefficients $\boldsymbol{y}^\vee$ and $\mathcal{X}$-variables $\boldsymbol{x}^\vee$ of the initial seed, we get a different $\boldsymbol{g}$-vector associated to the cluster variable.

For example, in the case of the A_2 cluster algebra, we first notice that in the initial seed we have

$$x_1^\vee = a_2 (y_1)^{-1} \equiv (x_1)^{-1}\,, \quad x_2^\vee = (a_1)^{-1}(y_2)^{-1} \equiv (x_2)^{-1}\,. \tag{3.37}$$

Furthermore, after the mutation $t_0 \xrightarrow{1} t_1$, the mutated cluster variable $a_{1;1}$ is given by

$$a_{1;1}^\vee = \frac{1 + y_1^\vee a_2^\vee}{a_1^\vee (1 \hat{\oplus}\, y_1^\vee)} = \frac{1}{a_1^\vee} \cdot \frac{1 + x_1^\vee}{1 \hat{\oplus}\, y_1^\vee}\,. \tag{3.38}$$

First of all, substituting $\boldsymbol{a}_0^\vee = \boldsymbol{a}$, $\boldsymbol{y}^\vee = (y_1^{-1}, y_2^{-1})$, and $\boldsymbol{x}^\vee = (x_1^{-1}, x_2^{-1})$, it is easy to see that this is indeed the same variable as before, since

$$\frac{1}{a_1^\vee} \cdot \frac{1 + x_1^\vee}{1 \hat{\oplus}\, y_2^\vee} = \frac{1}{a_1} \left[\frac{1 + x_1}{x_1}\right] \left[\frac{1 \hat{\oplus}\, y_1}{y_1}\right]^{-1} = \frac{a_2}{a_1} \cdot \frac{1 + x_1}{1 \hat{\oplus}\, y_1} \equiv a_1 \tag{3.39}$$

and since $y_1 x_1^{-1} = a_2$. Furthermore, from eq. (3.38) it also follows that the $\boldsymbol{g}$-vector associated to the dual variable $a_{1;1}^\vee$ is given by $\boldsymbol{g}_{1;1}^\vee = (-1, 0)$, which is the same as the cluster ray of the variable $a_{1;1}$, see table 3.2.

Finally, in the dual cluster algebra, we can also find an interpretation for the, suggestively named, coefficient matrix. The coefficients of the cluster t_1 after the mutation $t_0 \xrightarrow{1} t_1$ are given by

$$y_{1;1}^\vee = (y_1^\vee)^{-1}\,, \quad y_{2;1}^\vee = y_2^\vee (1 \hat{\oplus}\, y_1^\vee)\,. \tag{3.40}$$

Noting that the F-polynomials are given by $F_{1;1}^\vee(u_1, u_2) = 1 + u_1$ and $F_{2;1}^\vee(u_1, u_2) = 1$, respectively, we can rewrite the coefficients as

$$y_{j;1}^\vee = (y_1^\vee)^{c_{1j;1}} (y_2^\vee)^{c_{2j;1}} \prod_{i=1}^{2} F_{i;t}^\vee|_{\mathbb{P}}(y_1^\vee, y_2^\vee)^{b_{ij;1}^\vee}\,, \tag{3.41}$$

whereas $b_{ij;1}^\vee$ denotes the components of the adjacency matrix $B_{t_1}^\vee$ and $c_{ij;1}$ the components of the coefficient matrix obtained from the mutation rule of eq. (3.34) and given in table 3.2. In fact, this relation is general and can be used as a definition for the coefficient matrix, which plays the analogous role of the $\boldsymbol{g}$-vectors for the coefficients.

To summarise, the coefficient matrix and cluster rays we have defined recursively via mutation relations are in fact the coefficient matrix and $\boldsymbol{g}$-vectors of the dual cluster algebra, respectively, see eg. [165] for more details on the duality of cluster properties. For our purposes, however, the prescription via the ray mutation rule of eq. (3.35) is much better suited as the rays can be computed via matrix manipulation, which is much faster than the algebraic calculations required when using mutations in the dual cluster algebra.

3.1.3. Convex geometry: polytopes and fans

In the previous section we have defined the cluster rays, half lines that are emanating from the origin, which are in a one-to-one association to the cluster variables. In the example of the A_2 cluster algebra, we have seen that these cluster rays split up the ambient space $\mathbb{R}^2$ into regions that are uniquely labelled by the clusters of the cluster algebra. Before we proceed to discuss this and other geometric structures associated to cluster algebras, we first review some basics of convex geometry. The reader that is already familiar with this content may skip the section. For a more detailed introduction to the topic, see eg. [166].

While some of the following discussions might appear trivial, they are included for completeness and in order to make this work self-contained. Also, while geometric intuition allows to easily see many of the properties of the geometric objects considered here when restricted to three dimensions, precise definitions are required to make use of them in arbitrary dimensions. We begin by introducing a few basic notions that lead to the definition of a polytope, which intuitively can be described as a geometric object with flat faces. First of all, we define the notion of convexity.

Definition 3.27 (Convex set)**.** A set of points $K \subset \mathbb{R}^d$ is *convex*, if for any two points $\boldsymbol{x}, \boldsymbol{y} \in K$ the straight line $\{\lambda \boldsymbol{x} + (1-\lambda)\boldsymbol{y} : 0 \leq \lambda \leq 1\}$ between the points is completely contained within the set K.

Definition 3.28 (Convex hull)**.** Given a set of points $K \subset \mathbb{R}^d$, its convex hull $\mathrm{conv}(K)$ is the smallest convex set that contains K. It can be constructed as

$$\mathrm{conv}(K) = \bigcap \left\{ \tilde{K} \subset \mathbb{R}^d : K \subset \tilde{K}\,,\ \tilde{K} \,\mathrm{convex} \right\}\,, \tag{3.42}$$

that is as the intersection of all convex sets that contain K.

Example 3.29 (Convex hull of finite set)**.** Consider for example a finite set $K = (\boldsymbol{u}_1, \ldots, \boldsymbol{u}_r) \subset \mathbb{R}^d$. Its convex hull is given by

$$\mathrm{conv}(K) = \left\{ \lambda_1 \boldsymbol{u}_1 + \cdots + \lambda_r \boldsymbol{u}_r : \lambda_i \geq 0\,,\ \sum_{i=1}^{r} \lambda_i = 1 \right\}\,. \tag{3.43}$$

To see this, first note that the right hand side of this equation is convex by construction and contains any of the points $\boldsymbol{u}_i \in K$ as its extreme point with $\lambda_i = 1$. Consequently, by the definition of eq. (3.42), this proves that $\mathrm{conv}(K)$ is contained within the right hand side of the equality. On the other hand, the right hand side of the equation is contained in $\mathrm{conv}(K)$, which can be proven inductively by noting that we may write

$$\sum_{i}^{r} \lambda_i \boldsymbol{u}_i = (1-\lambda_k) \left(\sum_{i}^{r-1} \frac{\lambda_i}{1-\lambda_k} \boldsymbol{u}_i \right) + \lambda_k \boldsymbol{u}_k\,, \tag{3.44}$$

when $\lambda_k < 1$. One example for the convex hull of a finite set of points in $\mathbb{R}^2$ is depicted in figure 3.8.

As the example depicted in figure 3.8 already suggests, it is this notion of the convex hull of a finite set of points that gives rise to the definition of a polytope in $\mathbb{R}^d$.

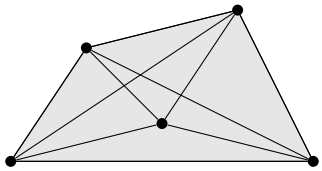

Figure 3.8: Example for the convex hull (shaded area) of a set of five points (black dots) in $\mathbb{R}^2$.

Definition 3.30 (Polytope from points)**.** A *convex polytope* P is the convex hull of a finite set of points $K = \{\boldsymbol{u}_1, \ldots, \boldsymbol{u}_r\}$ in $\mathbb{R}^d$, that is

$$P = \mathrm{conv}(K)\,. \tag{3.45}$$

The points $\boldsymbol{u}_i$ are the *extreme points* of the polytope. Note that we restrict our attention to convex polytopes and will thus omit the term convex from now on.

Alternatively, one can make the intuition of a polygon as the collection of flat surfaces precise and show that polytopes can equivalently be described in terms of hypersurfaces. A *half-space* is the region in $\mathbb{R}^d$ that is defined by an inequality $\lambda_1 \boldsymbol{x}_1 + \cdots + \lambda_d \boldsymbol{x}_d \leq z$ for some constant $z \in \mathbb{R}$ and coordinates $\boldsymbol{x}_i$ of $\mathbb{R}^d$. The hypersurface that splits $\mathbb{R}^d$ into the half-space and its complement is given by the points where the inequality becomes an equality. With this terminology, it can be proven that a polytope can equivalently be defined as follows.

Proposition 3.31 (Polytope from inequalities)**.** *A polytope can equivalently be described as the solution to a system of linear inequalities,*

$$P = \left\{\boldsymbol{x} \in \mathbb{R}^d : A\boldsymbol{x} \leq \boldsymbol{z}\right\}\,, \tag{3.46}$$

given by a matrix $A \in \mathbb{R}^{r\times d}$ *and constant* $\boldsymbol{z} \in \mathbb{R}^r$.[8]

Example 3.32. Consider the three half-spaces in $\mathbb{R}^2$ defined by the inequalities $x_1 \geq 0$, $x_2 \geq 0$, and $x_1 + x_2 \leq 0$. The intersection of these half-spaces forms the polygon depicted in fig. 3.9. As one can immediately see, the polygon is bounded by its faces, the intersections of the polygon with the hypersurfaces defined by those points, where the above inequalites become equalities. Similarly, the vertices of the polygon are given by the intersection of these hypersurfaces. Equivalently, the polygon could be defined as the convex hull of these vertices.

Remark 3.33. Note that for a generic collection of half-spaces the thus defined polytope might not be bounded, as one can immediately see by removing one of the half-spaces in the above example. All polytopes relevant to this work, however, are bounded such that we do not discuss this issue further.

[8] Note that inequalities of the form $A\boldsymbol{x} \geq \boldsymbol{z}$ are also covered by this definition by considering $A'\boldsymbol{x} \leq \boldsymbol{z}'$ with $A' = -A$ and $\boldsymbol{z}' = -\boldsymbol{z}$.

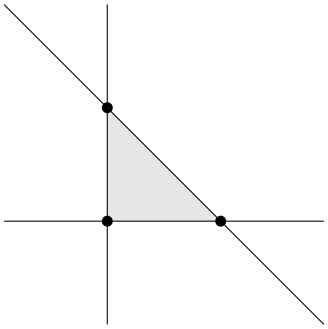

Figure 3.9: Example of a polytope (shaded area) defined as the intersection of half-spaces.

Using the description of a polytope in terms of hypersurfaces, we can discuss its boundary structure, the *faces*, as well as their dimensionality. Using the intuition that hypersurfaces form the boundaries of polytopes, we first define their faces as follows.

Definition 3.34 (Faces)**.** Consider a convex polytope $P \subset \mathbb{R}^d$. A linear inequality of the form $\boldsymbol{a} \cdot \boldsymbol{x} \leq z$ for $\boldsymbol{a} \in \mathbb{R}^d$ and $z \in \mathbb{R}$ on the coordinates $\boldsymbol{x} \in \mathbb{R}^d$ is *valid* for P, if it is satisfied for all points $\boldsymbol{u} \in P$. A *face* F of P is the set

$$F = P \cap \{\boldsymbol{x} \in \mathbb{R}^d : \boldsymbol{a} \cdot \boldsymbol{x} = z\}\,, \tag{3.47}$$

for some valid inequality $\boldsymbol{a} \cdot \boldsymbol{x} \leq z$. By specifying $\boldsymbol{a} = \boldsymbol{0}, z = 0$, we see that P itself is a face of P as well as the empty set $\emptyset$. The other, non-trivial faces are sometimes referred to as *proper faces*.

In the obvious way, we define the dimension of a face as the dimension of the linear subspace it generates,[9] which similarly applies to the dimension of the polytope itself. We also refer to a face of dimension p as a p-face of the polytope. In the obvious way, this also defines the codimension of any face as the codimension of its linear subspace.[10] The 0-faces of a d-dimensional polytope $P \subset \mathbb{R}^d$ are referred to as its *vertices*, the 1-faces as its *edges*. The codimension-0 or d-face is the polytope itself, while the codimension-1 or $(d-1)$-faces are referred to as *facets*.

Example 3.35. Continuing the previous example, it is easy to see that the dimension of the polytope is 2. Furthermore, the inequalities $x_2 \leq 1$ and $x_2 \geq 0$ are both valid for P with the resulting faces given by the vertex $\{(0,1)\}$ and the line segment $\{(\lambda, 0) : 0 \leq \lambda \leq 1\}$,

[9] More rigorously, since a face itself is bounded and thus not a proper vector space, we make use of the *affine hull*, which is defined for any set $K \in \mathbb{R}^d$ as

$$\mathrm{aff}(K) = \left\{ \lambda_1 \boldsymbol{u}_1 + \cdots + \lambda_r \boldsymbol{u}_r : r \geq 1\,,\, \boldsymbol{u}_i \in K\,,\, \sum_{i=1}^{r} \lambda_i = 1 \right\}\,, \tag{3.48}$$

that is as the set of affine linear combinations of points in K. It is easy to see that this is indeed a linear subspace of $\mathbb{R}^d$, allowing us to define the dimension of a face as the dimension of its affine hull.

[10] The codimension of a linear subspace essentially corresponds to the dimension of the orthogonal complement to that subspace.

respectively, which are depicted in figure 3.10. The linear subspace of the vertex is a single point and thus of dimension 0, the subspace of the line segment is of dimension 1.

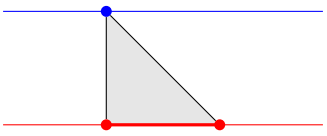

Figure 3.10: Examples for faces of the polytope constructed in the previous example 3.32.

With the notions of faces of a polytope and their dimension, we can introduce one further special class of polytopes, the *simple polytopes*. As it will turn out, all polytopes that are of relevance to the amplitudes of interest in this work are of this type.

Definition 3.36 (Simple polytope)**.** Given a polytope P of dimension d. If each of its vertices is adjacent to exactly d edges, that is if each 0-face has non-empty intersections with exactly d 1-faces, the polytope is called *simple*. Equivalently, each vertex is contained in exactly d facets of the polytope.

Beyond the geometric properties of polytopes, they also encode combinatorial information such as the number and adjacency of its faces. The main object to discuss these properties is the *face lattice*, defined as follows.

Definition 3.37 (Face lattice)**.** Given a polytope P, its *face lattice* $L(P)$ is the set of all faces $F \in P$. Set inclusion of lower-dimensional faces into higher-dimensional ones, such as eg. a vertex that is contained in one of its adjacent edges, forms a partial order[11] on the face lattice, which correspondingly is a partially ordered set.

Definition 3.38 (Combinatorial equivalence)**.** Two polytopes P, P' are considered to be *combinatorially equivalent* if there exists a function ϕ that bijectively maps the faces of $F \in P$ to faces $F' \in P'$ while being compatible with the inclusion relation, that is

$$\phi(F_1 \subset F_2) = \phi(F_1) \subset \phi(F_2)\,. \tag{3.49}$$

In this sense, ϕ is a lattice isomorphism between the face lattices of P and P'.

Restricting the face lattice of a polytope to its vertices and edges, we obtain an undirected graph $G(P)$, that is referred to as the *polytope graph* or its *1-skeleton*. It turns out that this graph completely captures the combinatorial structure in the form of the face lattice of a simple polytope, as is demonstrated by the following theorem.

Theorem 3.39 (Blind, Mani [167], Kalai [168])**.** *Consider two simple polytopes P, P'. If their polytope graphs are isomorphic,[12] the polytopes are combinatorially equivalent, that is their full face lattices are isomorphic as well.*

[11] In contrast to a total ordering, a partial ordering is an operation $\leq$ on a set S that is reflexive ($x \leq x$ for all $x \in S$), transitive (if $x \leq y$ and $y \leq z$ then $x \leq z$), and antisymmetric (if $x \leq y$ and $y \leq x$ then $y = x$), but is not required to be strongly connected (for all $x, y \in S$ we have $x \leq y$ or $y \leq x$.)

[12] Two graphs are isomorphic if there exists a bijective map between their vertices and edges that respects the connectivity among them.

Remark 3.40. In this way, we can consider a d-regular graph[13] g as an abstract definition for a simple d-dimensional polytope and refer to any polytope P in the form of definition 3.30 or proposition 3.31 with $G(P) = g$ as the *polytopal realisation* of that abstract polytope.

Example 3.41. We consider again the polytope constructed in example 3.32. Its face lattice is depicted in figure 3.11 as a Hasse diagram. In this diagram, each face F of the face lattice is a vertex and is connected by an edge going upward to a vertex G if $F \subset G$. The faces are labelled by the vertices of the polytope that are contained in that face, such that eg. the entire polytope is labelled as $P = (a, b, c)$. Clearly, the polytope graph consists

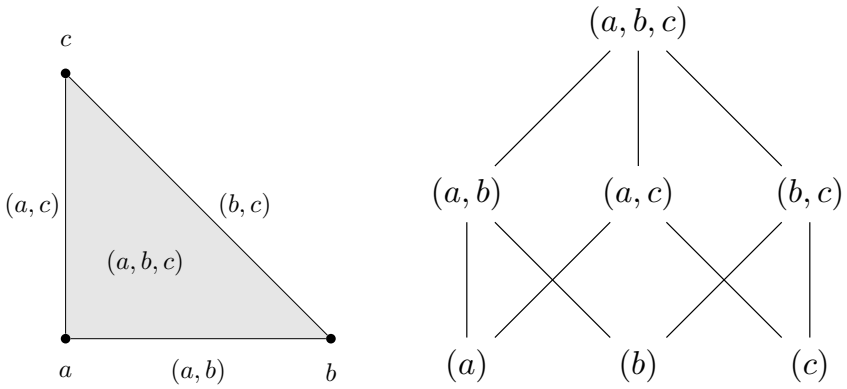

(a) polytope (b) face lattice

Figure 3.11: Face lattice (b) of the triangle (a) drawn as a Hasse diagram. The faces are labelled by the vertices a, b, c that are contained in that face.

of the bottom two layers of the face lattice as depicted in the figure.

As we will see in the following sections, see especially section 3.1.4, it is often beneficial to describe the geometric structures for example associated to cluster algebras in terms of another, dual object: a *fan*. To define it, first consider the following definition of its building blocks, the *convex cones*.

Definition 3.42 (Convex cone)**.** A *convex cone* is a nonempty set of vectors $C \subset \mathbb{R}^d$ that is closed under linear combinations with positive coefficients. The *conical hull* or positive span $\text{cone}(K)$ of a subset $K \subset \mathbb{R}^d$ is the intersection of all cones containing K or equivalently

$$\text{cone}(K) = \{\lambda_1 \boldsymbol{u}_1 + \cdots \lambda_r \boldsymbol{u}_r : r \geq 1\,,\, \boldsymbol{u}_i \in K\,,\, \lambda_i \geq 0\}\,. \tag{3.50}$$

Any conical hull $\text{cone}(K)$ is itself a cone and contains the origin $\mathbf{0} \in \text{cone}(K)$ and is thus also referred to as the cone of K. The cone of the empty set is defined to be $\{\mathbf{0}\}$.

For example, the cone of a single vector is the half-line emanating from the origin, and pointing in the direction of that vector, see figure 3.12 for an example. Such a half-line is

[13] A d-regular graph is a graph where each vertex is connected to exactly d edges.

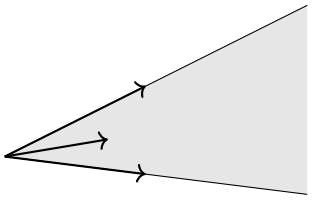

Figure 3.12: The cones obtained from the vectors $(8,4)$, $(6,1)$, and $(8,-1)$ are the rays (black lines) pointing in the direction of the vectors, respectively. The cone obtained from these rays (or equivalently the vectors) corresponds to the shaded area.

referred to as a *ray*. Furthermore, the cone of any finite set K of rays given in terms of the vectors $\{\boldsymbol{u}_1, \ldots, \boldsymbol{u}_r\} \subset \mathbb{R}^d$ can also be written as

$$\text{cone}(K) = \{\lambda_1 \boldsymbol{u}_1 + \cdots + \lambda_r \boldsymbol{u}_r : \lambda_i \geq 0\} \,. \tag{3.51}$$

In terms of the matrix $\mathcal{K} \in \mathbb{R}^{d\times r}$ whose columns are the vectors $\boldsymbol{u}_i$, this could also be written as $\text{cone}(K) = \mathcal{K}\mathbb{R}^r_{\geq 0}$, namely the image of the multiplication of $\mathcal{K}$ with vectors from $\mathbb{R}^r_{\geq 0}$. Consequently, the dimension of such a cone is given by the rank of the matrix $\mathcal{K}$. In what follows, we will only consider cones that are spanned by rays in this way and consequently not distinguish any further.

Similar to the faces of a polytope, a face F of a cone $C \subset \mathbb{R}^d$ is the intersection of the cone with a hypersurface defined by $\boldsymbol{a} \cdot \boldsymbol{x} = 0$ for $\boldsymbol{a} \in \mathbb{R}^d$ and the coordinates $\boldsymbol{x} \in \mathbb{R}^d$, such that the inequality $\boldsymbol{a} \cdot \boldsymbol{x} \leq 0$ is valid for C, that is it is satisfied by all points in C. It is easy to see that the face of a cone is itself a cone, since the hypersurface is closed under arbitrary linear combinations. Furthermore, for a cone given as the positive span of some rays, the positive span of any subset of rays that are not in the interior of the cone forms a face of that cone. Finally, one can convince oneself that the converse is also true. Namely, for a cone spanned by a finite set of rays, any face is given as the positive span of some subset of the rays.[14]

In a somewhat analogous way to the organisation of the faces of a polytope in its face lattice, we define a fan as a specific collection of cones as follows.

Definition 3.43 (Fan)**.** A fan $\mathcal{F}$ in $\mathbb{R}^d$ is a collection of cones

$$\mathcal{F} = \{C_1, \ldots, C_r\} \,, \tag{3.52}$$

with $C_i \subset \mathbb{R}^d$ nonempty, such that

[14] To see this, consider the intersection F of a valid hypersurface $H = \{\boldsymbol{a} \cdot \boldsymbol{x} = 0\}$ with a cone $C = \text{cone}(\boldsymbol{u}_1, \ldots, \boldsymbol{u}_r)$ spanned by rays $\boldsymbol{u}_i$. Arrange the rays such that the subset of rays contained in H is given by $u_1, \ldots, u_l$ for some $l \geq 0$. Obviously, the positive span of these rays is contained in both, C and H. On the other hand, some point $\boldsymbol{u} \in C \cap H$ can be written as $\boldsymbol{u} = \sum_i \lambda_i \boldsymbol{u}_i$ with $\lambda_i \geq 0$ and satisfies $\sum_{i=1}^r \lambda_i \boldsymbol{a} \cdot \boldsymbol{u}_i = 0$. Since the first l of the rays are contained in H, this simplifies to $\sum_{i=l+1}^r \lambda_i \boldsymbol{a} \cdot \boldsymbol{u}_i = 0$ whereas for $l+1 \leq i \leq r$ we have that $\boldsymbol{a} \cdot \boldsymbol{u}_i < 0$. Consequently, this can only hold when $\lambda_i = 0$ for $l+1 \leq i \leq r$, such that $\boldsymbol{u} \in \text{cone}(\boldsymbol{u}_1, \ldots, \boldsymbol{u}_l)$.

1. the intersection of any two cones in $\mathcal{F}$ is a face of both, and

2. each nonempty face of a cone in $\mathcal{F}$ is also a cone in $\mathcal{F}$.

If the union of all cones of the fan covers the entire ambient space $\mathbb{R}^d$, that is $\bigcup \mathcal{F} = \mathbb{R}^d$, the fan is said to be *complete*. By the second property, we refer to the p-dimensional cones of the fan also as its p-faces. We say that a fan is *simplicial* if all of its cones are *simplicial*, that is they are spanned by linearly independent vectors.

From this definition, it is easy to see that a single cone $C \subset \mathbb{R}^d$ together with all of its faces, which themselves are cones, forms a fan in $\mathbb{R}^d$.

Similar to the faces of a polytope, the fan consists of many cones that are contained within each other. In the obvious way, we say that two fans are combinatorially equivalent, if there exists a bijection between their cones that is compatible with the two axioms of the above definition. Some of the combinatorics of this data is encoded by the so-called *f-vector*, which is defined as follows.

Definition 3.44 (f-vector)**.** Given a fan $\mathcal{F}$ in $\mathbb{R}^d$, its f-vector $f \in \mathbb{Z}^d_{\geq 0}$ is the vector

$$f = (f_1, \ldots, f_d)\,, \tag{3.53}$$

whereas the component f_i counts the number of i-faces or i-dimensional cones in $\mathcal{F}$. Note that f_1 is the number of rays and f_d the number of cones in the fan.

To give some concrete realisations and to define the special classes of fans we will encounter in this work, we next consider the following two examples.

Example 3.45 (Normal fan)**.** One important example for convex fans are the *normal fans*, that can be obtained for any polytope $P \in \mathbb{R}^d$. Albeit not the most rigorous construction, for our purposes it is sufficient to first construct one cone for each of the vertices obtained as the positive span of the vectors that are normal to the facets that contain this vertex. The normal fan is then obtained as the collection of these cones as well as their intersections.[15] See also figure 3.13 for an example. By construction, it is dual to the polytope in the sense that each d-face (full-dimensional cone) of the fan corresponds to a 0-face (vertex) of the polytope, each $(d-1)$-face of the fan (facet) corresponds to a 1-face (edge) of the polytope, and so on. Note that the normal cones for each vertex do not overlap due to the convexivity of the polytope. If the polytope were not convex, it could contain inward pointing vertices such that some of the normal cones might intersect in their interior.

Example 3.46 (Fan from hypersurface arrangement)**.** Consider a finite set of hypersurfaces $\{H_1, \ldots, H_r\}$ through the origin, given by $H_i = \{\boldsymbol{x} \in \mathbb{R}^d : \boldsymbol{a}_i \cdot \boldsymbol{x} = 0\}$ for some $\boldsymbol{a}_1, \ldots, \boldsymbol{a}_r \in \mathbb{R}^d$. In the obvious way, these hypersurfaces split up $\mathbb{R}^d$ into several regions, each containing the origin. It can be shown that these regions are in fact convex cones,

[15] This construction can be made precise and proven to be a fan by the notion of a *normal cone* that is attached to each proper face of the polytope. In fact, instead of taking the intersections of the cones constructed from the vertices of the polytope, one would construct such cones for every proper face and then prove that the set of all such cones indeed is a fan.

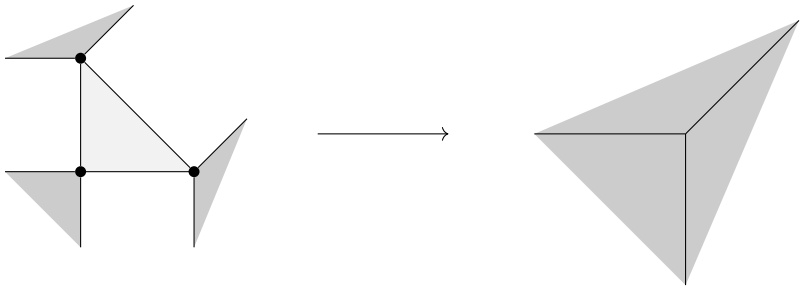

Figure 3.13: Construction of the normal fan (on the right, dark gray) of the polytope (on the left, light gray) of the previous example 3.32.

spanned by the rays which are obtained as the 1-dimensional intersections of $(d-1)$ linearly independent hypersurfaces.[16] In this way, the hypersurfaces form a complete fan in $\mathbb{R}^d$. Note that we could also consider hypersurfaces that are (partially) bounded by adding inequalities to their definition, see also example 3.49 and figure 3.14.

Before we conclude this section, we discuss one final concept. As we will see later on, especially in section 4.2, the triangulation of a fan by another fan is a crucial step in the construction of the symbol alphabet for the amplitudes of interest. Roughly speaking, a fan $\mathcal{F}$ triangulates another fan $\mathcal{G}$ if it is simplicial[17] and splits up the cones of $\mathcal{G}$ into smaller cones without $\mathcal{G}$ splitting up the cones of $\mathcal{F}$.[18] In the following definitions, we state what we understand as triangulation in the remainder of this work.

Definition 3.47 (Common refinement)**.** Given two fans $\mathcal{F}, \mathcal{G}$ in $\mathbb{R}^d$, their *common refinement* is defined as

$$\mathcal{F} \wedge \mathcal{G} = \left\{ C \cap C' : C \in \mathcal{F}\,,\, C' \in \mathcal{G} \right\}\,, \tag{3.54}$$

that is as the collection of the intersections of all cones of $\mathcal{F}$ and $\mathcal{G}$.

Definition 3.48 (Triangulation)**.** We say that a fan $\mathcal{F}$ in $\mathbb{R}^d$ *triangulates* a fan $\mathcal{G}$ in $\mathbb{R}^d$ if $\mathcal{F}$ is simplicial and satisfies

$$\mathcal{F} \wedge \mathcal{G} = \mathcal{F}\,, \tag{3.55}$$

that is if the common refinement of both fans is given by $\mathcal{F}$.

Clearly, in this definition any simplicial fan $\mathcal{F}$ in $\mathbb{R}^d$ triangulates itself. Furthermore, if the common refinement of two fans is simplicial, it triangulates both of these fans. Note that when dropping the requirement for $\mathcal{F}$ to be simplicial, we could say that a fan satisfying eq. (3.55) *refines* the fan $\mathcal{G}$. In this way, the common refinement of any two fans is a refinement of those two fans. Note also that the common refinement of a fan with another fan that is not complete is itself not complete. In this sense, our notion of triangulation

[16] Linear independence of hypersurfaces in this case means the linear independence of their normal vectors.
[17] With a simplicial cone being the higher-dimensional generalisation of the triangle.
[18] The last statement can also be phrased as the condition that each p-dimensional cone of $\mathcal{F}$ is contained in at most one p-dimensional cone of $\mathcal{G}$.

might differ from other definitions, in that it does not require the triangulating fan to be complete such that it might cover only parts of the triangulated fan.

Consider also the following two examples that visualise these abstract definitions.

Example 3.49 (Common refinement)**.** In figure 3.14, examples for two fans $\mathcal{F}$ and $\mathcal{G}$ in $\mathbb{R}^3$ obtained from hypersurface arrangements are illustrated. The f-vectors of these fans are given by

$$f_{\mathcal{F}} = (6, 12, 8)\,, \quad f_{\mathcal{G}} = (7, 15, 10)\,. \tag{3.56}$$

To obtain the fan $\mathcal{G}$, depicted on the right hand side in this figure, we include the hypersurface defined by $x_2 - x_3 = 0$ which is bounded by the condition $x_2 \geq 0$. Both of these fans are complete and simplicial, since each of their cones is spanned by three linearly independent vectors. The common refinement $\mathcal{F} \wedge \mathcal{G}$ is depicted in the center of the figure.

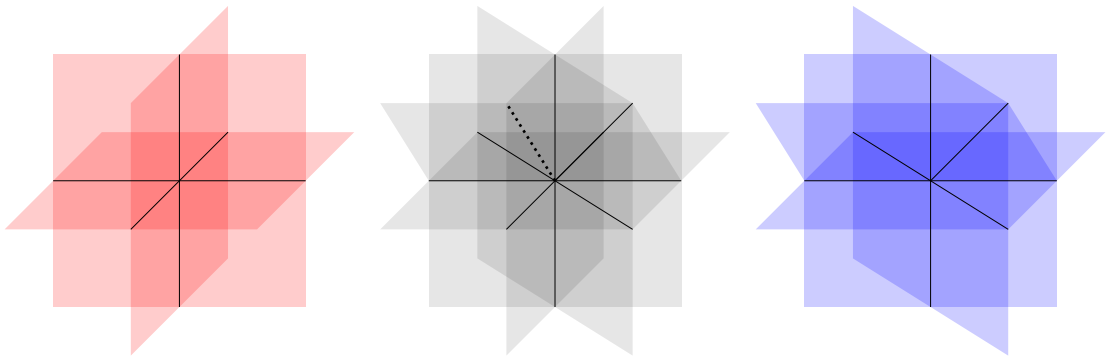

(a) $\mathcal{F}$ (b) $\mathcal{F} \wedge \mathcal{G}$ (c) $\mathcal{G}$

Figure 3.14: Examples for two fans $\mathcal{F}, \mathcal{G}$ obtained from hypersurface arrangements in (a) and (c). The fan $\mathcal{G}$ contains a hypersurface that is bounded by $x_2 \geq 0$. The common refinement $\mathcal{F} \wedge \mathcal{G}$ is depicted in (b). The dotted ray in there is a new ray, which is not included in either $\mathcal{F}$ or $\mathcal{G}$. Note that the common refinement is not simplicial.

Interestingly, even though the two fans consist of a total of 9 unique rays, the f-vector of the common refinement is given by

$$f_{\mathcal{F}\wedge\mathcal{G}} = (10, 23, 15)\,, \tag{3.57}$$

that is the common refinement contains a new ray that is not present in either $\mathcal{F}$ or $\mathcal{G}$. Also, the common refinement contains a cone that is spanned by four rays and is thus not simplicial. This demonstrated that the common refinement is a more intricate operation than just collecting the cones of both fans.

Example 3.50 (Triangulation)**.** In figure 3.15, we illustrate again the fan $\mathcal{F}$ together with another fan $\mathcal{F}'$ in $\mathbb{R}^3$, consisting of 9 rays and 14 cones, that triangulates the former. To see this note that each maximal cone of $\mathcal{F}'$ is completely contained within one cone of $\mathcal{F}$ and splits its (already simplicial) cones into smaller simplicial cones. Finally, as we will also encounter later on, we see that the triangulation of $\mathcal{F}$ by $\mathcal{F}'$ contains what we refer

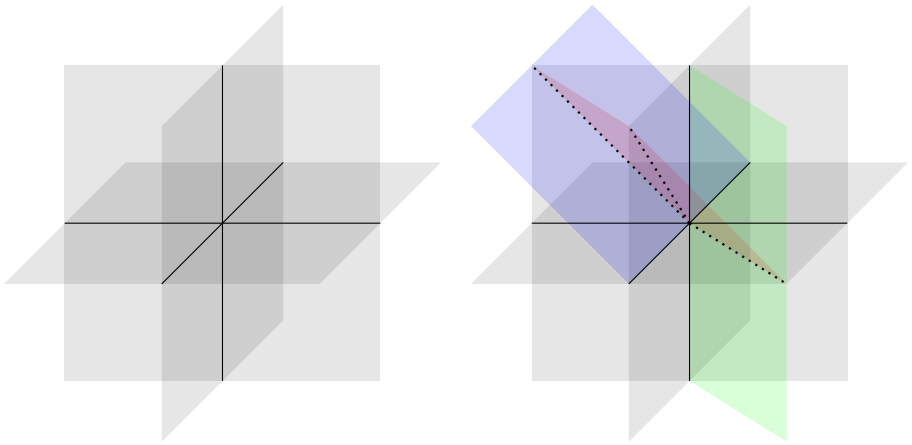

(a) $\mathcal{F}$ (b) $\mathcal{F}'$

Figure 3.15: Example for a fan in (b) that triangulates the fan $\mathcal{F}$ in (a). The dotted rays are redundant, since they are not rays of $\mathcal{F}$.

to as *redundant rays*, rays of $\mathcal{F}'$ that are not rays of $\mathcal{F}$. These rays are located on the intersection of less than $(d-1)$ linearly independent hypersurfaces of $\mathcal{F}$ and are depicted as dotted lines in the figure.

3.1.4. Cluster polytope & fan

We have paused the discussion of cluster algebras with coefficients in section 3.1.2 at the review of the cluster rays and the resulting structure that is obtained by collecting all rays at the origin of $\mathbb{R}^r$, with r the rank of the cluster algebra, to first set the stage of convex geometry in section 3.1.3. With these foundations laid out, we can now look back at the right hand side of figure 3.7. As might have become obvious by now, this collection of cluster rays indeed forms a complete fan in $\mathbb{R}^2$. Furthermore, we can recognize the same fan on the right hand side of figure 3.15 embedded on the hypersurface defined by $x_3 = 0$. Finally, the exchange graph of a cluster algebra consisting of its clusters as vertices and mutations as edges closely resembles what we have introduced in the previous section as the graph of a polytope. In this section, we introduce and define the cluster polytope and cluster fan that make these observations precise.

In [169], the authors demonstrated that the $\boldsymbol{g}$-vectors of a finite cluster algebra do form a fan, see also eg. [170, 171]. Using the cluster rays we have introduced in section 3.1.2, we correspondingly define the *cluster fan* as follows.

Definition 3.51 (Cluster fan)**.** Given a cluster algebra of rank r, we define a cone for each of its clusters as the positive span of the cluster rays of the variables of that cluster. The *cluster fan* is defined as the common refinement of all those cones, which is a fan in $\mathbb{R}^r$.

In fact, the cones defined for every cluster as above only intersect on their boundaries (that is on their proper faces) and thus do not overlap. Furthermore, each cluster of a cluster algebra of rank r consists of exactly r cluster rays, suggesting that the cluster fan is simplicial. For finite cluster algebras, the following statement has been proven in [169].

Proposition 3.52 (Fomin, Zelevinsky [169]). *The cluster fan of a finite cluster algebra of rank r defined as above is a complete, simplicial fan in $\mathbb{R}^r$.*

Remark 3.53. Note that due to using the cluster rays, which as discussed in remark 3.26 are the $\boldsymbol{g}$-vectors of the dual cluster algebra, instead of the $\boldsymbol{g}$-vectors of the cluster algebra itself, the cluster fan is strictly speaking the fan of the dual cluster algebra. Since these two fans are combinatorially equivalent (the two cluster algebras have the same cluster variables and mutations among those variables) and we are only considering the cluster fan as defined above, we will not distinguish any further.

We have seen in the previous section that we can construct the normal fan for any polytope. Furthermore, the exchange graph of a cluster algebra is very similar to what we have seen as the polytope graph. This raises the question whether the cluster fan is the normal fan of some polytope that can be constructed for the cluster algebra. In fact, as the following theorem demonstrates, this is indeed the case.

Theorem 3.54 (Chapoton, Fomin, Zelevinsky [170]). *The cluster fan of a finite cluster algebra of rank r is the normal fan of a simple r-dimensional polytope. Its graph polytope or 1-skeleton is given by the exchange graph of the cluster algebra.*

By this theorem, we define the *cluster polytope* as the polytope obtained from the exchange graph of a cluster algebra, whose normal fan is the cluster fan. By construction, each vertex of the polytope is associated to a cluster. Two vertices are connected by an edge if the two associated clusters are connected by one mutation. In general, for a cluster algebra of rank r, a p-face of the cluster polytope is associated to the cluster subalgebra that is obtained by freezing out $r-p$ of the variables in a cluster, and can thus be labelled by the variables that are frozen out. Furthermore, such a face contains all the vertices corresponding to clusters that contain the $r-p$ cluster variables that are frozen out.

For example, the cluster subalgebra obtained by freezing out all r variables of one cluster is just the cluster itself. Correspondingly, the vertex is labelled by these r variables and associated to the cluster. The cluster subalgebra obtained by freezing one of the variables in a cluster is of rank $r-1$ and is associated to a facet of the polytope. This facet is thus associated to the one variable that is frozen out and contains all vertices corresponding to the clusters that contain this variable.

The analogous statements for the cluster fan are obtained by replacing p with $r-p$ in the above discussion. The association of the algebraic objects of a cluster algebra with its geometric realisations in the cluster polytope and fan is also summarised in table 3.3.

Finally, using the previously constructed A_2 cluster algebra as well as the A_3 cluster algebra, whose rays can be similarly obtained by the mutation rule of eq. (3.35), we visualise their cluster polytopes and fans in the following two examples.

Example 3.55 (A_2 cluster algebra). We have previously seen that the cluster algebra of A_2 Dynkin type consists of 5 cluster variables in 5 clusters. The associated cluster polytope and cluster fan are depicted in figure 3.16.

In this figure, we have highlighted the association of the algebraic objects of the cluster algebra to the geometric structures. Here, the five distinct variables of tables 3.1 and 3.2 are

Algebra	Polytope		Fan	
	Dim.	Type	Dim.	Type
Cluster	0	Vertex	r	Cone
Mutation	1	Line	$r-1$	Facet
⋮	⋮		⋮	
$\mathcal{A}$-variable	$r-1$	Facet	1	Ray
Cluster algebra	r	Polytope	0	Point ($\mathbf{0}$)

Table 3.3: Comparison of the faces of a cluster algebra of rank r, its polytope and the cluster fan.

labelled as $a_1 = a_{1;0}$, $a_2 = a_{2;0}$, $a_3 = a_{1;1}$, $a_4 = a_{2;2}$, and $a_5 = a_{1;3}$, whereas the associated cluster ray is labelled as $\boldsymbol{\rho}_i$ with $i = 1, \ldots, 5$. Using this notation, the clusters are given by $\Sigma_0 = (a_1, a_2)$, $\Sigma_1 = (a_3, a_2)$, $\Sigma_2 = (a_3, a_4)$, $\Sigma_3 = (a_5, a_4)$, $\Sigma_4 = (a_5, a_1)$, whereas we have only indicated the cluster variables for brevity. In the figure, the vertices of the polytope are labelled by the cluster variables of the associated cluster and the edges/facets by the associated cluster variable. Note that for example the facet labelled by a_5 contains the two vertices whose clusters contain that variable. Due to the low dimension, this facet also corresponds to the mutation of a_1 in the cluster (a_5, a_1) or of a_4 in the cluster (a_5, a_4), respectively. The rays of the cluster fan are the cluster rays $\boldsymbol{\rho}_i$ of the variables a_i. As can be seen by comparing the right and left hand side of the figure, $\boldsymbol{\rho}_i$ is the normal vector to the face of a_i.

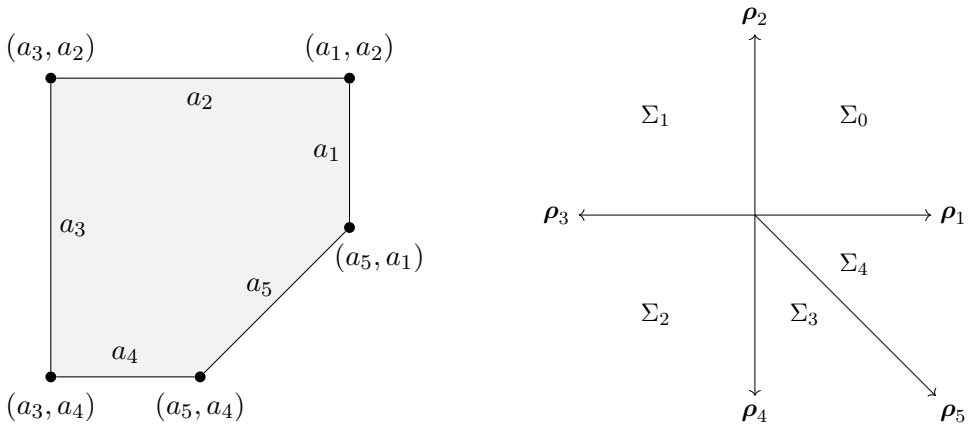

(a) cluster polytope (b) cluster fan

Figure 3.16: A polytopal realisation of the cluster polytope of the A_2 cluster algebra (a) and the corresponding cluster fan (b).

Example 3.56 (A_3 cluster algebra)**.** The cluster algebra of A_3 Dynkin type is constructed from the initial seed

$$a_1 \longrightarrow a_2 \longrightarrow a_3$$

and consists of a total of 9 cluster variables in 14 clusters. The cluster polytope correspondingly consists of 9 facets and 14 vertices, whereas the cluster fan consists of 9 rays in one-to-one association to the cluster variables that span 14 cones in one-to-one association to the clusters. Both, the cluster polytope and fan, are depicted in fig. 3.17.

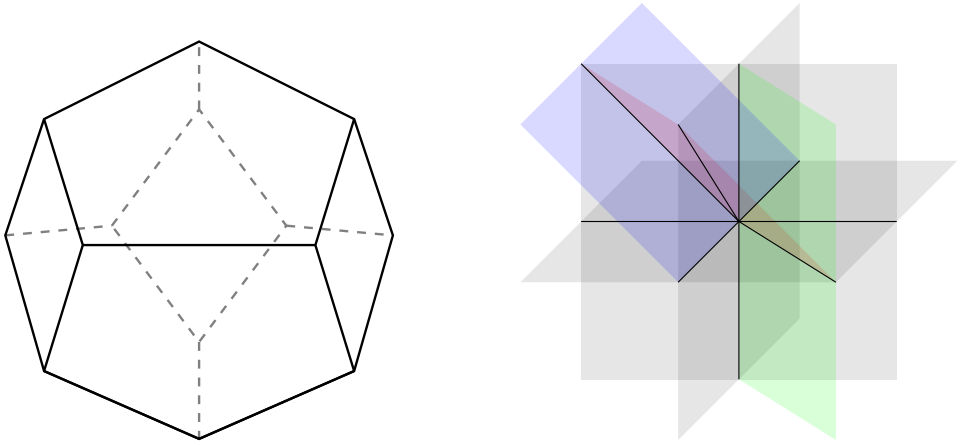

(a) cluster polytope (b) cluster fan

Figure 3.17: A polytopal realisation of the cluster polytope of the A_3 cluster algebra (a) and the corresponding cluster fan (b).

Remark 3.57 (Cluster polytope of A_n cluster algebras)**.** In fact, the cluster polytopes of the cluster algebras of A_n Dynkin type correspond to the previously known n-dimensional *associahedra*. Their face complex was first introduced by Stasheff as a tool to study the homotopy associative H-spaces [172, 173] and they were later realised to be convex polytopes [174, 175]. For this reason, the cluster polytope of any finite cluster algebra is sometimes also referred to as a *generalised associahedron*.

Remark 3.58 (Cluster fan of infinite cluster algebras)**.** So far, the construction of the cluster polytope and fan strictly speaking only applied to finite cluster algebras. One of the main reasons for us to introduce them is, however, to study infinite cluster algebras, see in particular section 3.2.4. We will not discuss the subtleties of defining a (fractal-like) polytope consisting of infinitely many faces, since we will be mostly be working with the cluster fan and only use the cluster polytope to visualise some of the results. Looking back at definition 3.43 of a fan, we see that it naturally carries over to an infinite collection of cones, as do the notions of the f-vector, refinement, and triangulation. In this way, we extend the definition of the cluster fan to also include infinite cluster algebras. Note however, that while the fan of an infinite cluster algebra is still simplicial, in contrast to finite cluster algebras it is not necessarily complete.

3.2. Cluster bootstrap

As was discussed in section 2.3, the functions that describe the BDS-like normalised MHV and NMHV amplitudes with L loops in $\mathcal{N} = 4$ pSYM are given by weight-$2L$ multiple

polylogarithms. In section 2.3.5, we reviewed how this knowledge has been used to formulate the symbol boostrap programme. In this programme, without ever resorting to explicit calculations via Feynman diagrams, one constructs the amplitude from its analytic structure by first determining its symbol alphabet, whose letters describe the singularities of the amplitude. Facilitating physical constraints or additional knowledge about the amplitude in certain kinematic regimes, the space of all possible symbols obtained from the alphabet can be reduced to obtain the symbol of the amplitude.

This, however, leaves the question with which symbol alphabet to start this construction. Remarkably, in [118] the authors observed that the alphabet of known six- and seven-particle MHV amplitudes is equivalent to the set of cluster variables of the cluster algebra of $\mathrm{Gr}(4,6)$ and $\mathrm{Gr}(4,7)$, respectively. Note that, as reviewed in 2.3.3, the kinematic space of such n-particle amplitudes is given by the quotient of $\mathrm{Gr}(4,n)$ by the torus action $(\mathbb{C}^*)^{n-1}$, see also eq. (2.93). In this way, it might not come as a surprise that further algebraic properties of the Grassmannian are relevant for the description of the amplitude.

This observation of the relation of certain cluster algebras to the symbol alphabet of n-particle scattering can be turned around and used as the starting point of the so-called *cluster bootstrap* programme. Consequently, the starting point of this work is the following conjecture, generalising from six- and seven- to the case of n-particle amplitudes.

Conjecture 3.59. *The alphabet of n-particle MHV and NMHV amplitudes in planar $\mathcal{N}=4$ super Yang-Mills theory is given by the cluster variables of the cluster algebra of* $\mathrm{Gr}(4,n)$.

Starting from this working assumption, one begins by constructing the cluster algebra of the Grassmannian $\mathrm{Gr}(4,n)$. The initial seeds of these cluster algebras are depicted in figure 3.18 in terms of the cluster and frozen variables, which are given by Plücker variables. Using the mutation rule, eq. (3.6), one then performs all possible mutations to generate the clusters of the cluster algebra as well as their cluster variables. With the set of cluster variables serving as the symbol alphabet, the amplitude itself is obtained by the symbol bootstrap procedure. That is, one first constructs all possible symbols that can be formed from the alphabet. Using physical constraints, this space is reduced to get an ansatz for the symbol of the amplitude itself. Using known values of the amplitude in certain kinematic regimes, one can finally fix the remaining ambiguities and integrate the symbol to obtain the amplitudes functional form.

There is, however, one further subtlety. As was reviewed in section 2.3.3, the amplitude is invariant under dual conformal symmetry which acts via the fundamental representation of $\mathrm{SL}(4,\mathbb{C})$ on the momentum twistors. The Plücker variables form the basic invariants under these transformations but are by themselves not projectively invariant. Consequently, the amplitude must be parameterised in terms of dual conformally invariant cross-ratios of these variables, that is coordinates of the kinematic space $\widetilde{\mathrm{Gr}}(4,n)$. This also translates to the symbol of the alphabet, with its letters being closely related to the arguments of the multiple polylogarithm describing the amplitude. Similarly, we require the alphabet to also obey the discrete symmetries of the amplitudes such as dihedral or parity symmetry.

However, the cluster variables of the cluster algebra of $\mathrm{Gr}(4,n)$ are coordinates on the

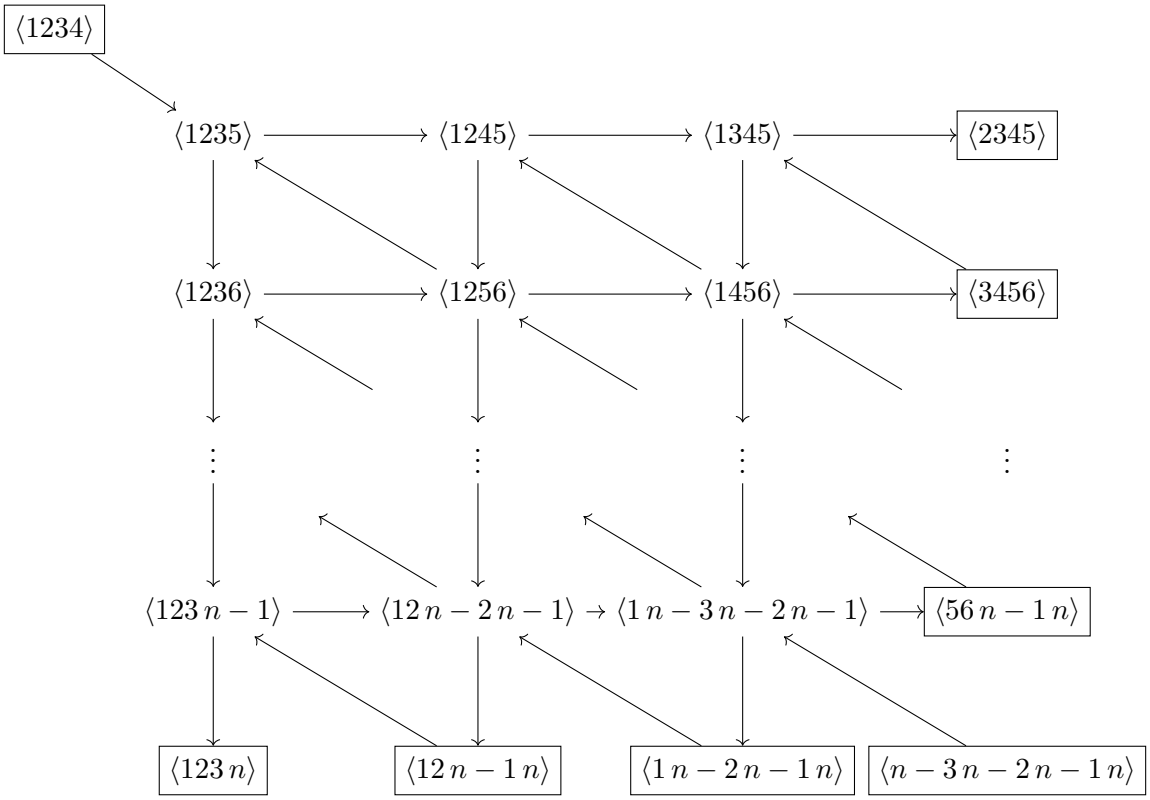

Figure 3.18: Initial seeds of the cluster algebras of $\mathrm{Gr}(4,n)$. The boxed variables are frozen and hence not mutated.

Grassmannian and not the kinematic space.[19] This can already be seen from the initial seed of the cluster algebra, see figure 3.18, which demonstrates that the cluster variables of $\mathrm{Gr}(4,n)$ contain Plücker variables, which by themselves are not dual conformally invariant. In fact, as we will also discuss later on, all cluster variables of these Grassmannian cluster algebras can be expressed as polynomials of a set of (dependent) Plücker variables by making use of the Plücker relations. Consequently, we obtain the symbol alphabet of the n-particle amplitude as dual conformally invariant products of the union of $\mathcal{A}$-variables and frozen variables. The resulting alphabet is equivalent to the set of $\mathcal{A}$-variables and frozen variables up to multiplicative relations, which from the perspective of the symbol amounts to a linear change of basis.

The remainder of this section is devoted to a review of explicit results obtained from the cluster bootstrap for six- and seven-particle amplitudes. However, before we turn to these examples, in section 3.2.1 we first review the so-called *cluster adjacency* property, a powerful set of constraints for the symbol that can also be obtained from the cluster algebra. Finally,

[19] In contrast to the $\mathcal{A}$-variables, the $\mathcal{X}$-variables do form valid coordinates on $\widetilde{\mathrm{Gr}}(k,n)$. In fact, one can show that the $\mathcal{X}$-variables of the initial seed of fig. 3.18 are dual conformally invariant, since each particle label appears with the same multiplicity in both the numerator and denominator of the variable. Since all other $\mathcal{X}$-variables are rational functions of the initial ones, they are dual conformally invariant as well.

this chapter will be concluded by an observation that poses a major obstruction when applying this procedure to eight and more particles and ultimately requires a modification of conjecture 3.59, to which we turn to in section 4.2.

3.2.1. Cluster adjacency

One important class of physical constraints that allows to reduce the space of all possible symbols are the Steinmann relations. As we have already discussed in section 2.3.4, the Steinmann relations put limits on the appearance of consecutive discontinuities of the amplitude. On the level of the symbol, they determine which letters can appear in the first two slots of the symbol [51, 56]. In fact, it has been argued that instead the more strict *extended Steinmann relations* do hold [53], which extend these constraints to any two consecutive slots of the symbol.

Remarkably, in [57, 176, 177] it was discovered that the extended Steinmann relations can equivalently be described by the cluster algebra of $\mathrm{Gr}(4,n)$. More precisely, it was found that for all known cases the extended Steinmann relations are implied by the *cluster adjacency* property, as expressed by the following conjecture.

Conjecture 3.60 (Cluster adjacency)**.** *Two distinct $\mathcal{A}$-variables can appear consecutively in a symbol only if there exists a cluster where they both appear.*

Even more, for the case of six and seven particles, it was found that the extended Steinmann relations together with the first entry and integrability conditions imply the cluster adjacency property. A pair of two cluster variables appearing in a cluster together is also referred to as *admissible pair*, whereas the *neighbour set* of a cluster variable a is the set inlcuding a[20] as well as all cluster variables b such that $\{a,b\}$ is an admissible pair. With this evidence and the equivalence to the Steinmann relations and first entry conditions (together with integrability), adopting the cluster adjacency property allows to also obtain valuable structural information about the symbol from the cluster algebra, beyond just the alphabet that is obtained from the cluster variables.

Interestingly, cluster adjacency can be given a geometric interpretation by the cluster polytope (or equivalently cluster fan). First, by freezing two cluster variables that appear together in some cluster of a cluster algebra of rank r, that is an admissible pair, we obtain a rank-$(r-2)$ cluster subalgebra. This corresponds to a codimension-2 (dimension-2) face of the cluster polytope (fan). Furthermore, given a cluster variable a which is associated to a codimension-1 facet of the cluster polytope, its neighbour set can easily be seen to consist of all cluster variables b whose associated facets intersect the facet of a. This intersection precisely corresponds to the codimension-2 face associated to the (admissible) pair $\{a,b\}$.

In this way, not only the facets of the polytope, which determine the symbol alphabet, but also its lower dimensional faces have a physical significance. In fact, beyond the codimension-2 faces, it has been speculated that the cluster algebra also contains information on admissible triples of consecutive letters in the symbol. In [177], it was observed

[20] Note that cluster adjacency explicitly does not place constraints on the repeated appearance of the same cluster variable.

that the three letters of all triplets $a \otimes b \otimes c$ that appear in the symbol either all appear together in a cluster, thus corresponding to a codimension-3 face of the cluster polytope, or c can be obtained from a via one mutation and b is the $\mathcal{X}$-variable of this *mutation pair*.[21] These mutation pairs correspond to edges, or 1-faces, of the polytope, where all but one variable are frozen and the edge contains the two vertices corresponding to the clusters that contain either a or c as well as the variables that are frozen out. See also figure 3.20 for an example.

Following this observation, one might ask whether other faces of the cluster polytope of lower dimension place further constraints on the structure of the letters appearing in the symbol. In fact, one hint for such more general cluster adjacency properties is given by the integrability condition that the symbol satisfies. Relating consecutive entries of the symbol with each other, it transfers the cluster adjacency principle to larger consecutive sets of letters. The precise form of such a generalisation as well as its physical significance are under active research.

3.2.2. Example: $\mathrm{Gr}(4,6)$ and six-particle scattering

As described in the introduction to this section, we begin with the initial seed of the $\mathrm{Gr}(4,6)$ cluster algebra, which is depicted in figure 3.19 and, as can also be seen in the figure, is of A_3 Dynkin type. Performing all possible mutations, we obtain the nine cluster variables of

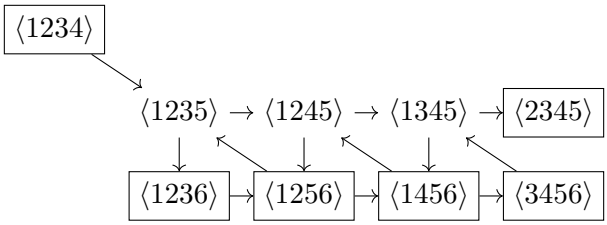

Figure 3.19: Initial seed of the cluster algebra of $\mathrm{Gr}(4,6)$.

this cluster algebra as the Plücker variables

$$\begin{aligned} a_1 &= \langle 1235\rangle\,, & a_2 &= \langle 1245\rangle\,, & a_3 &= \langle 1345\rangle\,, \\ a_4 &= \langle 1246\rangle\,, & a_5 &= \langle 1346\rangle\,, & a_6 &= \langle 1356\rangle\,, \\ a_7 &= \langle 2346\rangle\,, & a_8 &= \langle 2356\rangle\,, & a_9 &= \langle 2456\rangle\,, \end{aligned} \tag{3.58}$$

which appear in a total of 14 clusters and whereas a_1, a_2, a_3 are in the initial seed. Together with the six frozen variables $\langle 1234\rangle, \langle 2345\rangle, \langle 3456\rangle, \langle 1456\rangle, \langle 1256\rangle$, and $\langle 1236\rangle$, the set of cluster and frozen variables precisely corresponds to the 15 Plücker variables of $\mathrm{Gr}(4,6)$. Note again that, naively, the cluster variables obtained from the mutation relation, eq. (3.6), are rational functions of the (independent) variables of the initial seed. However, by using the Plücker relations, eq. (2.95), one can easily show that in this case these rational functions are equal to the Plücker variables.

[21] Note that if c is obtained as the mutation of a, the $\mathcal{X}$-variable associated to c is the inverse as that of a, which on the level of the symbol determines the sign of the term.

Since the cluster algebra is of A_3 Dynkin type, we have already seen its cluster polytope and fan in figure 3.17. To highlight the association of the cluster variables to its facets, the 3-dimensional cluster polytope of the $\mathrm{Gr}(4,6)$ cluster algebra is also depicted in fig. 3.20. In this figure, we have also highlighted examples for admissible and mutation pairs in this

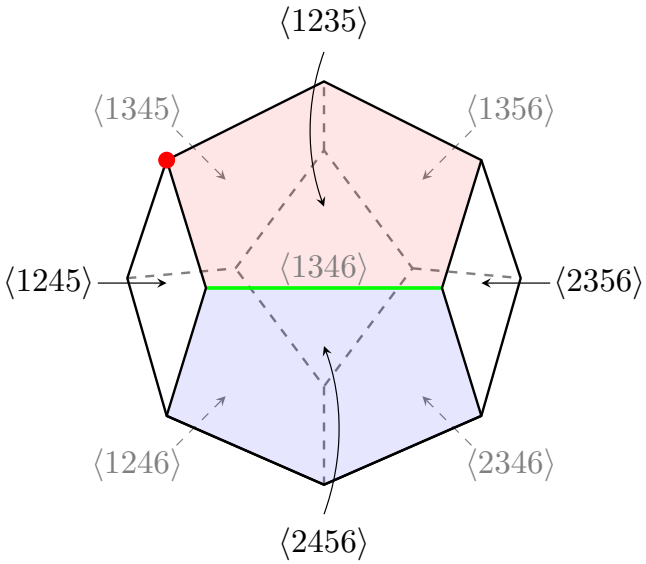

Figure 3.20: The cluster polytope of the cluster algebra of $\mathrm{Gr}(4,6)$ as well as its cluster variables. The initial seed is highlighted by the red dot, the facets associated to the cluster variables $\langle 1235\rangle$ and $\langle 2456\rangle$ are drawn in a red and blue shade, respectively. Since they intersect at the green line, these two variables can appear in consecutive slots of the symbol. Due to the low dimension of the polytope, this edge also corresponds to the mutation of $\langle 1245\rangle$ into $\langle 2356\rangle$ and vice versa, which thus can appear as a triple with their $\mathcal{X}$-variable in between the two $\mathcal{A}$-variables.

cluster algebra. In fact, we can easily read off the admissible and mutation pairs of $\mathrm{Gr}(4,6)$ from this cluster polytope. These are listed in table 3.4.

As was also mentioned in the introduction to this section, the cluster variables a_i with $i = 1,\ldots,9$ by themselves are not dual conformally invariant. A multiplicatively equivalent alphabet of DCI letters is for example given by

$$u_1 = \frac{\langle 3456\rangle\,\langle 1236\rangle}{\langle 2356\rangle\,\langle 1346\rangle}\,, \qquad u_2 = \frac{\langle 1356\rangle\,\langle 2346\rangle}{\langle 2356\rangle\,\langle 1346\rangle}\,, \qquad u_3 = \frac{\langle 1345\rangle\,\langle 2456\rangle\,\langle 1236\rangle}{\langle 1235\rangle\,\langle 1246\rangle\,\langle 3456\rangle}\,, \tag{3.59}$$

as well as six more letters obtained from cyclic permutations $i \to i+1$ of the indices of the Plücker variables, see also eg. [32, 46, 47]. Note that in eq. (3.59), the cluster variables are highlighted in a blue colour whereas the frozen variables are written in black colour.

On the other hand, in the literature, see eg. [28, 32, 46–53] or the review [33], the symbol alphabet of the six-particle MHV and NMHV amplitudes with up to seven loops was shown

	a_1	a_2	a_3	a_4	a_5	a_6	a_7	a_8	a_9
a_1	●	●	●	○	○	●	○	●	●
a_2	●	●	●	●	○	○	○	○	●
a_3	●	●	●	●	●	●	○	○	○
a_4	○	●	●	●	●	○	●	○	●
a_5	○	○	●	●	●	●	●	○	○
a_6	●	○	●	○	●	●	●	●	○
a_7	○	○	○	●	●	●	●	●	●
a_8	●	○	○	○	○	●	●	●	●
a_9	●	●	○	●	○	○	●	●	●

Table 3.4: Cluster adjacency of $\mathrm{Gr}(4,6)$ in terms of the variables a_i as defined by eq. (3.58). In this case, all pairs either appear together in a cluster (denoted by ●) or are related by a mutation (denoted by ○).

to be given by the set

$$\mathcal{S}_6 = \{u, 1-u, y_u, v, 1-v, y_v, w, 1-w, y_w\} \,, \tag{3.60}$$

whereas the dual conformal cross ratios u, v, w are given in terms of the dual variables x_i, defined by $x_i - x_{i+1} = p_i$, see section 2.3.3, as

$$u = \frac{x_{13}^2 x_{46}^2}{x_{14}^2 x_{36}^2} \,, \qquad v = \frac{x_{24}^2 x_{15}^2}{x_{25}^2 x_{14}^2} \,, \qquad w = \frac{x_{35}^2 x_{26}^2}{x_{36}^2 x_{25}^2} \,, \tag{3.61}$$

$$y_u = \frac{u - z_+}{u - z_-} \,, \qquad y_v = \frac{v - z_+}{v - z_-} \,, \qquad y_w = \frac{w - z_+}{w - z_-} \,, \tag{3.62}$$

where as before $x_{ij}^2 = (x_i - x_j)^2$ and

$$z_\pm = \frac{1}{2}\left[-1 + u + v + w \pm \sqrt{\Delta}\right] \,, \quad \Delta = (1-u-v-w)^2 - 4uvw \,. \tag{3.63}$$

Parity acts on these variables as $u \to u$, $v \to v$, $w \to w$ and $y_i \to 1/y_i$, such that the cross ratios u, v, w are parity-even variables. Equivalently, the parity operation switches the sign of the square root of Δ, that is $\sqrt{\Delta} \to -\sqrt{\Delta}$. Finally, the variables transform as $u \to v \to w \to u$ and $y_u \to 1/y_v \to y_w \to 1/y_u$ under cyclic transformations of the particle labels.

At first sight, the appearance of the square root $\sqrt{\Delta}$ might seem problematic. First of all, in the previous discussion we have only considered symbol letters given as rational functions of some arguments. Even more, by construction all cluster variables are rational functions of the initial variables, since mutation is a birational transformation, and can thus not describe square-root letters.

However, in section 2.3.3 we have seen that instead of the dual variables x_i, momentum twistors are in fact better suited to parameterise the kinematics of planar $\mathcal{N} = 4$ super Yang-Mills amplitudes. They are essentially the double cover of the cross ratios u, v, w and

do contain parity-odd variables. Indeed, when parameterising the hexagon alphabet in terms of momentum twistors, the radicand Δ becomes a perfect square so that all letters become rational. As we will discuss in later sections, the case where the letters of the alphabet are irrational functions of the Plücker variables will require more sophisticated tools which we develop in section 5.

To be precise, by noting that the letters u, v, and w are the conformal cross ratios u_{36}, u_{14}, and u_{25}, respectively, as defined in eq. (2.82), we can use eq. (2.92) to express the entire six-particle alphabet in terms of momentum twistors. In fact, this demonstrates that

$$u = \frac{\langle 1236\rangle\langle 3456\rangle}{\langle 2356\rangle\langle 1346\rangle} \equiv u\,, \quad 1-u = \frac{\langle 1356\rangle\langle 2346\rangle}{\langle 2356\rangle\langle 1346\rangle} \equiv u_2\,, \quad y_u = \frac{\langle 1345\rangle\langle 2456\rangle\langle 1236\rangle}{\langle 1235\rangle\langle 1246\rangle\langle 3456\rangle} \equiv u_3\,, \tag{3.64}$$

whereas the last two equations are obtained by making use of the Plücker relations. Similarly, the cyclic images of u_1 correspond to v and w, respectively, such that one can show that the symbol alphabet of six-particle scattering precisely corresponds to the dual conformally invariant set of letters obtained from the cluster algebra of $\mathrm{Gr}(4,6)$.

Using this alphabet, one next proceeds as described for the symbol bootstrap. Picking one of the many concrete results obtained in this way, we briefly discuss the high-level steps in the example of the so-called *hexagon functions* $\mathscr{H}_{6,m}$, the space of functions, weight $m = 2L$ MPLs, of the six-particle amplitude at L loops. This space can be constructed recursively as follows, see eg. [47, 51]:

1. First, the recursion starts at weight 1 with the elementary logarithms

$$\mathscr{H}_{6,1} = \{\log u, \log v, \log w\}\,, \tag{3.65}$$

which is a consequence of the first entry condition [135], ensuring that the amplitude can only have singularities when intermediate particles go on-shell.

2. Next, assuming we have already constructed the hexagon functions with weight up to $m-1$, we make an ansatz for the $(m-1)\times 1$-component of the coproduct of a weight-m hexagon function F_m in terms of the weight-$(m-1)$ hexagon functions F^{φ}_{m-1} as

$$\Delta_{m-1,1}F_m = \sum_{\varphi\in\mathcal{S}} F^{\varphi}_{m-1}\otimes\log\varphi\,. \tag{3.66}$$

Note that for this ansatz to actually correspond to a coproduct, it has to satisfy the integrability condition. Since the coproduct has a non-trivial kernel, the ansatz for the actual function also contains transcendental constants such as zeta-values of weight m.

3. Next, the space of hexagon functions is further reduced by imposing physical constraints such as the (extended) Steinmann relations, the cluster adjacency property, or the requirement for physical branch points. For this reason, the functions obtained up to this point are also referred to as *(extended) Steinmann basis*.

4. Finally, comparing the remaining ansatz to known values of the amplitude obtained from alternative means or certain kinematic regimes such as the collinear limit, where the

momenta of two particles become collinear, one obtains the unique functional form of the six-particle scattering amplitude with up to six loops.

Beyond this general algorithm, there also exist approaches for a more efficient construction of the hexagon functions, such as splitting the space into parity-even and -odd functions [47], which is required in order to push these computations to higher loops.

3.2.3. Example: Gr(4, 7) and seven-particle scattering

Similar to the six-particle case, we begin by constructing the cluster algebra of Gr(4, 7). The initial seed of this rank-6 cluster algebra is depicted in figure 3.21. It can be shown

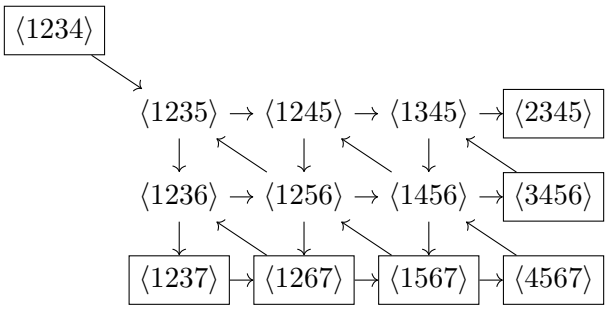

Figure 3.21: Initial seed of the cluster algebra of Gr(4, 7).

that the principal part of the quiver obtained by performing the mutations on the nodes which are in the initial seed labelled by $\{\langle 1236\rangle, \langle 1235\rangle, \langle 1245\rangle, \langle 1236\rangle, \langle 1256\rangle, \langle 1456\rangle\}$ corresponds to the exceptional E_6 Dynkin diagram, implying that the cluster algebra is finite. For our purposes, it is more suitable to consider instead another, equivalent cluster algebra. As was demonstrated in [55], one can use the frozen variables to recast the $\mathcal{A}$-variables into a projectively invariant form. Consequently, we will use the initial seed depicted in figure 3.22 with the homogeneous cluster variables defined by

$$\begin{aligned} a_{11} &= \frac{\langle 1234\rangle\,\langle 1567\rangle\,\langle 2367\rangle}{\langle 1237\rangle\,\langle 1267\rangle\,\langle 3456\rangle}\,, & a_{21} &= \frac{\langle 1234\rangle\,\langle 2567\rangle}{\langle 1267\rangle\,\langle 2345\rangle}\,, \\ a_{31} &= \frac{\langle 1567\rangle\,\langle 2347\rangle}{\langle 1237\rangle\,\langle 4567\rangle}\,, & a_{41} &= \frac{\langle 2457\rangle\,\langle 3456\rangle}{\langle 2345\rangle\,\langle 4567\rangle}\,, \\ a_{51} &= \frac{\langle 1(23)(45)(67)\rangle}{\langle 1234\rangle\,\langle 1567\rangle}\,, & a_{61} &= \frac{\langle 1(34)(56)(72)\rangle}{\langle 1234\rangle\,\langle 1567\rangle}\,, \end{aligned} \tag{3.67}$$

as well as their cyclic images a_{ij} obtained from a_{i1} by replacing the indices of the Plücker variables according to $l \to l+j-1$. Note that again the cluster variables are highlighted in a blue colour. In this definition, we make use of a short-hand notation for certain bilinears in the Plücker variables, which are given by

$$\langle a(bc)(de)(fg)\rangle = \langle abcd\rangle\,\langle efga\rangle - \langle abce\rangle\,\langle dfga\rangle\,. \tag{3.68}$$

The resulting cluster algebra consists of 42 cluster variables distributed among 833 clusters. Consequently, the 6-dimensional cluster polytope, also referred to as the E_6

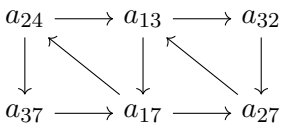

Figure 3.22: Initial seed of the cluster algebra of $\mathrm{Gr}(4,7)$ in terms of the homogenised cluster variables a_{ij}.

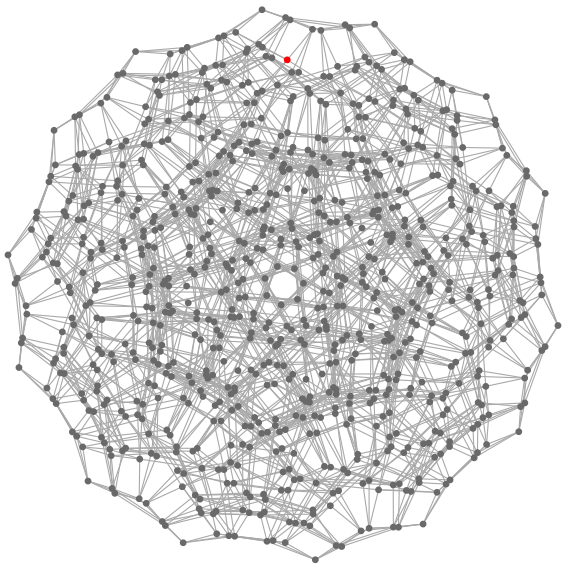

Figure 3.23: Illustration of the cluster polytope of $\mathrm{Gr}(4,7)$, depicted in terms of its exchange or polytope graph. The initial seed is again highlighted by a red dot.

polytope, contains 42 vertices and 833 facets. Its polytope graph, or equivalently the cluster exchange graph, is illustrated in figure 3.23.

The presentation of the seven-particle alphabet, consisting of the 42 homogenised cluster variables defined in eq. (3.67), already suggests that the alphabet is invariant under cyclic transformations of the Plücker indices. While it is straightforward to verify this property given the letters, there exists a general argument that demonstrates that in fact the cluster algebra of any $\mathrm{Gr}(k,n)$ are invariant under cyclic transformations [177].[22] In addition, one can explicitly verify that the alphabet is also invariant under the dihedral flip or reflection $i \to 8-i$ of the Plücker indices, such that it is in fact invariant under the entire dihedral group. As discussed in section 2.3.2, this is to be expected or required of the symbol alphabet, since the amplitude itself is invariant under the dihedral symmetry.

Using this alphabet, the symbols of the seven-particle MHV and NMHV amplitudes have been obtained by a similar procedure as described for the six-particle case with up to four loops in [33, 55, 56], whereas in particular the cluster adjacency property has been

[22] This is proven by constructing a sequence of mutations from the initial seed of the cluster algebra of $\mathrm{Gr}(k,n)$ to a seed with the same quiver topology but where all Plücker indices are cyclically shifted compared to the initial cluster. Since this can be done for any number of cyclic shifts, this proves that the resulting cluster algebra is invariant under cyclic transformations.

used for the four-loop NMHV result in [57]. More recently, these symbols were successfully integrated and the functional form of the amplitude were presented in [58].

Finally, before concluding this section let us comment on the cluster adjacency of the seven-particle amplitude. While cluster adjacency restricts the consecutive pairs of letters in the symbol that can appear, it does not require all of these admissible pairs to actually appear. In this case, cluster adjacency implies that only 840 out of the total $42 \times 41 = 1722$ ordered pairs of letters can appear next to each other. In [176], it was checked that all then known seven-particle property were consistent with this restriction, but in fact only a subset of 784 out of 840 adjacencies occurred. In particular, the following cluster-adjacent pairs[23]

$$(a_{21}, a_{64}) \quad \& \text{ cyclic} \tag{3.69a}$$

$$(a_{31}, a_{65}) \quad \& \text{ cyclic} \tag{3.69b}$$

$$(a_{11}, a_{41}) \quad \& \text{ cyclic + parity} \tag{3.69c}$$

were seen to be missing from the then known amplitudes (although the pairs (3.69c) do appear in certain integrals contributing to the amplitude). We will refer to these putative missing pairs as *beyond-cluster adjacency* restrictions. We will come back to this issue in section 4.3.2, where we present our findings on the appearance of these missing pairs in known seven-particle symbols and discuss the consequences for the geometry of the cluster polytope.

In particular, the $840 = 399 \times 2 + 42$ ordered admissible pairs of the seven-particle amplitude consist of 42 pairs of the same cluster variable plus 399 pairs of distinct cluster variables, which are associated to the 399 codimension-2 faces of the E_6 cluster polytope. In this picture, the 14 pairs further removed in beyond–cluster adjacency correspond to the removal of the associated codimension-2 faces from the cluster polytope.

3.2.4. Beyond seven particles

In the previous sections we have seen how starting with the working assumption of conjecture 3.59 that the symbol alphabet of n-particle scattering is given by the cluster algebra of $\mathrm{Gr}(4, n)$, one can construct the functional representation of six-particle amplitudes with up to seven loops and of seven-particle amplitudes with up to four loops. Furthermore, we have seen that the cluster algebra also describes the extended Steinmann relations, constraints on which letters can appear next to each other in the symbol, in terms of the principle of cluster adjacency.

Beyond continuing these calculations to higher loops, the obvious next step for the cluster bootstrap programme is to apply it to eight and more particles. However, starting at eight particles, there has been a long-standing major obstruction: the cluster algebras of $\mathrm{Gr}(4, n)$ are infinite for $n \geq 8$. Consequently, these cluster algebras consist of infinitely many cluster variables. In fact, while the cluster algebra of $\mathrm{Gr}(4, 8)$ is of finite mutation type, see eg. [178], such that up to quiver isomorphism it contains only a finite number of

[23] Note that the sets (3.69a) and (3.69b) are related by a dihedral reflection.

inequivalent quivers, the cluster algebras of $\mathrm{Gr}(4, n)$ for $n \geq 9$ are of infinite mutation type and thus consist of infinitely many clusters with inequivalent quivers.

If conjecture 3.59 were to hold for $n \geq 8$, this would imply that the symbol alphabet contains infinitely many letters. Even if it might be possible that the amplitude actually has infinitely many singularities with possibly ever more appearing with increasing loop number, or that the actual, finite symbol alphabet is contained within the infinitely large, predicted one, the infinity of the symbol alphabet poses a practical obstruction to the application of the cluster bootstrap programme. In fact, the analysis of Landau equations, which encode an important class of singularities of the amplitude, exhibits only a finite number of such Landau singularities for any massless planar theory at any loop order [59]. Even more, in there the authors show that for the six-particle amplitude in planar $\mathcal{N} = 4$ SYM the Landau singularities precisely correspond to the zero loci of the symbol letters suggesting that the symbol alphabet is finite. As one of the main contributions of this work, in what follows we will see how the relation of Grassmannian cluster algebras to so-called *tropical geometry* offers a solution for this obstruction.

4. Finiteness from tropical geometry

In the previous sections we have reviewed cluster algebras and their application to loop amplitudes of planar $\mathcal{N} = 4$ super Yang-Mills theory. Specifically, we have seen how the set of cluster variables, or equivalently the codimension-1 facets of the cluster polytope, allow us to construct the symbol alphabet and thus form the starting point of the cluster bootstrap programme. Beyond this data, the cluster algebra also contains structural information about the symbol. By the cluster adjacency property, the codimension-2 faces of the cluster algebra determine which letters can appear in consecutive slots of the symbol, referred to as admissible pairs.

However, while this approach has led to a plethora of results for six- and seven-particle scattering, starting at eight particles the cluster algebra becomes infinite, which in turn poses an obstruction for the bootstrap programme. Even more subtly, we have seen that the cluster adjacency property is in fact too broad: 28 of the 399 admissible pairs associated to the codimension-2 faces of the $\mathrm{Gr}(4,7)$ cluster polytope have not been observed to appear in the symbols of known seven-particle amplitudes. Note that 14 of these pairs, however, do appear in certain integrals contributing to the amplitude, such that there remain 14 codimension-2 faces unaccounted for. These subtleties seem to suggest that while the geometric structure of the cluster algebra in principle is a crucial input for the scattering amplitude, it is not quite the right geometry: for seven-particle scattering, it contains too many codimension-2 faces, for eight-particle scattering too many (infinitely many, to be precise) codimension-1 facets. Instead, a more coarse-grained geometry is required to accurately describe the amplitude.

In fact, in [71] Speyer and Williams introduced and discussed another geometric object associated to the Grassmannians $\mathrm{Gr}(k,n)$, the fan of the *tropical totally positive Grassmannian* $\mathrm{Tr}_+(k,n)$, referred to as the *tropical fan*. Remarkably, the fan of $\mathrm{Tr}_+(4,7)$ is a coarser version of the cluster fan of $\mathrm{Gr}(4,7)$, that is the cluster fan refines the tropical fan. While the tropical fan contains the same 42 rays as the cluster fan, which in there correspond to the 42 cluster variables, it contains the same dimension-2 faces as the cluster fan except for the seven faces corresponding to the seven missing cluster adjacency pairs of eq. (3.69b).[1] Finally, since the tropical fan is finite by construction, one might wonder whether this is the correct geometry to describe the symbols of loop amplitudes in $\mathcal{N} = 4$ pSYM.

To answer this question, we begin this chapter in section 4.1 by first reviewing the mathematics of tropical geometry, which is then used to construct the tropical fans associated to the Grassmannians $\mathrm{Gr}(k,n)$. Following that, we reformulate the cluster bootstrap programme using the insights from tropical geometry in section 4.2 and discuss the appli-

[1] Remember that admissible pairs correspond to codimension-2 faces of the cluster polytope, which equvialently corresponds to dimension-2 faces of the fan.

cation of this *tropical cluster bootstrap* to the seven-particle amplitude as an example in section 4.3.

4.1. Tropical geometry

In essence, tropical geometry is the algebraic geometry over the tropical semifield $(\mathbb{R} \cup \{\infty\}, \oplus, \otimes)$, which is the set of real numbers together with infinity on which addition is given by taking the minimum and multiplication by addition, referred to as *tropical addition* $\oplus$ and *tropical multiplication* $\otimes$, respectively. Starting with an affine variety, which can be defined as the zero locus of one or more polynomials, such as for example the Plücker relations that are used to construct the Grassmannians $\mathrm{Gr}(k, n)$, tropical geometry revolves around the geometric structures that are attached to the tropicalised versions of these polynomials, which are obtained by replacing addition and multiplication with their tropical counterparts.

We begin this section with an introduction to tropical geometry in section 4.1.1, where we review the main ideas and concepts following [62, 71, 179] with a focus on the tropical geometry of the Grassmannian and configuration space. The interested reader is referred to the many good introductory texts such as [180] as well as reviews on the subject [179, 181, 182] for further details. Following this, we discuss an alternative construction of the so-called positive part of the tropical configuration space, the totally positive tropical configuration space $\widetilde{\mathrm{Tr}}_+(k, n)$, in sections 4.1.2 and 4.1.3. It is this object that plays a central role in the tropical cluster bootstrap, as discussed in section 4.3.

4.1.1. Tropical varieties

As alluded to in the introduction, we begin the construction of a *tropical variety* by introducing the *tropical semifield*. It is defined as follows.[2]

Definition 4.1 (Tropical semifield)**.** The tropical semifield is $\mathbb{R} \cup \{\infty\}$ with operations $\oplus$ and $\otimes$, tropical addition and multiplication, respectively, given by $a \oplus b = \min(a, b)$ and $a \otimes b = a + b$.

It is easy to see that tropical addition and multiplication as defined above are associative, commutative, and distributive with additive identity ∞ and multiplicative identity 0. Since the addition does not have an inverse, this is indeed a semifield. Many algebraic expressions are considerably simpler in the tropical semifield compared to regular arithmetic, as highlighted by the following examples.

Example 4.2. 1. The tropical polynomial $F(x) = 0 \oplus 3 \otimes x^2 \oplus x^3$ can be written as $\min(0, 3 + 2x, 3x)$ in regular arithmetic, which is a piecewise linear function from $\mathbb{R} \cup \{\infty\}$ to $\mathbb{R}$. Note that we cannot drop the 0, since it is the multiplicative and not the additive identity on the tropical semifield.

[2] Note the similarity of the tropical semifield to the cluster-tropical semifield defined in def. 3.5, whereas the latter could be considered an exponential version of the tropical semifield defined in here.

2. By considering $(x \oplus y)^n$ for some positive integer n as the n-fold tropical multiplication of the term $(x \oplus y)$ with itself, we can write it as $n \cdot \min(x, y)$ in regular arithmetic. Consequently, we see we see that it is equal to $x^n \oplus y^n$, which can also be written as $\min(nx, ny)$.

Before we move on to apply the tropical semifield to algebraic varieties and explain their tropicalisation, we first introduce the notion of a *valuation*. It is defined as follows.

Definition 4.3 (Valuation)**.** Fix a field K. A *valuation* on that field is a map $\mathrm{val} : K \to \mathbb{R} \cup \{\infty\}$ that satisfies

1. $\mathrm{val}\,(ab) = \mathrm{val}\,(a) + \mathrm{val}\,(b)$, and
2. $\mathrm{val}\,(a + b) \geq \min(\mathrm{val}\,(a)\,, \mathrm{val}\,(b))\,,$

and whereas the zero element is mapped to infinity.

While the valuation is defined for any field K, we will from now on only consider algebraically closed fields and thus not distinguish any further. Consider the following examples that are of relevance to tropical geometry.

Example 4.4. 1. Fix $K = \mathbb{C}$. The *trivial valuation* on K is given by $\mathrm{val}\,(a) = 0$ for all $a \in \mathbb{C}^*$, that is all non-zero complex numbers are mapped to zero.

2. Consider $K = \mathbb{C}\{\{t\}\}$, the field of Puiseux series. It is the algebraic closure of the field of Laurent polynomials with complex coefficients and its elements are given by Laurent series with rational exponents with a common denominator in each series. By ordering the exponents appearing in an element $a \in K$, we define the valuation map evaluated on a to be its smallest exponent. For example, the valuation of $a = t^{-3/2} - t^{1/2}$ is given by $\mathrm{val}\,(a) = -3/2$.

Note that the restriction of the underlying field K to the complex numbers is referred to as tropical geometry with constant coefficients. While this is the case for the tropicalisation of the Grassmannian and configuration space, we keep K general for now.

With the essential tools in place, we turn to the tropicalisation of an affine variety, which can be defined as the zero locus of one or more polynomials. Consequently, we begin by defining the tropicalisation of a polynomial. It is defined in the obvious way as follows

Definition 4.5 (Tropical polynomial)**.** Fix a field K with valuation val. Given a polynomial $f \in K[x_1^{\pm 1}, \ldots, x_r^{\pm 1}]$ of the form

$$f = \sum_{a \in M_f} c_a x_1^{m_1^a} \ldots x_r^{m_r^a}\,, \tag{4.1}$$

with coefficients $c_a \in K$ and whereas M_f is an index set labeling the monomials, we define the tropicalisation of f, the *tropical polynomial* $\mathrm{Tr}f : (\mathbb{R} \cup \{\infty\})^r \to \mathbb{R}$, as

$$\mathrm{Tr}f = \min_{a \in M_f} \left(\mathrm{val}\,(c_a) + \sum_{j=1}^{r} m_j^a \cdot x_j \right)\,, \tag{4.2}$$

that is we replace addition by taking the minimum and multiplication by addition. Similar to usual polynomials, we refer to the arguments of the minimum, that is terms of the form

$$\mathrm{val}\,(c_a) + \sum_{j=1}^{r} m_j^a \cdot x_j\,, \tag{4.3}$$

as the monomials of the tropical polynomial.

Example 4.6. We demonstrate this and the following constructions using a simple example. Consider for this $K = \mathbb{C}$ with trivial valuation and the polynomial $g \in \mathbb{C}[x_1, x_2]$, which is given by

$$g(x_1, x_2) = 2x_1^3 + x_1^{-1}x_2 - x_2^2\,. \tag{4.4}$$

When passing to the tropical version, the three constant coefficients 2, 1, and -1 are mapped to zero under the valuation. We thus obtain the tropical polynomial

$$\mathrm{Tr}g(x_1, x_2) = \min\left(3x_1, -x_1 + x_2, 2x_2\right)\,, \tag{4.5}$$

consisting of the three tropical monomials $3x_1$, $-x_1 + x_2$, and $2x_2$.

Given some polynomial $f \in K[x_1^{\pm 1}, \ldots, x_r^{\pm 1}]$, we can attach to it the hypersurface $V(f)$ as the zero-locus of the polynomial, that is $V(f) = \{x \in (K^*)^r : f(x) = 0\}$, whereas as always $K^* = K\backslash\{0\}$. Similar to the tropicalisation of the polynomial f, we also define the tropicalisation of the associated hypersurface. To do so, note that the tropical polynomial $\mathrm{Tr}f$ is a piecewise linear function from $(\mathbb{R} \cup \{\infty\})^r$ to $\mathbb{R}$. This function is linear and differentiable everywhere except where the minimum is attained by at least two tropical monomials, which corresponds to the points where the function passes between regions of linearity. This leads to the following definition.

Definition 4.7 (Tropical hypersurface)**.** Given a polynomial $f \in K[x_1^{\pm 1}, \ldots, x_r^{\pm 1}]$, the *tropical hypersurface* $V\left(\mathrm{Tr}f\right)$ is the set of points where the tropicalised polynomial $\mathrm{Tr}f$ is not differentiable. Equivalently, this is the set of points in $\mathbb{R}^r$ where the minimum is attained by (at least) two tropical monomials.

In this way, a tropical polynomial gives rise to a number of *tropical hypersurface conditions*, each being defined by setting two tropical monomials equal to each other and smaller or equal then the remaining monomials. The tropical hypersurface consists of those points that satisfy any one of these hypersurface conditions and splits up the ambient space $\mathbb{R}^r$ into the regions of linearity, each defined by the tropical monomial that attains the minimum in this region, as can also be seen in the following example.

Example 4.8. Continuing our previous example, the tropical hypersurface associated to the polynomial g of eq. (4.4) is given by the union of solutions to each of the equations

$$\begin{aligned} 3x_1 &= -x_1 + x_2 \leq 2x_2\,, \\ 3x_1 &= 2x_2 \leq -x_1 + x_2\,, \\ 2x_2 &= -x_1 + x_2 \leq 3x_1\,, \end{aligned} \tag{4.6}$$

which is where the tropical polynomial is non-linear. This region is given by the union $V(\mathrm{Tr}g) = V_1 \cup V_2 \cup V_3$ of the three hypersurfaces $V_1 = \{\boldsymbol{x} \in \mathbb{R}^2 : x_2 = 4x_1, x_1 \geq 0\}$, $V_2 = \{\boldsymbol{x} \in \mathbb{R}^2 : x_2 = 3/2x_1, x_1 \leq 0\}$, and $V_3 = \{\boldsymbol{x} \in \mathbb{R}^2 : x_2 = -x_1, x_1 \geq 0\}$ and is illustrated in figure 4.1. Note that in this case the tropical hypersurface is the union of three

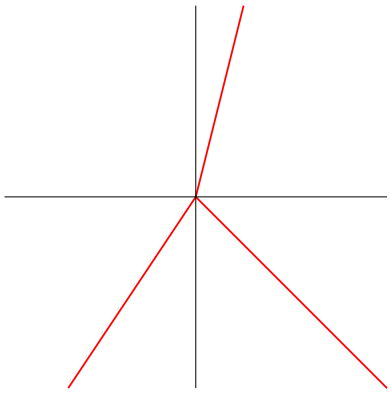

Figure 4.1: The tropical hypersurface associated to $g = 2x_1^3 + x_1^{-1}x_2 - x_2^2$ is depicted in red.

bounded hyperplanes in $\mathbb{R}^2$. Also note that, as is always the case, the tropical hypersurface conditions of eqs. (4.6) are invariant under the simultaneous positive rescaling $x_i \to \lambda x_i$ for any $\lambda \in \mathbb{R}_{\geq 0}$.

Finally, consider a polynomial ideal $I \subset K[x_1^{\pm 1}, \ldots, x_r^{\pm 1}]$. The associated affine variety $V(I)$ in the r-dimensional algebraic torus T over K, where $T = (K^*)^r$, is the space of points in T where all elements of I are simultaneously zero. Equivalently, the affine variety can be constructed as the intersection of the hypersurfaces of the polynomials $f \in I$, that is we have

$$V(I) = \{x \in T : f(x) = 0 \text{ for all } f \in I\} = \bigcap_{f \in I} V(f)\,. \tag{4.7}$$

Following this approach, we define the tropicalisation of a variety $V(I)$ in the obvious way via the tropical hypersurfaces as follows.

Definition 4.9 (Tropical variety)**.** Given an ideal $I \subset K[x_1^{\pm 1}, \ldots, x_r^{\pm 1}]$, the tropicalisation of the affine variety $V(I)$, the *tropical variety*, is defined as

$$\mathrm{Tr}V(I) = \bigcap_{f \in I} V(\mathrm{Tr}f)\,, \tag{4.8}$$

that is as the intersection of the tropical hypersurfaces of all $f \in I$. Equivalently, the tropical variety consists of all those points that simultaneously satisfy the tropical hypersurface conditions for all polynomials $f \in I$.

If the ideal is finitely generated, that is $I = \langle f_1, \ldots, f_l \rangle$, we can express the variety $V(I)$ as the zero locus of the polynomials $f_1, \ldots, f_l$ only, that is $V(I) = \{x \in T : f_1(x) = \cdots = f_l(x) = 0\}$. However, the same is not true for the tropical variety. For a finitely generated

ideal I, the tropical variety is not necessarily given by the intersection of the associated tropical hypersurfaces $\cap_{i=1}^{l} V(\mathrm{Tr} f_i)$. Any finite subset of polynomials of the ideal I that allows to write the tropical variety of I in such a way as the intersection of their tropical hypersurfaces is referred to as a *tropical basis* for I. Such a finite basis always exists, as the following result from [62] highlights. See also [183] for further details on tropical bases.

Proposition 4.10 (Finiteness of tropical varieties)**.** *Given an ideal I in $K[x_1^{\pm 1}, \dots, x_r^{\pm 1}]$ we can compute its universal Gröbner basis* $\mathrm{UGB}(I)$*, a finite subset of I which contains a Gröbner basis for I. The tropical variety $\mathrm{Tr}V(I)$ is the intersection of the tropical hypersurfaces $V(\mathrm{Tr}f)$ for $f \in \mathrm{UGB}(I)$.*

In particular, this result guarantees that the tropical variety $\mathrm{Tr}V(I)$ of any ideal $I \subset K[x_1^{\pm 1}, \dots, x_r^{\pm 1}]$ can be written as the intersection of a finite number of tropical hypersurfaces. In this way, we can consider tropical varieties as finite objects.

As it will turn out, for our purposes we do not need the entire tropical variety $\mathrm{Tr}V(I)$ but only its so-called *positive part* $\mathrm{Tr}_+V(I)$. To construct the positive part, consider again the tropicalisation of a polynomial, as defined by eqs. (4.1) and (4.2). As we can see in there, the tropical polynomial loses the information on the coefficient c_a of each monomial and especially for real coefficients its sign. To restore this data, we attach to each tropical monomial and correspondingly the region in $\mathbb{R}^r$ where the monomial attains the minimum, labelled by $a \in M_f$, the sign of its coefficient c_a. Next, we define the positive part of the tropical variety as those components that separate regions of different signs, see also [71, 184]. Equivalently, the positive part consists of those tropical hypersurfaces that are obtained by setting two tropical monomials of different signs equal to each other and smaller or equal than the other tropical monomials. In this way, passing from the full tropical variety to its positive part amounts to the removal of those hypersurfaces that are defined via monomials of equal sign.

Example 4.11. From eq. (4.4) of our previous examples we see that the tropical monomials $3x_1$ and $-x_1 + x_2$ have a positive sign whereas $2x_2$ has negative sign. Correspondingly, the positive part of the tropical variety consists only of the two hypersurfaces V_2 and V_3, since they arise from setting one of the positive monomials equal to the negative monomial. The positive part is also depicted in fig. 4.2.

Before we conclude this section with a general review of the tropical Grassmannian and configuration space, we first demonstrate in the following example how the tropical Grassmannian $\mathrm{Tr}(2,n)$ and its positive part $\mathrm{Tr}_+(2,n)$, the totally positive tropical Grassmannian, are constructed.

Example 4.12 (Tropical Grassmannian $\mathrm{Tr}(2,n)$)**.** Back in section 2.3.3, we reviewed the construction of the Grassmannian $\mathrm{Gr}(k,n)$ as the projective variety of the Plücker ideal. This ideal is defined via the homogeneous polynomials in the Plücker variables that make up the Plücker relations. In the case of $\mathrm{Gr}(2,n)$, these relations are given by

$$p_{ij}p_{kl} - p_{ik}p_{jl} + p_{il}p_{jk} = 0\,, \quad 1 \leq i < j < k < l \leq n\,, \tag{4.9}$$

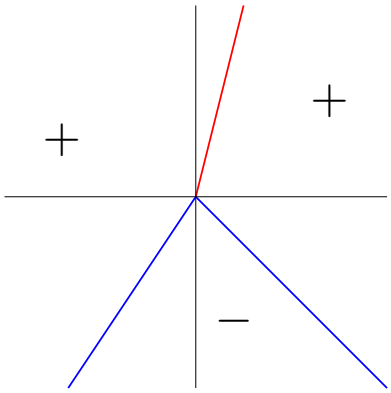

Figure 4.2: The tropical variety of the polynomial g is depicted in red and blue. The blue hypersurfaces constitute the positive part and each region is labelled by the sign of its tropical monomial.

in terms of the $D = \binom{n}{2}$ Plücker coordinates p_{ij}. The corresponding tropical polynomials are given by

$$\min\left(w_{ij} + w_{kl}\,, w_{ik} + w_{jl}\,, w_{il} + w_{jk}\right)\,, \tag{4.10}$$

whereas it is customary to denote the tropicalised Plücker variables by w_{ij} to avoid confusion. Note in particular that the tropical monomials have no information on the sign of the term they originated from. By the above construction, we assign "+" to the first and last monomial, and "−" to the tropical monomial in the middle.

Organising the tropicalised Plücker variables w_{ij} in lexicographical order, they form coordinates on $\mathbb{R}^D$. The tropical hypersurfaces of each of the Plücker relation polynomials are obtained by the following hypersurface conditions

$$w_{ij} + w_{kl} = w_{ik} + w_{jl} \leq w_{il} + w_{jk}\,, \tag{4.11}$$

$$w_{ij} + w_{kl} = w_{il} + w_{jk} \leq w_{ik} + w_{jl}\,, \tag{4.12}$$

$$w_{ik} + w_{jl} = w_{il} + w_{jk} \leq w_{ij} + w_{kl}\,, \tag{4.13}$$

whereas a point in $\mathbb{R}^D$ has to satisfy any one of these equations to be on the tropical hypersurface. These hypersurfaces split up the ambient space $\mathbb{R}^D$ into the regions of linearity of the tropical monomial. The entire tropical Grassmannian $\mathrm{Tr}(2,n)$ is given by those points that simultaneously satisfy the hypersurface conditions for all tropical Plücker relation polynomials.

Finally, since the tropical monomials $w_{ij}+w_{kl}$ and $w_{il}+w_{jk}$ have a positive sign whereas $w_{ik} + w_{jl}$ has a negative sign, the positive part of the tropical Grassmannian, the totally positive tropical Grassmannian $\mathrm{Tr}_+(2,n)$ is given by the intersection of all hypersurfaces defined only by the equations (4.11) and (4.13), since for these monomials of different signs are set to be equal.

In a similar way to this example, we construct the tropical Grassmannian $\mathrm{Tr}(k,n)$ start-

ing with the general Plücker relations, given by

$$\sum_{r=1}^{k+1}(-1)^r p_{i_1\dots i_{k-1}j_r} p_{j_1\dots\hat{j}_r\dots j_{k+1}} = 0\,, \tag{4.14}$$

for any two ordered sequences $1 \leq i_1 < \cdots < i_{k-1} \leq n$ and $1 \leq j_1 < \cdots < j_{k+1} \leq n$. The polynomials on the left hand side of this equation, also referred to as Plücker relation polynomial, form the Plücker ideal, whose projective variety corresponds to the Grassmannian $\mathrm{Gr}(k,n)$. The tropicalised version of the Plücker relation polynomials is

$$\min_{r=1,\dots,k+1}\left(w_{i_1\dots i_{k-1}j_r} + w_{j_1\dots\hat{j}_r\dots j_{k+1}}\right)\,, \tag{4.15}$$

where again we label the tropicalised Plücker variables by $w_{i_1\dots i_k}$. The tropical variety of the Plücker ideal, that is the intersection of the tropical hypersurfaces of all tropicalised Plücker relation polynomials, is a fan in $\mathbb{R}^D$ with $D = \binom{n}{k}$ whose maximal cones are of dimension $k(n-k)+1$, as was demonstrated in [62].[3]

Note that this is not quite the same as the dimension of the Grassmannian $\mathrm{Gr}(k,n)$, which is $k(n-k)$. In fact, we can observe that the Plücker relations are invariant under the overall scaling $p_{i_1\dots i_k} \to t \cdot p_{i_1\dots i_k}$ for any $t \in \mathbb{C}^*$. On the tropicalised Plücker relations, this translates to the invariance of the tropical hypersurface equations under the scaling $w_{i_1\dots i_k} \to t + w_{i_1,\dots,i_k}$ for any $t \in \mathbb{R}$. This leads to the following definition.

Definition/Proposition 4.13 (Speyer, Sturmfels [62])**.** The tropicalisation of the Grassmannian, the *tropical Grassmannian* $\mathrm{Tr}(k,n)$, is the quotient of the tropical variety of the Plücker ideal by the global scaling $w_{i_1\dots i_k} \to t + w_{i_1\dots i_k}$ for any $t \in \mathbb{R}$. It is a fan in $\mathbb{R}^D$ of dimension $k(n-k)$.

Remark 4.14. We refer to this quotient, and not the tropical variety of the Plücker ideal itself, as the tropical Grassmannian due to it matching the dimension of the classical Grassmannian. As is discussed in eg. [62], there exist multiple, closely related tropical varieties that can be constructed from the Grassmannian that are sometimes used interchangeably in the literature.

In section 2.3.3, we have seen that instead of the Grassmannian, the configuration space $\widetilde{\mathrm{Gr}}(k,n)$ is in fact the kinematic space of loop amplitudes in $\mathcal{N}=4$ pSYM. Its coordinates are invariant under dual conformal transformations as well as the projective equivalence of the momentum twistors $Z_i \sim t_i Z_i$ for $t_i \in \mathbb{C}^*$. The latter translates to the Plücker variables, which are essentially the minors of the matrix whose columns are the momentum twistors, as the scaling $p_{i_1\dots i_k} \to t_{i_1}\cdots t_{i_k} p_{i_1\dots i_k}$ for $t_{i_1},\dots,t_{i_k} \in \mathbb{C}^*$. It can be shown that the Plücker relations are invariant under this scaling. The configuration space is obtained as the quotient of the Grassmannian by this local scaling, as was discussed in section 2.3.3.

Passing again to the tropical version, the local scaling translates to $w_{i_1\dots i_k} \to t_{i_1} + \cdots + t_{i_k} + w_{i_1\dots i_k}$ for $t_{i_1},\dots,t_{i_k} \in \mathbb{R}$, which is also referred to as *lineality*. In fact, the

[3] Note that the coordinates on $\mathbb{R}^D$ are given by the D tropical Plücker variables $w_{i_1\dots i_k}$ for any ordered sequence $1 \leq 1_i < \cdots < i_k \leq n$.

hypersurface conditions obtained from the tropicalised Plücker relations, eq. (4.15), are also invariant under this local scaling. This can be seen by noting that the two terms of each tropical monomial together contribute the same Plücker indices $i_1, \ldots, i_{k-1}, j_1, \ldots, j_{k+1}$. Consequently, we define the *tropical configuration space* $\widetilde{\mathrm{Tr}}(k,n)$ as follows.

Definition/Proposition 4.15 (Speyer, Sturmfels [62])**.** The tropicalisation of the configuration space, the *tropical configuration space* $\widetilde{\mathrm{Tr}}(k,n)$, is the quotient of the tropical variety of the Plücker ideal by the local scaling relation $w_{i_1\ldots i_k} \to t_{i_1} + \cdots + t_{i_k} + w_{i_1\ldots i_k}$ for $t_{i_1}, \ldots, t_{i_k} \in \mathbb{R}$. It is a fan in $\mathbb{R}^D$ of dimension $(k-1)(n-k-1)$.

Similar to before, the positive parts, the *totally positive tropical Grassmannian* $\mathrm{Tr}_+(k,n)$ and the *totally positive tropical configuration space* $\widetilde{\mathrm{Tr}}_+(k,n)$, respectively, are obtained by limiting the above constructions to those tropical hypersurface conditions that arise from monomials with different sign. These are the tropical equivalents of the totally positive Grassmannian and totally positive configuration space $\widetilde{\mathrm{Gr}}_+(k,n)$, respectively, which are obtained from the full Grassmannian and configuration space by restricting all Plücker variables $p_{i_1\ldots i_k}$ for ordered sequences $1 \leq i_1 < \cdots < i_k \leq n$ to real, positive values.

4.1.2. Web-parameterisation of $\widetilde{\mathrm{Gr}}_+(k,n)$

In the previous section we have introduced the totally positive tropical configuration space $\widetilde{\mathrm{Tr}}_+(k,n)$ as a fan in $\mathbb{R}^D$ with dimension $(k-1)(n-k-1)$. However, the actual construction as reviewed above is impractical, also due to the embedding of the fan in the higher-dimensional space parameterised by the $D = \binom{n}{k}$ (tropical) Plücker variables. For this reason, we now turn to an alternative construction that was presented in [71]. Since this is based on a parameterisation of the positive configuration space $\widetilde{\mathrm{Gr}}_+(k,n)$, we first devote this section to review the so-called *web-parameterisation*.

First, we draw the web graph $\mathrm{Web}_{k,n}$ as follows. Starting with a k by $n-k$ grid, with k ingoing edges from the left and $n-k$ outgoing edges on the top, we label these external edges from 1 to n clockwise starting on the bottom left. We furthermore label the $d = (k-1)(n-k-1)$ internal chambers starting from the top left by filling the columns with $x_1, \ldots, x_d$. The horizontal and vertical internal edges are all directed, pointing to the right and top, respectively.

Example 4.16. In figure 4.3, the web graphs $\mathrm{Web}_{2,5}$ and $\mathrm{Web}_{3,7}$ used to obtain the parameterisations for $\widetilde{\mathrm{Gr}}_+(2,5)$ and $\widetilde{\mathrm{Gr}}_+(3,7)$, respectively, are depicted.

With the use of the web graph $\mathrm{Web}_{k,n}$, we introduce the functions $P_K : (\mathbb{R}_{\geq 0})^d \to (\mathbb{R}_{\geq 0})^D$ for any ordered sequence $K = (i_1, \ldots, i_k)$ with $1 \leq i_1 < \cdots i_k \leq n$ as

$$P_{i_1\ldots i_k}(x_1, \ldots, x_d) = \sum_{S \in \mathrm{Path}(i_1,\ldots,i_k)} \mathrm{Prod}_S(x_1, \ldots, x_d) \,, \tag{4.16}$$

whereas the functions on the right hand side are defined as follows. Given $K = (i_1, \ldots, i_k)$ we construct all possible paths along the web graph in the following way. Denoting $[m] = (1, \ldots, m)$, any such path may start at $[k] \setminus (K \cap [k])$, that is at any of the ingoing edges

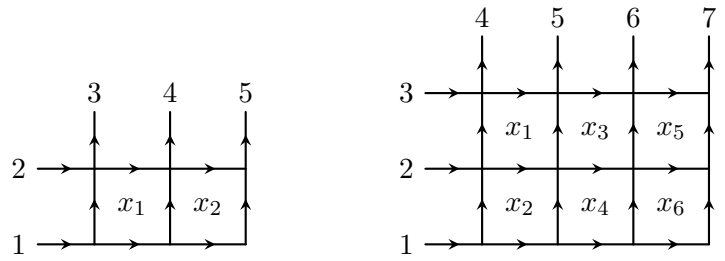

(a) $\mathrm{Web}_{2,5}$ (b) $\mathrm{Web}_{3,7}$

Figure 4.3: Two examples for web graphs, (a) $\mathrm{Web}_{2,5}$ and (b) $\mathrm{Web}_{3,7}$.

except those whose label is contained in K. Furthermore, any path may end at $K\backslash(K \cap [k])$, that is at any of the outgoing edges whose label is contained in K. The set $\mathrm{Path}\,(K)$ is then given as all collections of non-intersecting paths such that all ingoing and outgoing labels that are allowed as start- and endpoints for the paths are covered by a path. Note that for $K = [k]$ there is no such path. However, in this case we include the empty set as a valid path.

Example 4.17. An example for the collections of non-intersecting paths in $\mathrm{Path}\,(2,5)$ is depicted in figure 4.4.

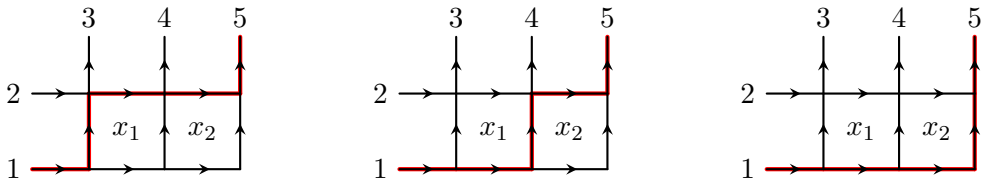

(a) (b) (c)

Figure 4.4: For $\mathrm{Web}_{2,5}$ there are three complete collections of non-intersecting paths in $\mathrm{Path}\,(2,5)$, each consisting of one path.

For any complete collection of non-intersecting paths $S \in \mathrm{Path}\,(K)$, we obtain the monomial $\mathrm{Prod}_S\,(x)$ by multiplying for each path in S the x variables of those chambers, that are located above the path. This also includes those chambers that are not directly above the path but separated by other internal chambers. If there are no such chambers, we associate 1 to the path.

Example 4.18. We conclude our examples for $\mathrm{Web}_{2,5}$ and $\mathrm{Web}_{3,7}$. Consider for example the function P_{25} of $\mathrm{Web}_{2,5}$. The three collections of non-intersecting paths are depicted in figure 4.4. The path on the left hand side contributes by x_1, whereas the right hand path contributes by 1. We thus obtain

$$P_{25}(x_1, x_2) = 1 + x_1 + x_1 x_2\,. \tag{4.17}$$

For the function P_{356} of $\text{Web}_{3,7}$, the collections of non-intersecting paths are depicted in figure 4.5. Summing over these collections, we obtain

$$P_{356}(x_1, x_2, x_3) = x_1^2 x_2 x_3 x_4 + x_1 x_2 x_3 x_4 + x_1 x_2 x_3 \,. \tag{4.18}$$

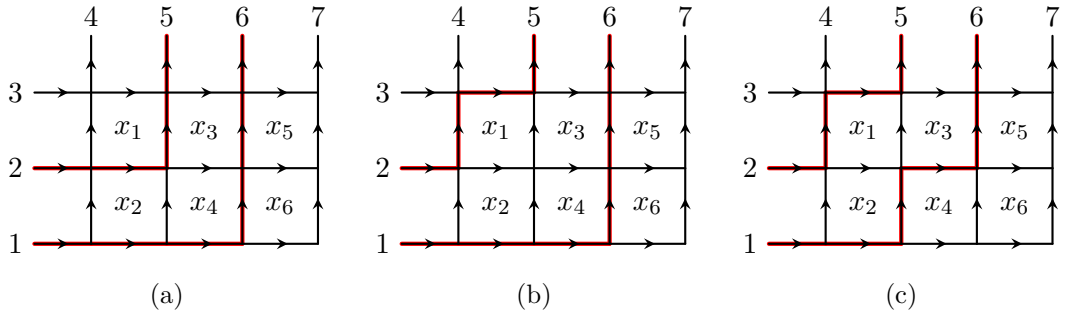

Figure 4.5: Collections of non-intersecting paths in Path $(3, 5, 6)$ of $\text{Web}_{3,7}$.

Finally, we use the previously defined map P_K to construct the parameterisation of the positive configuration space. It is obtained by parameterising each Plücker variable p_K for an ordered sequence $K = (i_1, \ldots, i_k)$ by P_K, with the Plücker variables of any unordered sequence K' being equal to P_K up to the appropriate sign and K being the ordered version of K'. Collecting the D ordered Plücker variables in a vector, we can also express the parameterisation as the function

$$\Phi : (\mathbb{R}_{\geq 0})^d \to \widetilde{\text{Gr}}_+(k, n) \,, \quad (x_1, \ldots, x_d) \mapsto \{P_K(x_1, \ldots, x_d)\}_K \,, \tag{4.19}$$

that is the web variables $x_1, \ldots, x_d$ are mapped to the D-vector whose $K = (i_1, \ldots, i_k)$ component is given by $P_K(x_1, \ldots, x_d)$. As proven in [71], the map Φ is indeed a bijection.

4.1.3. Fans of the totally positive tropical configuration space

In [71], the authors not only introduced the totally positive tropical configuration space and demonstrated that it is a fan in $\mathbb{R}^D$ of dimension $d = (k-1)(n-k-1)$, but also introduced another, full-dimensional fan in $\mathbb{R}^d$ that is combinatorially equivalent to the former. In this section, we review its construction based on the web-parameterisation and conclude with a complete example of the construction of $\widetilde{\text{Tr}}_+(2, 5)$.

The starting point of the construction is the following general result which relates a parameterisation of an affine variety to its tropicalisation. It is stated in terms of $\mathcal{C}$ and $\mathcal{R}$, the fields of Puiseux series with complex and real coefficients, respectively, and whereas by $\mathcal{R}^+$ we denote the restriction of $\mathcal{C}$ to those series where the coefficient of the monomial with the lowest exponent is real and positive.

Proposition 4.19 (Speyer, Williams [71])**.** *Consider two affine varieties $V(I) \subset \mathcal{C}^m$ and $V(J) \subset \mathcal{C}^l$ and a rational map $f : \mathcal{C}^m \to \mathcal{C}^l$ that can be written without using subtraction and that takes $V(I)$ to $V(J)$ such that $V(I) \cap (\mathcal{R}^+)^m$ is mapped surjectively onto $V(J) \cap (\mathcal{R}^+)^l$. Then the tropicalised function Trf maps $Tr_+V(I)$ surjectively onto $Tr_+V(J)$.*

Up to some subtleties,[4] this allows us to transfer the parameterisation Φ of the positive configuration space to its tropical version. Skipping some of the technical details, we consequently consider the tropicalisation $\mathrm{Tr}\Phi$, which maps the tropicalised web-variables $\tilde{x}_1, \ldots, \tilde{x}_k$ to the D-vector whose $K = (i_1, \ldots, i_k)$ component is given by

$$(\mathrm{Tr}P_K)(\tilde{x}_1, \ldots, \tilde{x}_k) = \min_{S \in \mathrm{Path}(i_1,\ldots,i_k)} (\mathrm{Sum}_S(\tilde{x}_1, \ldots, \tilde{x}_k)) \,, \tag{4.20}$$

where Sum_S is obtained in the obvious way from Prod_S by replacing multiplication with addition. Note that $\mathrm{Tr}P_K$ in this way corresponds to a parameterisation of the tropical Plücker variable $w_{i_1\ldots i_k}$. By proposition 4.19, the function $\mathrm{Tr}\Phi$ is a surjective map from $\mathbb{R}^d$ to the totally positive tropical configuration space $\widetilde{\mathrm{Tr}}_+(k,n)$.

Being a tropical polynomial, we can construct an associated tropical hypersurface in $\mathbb{R}^d$, which splits up the space $\mathbb{R}^d$ into the regions of linearity of this map. This hypersurface arrangement in fact constitutes a complete fan in $\mathbb{R}^d$, whose maximal, that is d-dimensional, cones are given by the regions of linearity of the tropical polynomial. To construct the entire positive tropical configuration space $\widetilde{\mathrm{Tr}}_+(k,n)$, we tropicalise all Plücker variables $p_{i_1\ldots i_k}$ parameterised by $P_{i_1\ldots i_k}$ and obtain their tropical hypersurfaces resulting in such a fan in $\mathbb{R}^d$ for each of the Plücker variables. The fan $F_{k,n}$ of $\widetilde{\mathrm{Tr}}_+(k,n)$ is then given as the common refinement of the individual fans. This is made precise by the following definition.

Definition 4.20 (Fan $F_{k,n}$ of $\widetilde{\mathrm{Tr}}_+(k,n)$ [71])**.** The fan $F_{k,n}$ is the complete fan in $\mathbb{R}^d$ with $d = (k-1)(n-k-1)$ whose maximal cones are the domains of linearity of the piecewise linear map $\mathrm{Tr}\Phi$.

Note in particular that in contrast to the construction of a tropical variety as the intersection of tropical hypersurfaces, see definition 4.9, all points in $\mathbb{R}^d$ are in fact part of the fan $F_{k,n}$ and not only the points of the tropical hypersurfaces of the polynomials P_K. Furthermore, by using the tropicalised Plücker parameterisation, eq. (4.20), we can alternatively obtain an embedding of the d-dimensional fan $F_{k,n}$ into $\mathbb{R}^D$. It is the image of $\mathbb{R}^d$ under this map that corresponds to the totally positive tropical configuration space $\widetilde{\mathrm{Tr}}_+(k,n)$ as constructed in section 4.1.1, which itself is a fan in $\mathbb{R}^D$ of dimension d and combinatorially equivalent to $F_{k,n}$.

Example 4.21 ($F_{2,5}$)**.** Proceeding as in the examples of the previous section, we get the parameterisation of $\widetilde{\mathrm{Gr}}_+(2,5)$ in terms of the web-variables x_1, x_2 as

$$P_{1l} = P_{23} = 1 \,, \qquad P_{24} = 1 + x_1 \,, \qquad P_{25} = 1 + x_1 + x_1x_2 \,, \tag{4.21}$$

$$P_{34} = x_1 \,, \qquad P_{35} = x_1 + x_1x_2 \,, \qquad P_{45} = x_1x_2 \,. \tag{4.22}$$

The tropicalisation of these polynomials is given by

$$W_{1l} = W_{23} = 0 \,, \qquad W_{24} = \min(0, \tilde{x}_1) \,, \qquad W_{25} = \min(0, \tilde{x}_1, \tilde{x}_1 + \tilde{x}_2) \,, \tag{4.23}$$

[4] In order to apply this result, one first has to extend the Plücker ideal to an ideal in the field of rational functions with coefficients from $\mathcal{R}$, the set of Puiseux series with real coefficients, and show that the extension of the parameterisation Φ to this field still is a bijection. To this map we can then apply the proposition, see also section 4 in [71].

$$W_{34} = \tilde{x}_1\,, \qquad W_{35} = \min(\tilde{x}_1, \tilde{x}_1 + \tilde{x}_2)\,, \qquad W_{45} = \tilde{x}_1 + \tilde{x}_2\,, \tag{4.24}$$

whereas similar to the Plücker variables we denote $W_K = \mathrm{Tr}P_K$. Constructing the tropical hypersurfaces of these polynomials, we get $V_1 = \{\tilde{\boldsymbol{x}} \in \mathbb{R}^2 : \tilde{x}_1 = 0\}$ from W_{24}, $V_2 = \{\tilde{\boldsymbol{x}} \in \mathbb{R}^2 : \tilde{x}_2 = 0\}$ from W_{45} as well as $V_3 = \{\tilde{\boldsymbol{x}} \in \mathbb{R}^2 : \tilde{x}_1 = 0\,, \tilde{x}_2 \geq 0\}$, $V_4 = \{\tilde{\boldsymbol{x}} \in \mathbb{R}^2 : \tilde{x}_2 = 0\,, \tilde{x}_1 \leq 0\}$, and $V_5 = \{\tilde{\boldsymbol{x}} \in \mathbb{R}^2 : \tilde{x}_1 + \tilde{x}_2 = 0\,, \tilde{x}_2 \leq 0\}$ from W_{25}. These hypersurfaces split up $\mathbb{R}^2$ into five 2-dimensional cones that are spanned by a total of 5 rays. The fan $F_{2,5}$ that results from this hypersurface arrangement is depicted in fig. 4.6.

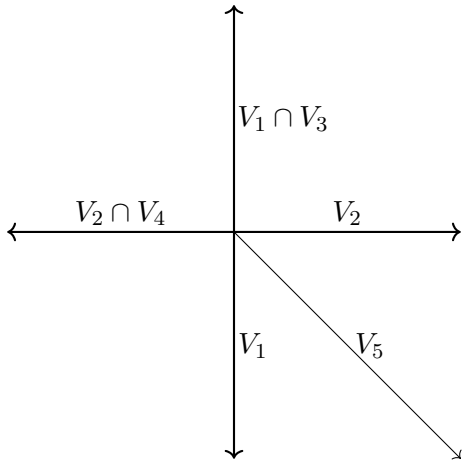

Figure 4.6: Fan $F_{2,5}$. Each segment is labelled by the hypersurfaces that constitute it.

Remark 4.22. Whereas this construction is the canonical way to tropicalise the positive configuration space, we may choose to only tropicalise a subset of all Plücker variable parametrisations. The resulting fan is the common refinement of the corresponding subset of fans associated to the Plücker variables and thus a coarser version of the fully tropicalised fan. This means that the partial fan consists of less rays and cones with some of the cones of the full refining those of the partial fan. In the remainder of this work we will be almost exclusively focusing on the following *partial tropicalisation* of the configuration space $\widetilde{\mathrm{Gr}}_+(4,n)$,

$$\widetilde{\mathrm{pTr}}_+(4,n): \begin{array}{l} \langle ii+1jj+1\rangle \to \mathrm{Tr}\left(\langle ii+1jj+1\rangle\right), \\ \langle ij-1jj+1\rangle \to \mathrm{Tr}\left(\langle ij-1jj+1\rangle\right), \end{array} \quad i = 1,\ldots,n\,, \tag{4.25}$$

namely we only tropicalise the Plücker variables with indices either pairwise adjacent, or forming an adjacent triplet. The associated fan will be denoted by $pF_{4,n}$. As we will see in later sections, this choice is believed to be the most relevant for n-particle amplitudes in $\mathcal{N} = 4$ pSYM, as it leads to predictions for their singularities that agree with the known $n = 6, 7$ cases, and more generally respects the parity symmetry of MHV amplitudes in a minimal way [72, 185, 186]. In contrast, $\widetilde{\mathrm{Tr}}_+(4,n)$ is not parity invariant.

4.2. Tropical cluster bootstrap

As we reviewed in section 2.3.3, the space of kinematics of n-particle scattering in planar $\mathcal{N} = 4$ super Yang-Mills theory is the configuration space $\widetilde{\mathrm{Gr}}(4,n)$, a quotient of the Grassmannian $\mathrm{Gr}(4,n)$ by the torus action $(\mathbb{C}^*)^{n-1}$. Up to this point, we have seen two very different constructions that allow to associate a fan to the configuration space. First, in section 3.1.4 we discussed the cluster fan of the cluster algebra of $\mathrm{Gr}(k,n)$, a fan in $\mathbb{R}^d$ with $d = (k-1)(n-k-1)$ which is infinite and not complete for $k = 4$ and $n \geq 8$. Second, in the previous section we discussed the fan $F_{k,n}$ of the totally positive tropical configuration space $\widetilde{\mathrm{Tr}}_+(k,n)$, a finite and complete fan in $\mathbb{R}^d$.

For the simpler, two-dimensional examples of the cluster algebra of $\mathrm{Gr}(2,5)$ and the totally positive tropical confiugration space $\widetilde{\mathrm{Tr}}_+(2,5)$, we have explicitly constructed the respective fans, see figs. 3.16 and 4.6, respectively. In figure 4.7 we depict both of these fans again. Remarkably, the two fans created by very different procedures are in fact equal!

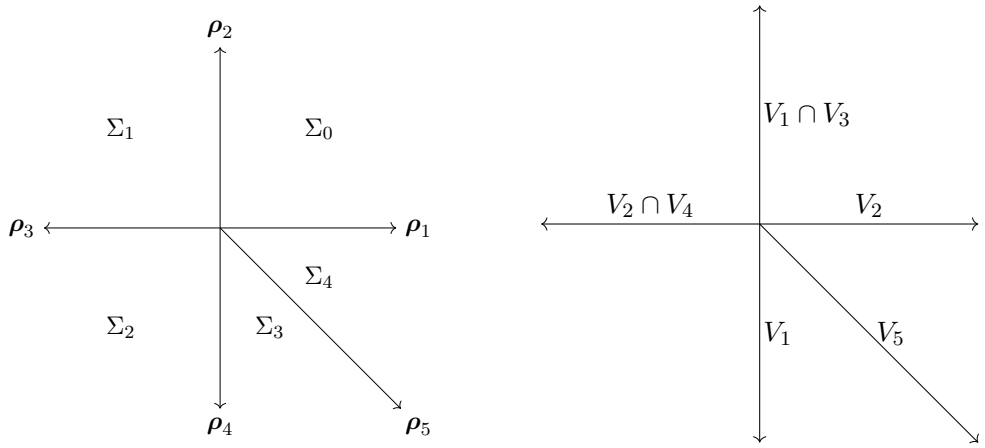

(a) cluster fan (b) $F_{2,5}$

Figure 4.7: Comparison of (a) the cluster fan of $\mathrm{Gr}(2,5)$ and (b) the fan $F_{2,5}$ of the totally positive tropical configuration space $\widetilde{\mathrm{Tr}}_+(2,5)$.

As we will discuss in the remainder of this chapter, while not in general equal, the cluster fan of $\mathrm{Gr}(k,n)$ and the fan $F_{k,n}$ are closely related. With the tropical fan being inherently finite, it is this relation that will allow us to formulate a new approach, the *tropical cluster bootstrap*, to obtain a finite symbol alphabet for $n \geq 8$ particles while reproducing the previously known results for $n < 8$.

4.2.1. Triangulating tropical geometries

As was first demonstrated by general techniques for the cluster algebra of $\mathrm{Gr}(3,7)$ in [71] and for many other cluster algebras in [70], the cluster fan of a finite cluster algebra of $\mathrm{Gr}(k,n)$ is a refinement of the fan of the totally positive tropical configuration space $\widetilde{\mathrm{Tr}}_+(k,n)$. That is, the cones of the cluster fan are all contained within cones of the tropical fan. Since the cones of the cluster fan are all simplicial, it triangulates $\widetilde{\mathrm{Tr}}_+(k,n)$. Note

that this relation allows to compute the fan $F_{k,n}$ of $\widetilde{\mathrm{Tr}}_+(k,n)$ by using the simple algebraic operations on the cluster algebra of $\mathrm{Gr}(k,n)$.

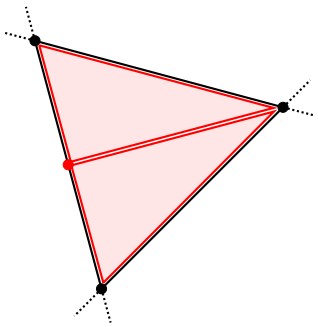

Figure 4.8: The intersection of a simplicial cone of a 3-dimensional fan with the unit sphere S^2 in black and that of two simplicial cones of another fan in red. The black lines correspond to the tropical hypersurfaces with rays of the associated fans at their intersections. The cone is triangulated by two simplicial cones (red) due to the redundant ray that only lies on one of the hypersurfaces.

In this triangulation, however, the cluster algebra sometimes introduces *redundant rays* – rays of the cluster fan that are not tropical rays. Geometrically, redundant rays are not on a 1-dimensional but a higher dimensional intersection of tropical hypersurfaces. Instead they are the positive linear combination of two tropical rays spanning some cone. This is illustrated in figure 4.8 and the left hand side of figure 4.9. In general, a ray is redundant if the number of linearly independent tropical hypersurfaces it lies on, the *ray rank*, is less then the maximal value $d-1$. In this case, the ray does not lie on a 1-dimensional intersection of tropical hypersurfaces and is thus redundant.

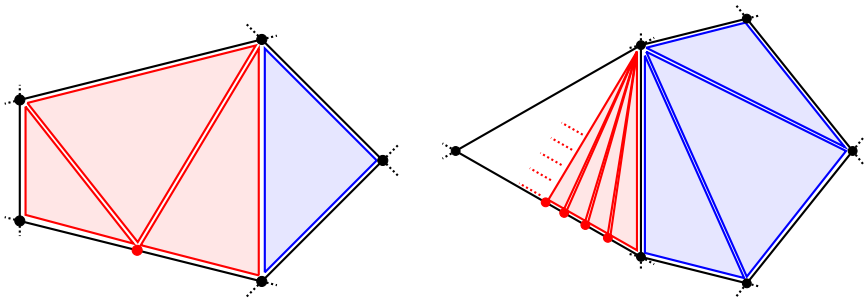

(a) Finite case (b) Infinite case

Figure 4.9: Illustrative examples of the (redundant) triangulation of a tropical fan by a (a) finite and (b) infinite cluster algebra. Each of the figures depicts two cones of a 3-dimensional fan intersected with the unit sphere S^2 in black. The cones and the redundant rays from the redundant triangulation are drawn in red, those from the non-redundant triangulation in blue.

If the cluster algebra is infinite, e.g. in our case of $\mathrm{Gr}(4,n)$ for $n \geq 8$, it consists of infinitely many $\mathcal{A}$-variables and thus also rays. In the regions of the ambient space $\mathbb{R}^d$ that

are covered by the cluster fan, it again refines the fan $F_{k,n}$ of the tropical configuration space. Since the latter is by construction always finite, almost all of the cluster rays are redundant. It is therefore natural to expect that the nature of the infinities of the cluster algebra can be interpreted as a redundant triangulation of $F_{k,n}$ with infinitely many cones of the cluster fan containing redundant rays, as is illustrated on the right hand side of figure 4.9.

Note that these (redundant) triangulation properties also applies to the fan of any partial tropicalisation of $\widetilde{\mathrm{Gr}}_+(k,n)$, such as $pF_{4,n}$, which is a coarser version of the fully tropicalised fan and hence also triangulated by the cluster fan. In fact, as is discussed in [186], in the finite cases one can also go in the other direction and include additional polynomials in the Plücker variables, parameterise those with the web-parameterisation and also tropicalise the resulting polynomial. If we tropicalise all cluster variables, which are polynomials of the initial Plücker variables, the resulting tropical fan is exactly the cluster fan.

Finally, the cones of the cluster fan can be fused along redundant faces to obtain the fan of the totally positive tropical configuration space. We consider a face of the cluster fan as a redundant face if it is not actually a face of $F_{k,n}$ but only apparent due to the triangulation of a non-simplicial cone by simplicial cones of the cluster algebra. Just as for redundant rays, we can determine whether a face is redundant or not by computing its face rank, the number of linearly independent tropical hypersurfaces on which the face lies. A dimension-m face is non-redundant if this number assumes the maximal value of

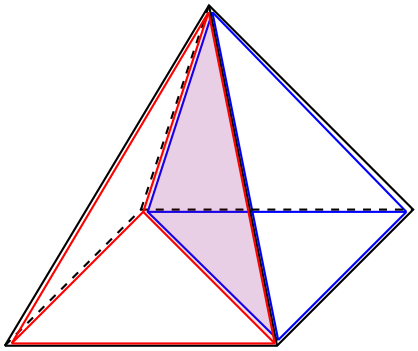

Figure 4.10: The intersection of a non-simplicial cone (the pyramid) of a 4-dimensional fan with the unit sphere S^3. This cone is triangulated by two simplicial cones, drawn in red and blue. These two cones share a codimension-1 face along which we fuse. When doing so, the codimension-2 face on the base of pyramid is also fused and thus deleted.

$d-m$. In practice, for any m we consider all dimension-m faces and fuse them along their redundant dimension-$(m-1)$ boundaries, which are thus removed. This is illustrated in 4.10 for a pyramid with square base which is triangulated by two simplices.

4.2.2. Truncated cluster algebra

To tame the infinity of the cluster algebra, we utilize the relation between the cluster fan and the inherently finite fan $(p)F_{4,n}$ of the (partially) tropicalised positive configuration

space and introduce the following selection rule: whenever we encounter a cluster containing a redundant ray we stop mutation in this direction and discard all such redundant clusters. This results in the *truncated cluster algebra*, defined as follows.

Definition 4.23 (Truncated cluster algebra)**.** Consider a cluster algebra $\mathscr{A}$ of $\mathrm{Gr}(k,n)$ with initial seed Σ_0. We say that a cluster is *non-redundant* with respect to $(p)F_{k,n}$, if the rays associated to all cluster variables in that cluster are non-redundant rays of $(p)F_{k,n}$. The *cluster algebra truncated by* $(p)F_{k,n}$ is the subset of clusters which are non-redundant with respect to $(p)F_{k,n}$ and which are connected to Σ_0 via a sequence of mutations along non-redundant clusters.

Remark 4.24. Note that in theory we can choose the fan $\tilde{F}_{k,n}$ of any (partial) tropicalisation of the totally positive configuration space. If this choice is clear from context, we usually drop the explicit reference to the fan and refer to the cluster algebra truncated by that fan as the *truncated cluster algebra*.

To construct the truncated cluster algebra, we start from the initial cluster, which by construction does not contain redundant rays and is thus part of the truncated cluster algebra.[5] Next, we perform all possible mutations stopping whenever we obtain a cluster containing a redundant ray. Once we have exhausted all mutations that lead to new, non-redundant clusters, we have obtained the entire truncated cluster algebra. Each of the rational $\mathcal{A}$-variables in this subset is then by construction in one-to-one correspondence to a tropical ray of $(p)F_{4,n}$.

With the finite, truncated cluster algebra, we can modify conjecture 3.59, which formed the starting point of the cluster bootstrap, to obtain a finite symbol alphabet. The *tropical cluster bootstrap* is based on the following conjecture.

Conjecture 4.25 (Tropical cluster bootstrap)**.** *The alphabet of n-particle MHV and NMHV amplitudes in planar $\mathcal{N}=4$ super Yang-Mills theory is given by the cluster variables of the finite cluster algebra of* $\mathrm{Gr}(4,n)$ *truncated by the fan of* $\widetilde{\mathrm{pTr}}_+(4,n)$.

We explore the finite symbol alphabets that can be obtained from the different truncations of the cluster algebra in section 4.3 as well as sections 6.2 and 6.3. Note though that this conjecture is still not in its final form. In chapter 5, we discuss another modification that also incorporates non-rational letters in addition to the rational letters obtained from the (truncated) cluster algebra itself.

4.3. Example: $\widetilde{\mathrm{pTr}}_+(4,7)$ and seven-particle scattering

Having reviewed the basics of tropical geometry, the construction of the totally positive tropical configuration space, as well as its relation to the cluster fan, we now put the newly formulated tropical cluster bootstrap to its first test. While we have introduced tropical geometry as a way to obtain a finite subset of the infinite cluster algebras of $\mathrm{Gr}(4,n)$ for

[5] The rays of the initial cluster of a cluster algebra of $\mathrm{Gr}(k,n)$ are by definition the unit vectors of $\mathbb{R}^d$. It can be shown that these are non-redundant rays of $F_{k,n}$.

$n \geq 8$, the truncated cluster algebra is also well-defined for $n < 8$, where the cluster algebra itself already is finite. For the tropical cluster bootstrap to be well-defined, it has to be consistent with this case and reproduce the well-known, finite symbol alphabet. For this reason, we apply it to the case of seven-particle scattering in this section and demonstrate that this is indeed the case. In doing so, we also explore in how far the fan of the totally positive tropical configuration space might be used to explain the beyond-cluster adjacency restrictions we discussed in section 3.2.3 and how the two, full and partial, tropicalisations differ from each other in their application to the tropical cluster bootstrap.

4.3.1. Truncated cluster algebra of $\mathrm{Gr}(4,7)$

In section 3.2.3 we have already constructed the cluster algebra of $\mathrm{Gr}(4,7)$ and have found that it consists of 42 variables in 833 clusters, which correspond to the 42 rays and 833 cones of the cluster fan, respectively. To construct the whole fan, we start at the initial seed and perform all possible mutations of the ray matrix using eq. (3.35). The columns of this ray matrix correspond to the rays of the cluster fan with all rays from one matrix spanning the cone associated to that cluster. By simple counting we can compute the f-vector, as defined in 3.44, of the cluster fan, which in this case is a complete fan in $\mathbb{R}^6$, and find that it in accordance with the literature is given by

$$f_{E_6} = (42, 399, 1547, 2856, 2499, 833)\,, \tag{4.26}$$

whereas we label it by E_6 since the cluster algebra is of that Dynkin type.

Next, we turn to the tropical fans $F_{4,7}$ and $pF_{4,7}$ of the full and partial tropicalisation, respectively, whereas from now on the partial tropicalisation always refers to the subset defined eq. (4.25). Starting with the full tropicalisation, we first use the web-parameterisation to parameterise the positive configuration space in terms of the six independent web-variables $x_1, \ldots, x_6$. Examples for this are given in section 4.1.2, where we discussed the dual space $\widetilde{\mathrm{Gr}}_+(3,7)$.[6] To construct the tropical fan $F_{4,7}$ we next tropicalise this parameterisation and use a computer program to obtain the tropical hypersurface for each parameterisation polynomial. Each of them splits up $\mathbb{R}^6$ into the regions of linearity of its polynomial and forms a complete fan in $\mathbb{R}^6$. As defined in general in section 4.1.3, the fan $F_{4,7}$ is finally obtained as the common refinement of all these fans, again using a computer program. Its f-vector $f_{4,7}$ is

$$f_{4,7} = (42, 392, 1463, 2583, 2163, 693)\,, \tag{4.27}$$

which is precisely what was reported in [71].

With the data of these two fans, it can be explicitly checked that the interior of the obtained cones does not intersect any tropical hypersurfaces as well as that all faces actually lie on tropical hypersurfaces and together form a complete fan, implying that the cluster fan actually refines and thus triangulates $F_{4,7}$. Furthermore, with all computations taking

[6] Note that in general the space $\mathrm{Gr}(k,n)$ is equivalent to $\mathrm{Gr}(n-k,n)$ and consequently also their positive parts. Similarly, there exists an isomorphism between the corresponding positive configuration spaces.

only on the order of minutes to complete, this highlights the efficiency of using cluster algebras as a computational tool for totally positive tropical configuration spaces.

Having verified empirically that the cluster fan indeed triangulates the fan $F_{4,7}$, we can construct the truncated cluster algebra. Since the set of rays of the cluster fan and the tropical rays of $F_{4,7}$ precisely match, the cluster fan does not contain any redundant rays such that all clusters are non-redundant. Consequently, the truncated cluster algebra in this case contains all clusters of the original cluster algebra. Even more, this implies that the truncated cluster algebra gives rise to the same, already known, finite symbol alphabet that was previously obtained from the cluster algebra alone. For this finite case, and in fact similarly for the case of six-particle scattering, the tropical cluster bootstrap thus reduces to the original cluster bootstrap.

Finally, we can also make use of the fusing procedure outlined above to remove redundant rays and faces from the cluster fan and thus pass to the coarser fan $F_{4,7}$. As can be seen from the f-vectors, this results in the removal of seven dimension-2 faces from the cluster fan, which in turn correspond to admissible pairs of cluster variables that appear together in a cluster. The removed faces and pairs are given in table 4.1. It turns out that the seven faces removed in $F_{4,7}$ with respect to the cluster fan of $\mathrm{Gr}(4,7)$ are precisely those given by the extended cluster adjacency restrictions, eq. (3.69b), pairs that are admissible from the perspective of the cluster algebra but have been conjectured to not appear in any symbol of seven-particle scattering.

$-e_1$	$e_2+e_4-e_6$	(a_{35},a_{62})
e_3	$-e_2+e_5$	(a_{32},a_{66})
e_4	$-e_1+e_3+e_5-e_6$	(a_{37},a_{64})
$-e_6$	$e_1+e_2-e_3-e_5$	(a_{31},a_{65})
e_1-e_2	$e_1-e_2-e_4+e_6$	(a_{34},a_{61})
e_2-e_3	$e_2+e_4-e_5-e_6$	(a_{33},a_{67})
e_1-e_4	$e_1-e_3-e_5$	(a_{36},a_{63})

Table 4.1: Dimension-2 faces that are missing in $F_{4,7}$ compared to the E_6 cluster fan. In the first two columns, the two rays spanning the face are given in terms of the canonical unit vectors e_i of $\mathbb{R}^6$. In the final column we list the cluster variable associated to these rays in the notation of eqs. (3.67).

Note that only the faces related to eq. (3.69b) and not their reflected counterparts, eq. (3.69a), are missing in $\widetilde{\mathrm{Tr}}_+(4,7)$. This implies that the totally positive tropical configuration space is not symmetric under a dihedral reflection, which is a symmetry of the cluster algebra and the associated superamplitudes. For this reason, we also consider the fan $pF_{4,7}$ of the partially tropicalised positive configuration space, which is obtained by only tropicalising the parameterisations of the Plücker variables of the form $\langle ii+1jj+1\rangle$ and $\langle ij-1jj+1\rangle$, see eq. (4.25). It can be constructed in the same way as the fan of the full tropicalisation, but whereas we tropicalise only the specified subset of polyonmials. The resulting fan is compatible with all expected symmetries of the amplitude and, as first

computed in [186], its f-vector is given by

$$f_{4,7}^{(p)} = (42, 385, 1393, 2373, 1918, 595)\,. \tag{4.28}$$

Note that the truncation of the cluster algebra by this fan also yields all 42 symbol letters. The 14 dimension-2 faces that are missing in $pF_{4,7}$ with respect to the cluster fan correspond to the pairs of eqs. (3.69a) and (3.69b).

4.3.2. Cluster adjacency of seven-particle amplitudes

In the previous section we have seen that both fans $F_{4,7}$ and $pF_{4,7}$ yield all 42 letters of the cluster algebra of $\mathrm{Gr}(4,7)$. Consequently, the cluster bootstrap would be compatible with this finite case regardless of which of the two fans we choose. However, as we have also seen, the fan $pF_{4,7}$ respects all symmetries of the amplitude whereas the fan of the full tropicalisation is not symmetric under dihedral reflections. Even more, the 385 dimension-2 faces $pF_{4,7}$ seem to best describe cluster adjacency by also incorporating the extended cluster adjacency restrictions of eqs. (3.69a)–(3.69c). In this section, we will further analyse this last point and gather the symbols of MHV and NMHV amplitudes computed by other means to analyse the adjacent pairs of letters appearing in them.

In [55, 56] the symbols of the seven-particle MHV amplitude up to four loops are given. We found that up to two loops the set of pairs of consecutive letters is smaller then dictated by the three restrictions of eqs. (3.69a), (3.69b) and (3.69c). Starting at three loops, however, the set of pairs of consecutive letters in these amplitudes appears to stabilize with a total number of 371 pairs. These are all pairs allowed by cluster adjacency with the exception of those stated in all three restrictions.

In [56, 57, 187] the symbols of NMHV seven-particle amplitudes up to four loops are given. Up to three loops, we again find that the set of pairs of consecutive letters is smaller than dictated by beyond–cluster adjacency. At four loops, however, we find all 399 pairs of consecutive letters in agreement with cluster adjacency, that is also the pairs of eqs. (3.69a) and (3.69b) do appear. These results are also summarised in table 4.2.

Loops	1	2	3	4
MHV	42	210	371	371
NMHV	63	294	343	399
Cluster adjacency	399			
+ eqs. (3.69a) & (3.69b)	385			
+ eqs. (3.69c)	371			

Table 4.2: Number of unordered pairs of distinct consecutive letters in the symbols of the seven-particle amplitudes at given loop level. Note that all the found pairs obey general cluster adjacency, that is the letters appear together in a cluster of the E_6 cluster algebra. In the last three rows we give the number of consecutive pairs of letters that are theoretically possible considering the seven-particle alphabet and imposing only cluster adjacency or also the restrictions to it.

The analysis of the adjacent letters in the MHV and NMHV seven-particle amplitudes thus suggests that while the fan of the partially tropicalised configuration space $\widetilde{\text{pTr}}_+(4,7)$ appears to be too large to describe the adjacency properties of the MHV amplitudes, at least up to loop four, it best captures the adjacency properties of seven-particle scattering, especially when including the pairs of eq. (3.69c), which were observed to appear in certain integrands. On the other hand, the fan $pF_{4,7}$ is too small to describe the adjacency properties of the NMHV amplitudes, whose pairs of adjacent letters fully saturate those obtained by imposing cluster adjacency only.

From the above analysis as well as the comparison to other explicit results obtained from different approaches, see the next section, we conclude that the partial tropicalisation as defined by eq. (4.25) is the most appropriate choice for our purposes. As argued above, we expect the cluster algebra of $\text{Gr}(4,n)$ truncated by $pF_{4,n}$ to give the correct alphabet for both, MHV and NMHV amplitudes of n particles in planar $\mathcal{N}=4$ super Yang-Mills theory, albeit the fan is expected to describe the adjacency properties of MHV amplitudes only.

4.3.3. Weight-2 words in seven-particle amplitudes

Beyond the cluster adjacency properties, we can analyse further properties of the seven-particle symbols to compare the two different tropicalisations. As we have seen before, not every tensor is the symbol of some function. A necessary and sufficient condition for a tensor of the form

$$\sum_{i_1,\ldots,i_k} c_{i_1\ldots i_k} \log a_{i_1} \otimes \cdots \otimes \log a_{i_k} \tag{4.29}$$

to be the symbol of some function is the integrability condition [82]. Considering weight-2 words, that is symbols consisting of two letters, this condition is given by

$$\sum_{i,j} c_{ij} d\log a_i \wedge d\log a_j = 0\,. \tag{4.30}$$

We hence analyse the independent integrable weight-2 words that appear in the symbols of the MHV and NMHV seven-particle amplitudes. In theory, the weight-2 words could be formed out of all 42 seven-particle letters. Being the symbols of amplitudes, integrability has to be imposed on these combinations. Further imposing cluster adjacency, we obtain 573 independent integrable weight-2 words. If we also impose the beyond–cluster adjacency restrictions (3.69a) and (3.69b), this number is further reduced to 559. These numbers are listed in table 4.3.

Based on the same data as the analysis of cluster adjacency for seven-particle amplitudes, the number of independent integrable weight-2 words that appear in these amplitudes are displayed in table 4.3. Similar to before, we find that while the weight-2 integrable words appearing in the MHV amplitudes up to four loops do not saturate the maximally possible number and are thus compatible with beyond–cluster adjacency, the NMHV amplitudes only follow cluster adjacency. At four loops, the restrictions of eqs. (3.69a) and (3.69b) are too strict and do not hold for the NMHV seven-particle amplitude.

Loops	1	2	3	4
MHV	1	98	489	531
NMHV	15	294	496	573
Integrability	1035			
+ Cluster adjacency	573			
+ eqs. (3.69a) & (3.69b)	559			
+ eqs. (3.69c)	545			

Table 4.3: Number of independent integrable weight-2 words appearing in the seven-particle amplitudes at given loop level. The sets are inclusive with increasing loop number, that is the words appearing at lower loop are part of those at higher loop. The last four rows show the number of independent weight-2 words that are theoretically possible considering the seven-particle alphabet and imposing only integrability or also cluster adjacency or also the restrictions, respectively, to it.

As for the pairs of adjacent letters, this data suggests that the totally positive tropical configuration space is too small to properly describe the seven-particle NMHV amplitudes, as the integrable weight-2 words again saturate those obtained by imposing cluster adjacency only. However, up to four loops the integrable weight-2 words in the seven-particle MHV amplitude do not even saturate those obtained from beyond–cluster adjacency, even with all three restrictions imposed. To confirm whether MHV amplitudes indeed saturate this 545-dimensional space, it would be interesting to compute their 5-loop correction.

5. Non-rationality from infinite mutation sequences

In the previous chapter, we have seen how the fan of the totally positive tropical configuration space gives rise to a selection rule that can be used to select a finite subset of the infinite cluster algebras of $\mathrm{Gr}(4,n)$ for $n \geq 8$ which is also compatible with the finite cases of $n < 8$. While this is an important step forward, the infinite number of cluster variables is not the only obstruction when trying to extend the cluster bootstrap to this case.

By construction, all the letters obtained from the $\mathcal{A}$-variables of a (truncated) cluster algebra are rational. This is easy to see from the mutation rule, which is a birational transformation, such that all cluster variables are rational functions of the variables of the initial seed. However, as was described for example in [188], rational letters are not sufficient to describe the symbol of the amplitudes at eight or more particles already at one-loop. For example, the so-called double-pentagon integrals contribute non-rational letters of the form

$$1 \pm u \mp v + \sqrt{\Delta}\,, \tag{5.1}$$

whereas the conformal cross ratios are given by $u = (\langle 1238\rangle \langle 4567\rangle)/(\langle 1458\rangle \langle 2367\rangle)$ and $v = (\langle 2345\rangle \langle 1678\rangle)/(\langle 1458\rangle \langle 2367\rangle)$, respectively. The radicand Δ of this letter corresponds to the Gram determinant of one of the two four-mass one-loop boxes formed by eight massless legs, see for example [74]. The latter are given by

$$\Delta_{1,3,5,7} = \left(1 - \frac{\langle 1234\rangle \langle 5678\rangle}{\langle 1256\rangle \langle 3478\rangle} - \frac{\langle 1278\rangle \langle 3456\rangle}{\langle 1256\rangle \langle 3478\rangle}\right)^2 - 4\frac{\langle 1278\rangle \langle 1234\rangle \langle 3456\rangle \langle 5678\rangle}{(\langle 1256\rangle \langle 3478\rangle)^2}\,, \tag{5.2}$$

$$\Delta_{2,4,6,8} = \left(1 - \frac{\langle 2345\rangle \langle 1678\rangle}{\langle 2367\rangle \langle 1458\rangle} - \frac{\langle 1238\rangle \langle 4567\rangle}{\langle 2367\rangle \langle 1458\rangle}\right)^2 - 4\frac{\langle 1238\rangle \langle 2345\rangle \langle 4567\rangle \langle 1678\rangle}{(\langle 2367\rangle \langle 1458\rangle)^2}\,, \tag{5.3}$$

whereas $\Delta \equiv \Delta_{2,4,6,8}$ is related to $\Delta_{1,3,5,7}$ by the cyclic shift $\langle ijkl\rangle \to \langle i+1\, j+1\, k+1\, l+1\rangle$. In particular, the square root in (5.1) is not rationalised by the momentum twistor parameterisation in the form of the Plücker variables. Such letters are referred to as non-rational or also *algebraic* letters.[1]

Further to this result, in [61] an alphabet for the eight-point NMHV amplitude constructed via the so-called $\bar{Q}$-equations was proposed, consisting of a total of 18 multiplicatively independent non-rational or algebraic letters. The square roots contained in these letters precisely correspond to the square roots of the two four-mass boxes above.

These non-rational letters can never appear in the purely rational alphabet obtained from the set of cluster variables of some cluster algebra. However, as we review in section 5.1, while not directly part of the cluster variables, we can use the infinity of some cluster algebras to obtain square-root expressions from certain limits. For this reason, the

[1] This is in abuse of notation, since of course the rational letters are algebraic as well.

remainder of this chapter is devoted to the study of such limits and how to utilise them to obtain the square-root letters of the alphabet for the scattering of eight and more particles.

In section 5.2, we first formalise how a certain notion of periodicity leads to the infinite mutation sequences as we consider them in here. Next, we continue to present general results for the sequences of $A_m^{(1)}$ cluster algebras in section 5.3. Finally, in section 5.4 we conclude this chapter with a discussion on how these general results can be used to obtain square-root letters and present our final modification of the cluster bootstrap conjecture.

5.1. Continued fractions and square-roots

There is a notion in which the infinity of a cluster algebra does produce square-root variables. In [189] the connection between cluster algebras and continued fractions was used to study the cluster algebra of affine $A_1^{(1)}$ Dynkin type, whose initial seed consists of two variables a_1 and a_2 connected by two arrows. This cluster algebra is infinite, that is it consists of infinitely many different clusters and $\mathcal{A}$-variables. Specifically, in this cluster algebra there exist two directions in which mutation yields infinitely many letters, as depicted in figure 5.1: one can either repeatedly mutate at the source of the quiver (the node where the arrows originate) or at the sink of the quiver (the node where the arrows point to), denoted by $\mu_1\mu_2\mu_1\cdots$ and $\mu_2\mu_1\mu_2\cdots$, respectively.

$$\cdots \quad \xleftarrow{\mu_1} \quad a_1 \leftleftarrows a_0 \quad \xleftarrow{\mu_2} \quad a_1 \rightrightarrows a_2 \quad \xrightarrow{\mu_1} \quad a_3 \leftleftarrows a_2 \quad \xrightarrow{\mu_2} \quad \cdots$$

Figure 5.1: Infinite mutation sequences $\mu_1\mu_2\mu_1\cdots$ and $\mu_2\mu_1\mu_2\cdots$ in the $A_1^{(1)}$ cluster algebra starting from the initial cluster consisting of a_1 and a_2.

Using the theory of infinite continued fractions, the authors of [189] have demonstrated that in the $A_1^{(1)}$ cluster algebra with no frozen variables[2] the ratio of variables a_i/a_{i-1} along the infinite mutation sequence $\mu_1\mu_2\mu_1\cdots$ converges in the limit of $i \to \infty$ to

$$\lim_{i\to\infty} \frac{a_i}{a_{i-1}} = \frac{a_1' + a_1 + \sqrt{(a_1' - a_1)^2 + 4}}{2a_2}\,, \tag{5.4}$$

with $a_1' = (1 + a_2^2)/a_1$. A similar and somewhat more general result, derived from the perspective of so-called *scattering diagrams*, was also presented in [190]. Note in particular the structural similarity of this limit to the square-root letter of eq. (5.1).

How can we utilise this result to obtain non-rational letters from the cluster algebra? The most direct approach would be to first systematically scan the (truncated) cluster algebra of $\mathrm{Gr}(4,8)$ for appearances of $A_1^{(1)}$ cluster subalgebras, compute the limits of all these subalgebras and finally analyse the resulting set of square-root letters as to whether it is mutliplicatively equivalent to the previously known ones. However, this would require to manually compute the limit of each mutation sequence as the mutations and thus the variables along the sequence depend on the cluster variables connected to the subalgebra.

[2]Equivalently, one can set all coefficients to 1 such that they do not contribute.

When calculating the limit of some mutation sequences, we are effectively restricting mutation to a subalgebra. In this way, the variables connected to it can be considered frozen variables from the perspective of the subalgebra. In theory, one could thus compute the limit of the $A_1^{(1)}$ cluster algebra with a fixed but generic number of frozen variables, say m, and fixed but generic connections to the nodes of the subalgebra, encoded by a $2 \times (2+m)$ extended adjacency matrix, and specify the actual values encountered within the larger cluster algebra after having performed all calculations. Using the framework of frozen variables, which we discussed in section 3.1.1, in this general setting, however, is very complicated.

Instead, the framework of cluster algebras with coefficients, as discussed in section 3.1.2, is much better suited to handle this kind of calculation. Keeping the coefficients general at first, it requires much less effort to consider the infinite mutation sequence, write down its recurrence relation and solve for its limit. After having obtained these results, we can then specify the coefficient semifield as discussed in remark 3.9 to adapt to the actual embedding. In the cases discussed in this work, we can express all relevant results in terms of the $\mathcal{X}$-variables of the initial seed. Since they are obtained as a product over all connected $\mathcal{A}$-variables, see eq. (3.18), these results are well-defined for any embedding.

5.2. Cluster-mutation periodicity

Considering again the infinite mutation sequences in the $A_1^{(1)}$ cluster algebra, see figure 5.1, we observe that up to the labelling of the nodes, the quivers are all isomorphic to the quiver of the initial cluster. In fact, it is this property that makes the sequence treatable as an infinite continued fraction. This *periodicity* property has previously been studied in [191]. For general cluster algebras, it is defined as follows.

Definition 5.1 (Cluster-mutation periodicity)**.** A seed Σ is said to be *cluster-mutation periodic* of period p, if there exists a sequence of p mutations from Σ to another seed Σ' whose quiver is isomorphic to that of Σ.

Example 5.2. According to this definition, any seed of the $A_1^{(1)}$ cluster algebra is cluster-mutation periodic of period 1, since a mutation only flips the arrows resulting in the same quiver up to the labelling of the nodes.

If a quiver is periodic in this sense, we can repeat the same mutation infinitely many times thus giving rise to an infinite mutation sequence. Since the rational functions, eqs. (3.19) and (3.20), that realise the mutation are determined by the quiver, the periodicity allows us to write down a recurrence relation for all clusters along the sequence,

$$a_{i;j+1} = M_i\left(a_{1;j}, \ldots, a_{r;j}; y_{1;j}, \ldots, y_{r;j}\right) , \tag{5.5}$$

whereas we label the clusters and its elements along the sequence by the integer j. Unlike for generic cluster algebras, due to the periodicity of the quiver, the rational function M_i does not depend on j but is the same for all clusters along the sequence.

Note that in general, while we may repeat the mutation infinitely many times, the resulting sequence may be periodic, that is consisting of only a finite set of different $\mathcal{A}$-variables. This is the case whenever the considered cluster algebra is finite, like for example for the cluster algebra of A_2 Dynkin type, whose initial quiver is given by two nodes connected by one arrow. Each of the clusters of the corresponding cluster algebra is mutation-periodic of period 1 but the cluster algebra is finite consisting of five clusters and five variables.

Periodic clusters have been studied and classified in [191] for period one and two. Using this perspective, in this section we consider cluster algebras of $A_m^{(1)}$ Dynkin type for $m \in \mathbb{N}$, which are the largest class of period one *primitives*, the building blocks of all period one cluster algebras. To the best of our knowledge the analysis of their infinite mutation sequences is new, and thus may be of intrinsic mathematical interest irrespective of the application to the loop amplitudes of planar $\mathcal{N} = 4$ super Yang-Mills theory. Some calculations and proofs are omitted in the main text, we refer the interested reader to appendix A for further details.

5.3. Infinite mutation sequences of type $A_m^{(1)}$

The cluster algebras of $A_m^{(1)}$ Dynkin type are rank-$(m+1)$ cluster algebras whose eponymous quivers are depicted in figure 5.2. As can be easily seen, mutating at either the source or sink (ie. the node of $a_{1;j}$ or $a_{m+1;j}$) leads to the same quiver with the labels of the nodes rotated clockwise by one position. In this section, we will discuss the repeated mutation at the source, that is we always mutate $a_{1;j}$. For the other direction, see appendix A.

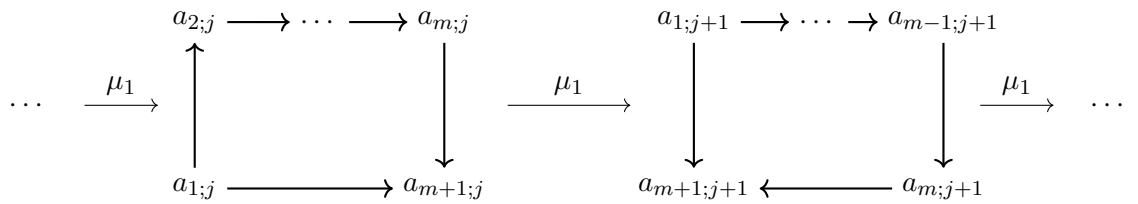

Figure 5.2: Clusters j and $j+1$ along the considered mutation sequence of the cluster algebra of $A_m^{(1)}$ Dynkin type. The coefficients are omitted in the figure.

Remark 5.3. The $A_m^{(1)}$ cluster algebras can also be considered as arising from the surface $A(m, 1)$, which is the annulus with m marked points on the outer and one marked point on the inner boundary. In this formalism, a cluster of the cluster algebra corresponds to a triangulation of this surface, in which each arc connecting two marked points (or one with itself) corresponds to a variable of the cluster, see fig. 5.3 for an example or [178] for details the relation of cluster algebras and triangulated surfaces.

The cluster algebras of $A_m^{(1)}$ Dynkin type are cluster-mutation periodic with period one by the above arguments. From the geometric perspective of the annulus we described, this periodicity corresponds to winding the arcs around the inner boundary, which can be considered as a redundancy in the cluster algebra [192, 193]. We may remove this redundancy by replacing it with quantities that are invariant under mutation or, geometrically

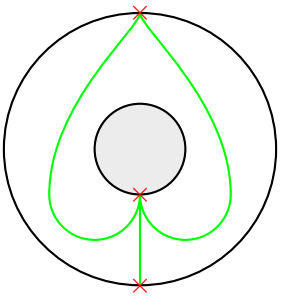

Figure 5.3: A triangulation of the annulus with two marked points on the outer and one marked point on the inner boundary. It corresponds to the initial cluster of the $A_2^{(1)}$ cluster algebra.

speaking, a winding by 2π along the sequence. As it will turn out later, see in particular proposition 5.4, these invariants play a central role in solving the infinite mutation sequences and obtaining algebraic letters from them.

The plan for this section is to obtain the closed form of $a_{i;j}$ along the infinite mutation sequence. We do this by first applying the general equations for the mutation relation, eqs. (3.19), (3.20), and (3.22), to the mutations depicted in fig. 5.2, which results in a recursion relation for the variables along the sequence, eqs. (5.6)–(5.8). Next, we construct quantities that are invariant along this sequence, eqs. (5.27) and (5.28), which in turn can be used to linearise the recursion relations. To obtain a linear recursion relation with constant coefficients, we introduce another sequence α_j in eq. (5.30) and present a closed form for its solution in eq. (5.50). Finally, this solution can in turn be used to obtain a solution for $a_{1;j}$. The reader not interested in the details of this calculation may directly skip to this part and especially eq. (5.51), which defines the objects that have a direct physical application.

Recursion relation

Consider now the infinite mutation sequence depicted in fig. 5.2, which starts at the initial seed denoted by $j = 0$. We can immediately write down the mutation relations for the variables and coefficients along this sequence by applying eqs. (3.19) and (3.20) to the depicted clusters. They are given for any $j \in \mathbb{Z}$ by

$$a_{m+1;j+1} = \frac{a_{2;j}a_{m+1;j}}{a_{1;j}} \frac{1 + x_{1;j}}{1 \hat{\oplus} y_{1;j}} , \tag{5.6}$$

$$y_{1;j+1} = \frac{y_{2;j}\, y_{1;j}}{(1 \hat{\oplus} y_{1;j})} , \quad y_{m;j+1} = \frac{y_{m+1;j}\, y_{1;j}}{(1 \hat{\oplus} y_{1;j})} , \quad y_{m+1;j+1} = (y_{1;j})^{-1} , \tag{5.7}$$

$$x_{1;j+1} = \frac{x_{2;j}\, x_{1;j}}{(1 + x_{1;j})} , \quad x_{m;j+1} = \frac{x_{m+1;j}\, x_{1;j}}{(1 + x_{1;j})} , \quad x_{m+1;j+1} = (x_{1;j})^{-1} . \tag{5.8}$$

Again, it is the periodicity of the quivers that allows us to write down one set of equations that is valid for all clusters j along the sequence. Note that the mutation rule of the $\mathcal{X}$-variables is that of the coefficients with tropical addition changed to normal addition. Also

note that the $\mathcal{X}$-variable associated to $a_{1;j}$ is given by $x_{1;j} = (a_{2;j}a_{m+1;j})^{-1}\, y_{1;j}$, which we used to arrive at eq. (5.6). The other variables and coefficients are not mutated but only shifted in their first index by

$$a_{i;j+1} = a_{i+1;j} \quad \text{for } i \neq m+1\,, \tag{5.9}$$
$$y_{i;j+1} = y_{i+1;j} \quad \text{for } i \notin \{1, m, m+1\}\,, \tag{5.10}$$
$$x_{i;j+1} = x_{i+1;j} \quad \text{for } i \notin \{1, m, m+1\}\,. \tag{5.11}$$

We can use these relations to relate all variables $a_{i;j}$ for $i > 0$ to some $a_{1;j'}$ for an appropriate choice of j'. Consequently, we only need to solve the above recursion relations for $a_{1;j}$ in order to get a solution for all variables in each cluster j along the sequence.

While these recursion relations are defined for any $j \in \mathbb{Z}$, we will only consider the *source-direction* in the remainder of this section, that is we consider $j \geq 0$ and the limit $j \to \infty$. For the other infinite mutation sequence, the *sink-direction*, see appendix A.

Auxiliary sequences

In [191], infinite mutation sequences of type $A_m^{(1)}$ without coefficients[3] were analysed by linearising the recursion relations. Following this approach, we first introduce the auxiliary sequence β_j of ratios, which is defined as

$$\beta_j = \frac{a_{m+1;j}}{a_{1;j}}\,, \tag{5.12}$$

and corresponds to the ratio of the sink-variable over the source-variable. Note that we can use eq. (5.9) to express β_j as $a_{1;j+m}/a_{1;j}$ or similar equivalent ways. Specifying $m = 1$, we see that this is the same sequence whose limit we presented in eq. (5.4) and which sparked the motivation to study these infinite mutation sequences in a more general setting. While β_j and its limit do not quite correspond to the algebraic letters, they nonetheless play an essential role when solving for $a_{1;j}$.

Finally, we also define the auxiliary sequence γ_j as

$$\gamma_j = 1 \,\hat{\oplus}\, y_{1;j} \,\hat{\oplus}\, y_{1;j}\, (y_{1;j-m})^{-1}\,. \tag{5.13}$$

Note that when restricting to the case of no coefficients, we effectively set all $y_{i;j}$ to one such that also γ_j is one for all j along the sequence in this case.

Invariants

Again taking inspiration from the approach used in [191], we attempt to reformulate the recursion relation for $a_{1;j}$ as a single, linear recursion relation with constant coefficients. To refactor eqs. (5.6)–(5.11) accordingly, we next introduce the following two quantities $K_{1;j}$ and $K_{2;j}$, and prove that they are invariant along the sequence.

[3] The cluster algebra without coefficients can be obtained from that with general coefficients by setting the initial coefficients to one. Due to the mutation relations, the coefficients and $(1 \,\hat{\oplus}\, y_{1;j})$ will then be equal to one in every cluster and will not influence the other mutation relations.

Definition/Proposition 5.4. The two quantities $K_{1;j}$ and $K_{2;j}$, defined as

$$K_{1;j} = \left(\gamma_0\beta_0^{-1}\gamma_j^{-1}\beta_j\right)\left[1 + x_{1;j} + x_{1;j}\,(x_{1;j-m})^{-1}\right], \tag{5.14}$$

$$K_{2;j} = \left(\gamma_0\beta_0^{-1}\gamma_j^{-1}\beta_j\right)\left(\gamma_{1-m}\beta_{1-m}^{-1}\gamma_{j-m+1}^{-1}\beta_{j-m+1}\right)\left[x_{1;j}\,(x_{1;j-m})^{-1}\right], \tag{5.15}$$

are invariant along the infinite mutation sequence, whose mutation relations are given by eqs. (5.6)–(5.8). Note that we inserted the factor $\gamma_0\beta_0^{-1}$ and $\gamma_{1-m}\beta_{1-m}^{-1}$ in the definition of $K_{1;j}$ and $K_{2;j}$ to normalise these quantities at $j = 0$ for later convenience.

Proof. First of all, from eqs. (5.6) it follows that the ratio β_{j+1} is related to the quantities at the previous element j of the sequency as

$$\beta_{j+1} = \frac{a_{m+1;j+1}}{a_{1;j+1}} = \frac{a_{m+1;j}}{a_{1;j}}\frac{1 + x_{1;j}}{1 \hat{\oplus} y_{1;j}} = \frac{1 + x_{1;j}}{1 \hat{\oplus} y_{1;j}}\beta_j\,, \tag{5.16}$$

whereas we used that $a_{1;j+1} = a_{2;j}$. On the other hand, it follows from eqs. (5.8) that

$$x_{1;j+1}\,(x_{1;j-m+1})^{-1} = \frac{x_{1;j}x_{2;j}}{x_{1;j-m+1}\,(1 + x_{1;j})} = \frac{x_{1;j}x_{m;j-m+2}}{x_{1;j-m+1}\,(1 + x_{1;j})} \tag{5.17}$$

$$= (1 + x_{1;j})^{-1}\,(1 + x_{1;j-m+1})^{-1}\left[x_{1;j}\,(x_{1;j-m})^{-1}\right], \tag{5.18}$$

whereas we have used eqs. (5.11) to write

$$x_{2;j} = x_{3;j-1} = \cdots = x_{m;j-m+2}\,. \tag{5.19}$$

This also implies that

$$1 + x_{1;j+1} + x_{1;j+1}\,(x_{1;j-m+1})^{-1} = (1 + x_{1;j})^{-1}\left[1 + x_{1;j} + x_{1;j}\,(x_{1;j-m})^{-1}\right]$$

As is a general property of cluster algebras, the corresponding relations for the coefficients can be obtained from those of the $\mathcal{X}$-variables by replacing them with the coefficients and addition by cluster-tropical addition. We thus also have that

$$\gamma_{j+1} = \left(1 \hat{\oplus} y_{1;j}\right)^{-1}\gamma_j\,. \tag{5.20}$$

This implies that $\gamma_{j+1}^{-1}\beta_{j+1} = (1 + x_{1;j})\gamma_j^{-1}\beta_j$ such that the proposition follows. Note that this holds for all $j \in \mathbb{N}$. □

Being invariant along the sequence, these two quantities satisfy $K_{i;j} = K_{i;j'}$ for $i = 1, 2$ and any $j, j' \geq 0$. Using this property, we aim to express them in terms of the variables of the initial seed, that is $j = 0$, only. However, as defined above they still depend on variables from the seeds labelled by j, $j-m$, and $j-m+1$. We thus consider the following result relating $x_{1;j-m}$ to the variables of the cluster j.

Lemma 5.5. *Using the mutation rules in the opposite direction, that is mutating at $a_{m+1;j}$, we can express $x_{1;j-m}$ in terms of the seed labelled by j as*

$$(x_{1;j-m})^{-1} = x_{2;j}\,(1 + x_{3;j}\,(1 + \cdots x_{m;j}\,(1 + x_{m+1;j})))\,. \tag{5.21}$$

Proof. To prove the above relation. we consider the mutation sequence depicted in figure 5.2 in reverse. Since mutation is an involution, we can go from cluster $j+1$ to cluster j by mutating the former at node $m+1$. The relevant mutation relations are given by

$$x_{m+1;j} = x_{m;j+1}\left(1 + x_{m+1;j+1}\right) , \quad x_{1;j} = \left(x_{m+1;j+1}\right)^{-1} , \tag{5.22}$$

$$x_{i;j} = x_{i-1;j+1} \quad \text{for } i \notin \{1, 2, m+1\} . \tag{5.23}$$

As can be seen from these relations, mutating from the cluster j to the cluster $j-m$ along the sequence automatically results in a parmeterisation of $x_{1;j-m}$ in terms of the variables of cluster j. From these, we can immediately conclude that

$$x_{m;j-m+i} = x_{m-1;j-m+i+1} = \cdots = x_{i;j} , \tag{5.24}$$

for $2 \leq i \leq m$. With these relations in place, we can express the $\mathcal{X}$-variable $x_{1;j-m}$ in terms of the variables of cluster j as

$$\begin{aligned} x_{1;j-m}^{-1} &= x_{m+1;j-m+1} = x_{m;j-m+2}\left(1 + x_{m+1;j-m+2}\right) \\ &= x_{2;j}\left(1 + x_{m;j-m+3}\left(1 + x_{m+1;j-m+3}\right)\right) = \cdots \\ &= x_{2;j}\left(1 + x_{3;j}\left(1 + \cdots x_{m;j}\left(1 + x_{m+1;j}\right)\right)\right) , \end{aligned} \tag{5.25}$$

concluding the proof. □

Corollary 5.6. *From eq. (5.21), we can immediately follow the analogous statement relating $y_{1;j-m}$ to the coefficients of the cluster labelled by j. The relation is given by*

$$\left(y_{1;j-m}\right)^{-1} = y_{2;j}\left(1 \hat{\oplus} y_{3;j}\left(1 \hat{\oplus} \cdots y_{m;j}\left(1 \hat{\oplus} y_{m+1;j}\right)\right)\right) . \tag{5.26}$$

Proof. Since the mutation relations for the coefficients are the same as those for the $\mathcal{X}$-variables but with addition replaced by cluster-tropical addition, the relation follows by the same argument as above. □

Finally, with these results we can rephrase the invariants in terms of the $\mathcal{X}$-variables of the initial seed only, as expressed by the following corollary. Note in particular the simple form of these expressions due to the included normalisation factors.

Corollary 5.7. *The invariants, from now on labelled by K_1 and K_2, respectively, can be expressed in terms of the $\mathcal{X}$-variables $x_{1;0}, \ldots, x_{m+1;0}$ of the initial seed as*

$$K_1 \equiv K_{1;0} = 1 + x_{1;0}\left(1 + x_{2;0}\left(1 + x_{3;0}\left(1 + \cdots x_{m;0}\left(1 + x_{m+1;0}\right)\right)\right)\right) , \tag{5.27}$$

$$K_2 \equiv K_{2;0} = x_{1;0}x_{2;0}\left(1 + x_{3;0}\left(1 + \cdots x_{m;0}\left(1 + x_{m+1;0}\right)\right)\right) . \tag{5.28}$$

Proof. Insert eq. (5.21) into eqs. (5.14) and (5.15), respectively. □

Linearised recursion relation

We next proceed to linearise the recursion relation of $a_{1;j}$, eq. (5.6), in order to obtain a closed form for the cluster variables along the sequence and discuss their limits. Using the invariants K_1 and K_2, we can rewrite it as

$$\gamma_j^{-1}\gamma_{j+m}^{-1}a_{1;j+2m} - \gamma_0^{-1}\beta_0 K_1 \cdot \gamma_j^{-1}a_{1;j+m} + \gamma_0^{-2}\beta_0^2 K_2 \cdot a_{1;j} = 0\,. \tag{5.29}$$

While this is indeed a linear and homogeneous recursion relation, it does not have constant coefficients making it difficult to apply standard techniques used to solve recursion relations.

However, we may obtain a recurrence with constant coefficients by introducing yet another sequence, labelled by α_j. It is defined for $j \geq 0$ by

$$\alpha_j = \gamma_{j \bmod m}^{-1}\gamma_{(j \bmod m)+m}^{-1} \cdots \gamma_{j-2m}^{-1}\gamma_{j-m}^{-1} \cdot a_{1;j}\,. \tag{5.30}$$

Note that this is to be read that for $0 \leq i < m$ we have $\alpha_{m+i} = \gamma_i^{-1} \cdot a_{1;m+i}$, and $\alpha_{2m+i} = \gamma_i^{-1}\gamma_{m+i}^{-1} \cdot a_{1;2m+i}$, and so on. In terms of this sequence, the recursion relation eq. (5.29) can be written as

$$\alpha_{j+2m} - \gamma_0^{-1}\beta_0 K_1 \cdot \alpha_{j+m} + \gamma_0^{-2}\beta_0^2 K_2 \cdot \alpha_j = 0\,, \tag{5.31}$$

which is a linear, homogeneous recursion relation with constant coefficients for the sequence α_j for $j \geq 0$. It is defined in terms of the initial values $\alpha_0, \ldots, \alpha_{2m-1}$. We can now apply standard solving techniques to it to obtain a solution for α_j and next use the relation to $a_{1;j}$, eq. (5.30) to also obtain a solution for $a_{1;j}$. Before we continue to do so, we first further discuss the initial values of the recursion for α_j.

Using eq. (5.30), we can alternatively express these initial values in terms of the variables and coefficients of the initial cluster via the mutation relations, eqs. (5.6)–(5.8). In order to express them in a convenient way, we first define analogs for, or generalisations of, K_1 and K_2 by

$$K_i = x_{1;0} \cdots x_{i;0}\,(1 + x_{i+1;0}\,(1 + \cdots x_{m;0}\,(1 + x_{m+1;0})))\,. \tag{5.32}$$

Using these quantities, we can express the initial values $\alpha_0, \ldots, \alpha_{2m-1}$ in terms of the quantities of the initial seed, as expressed by the following lemma.

Lemma 5.8. *The initial values α_i and α_{i+m} for $0 \leq i \leq m-1$ are given by*

$$\alpha_i = a_{i+1;0}\,, \quad \alpha_{m+i} = a_{i+1;0} \cdot \gamma_0^{-1}\beta_0 F_i\,, \tag{5.33}$$

whereas the F_i are given by

$$F_0 = 1\,, \quad F_i = K_1 - K_{i+1}\,, \tag{5.34}$$

which are rational functions in the initial $\mathcal{X}$-variables.

Proof. While the equation on the left hand side of eq. (5.33) can be seen by noting that $\alpha_i = a_{1;i}$ and using eq. (5.9), to prove the second condition – and to determine the F_i – we first observe that $\alpha_{m+i} = \gamma_i^{-1}a_{1;m+i}$ and hence again by eq. (5.9) that $\alpha_{m+i} = \gamma_i^{-1}a_{m+1;i}$.

For $i = 0$, this immediately implies that $\alpha_m = \gamma_0^{-1} a_{m+1;0}$ and hence $F_0 = 1$. For $i \geq 1$, we can use the mutation rule (5.6) and eq. (5.20) to get

$$\alpha_{m+i} = a_{2;i-1}\gamma_{i-1}^{-1}\beta_{i-1}\left(1 + x_{1;i-1}\right) = a_{i+1;0}\gamma_0^{-1}\beta_0 \cdot \prod_{j=1}^{i}\left(1 + x_{1;i-j}\right) , \tag{5.35}$$

whereas we have repeatedly applied the relation $\gamma_{j+1}^{-1}\beta_{j+1} = (1+x_{1;j})\gamma_j^{-1}\beta_j$ in the last step, proving the second initial condition with F_i being the product over the $\mathcal{X}$-variables. To express F_i in terms of the variables of the initial cluster, we observe that by the mutation rules, eqs. (5.8) and (5.11), we have

$$\begin{aligned}
1 + x_{1;i-1} &= \left(1 + x_{1;i-2}\right)^{-1}\left(1 + x_{1;i-2}\left(1 + x_{2;i-2}\right)\right) && (5.36)\\
&= \left(1 + x_{1;i-2}\right)^{-1}\left(1 + x_{1;i-2}\left(1 + x_{i;0}\right)\right) && (5.37)\\
&= \left(1 + x_{1;i-2}\right)^{-1}\left(1 + x_{1;i-3}\right)^{-1}\left(1 + x_{1;i-3}\left(1 + x_{i-1;0}\left(1 + x_{i;0}\right)\right)\right) && (5.38)\\
&= \dots && (5.39)\\
&= \prod_{j=2}^{i}\left(1 + x_{1;i-j}\right)^{-1} \cdot \left(1 + x_{1;0}\left(1 + x_{2;0}\left(1 + \cdots x_{i-1;0}\left(1 + x_{i;0}\right)\right)\right)\right) . && (5.40)
\end{aligned}$$

Using this relation in eq. (5.35) and noting that $\left(1 + x_{1;0}\left(1 + \cdots x_{i-1;0}\left(1 + x_{i;0}\right)\right)\right) = K_1 - K_{i+1}$ completes the proof. □

Limits of auxiliary sequences

Before we turn to the solution of the recursion relation of α_j, and consequently that of $a_{1;j}$, we first discuss the limits of the auxiliary sequences β_j and γ_j. First of all, we have the following result, which is proven in appendix A.

Lemma 5.9. *There exists some $N \in \mathbb{N}$ such that*

$$\gamma_j = 1 , \quad \forall j \geq N . \tag{5.41}$$

The sequence γ_j consequently has the limit $\gamma_j \to 1$ for $j \to \infty$.

Proof. See section A.1. □

Next, we can use the recursion of α_j to discuss the limit of the auxiliary sequence β_j. Consider for this the following lemma.

Lemma 5.10. *Using the recursion relation for α_j, eq. (5.31), we see that, assuming convergence, the limit of the auxiliary sequence of ratios β_j has to be one of $\beta_\pm$ given by*

$$\beta_\pm = \beta_0 \frac{K_1 \pm \sqrt{K_1^2 - 4K_2}}{2\gamma_0} , \tag{5.42}$$

where $\beta_0 = a_{m+1;0}/a_{1;0}$ and $\gamma_0 = 1 \mathbin{\hat{\oplus}} x_{1;0}\left(1 \mathbin{\hat{\oplus}} y_{2;0}\left(1 \mathbin{\hat{\oplus}} y_{3;0}\left(1 \mathbin{\hat{\oplus}} \cdots y_{m;0}\left(1 \mathbin{\hat{\oplus}} y_{m+1;0}\right)\right)\right)\right)$.

Proof. First, note that $\alpha_{j+m}/\alpha_j = \gamma_j^{-1}\beta_j$. Since $\gamma_j \to 1$ for $j \to \infty$, as discussed above, this demonstrates that, assuming convergence, the limit of α_{j+m}/α_j is the same as that of β_j. Next, we divide the recursion relation, eq (5.31), by α_j and, again assuming convergence, take the limit of $j \to \infty$. This results in an equation for the limit β of β_j given by

$$\beta^2 - \gamma_0^{-1}\beta_0 K_1 \cdot \beta + \gamma_0^{-2}\beta_0^2 K_2 = 0\,. \tag{5.43}$$

Solving this equation for β proves the lemma. Note that we used corollary 5.6 to arrive at the expression of γ_0 in terms of the $y_{i;0}$. □

Remark 5.11. Note that for $m = 1$, depending on the sign of a_1, $\beta_\pm$ precisely corresponds to the limit of a_i/a_{i-1} as $i \to \infty$ given in eq. (5.4). To see this, first restrict to the case of $m = 1$, that is the $A_1^{(1)}$ cluster algebra that was considered in [189]. Consequently, the invariants K_1 and K_2 are given by

$$K_1 = 1 + x_1 + x_1x_2\,, \quad K_2 = x_1x_2\,, \tag{5.44}$$

whereas we denote the $\mathcal{X}$-variables of the initial cluster by x_1 and x_2, respectively. Further removing the coefficients by specifying $y_{1;0} = y_{2;0} = 1$, such that $y_{1;j} = y_{2;j} = \gamma_j = 1$ for all j, we see that the $\mathcal{X}$-variables are given by $x_1 = a_2^{-2}$ and $x_2 = a_1^2$, respectively, where again we have dropped the label j for the variables of the initial seed. Then, we can write the rational part of the expression as

$$\beta_0 K_1 = \frac{a_2}{a_1}\left(1 + a_2^{-2} + a_1^2 a_2^{-2}\right) = a_2^{-1}\left(\frac{a_2^2+1}{a_1} + a_1\right) = \frac{a_1' + a_1}{a_2}\,. \tag{5.45}$$

Next, the radicand of the square root can be rephrased as

$$K_1^2 - 4K_2 = (1 + x_1 + x_1x_2)^2 - 4x_1x_2 = (1 + x_1 - x_1x_2)^2 + 4x_1^2x_2 \tag{5.46}$$

$$= \left(\frac{a_2^2+1}{a_2^2} - a_1^2a_2^{-2}\right)^2 + 4a_1^2a_2^{-4} \tag{5.47}$$

$$= a_1^2a_2^{-4}\left[\left(a_1' - a_1\right)^2 + 4\right]\,. \tag{5.48}$$

Choosing the sign of $\beta_\pm$ to be the same as the sign of a_1, we can pull the factor $a_1^2a_2^{-4}$ out of the square-root and multiply it with $\beta_0 = a_2/a_1$ to obtain the same non-rational part as in eq. (5.4).

Finally, let us briefly comment on the associated limit ray. In the $j \to \infty$ limit, the ratio of consecutive cluster variables, eq. (5.42), obeys a generalized form of the separation principle of eq. (3.32). That is, it factorizes into a monomial in the initial $\mathcal{A}$-variables times a ratio of algebraic function with a cluster-tropical sum, which can be interpreted as the (generalized) cluster-tropical version of the algebraic function.[4] Analogously to the definition of g-vectors from the exponents of the $\mathcal{A}$-coordinate representation of eq. (3.32),

[4] In particular, γ_0 is the cluster-tropical version of K_1, and it is natural to consider it also as the (generalised) cluster-tropical version of $\sqrt{K_1^2 - 4K_2}$. This is motivated by the relation $\gamma_0^2 \hat{\oplus}\, y_{1;0}y_{2;0}\left(1 \hat{\oplus}\, y_{3;0}\left(1 \hat{\oplus} \cdots y_{m;0}\left(1 \hat{\oplus}\, y_{m+1;0}\right)\right)\right) = \gamma_0^2$.

from eq. (5.42) we may thus associate $\boldsymbol{g}_\beta = (-1, 0, \ldots, 0, 1) \in \mathbb{Z}^{m+1}$ to the limit. Indeed, considering the sequence of $\boldsymbol{g}$-vectors associated to the sequences of $\mathcal{A}$-variables $a_{i;j}$, we find that they all do converge to $\boldsymbol{g}_\beta$. In fact, the same also applies to the sink-direction, whose cluster rays have the same limit. Note, however, that this is the limit ray with reference to the $A_m^{(1)}$ cluster algebra only. In practice, to obtain the limit ray of some embedding of such a cluster algebra, we use the mutation relation for the cluster rays given by eq. (3.35).

Solving the recursion relations

With all the required results in place, we now turn to discussing the solution of the auxiliary recurrence α_j, eq (5.31). Being a linear recurrence with constant coefficients, it can be solved by standard methods based on its characteristic polynomial, which is given by

$$P_m(t) = t^{2m} - \gamma_0^{-1}\beta_0 K_1 \cdot t^m + \gamma_0^{-2}\beta_0^2 K_2 \,. \tag{5.49}$$

Its $2m$ roots are given by $\beta_\pm^{1/m}\eta_m^i$ for $i = 0, \ldots, m-1$ and whereas η_m is the m-th root of unity. To see this, note that we may first solve for the roots in terms of t^m resulting in $t^m = \beta_\pm$. Accordingly, the most general solution to the recurrence is given by

$$\alpha_j = C_+(j)\,(\beta_+)^{\frac{j}{m}} + C_-(j)\,(\beta_-)^{\frac{j}{m}} \,, \tag{5.50}$$

whereas the overall coefficients $C_\pm(j)$ multiplying $(\beta_\pm)^{j/m}$ are given by

$$C_\pm(j) = c_0^\pm + c_1^\pm \eta_m^j + \cdots + c_{m-1}^\pm \eta_m^{(m-1)j} \,. \tag{5.51}$$

The $2m$ coefficients $c_i^\pm$ for $i = 0, \ldots, m-1$ can be obtained from the initial values $\alpha_0, \ldots, \alpha_{2m-1}$ and can thus ultimately be expressed in terms of the quantities of the initial cluster. Note that since η_m is m-periodic, the overall coefficients $C_\pm(j)$ only depend on $(j \bmod m)$, implying that they assume a total of m different values.

We can explicitly calculate the coefficients $C_\pm(i)$ in terms of the variables of the initial seed by equating the general solution, eq. (5.50), with the expressions for the initial values of α_j, eq. (5.33). Together, these equations form a system of two linear equations for the coefficients $C_\pm(i)$ for any fixed $0 \leq i \leq m-1$, with one coming from α_i and one from α_{i+m}. It is solved by

$$C_\pm(i) = a_{i+1;0}\,(\beta_\pm)^{-i/m}\,\frac{\pm 2F_i \mp K_1 + \sqrt{K_1^2 - 4K_2}}{2\sqrt{K_1^2 - 4K_2}} \,, \tag{5.52}$$

whereas the functions F_i were defined in eq. (5.34).

Finally, we can use the solution for α_j, eq. (5.50), to obtain a solution for $a_{1;j}$ via the relation between them, eq. (5.30). Due to the relations of the other variables $a_{i;j'}$ in the clusters along the sequence to the value of $a_{1;j}$, see eqs. (5.9), this results in a solution for all $\mathcal{A}$-variables along the sequence. For our purposes, however, only ratios of the coefficients $C_\pm(j)$ have a physical significance, such that we do not explicitly present a closed form for $a_{i;j}$, which is proportional to that of α_j.

5.4. Generalised cluster variables

Having obtained the general solution of the infinite mutation sequences of type $A_m^{(1)}$, we now turn to the discussion of how we could attribute *generalised, algebraic cluster variables* to them. While the following construction might appear ad-hoc, it is a natural generalisation to infinite mutation sequences of type $A_m^{(1)}$ of the particular association that has been shown to correctly reproduce the eight-particle NMHV alphabet from mutation sequences of type $A_1^{(1)}$, as was first pointed out in [72]. Furthermore, this approach is also backed by a complimentary analysis via scattering diagrams, see section 6.2.4 or [73].

The procedure starts by considering again the general solution of $a_{1;j}$. As we have discussed before, it is proportional to α_j, eq. (5.50), and consists of the two terms with coefficients $C_\pm(j)$. In the limit of $j \to \infty$, $a_{1;j}$ does not converge and, since $\beta_+ > \beta_-$, the first term dominates over the second. The analogous argument holds for the infinite mutation sequence in the sink-direction, which has a similar solution with coefficients $\tilde{C}_\pm(j)$, as discussed in section A.2. Following and generalising the approach of [72], we thus adopt the following definition.

Definition 5.12 (Generalised cluster variables)**.** Consider a cluster algebra of type $A_m^{(1)}$. We associate the *generalised cluster variables* ϕ_i and $\tilde{\phi}_i$ for $0 \leq i \leq m-1$ to it, given by

$$\phi_i \equiv \frac{C_+(i)}{C_-(i)} = \left(\frac{K_1 - \sqrt{K_1^2 - 4K_2}}{K_1 + \sqrt{K_1^2 - 4K_2}}\right)^{i/m} \frac{2F_i - K_1 + \sqrt{K_1^2 - 4K_2}}{-2F_i + K_1 + \sqrt{K_1^2 - 4K_2}}\,, \tag{5.53}$$

$$\tilde{\phi}_i \equiv \frac{\tilde{C}_+(i)}{\tilde{C}_-(i)} = \left(\frac{K_1 - \sqrt{K_1^2 - 4K_2}}{K_1 + \sqrt{K_1^2 - 4K_2}}\right)^{i/m} \frac{2\tilde{F}_i K_2 - K_1 + \sqrt{K_1^2 - 4K_2}}{-2\tilde{F}_i K_2 + K_1 + \sqrt{K_1^2 - 4K_2}}\,, \tag{5.54}$$

whereas F_i and $\tilde{F}_i$ are rational functions of the $\mathcal{X}$-variables of the initial seed of the cluster algebra, which are given by

$$\tilde{F}_i = \frac{K_{m+1-i}}{K_{m+1}}\,, \qquad F_i = \begin{cases} 1 & \text{if } i = 0\,, \\ K_1 - K_{i+1} & \text{otherwise}\,, \end{cases} \tag{5.55}$$

and are defined in terms of the generalised invariants K_i, which are given by

$$K_i = x_{1;0} \cdots x_{i;0} \left(1 + x_{i+1;0} \left(1 + \cdots x_{m;0} \left(1 + x_{m+1;0}\right)\right)\right)\,. \tag{5.56}$$

Note that we have previously introduced these quantities in eqs. (5.34) and (5.32) and that $\tilde{F}_i$ arises from the sink-direction of the infinite mutation sequence, see sec. A.2.

In all relevant cases, we do not encounter cluster algebras of type $A_m^{(1)}$ by themselves but rather as cluster subalgebras in larger cluster algebras of the Grassmannians $\mathrm{Gr}(k,n)$. In the natural way, we obtain the generalised cluster variables in this case from any cluster $\mathcal{C}$ that contains an $A_m^{(1)}$ cluster subalgebra by the above equations, whereas the $\mathcal{X}$-variables are those of $\mathcal{C}$ that correspond to the $A_m^{(1)}$ subalgebra.

Finally, let us comment on the association of these variables to *generalised cluster rays*. For ordinary cluster variables, we have seen in section 3.1.2 how each of the $\mathcal{A}$-variables

in a rank-r cluster algebra is in a one-to-one correspondence to a cluster ray in $\mathbb{R}^r$. The generalised cluster variables of eqs. (5.53) and (5.54), however, demonstrate a different behaviour. As we have discussed in the previous section, the cluster rays of the variables $a_{i;j}$ all converge to $\boldsymbol{g}_\beta$. The same applies to the sink-direction, see appendix A.2. In this sense, $\boldsymbol{g}_\beta$ can be considered the cluster ray of the algebraic letters ϕ_i and $\tilde{\phi}_i$ with $0 \leq i \leq m-1$. Note that the major difference is that the generalised cluster variables are in a many-to-one correspondence to generalised cluster rays. In particular, for $m = 1$, we have two different variables, ϕ_1 and $\tilde{\phi}_1$, associated to one ray $\boldsymbol{g}_\beta$, depending on the direction of approach, that is whether we approach the ray from the source- or sink-direction. For $m > 1$, m generalised cluster variables are associated to the limit ray for each of the two directions of approach.

The results presented in here reduce to the special case discussed in [72] when restricting to $m = 1$ and the specific embedding of the $A_1^{(1)}$ cluster algebra discussed in there. However, in contrast to the previous constructions, our approach based on the study of infinite mutation sequences is more general and, due to working with general coefficients, can be directly applied to any embedding of an $A_m^{(1)}$ cluster algebra. Consequently, it can also be directly applied to the scattering of more than eight particles, as we will discuss in section 6.3. In how far the generalised cluster variables as defined in here are applicable to loop amplitudes of planar $\mathcal{N} = 4$ super Yang-Mills theory is discussed in there as well as in section 6.2.

6. Applications and examples

In chapters 2 and 3, we have reviewed how the so-called cluster bootstrap programme allows to construct amplitudes of planar $\mathcal{N} = 4$ super Yang-Mills theory directly without referring to direct calculations via Feynman diagrams. While this approach has led to remarkable results, see sections 3.2.2 and 3.2.3, there have been long-standing obstructions preventing a generalisations to higher particle numbers. First, starting at eight particles, the cluster algebra naively predicts infinitely many symbol letters. Second, letters obtained from cluster algebras are rational by construction and therefore cannot describe the non-rational letters known to appear for example in the eight-particle one-loop NMHV amplitude. In this work, we have proposed two novel approaches that address these issues: using tropical geometry to construct a finite subset of the infinite cluster algebra and infinite mutation sequences to construct generalised cluster variables containing square roots, see chapters 4 and 5, respectively. We now turn to applying these methods to various cases of physical significance, which is the main objective of this chapter.

We start in section 6.1 with a study of the totally positive tropical configuration space $\widetilde{\mathrm{Tr}}_+(3,8)$. While this also serves as a first concrete example of the abstract tools developed before, it has a direct application to the amplitudes of generalised biadjoint scalar theory discussed in section 2.2.3. Specifically, we use the fan of the cluster algebra of $\mathrm{Gr}(3,8)$ to obtain a minimal triangulation of the fan $F_{3,8}$ of $\widetilde{\mathrm{Tr}}_+(3,8)$. With the amplitude being the volume of this latter fan, its minimal triangulation results in an expression of the amplitude with a (near-)minimal amount of spurious poles.

Next, in section 6.2 we turn to eight-particle amplitudes in $\mathcal{N} = 4$ pSYM. By constructing the finite fan of the partially tropicalised, totally positive configuration space $\widetilde{\mathrm{pTr}}_+(4,8)$, we remove the infinity of the cluster algebra of $\mathrm{Gr}(4,8)$ and obtain a finite subset of 272 cluster variables, the truncated cluster algebra. We propose this set, which contains all previously known rational letters, as the alphabet of eight particle amplitudes. Furthermore, by studying all infinite mutation sequences of $A_m^{(1)}$ cluster subalgebras appearing in the truncated cluster algebra, which in this case are restricted to $m = 1$, we obtain a set of 18 multiplicatively independent non-rational letters. These are equivalent to the algebraic letters that have appeared in an explicit calculation of the two-loop amplitude in [61].

Finally, we extend these results to the case of $\widetilde{\mathrm{pTr}}_+(4,9)$ and nine-particle scattering in section 6.3. Again, by constructing the finite fan of $\widetilde{\mathrm{pTr}}_+(4,9)$, we obtain the truncated cluster algebra of $\mathrm{Gr}(4,9)$ and a corresponding candidate for the rational part of the symbol alphabet consisting of 3078 letters including all previously known rational letters. Studying the infinite mutation sequences of all $A_m^{(1)}$, we find that although in contrast to the eight-particle case, also sequences for $m > 1$ appear, there are reasons why the associated algebraic cluster variables should be considered unphysical and excluded from the alphabet. Limiting to the sequences for $m = 1$, we obtain 2349 square-root letters again including all previously known ones, such as the 99 square-root letters obtained in an explicit calculation of the two-loop NMHV amplitude in [75].

6.1. $\widetilde{\mathrm{Tr}}_+(3,8)$ and generalised biadjoint scalar amplitude

We have started in section 2.2 with a review of scattering equations $\mathbb{CP}^1$ and the CHY formalism. In there, we have seen how they can be used to efficiently compute the amplitude of biadjoint scalar ϕ^3 theory. On the other hand, extending the scattering equations to $\mathbb{CP}^{k-1}$ with $k > 2$, one can construct amplitudes of a generalised biadjoint scalar amplitude, see in particular section 2.2.3.

Interestingly, the amplitude of n particles in biadjoint scalar ϕ^3 theory can alternatively be obtained from the volume of the dual associahedron $\mathcal{A}_n$. Associahedra are ubiquitous objects appearing in many contexts in mathematics. For example, the cluster polytopes of the cluster algebras of $\mathrm{Gr}(2,n)$ are combinatorially equivalent to $\mathcal{A}_{n-3}$. Furthermore, in [71] it was shown that the fan of the totally positive tropical configuration space $\widetilde{\mathrm{Tr}}_+(2,n)$ is equivalent to the dual of $\mathcal{A}_{n-3}$. We can thus compute the volume of the dual of $\mathcal{A}_{n-3}$ and in this way the n-point amplitude of biadjoint scalar theory by triangulating $\widetilde{\mathrm{Tr}}_+(2,n)$.

The biadjoint scalar amplitudes associated to $\widetilde{\mathrm{Tr}}(k,n)$ were generalized in [63, 64] from $k = 2$ to general values of k by a generalization of the scattering equations from $\mathbb{CP}^1$ to $\mathbb{CP}^{k-1}$, for more recent work in this direction see also [65–68]. We can hence compute these generalized biadjoint scalar amplitudes by analysing $\widetilde{\mathrm{Tr}}(k,n)$ or its totally positive part, which corresponds to the amplitude with canonical ordering.

As was demonstrated in [70], using the fact that the cluster fan triangulates the fan of the totally positive tropical configuration space, we can compute its volume and obtain an expression for the generalised biadjoint scalar amplitude. Given a simplicial fan $\mathrm{Tri}F_{k,n}$ triangulating the fan of the totally positive tropical configuration space $\widetilde{\mathrm{Tr}}_+(k,n)$, the amplitude is given by

$$m_k^n(\mathbf{1}|\mathbf{1}) = \sum_{\substack{\text{max. cones} \\ C\in \mathrm{Tri}F_{k,n}}} \prod_{\substack{\text{rays} \\ \boldsymbol{g}\in C}} \frac{1}{y\cdot \mathrm{Tr}\Phi(\boldsymbol{g})}\,, \tag{6.1}$$

whereas $\mathrm{Tr}\Phi$ denotes the embedding of the totally positive tropical configuration space into the full tropical configuration space obtained via the web-parameterisation as given by the tropicalisation of eq. (4.19) and y is the vector of lexicographically ordered generalized Mandelstam invariants $s_{i_1\dots i_k}$ spanning the kinematic space. In the case where $\mathrm{Tri}F_{k,n}$ coincides with the cluster fan, as was previously considered, C amounts to a cluster of the cluster algebra, and $\boldsymbol{g}$ to a ray associated to an $\mathcal{A}$-variable. With the top-dimensional cones being simplicial they each consist of d rays, the dimension of the fan.

In this chapter we build on the work of [70] to analyse $\widetilde{\mathrm{Tr}}_+(3,8)$ and its properties. Using cluster algebras, we will compute a triangulation of its fan and obtain its full geometry, whose combinatorial structure is expressed in terms of its f-vector. Furthermore, we will show how to obtain a minimal, non-redundant triangulation which allows us to write down the generalised biadjoint scalar amplitude with the least amount of spurious poles. Finally, we briefly mention how this can be extended to obtain the amplitude associated to $\widetilde{\mathrm{Tr}}_+(4,8)$.

6.1.1. Mutating and fusing cones

In [194] the question was posed, whether it is feasible to compute the tropical Grassmannian $\mathrm{Tr}(3,8)$. Using cluster algebra techniques, at least computing the totally positive tropical configuration space $\widetilde{\mathrm{Tr}}_+(3,8)$ becomes not only feasible but also efficient.

Starting from the seed of the cluster algebra of $\mathrm{Gr}(3,8)$, we perform all possible mutations to obtain the full cluster fan. As stated in [70], this contains 128 rays, 8 of which are redundant. These rays arise from redundant triangulations, as for example from the triangulation of an already simplicial cone by smaller simplicial cones. However, we also observe such redundant triangulations in (parts of) non-simplicial cones with up to 13 rays. Such a scenario is illustrated in figure 6.1.

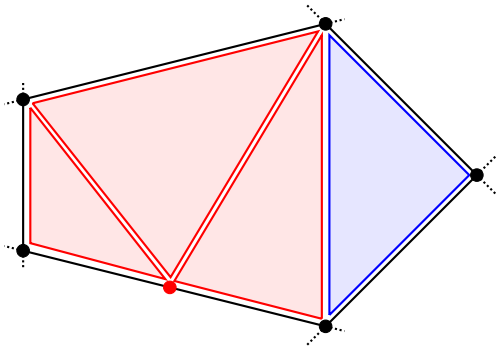

Figure 6.1: Illustrative example of a non-minimal triangulation of a non-simplicial cone. In this example, we consider a 3-dimensional fan and draw its intersection with the unit-sphere S^2. Note that the vertices correspond to the rays and lines to dimension-2 surfaces. Simplicial cones have three rays and thus three vertices. On the left hand, we draw in blue a minimal triangulation. On the right hand, we draw how a redundant ray, drawn in red, leads to a non-minimal triangulation.

Proceeding as for $\mathrm{Gr}(4,8)$, we can also compute the truncated cluster algebra, that is, we restrict mutation to those clusters, that contain only non-redundant rays. Therefore, we truncate the cluster algebra whenever we encounter a cluster with at least one redundant ray. As demonstrated in [70], this results in a truncated cluster fan with 120 rays and 21720 cones. This cluster fan, however, has holes resulting from the truncation. Thus, while it contains only non-redundant triangulations, it does not triangulate the full totally positive tropical configuration space $\widetilde{\mathrm{Tr}}_+(3,8)$.

As the cluster algebra is finite in this case, we can start from its full – and finite – fan and fuse the cones along the redundant faces to obtain $F_{3,8}$, see in particular section 4.2.1 where we discussed this fusion procedure. In this way, we were able to construct the totally positive tropical configuration space efficiently using the associated cluster algebra. The f-vector of this and of the cluster fans are stated in table 6.1.

Geometry	f-vector							
Full cluster	128	2408	17936	67488	140448	163856	100320	25080
Truncated cluster	120	2240	16584	61920	127568	146944	88560	21720
$\widetilde{\mathrm{Tr}}_+(3,8)$	120	2072	14088	48544	93104	100852	57768	13612

Table 6.1: f-vectors of the full and truncated cluster polytope as well as that of $\widetilde{\mathrm{Tr}}_+(3,8)$.

6.1.2. Minimal triangulation

In the case of $\widetilde{\mathrm{Tr}}_+(3,8)$ the full cluster algebra is finite, resulting in a complete triangulation. However, the cluster fan has 8 redundant rays resulting in parts of the totally positive tropical configuration space to be redundantly triangulated.

By comparing the cluster fans of the full and truncated algebra, we identify 8 holes in the truncated fan that correspond to the areas, where the cluster algebra produces redundant triangulations and was thus truncated. Fusing the cones of the full cluster algebra that lie in any of these holes, we can identify those cones of $F_{3,8}$ that are not yet minimally triangulated by the cluster algebra.[1]

Note that in this way we do not always find the complete non-minimally triangulated cone but only that part of the cone, that is not yet minimally triangulated. This can also be seen on the right hand side of figure 6.1, where the right part of the cone is non-redundantly triangulated by the cluster algebra and hence only the left part, drawn in red, actually lies inside the hole. In an abuse of language, we will nonetheless refer to this as the full cone.

Given any cone of $F_{3,8}$ we construct its minimal triangulation by first building all possible simplicial cones out of the rays of the non-simplicial cones (these are linearly independent combinations of 8 rays, which is equal to the dimension of the fan, as may be seen by specialising eq. (2.98) to our case). We then iteratively combine these cones to a triangulation by grouping them such that they share codimension-1 boundaries and do not intersect. This is illustrated in figure 6.2. When no such cones are left, we check whether all codimension-1 boundaries are shared between precisely two cones to verify whether the triangulation covers the entire cone. Finally, we simply choose the minimal triangulation out of the thus constructed ones.

Note that this algorithm is only applicable if there are no rays of the totally positive tropical configuration space inside of the hole of the truncated cluster algebra. For $\widetilde{\mathrm{Tr}}_+(3,8)$ this is indeed the case, as can be checked by comparing with the full cluster algebra, which is known to provide its complete triangulation. Due to the complexity of the problem, this algorithm is, however, not efficient for the largest non-simplicial cones encountered in these holes. In each of the 8 holes we find one non-simplicial cone consisting of 13 non-redundant rays which is redundantly triangulated by 24 simplicial cones of the cluster algebra. For this cone the algorithm does not terminate within a reasonable amount of time.

[1] Note that in higher dimensions, even when excluding redundant rays, it is possible to obtain triangulations with different numbers of simplices. While all of them are non-redundant, only one of them is truly minimal.

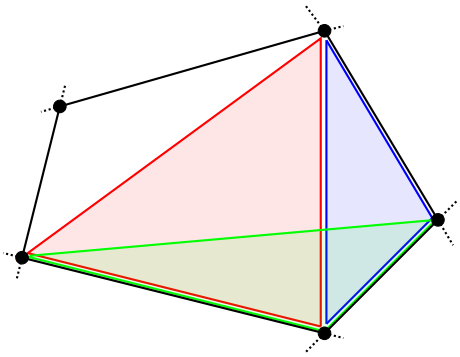

Figure 6.2: Illustrative example of the algorithm to triangulate a non-simplicial cone. Here we consider a 3-dimensional fan and draw its intersection with the unit-sphere S^2. The non-simplicial cone of the totally positive tropical configuration space is drawn in black. The red, green and blue cones are part of the set of all cones that may be used for the triangulation. If the algorithm has already picked the red one for the triangulation, only the blue one can be picked in the next step, as the green one intersects with the red cone and does not share a codimension-1 boundary with it.

In combination with the triangulation obtained from the truncated cluster algebra, we thus obtain a triangulation of the fan of $\widetilde{\mathrm{Tr}}_+(3,8)$ with 23496 simplicial cones. More precisely, we find that, not considering the largest non-minimally triangulated cones, there are 3168 simplicial cones corresponding to a redundant triangulation in the full cluster fan, 396 for each of the 8 holes. These cones redundantly triangulate 99 non-simplicial cones (or parts of such) in each hole. In the minimal triangulation, these non-simplicial cones are triangulated by 198 simplicial cones. Compared to the redundant triangulation, the amount of simplicial cones per non-simplicial cone is reduced by half.

Extrapolating this data to the largest non-minimally triangulated cones, which are redundantly triangulated by 24 simplicial cones, would suggest that they have a minimal triangulation with 12 simplicial cones. In this case, the minimal triangulation fan of $F_{3,8}$ would consist of 23400 simplicial cones.

6.1.3. Generalised biadjoint scalar amplitude

In [70], the simplicial fan of the full cluster algebra of $\mathrm{Gr}(3,8)$ was used to compute the respective generalised biadjoint scalar amplitude amplitude. However, having obtained the near-minimal triangulation, which consists of 1584 cones less than the full cluster triangulation, the amplitude can be written in a more economic way. The full result is contained in the ancillary file `Gr38AmpMin.m` attached to the `arXiv` submission of [164].

We demonstrate how the amplitude can be written in a shorter form when passing to the minimal triangulation by considering the example of a simplicial cone that is redundantly triangulated. The cluster algebra triangulates this cone with two also simplicial cones containing one of the redundant rays. This redundant triangulation leads to the

contribution

$$\begin{aligned}
&1/\Big((y\cdot b_{3,12345678})\,(y\cdot b_{3,78123456})\,(y\cdot b_{4,12345678})\,(y\cdot b_{5,34215678})\,(y\cdot b_{5,67548123}) \\
&\qquad \times (y\cdot b_{10,24513678})\,(y\cdot b_{8,78564123})\,(y\cdot b_e)\Big) \\
&+1/\Big((y\cdot b_{3,12345678})\,(y\cdot b_{3,78123456})\,(y\cdot b_{4,12345678})\,(y\cdot b_{5,34215678})\,(y\cdot b_{5,67548123}) \\
&\qquad \times (y\cdot b_{10,24513678})\,(y\cdot b_{8,12345678})\,(y\cdot b_e)\Big)\,, \qquad (6.2)
\end{aligned}$$

where the vectors b correspond to rays of $F_{3,8}$. These rays are elements of $\mathbb{R}^D$ with $D=\binom{8}{3}$, which is the space spanned by all (ordered) Plücker variables $\langle ijk\rangle$ of $\mathrm{Gr}(3,8)$. As outlined in [70], the 721 rays of $F_{3,8}$ are given by

$$b_{1,1234567} = e_{123}\,, \qquad (6.3)$$
$$b_{2,1234567} = e_{123}+e_{124}+e_{134}+e_{234}\,, \qquad (6.4)$$
$$b_{3,1234567} = e_{123}+e_{124}+e_{125}+e_{126}+e_{127}\,, \qquad (6.5)$$
$$b_{4,1234567} = e_{123}+e_{124}+e_{125}+e_{126}+e_{127}+e_{134}+e_{234}\,, \qquad (6.6)$$
$$b_{5,1234567} = e_{123}+e_{124}+e_{125}+e_{126}+e_{127}+e_{134}+e_{156}+e_{234}+e_{256}\,, \qquad (6.7)$$
$$b_{6,1234567} = b_{3,1234567}+b_{3,3456712}+b_{3,6712345}\,, \qquad (6.8)$$

whereas the e_{ijk} are the unit vectors in $\mathbb{R}^D$, with ijk corresponding to the indices of the Plücker variables, and the other rays are given by permutations of those listed. The same contribution in our minimal triangulation reads

$$\begin{aligned}
&1/\Big((y\cdot b_{3,12345678})\,(y\cdot b_{3,78123456})\,(y\cdot b_{4,12345678})\,(y\cdot b_{5,34215678})\,(y\cdot b_{5,67548123}) \\
&\qquad \times (y\cdot b_{10,24513678})\,(y\cdot b_{8,12345678})\,(y\cdot b_{8,78564123})\Big), \qquad (6.9)
\end{aligned}$$

and indeed, (6.2) simplifies to (6.9) upon taking the common denominator, and using the following identity

$$b_e = b_{8,12345678}+b_{8,78564123}\,, \qquad (6.10)$$

that the redundant ray b_e obeys. In general, the terms coming from the triangulation of non-simplicial cones are more complex and result, even for the minimal triangulations, in more than one term. These terms, however, cannot be further simplified while keeping the same structural form.

The advantage of writing the amplitude in this way is that such a minimal triangulation introduces the least possible amount of spurious poles into the amplitude. As can be seen from the simplification of the terms above, when using the minimal triangulation, the pole associated to $(y\cdot b_e)$, which in the redundant triangulation cancels between the two fractions, is not present at all.

In general, we see from eq. (6.1) that every ray introduces an apparent pole to the amplitude. The rays, which are dimension-1 faces of the triangulation fan, correspond to codimension-1 faces of the associated polytope in kinematic space. In this sense, if the cluster algebra introduces a redundant ray to triangulate the totally positive tropical configuration space, it introduces a codimension-1 boundary in the kinematic space that is associated to a non-physical pole whose contributions cancel between the terms.

6.2. $\widetilde{\mathrm{pTr}}_+(4,8)$ and eight-particle scattering

In this section we turn our attention to the symbol alphabet of eight-particle loop amplitudes in planar $\mathcal{N}=4$ super Yang-Mills theory. To construct its rational part, which is discussed in section 6.2.2, we apply the methods developed in chapter 4 and calculate the cluster algebra of $\mathrm{Gr}(4,8)$ and its truncations by both, the fan of the partially and the fully tropicalised, totally positive configuration space $\widetilde{\mathrm{pTr}}_+(4,8)$ and $\widetilde{\mathrm{Tr}}_+(4,8)$, respectively. As was discussed in section 4.1.3, the partial tropicalisation is obtained by only tropicalising Plücker variables of the form $\langle ii+1jj+1\rangle, \langle ij-1jj+1\rangle$, see eq. (4.25), and, in contrast to the full tropicalisation, respects the parity invariance of the amplitude. As was also discussed in there, the partial fan is essentially a subset of the full fan,[2] such that we can first construct the cluster algebra truncated by the latter and afterwards restrict to the partial case. This allows us to assess the applicability of both tropical geometries and results in a proposed rational alphabet consisting of 272 letters obtained from the cluster algebra truncated by the partial fan.

After discussing the rational part of the symbol alphabet, we turn to the non-rational letters in section 6.2.3. Applying the results of chapter 5, we first scan the truncated cluster algebra for all $A_m^{(1)}$ cluster subalgebras. Finding only subalgebras with $m=1$, we next construct a non-rational alphabet consisting of the generalised cluster variables associated to all these infinite mutation sequences. This results in a non-rational alphabet consisting of the 18 square-root letters that were also previously obtained by other means in [61].

Note that the results discussed in here were reported in [164, 195], see also [70, 72, 185, 186] for closely related work.

6.2.1. Truncated $\mathrm{Gr}(4,8)$ cluster algebra

To construct the truncated cluster algebra, we begin with the fan $F_{4,8}$ of the totally positive tropical configuration space $\widetilde{\mathrm{Tr}}_+(4,8)$. Using the algorithm described in section 4.1.2, we can calculate the web-parameterisation of the $D=\binom{8}{4}=70$ unique Plücker variables $\langle ijkl\rangle$ in terms of the $d=9$ web-variables $x_1,\ldots,x_9$. Each of these rational functions is then tropicalised by replacing addition by taking the minimum and multiplication by addition, which results in a set of 70 tropical polynomials, piecewise linear functions in the 9 tropical web-variables $\tilde{x}_1,\ldots,\tilde{x}_9$. For each of these polynomials, we can construct a fan in $\mathbb{R}^9$ by calculating the tropical hypersurfaces. As was discussed in section 4.1.3, the fan $F_{4,8}$ is then given by the common refinement of all these fans.

Since we are really only interested in the truncated cluster algebra itself, it is not necessary to solve the hypersurface equations and construct the fan explicitly. Instead, we can make use of the hypersurface conditions themselves to test if a cluster ray is a proper tropical ray or is redundant, which together with the mutation relations is sufficient to construct the truncated cluster algebra. To be precise, a ray in $\mathbb{R}^9$ is a non-redundant ray of $F_{4,8}$ if and only if it lies on the intersection of 8 linearly independent tropical hypersurfaces, that is it has a ray rank of 8. In this way, given any ray in $\mathbb{R}^9$, we first test on which of the

[2] To be precise, the full fan is a refinement of the partial one.

tropical hypersurfaces it lies by identifying the tropical hypersurface conditions[3] which it satisfies. Collecting the normal vectors to all these hypersurfaces, the ray rank is given as the rank of the matrix whose columns are the normal vectors.

With the basic setup in place, we consider the initial seed of the cluster algebra of $\text{Gr}(4,8)$, which is depicted in figure 6.3. The cluster rays associated to the variables in this seed are by construction the unit vectors of $\mathbb{R}^9$, which are non-redundant rays of $F_{4,8}$.

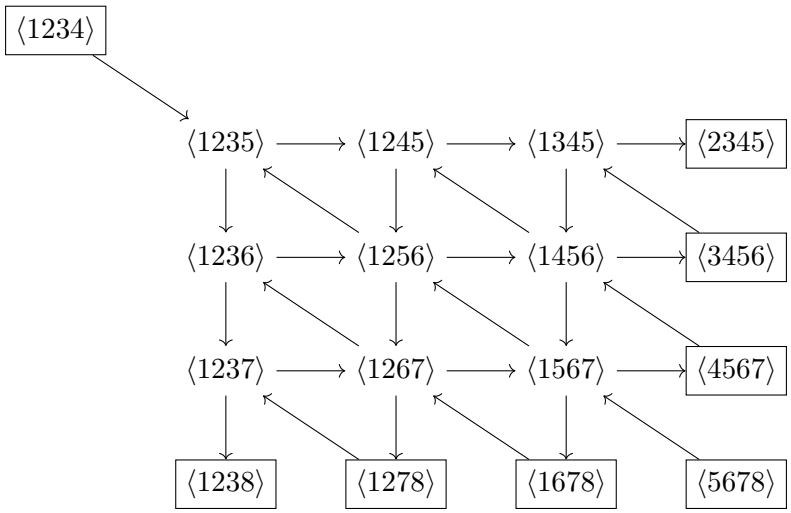

Figure 6.3: Initial seed of the cluster algebra of $\text{Gr}(4,8)$.

To construct the entire truncated cluster algebra, we start from this seed and perform all possible mutations. Using for simplicity the framework of cluster algebras with frozen variables, the variables are mutated according to eq. (3.6), whereas the associated cluster rays are mutated according to eq. (3.35). After each mutation, we use the algorithm described above to calculate the ray rank of the mutated cluster ray. If it is a redundant ray, we truncate the cluster algebra and exclude the cluster. After a large number of mutations, this algorithm stops as it has exhausted all possible mutations contributing non-redundant clusters resulting in a finite truncated cluster algebra with 356 cluster variables in 169,192 clusters. The f-vector of its fan is given by

$$f_{4,8} = (356, 9408, 90248, 428988, 1144532, 1796936, 1648184, 817178, 169192)\ . \tag{6.11}$$

Based on this result, we obtain the $\mathcal{A}$-variables of the cluster algebra truncated by $pF_{4,8}$ by repeating the above ray rank calculation for the non-redundant cluster rays but only including the tropical hypersurfaces obtained from the Plücker variables of the form $\langle ii+1jj+1\rangle, \langle ij-1jj+1\rangle$. This results in a subset of 272 $\mathcal{A}$-variables.

Before we present the proposed rational eight-particle alphabet, let us first discuss how we can write the letters in the most compact form as homogeneous polynomials by choosing a representation in which the denominator cancels out. The reader interested in the final form of the proposed alphabet may skip directly to the next section.

[3] We remind the reader that these conditions are given by the equations obtained from setting two terms of the piecewise linear function equal to each other and smaller or equal to the other terms.

As per the Laurent phenomenon, any cluster variable is a Laurent polynomial in the initial variables. While this parameterisation in terms of the independent Plücker variables has its advantages, for the applications to scattering amplitudes it is more practical to have the letters in the most compact form. Furthermore, from this perspective, it is perfectly fine if the letters depend on all, also dependent, Plücker variables.

In order to demonstrate the general algorithm used to obtain the octagon alphabet, we will make use of the example of a letter of degree two in the Plücker variables given by

$$a = \frac{\langle 1245\rangle \langle 1567\rangle \langle 3456\rangle + \langle 1256\rangle \langle 1345\rangle \langle 4567\rangle}{\langle 1456\rangle} . \tag{6.12}$$

By construction, we can parameterise all cluster variables as rational functions in the variables of any cluster. For small cluster algebras, this is obtained by taking the cluster as the initial seed and performing all possible mutations. This, due to its size, is not practical for the (truncated) cluster algebra of $\mathrm{Gr}(4,8)$. However, once we have the alphabet in terms of some initial cluster, we can identify the degree one letters that correspond to the Plücker variables by comparing them in the unique web-parameterisation.

This, for example, allows us to identify the following Plücker variable in the $\mathrm{Gr}(4,8)$ cluster algebra

$$\frac{\langle 1245\rangle \langle 1567\rangle \langle 3456\rangle + \langle 1256\rangle \langle 1345\rangle \langle 4567\rangle + \langle 1235\rangle \langle 1456\rangle \langle 4567\rangle}{\langle 1245\rangle \langle 1456\rangle} = \langle 3567\rangle . \tag{6.13}$$

Having identified a variable we can solve such rational expressions for any of the Plücker variables, allowing us to exchange any variable in the parameterisation, for example $\langle 1456\rangle$ by $\langle 3567\rangle$.

By cluster mutation any cluster variable is given as a rational function whose denominator is a monomial in the initial Plücker variables. To simplify this rational function, we thus change the parameterisation by exchanging any of the factors in the denominator with any of the other Plücker variables. In some cases, this causes the nominator to factor in such a way that parts of the denominator can be canceled. In our example, we therefore use the rational expression of the Plücker variables in terms of the initial ones to replace $\langle 1456\rangle$. Using the expression for $\langle 3567\rangle$ we obtain

$$a = \frac{\left(\langle 1245\rangle \langle 1567\rangle \langle 3456\rangle + \langle 1256\rangle \langle 1345\rangle \langle 4567\rangle\right)\left(\langle 1245\rangle \langle 3567\rangle - \langle 1235\rangle \langle 4567\rangle\right)}{\langle 1245\rangle \langle 1567\rangle \langle 3456\rangle + \langle 1256\rangle \langle 1345\rangle \langle 4567\rangle} , \tag{6.14}$$

such that the denominator cancels out completely and we obtain the letter in the fully simplified form of

$$a = \langle 1245\rangle \langle 3567\rangle - \langle 1235\rangle \langle 4567\rangle . \tag{6.15}$$

Whereas in this simple example one such replacement was sufficient, we can in general proceed in this way until there is no such change of parameterisation that simplifies the rational variable in the sense of reducing the number of factors in the denominator. If this does not result in the full denominator to cancel out, we attempt a different path of iterated changes of parameterisation. Note that in this way we effectively scan through all possible parameterisations. In fact, using this algorithm it was possible to eliminate the complete denominator of all cluster variables.

6.2.2. Rational octagon alphabet

In total, we find 356 distinct cluster $\mathcal{A}$-variables in the cluster algebra of $\mathrm{Gr}(4,8)$ truncated by the fan of the totally positive tropical configuration space $\widetilde{\mathrm{Tr}}_+(4,8)$ and 272 $\mathcal{A}$-variables in the cluster algebra truncated by the partially tropicalised configuration space $\widetilde{\mathrm{pTr}}_+(4,8)$. The full result is contained in the ancillary text file `OctagonAlphabet.m` attached to the `arXiv` submission of [164]. All of the variables can be reduced to homogeneous polynomials in the 70 Plücker variables. Together with the 8 frozen variables, the variables are given by (with those of the partial tropicalisation added in parantheses):

- 70 (70) variables of degree one, the distinct Plücker variables $\langle ijkl\rangle$,
- 120 (120) variables of degree two, 15 quadratic generators with cyclic orbit size 8,
- 132 (90) variables of degree three, 2 (1) cubic generators with 2 cyclic images, 2 (2) cubic generators with 4 cyclic images and 15 (10) cubic generators with 8 cyclic images,
- 32 (0) variables of degree four, 4 quartic generators with 8 cyclic images and
- 10 (0) variables of degree five, 1 quintic generator with 2 and 1 quintic generator with 8 cyclic images.

Out of these 364 (280) cluster variables, we obtain a candidate alphabet consisting of 356 (272) dual conformally invariant letters.

For simplicity, we state the variables only modulo cyclic transformations, that is up to shifts of the Plücker indices $i \to (i+j) \mod 8$. Not considering the Plücker variables $\langle ijkl\rangle$ themselves, the variables of the cluster algebra truncated by $F_{4,8}$ are cyclically generated by 40 distinct variables, which are summarised in tables 6.2 and 6.3, whereas in these tables the variables of the partially tropicalised fan are marked by colour coding. Note that we only give one possible representation, which is related to other choices by the Plücker relations. However, using the web-parameterisation of the Plücker variables as defined above, we can always express all the cluster $\mathcal{A}$-variables in terms of the initial x-variables. In this parameterisation, all Plücker relations are solved therefore resulting in a unique representation.

Before discussing the candidate alphabet for eight-particle scattering that can be derived from the truncated cluster algebra, let us first comment on the properties of these $\mathcal{A}$-variables. For general cluster algebras, the Laurent phenomenon assures that any cluster variable can be written as a Laurent polynomial in terms of the initial variables. As can be seen from the results in the case of $\mathrm{Gr}(4,8)$, in the case of cluster algebras of Grassmannians there seems to be the much stronger statement that the variables are actual polynomials in the Plücker variables with ± 1.

Even when taking into account that we have the freedom to add any Plücker relation, such that any integer coefficient may appear, the fact that we obtain actual polynomials with integer coefficients that also do have a representation with ± 1 coefficients only is quite surprising. This is also present when passing to the web-parameterisation – in contrast to

Degree	Cyclic Generator	#
2	$\langle 1457\rangle\langle 2367\rangle - \langle 1237\rangle\langle 4567\rangle$ $\langle 1235\rangle\langle 1467\rangle - \langle 1234\rangle\langle 1567\rangle$ $\langle 1245\rangle\langle 3567\rangle - \langle 1235\rangle\langle 4567\rangle$ $\langle 1256\rangle\langle 4678\rangle - \langle 1246\rangle\langle 5678\rangle$, $\langle 1235\rangle\langle 4678\rangle - \langle 1234\rangle\langle 5678\rangle$ $\langle 1256\rangle\langle 3467\rangle - \langle 1267\rangle\langle 3456\rangle$, $\langle 1256\rangle\langle 1478\rangle - \langle 1278\rangle\langle 1456\rangle$ $\langle 1245\rangle\langle 3467\rangle - \langle 1234\rangle\langle 4567\rangle$, $\langle 1236\rangle\langle 1478\rangle - \langle 1234\rangle\langle 1678\rangle$ $\langle 1256\rangle\langle 1347\rangle - \langle 1234\rangle\langle 1567\rangle$, $\langle 1256\rangle\langle 3678\rangle - \langle 1236\rangle\langle 5678\rangle$ $\langle 1245\rangle\langle 2367\rangle - \langle 1267\rangle\langle 2345\rangle$, $\langle 1346\rangle\langle 1578\rangle - \langle 1345\rangle\langle 1678\rangle$ $\langle 1267\rangle\langle 1358\rangle - \langle 1235\rangle\langle 1678\rangle$, $\langle 1347\rangle\langle 2356\rangle - \langle 1237\rangle\langle 3456\rangle$	8
3	$\langle 1236\rangle\langle 1578\rangle\langle 3457\rangle - \langle 1237\rangle\langle 1578\rangle\langle 3456\rangle - \langle 1235\rangle\langle 1678\rangle\langle 3457\rangle$ $\langle 1358\rangle\langle 1367\rangle\langle 2457\rangle - \langle 1267\rangle\langle 1358\rangle\langle 3457\rangle - \langle 1238\rangle\langle 1567\rangle\langle 3457\rangle$	2
	$\langle 1258\rangle\langle 1367\rangle\langle 2456\rangle - \langle 1238\rangle\langle 1567\rangle\langle 2456\rangle - \langle 1258\rangle\langle 1267\rangle\langle 3456\rangle$ $\langle 1236\rangle\langle 1567\rangle\langle 2458\rangle - \langle 1238\rangle\langle 1567\rangle\langle 2456\rangle - \langle 1236\rangle\langle 1245\rangle\langle 5678\rangle$	4
	$\langle 1245\rangle\langle 1567\rangle\langle 2378\rangle - \langle 1278\rangle\langle 1567\rangle\langle 2345\rangle - \langle 1237\rangle\langle 1245\rangle\langle 5678\rangle$ $\langle 1237\rangle\langle 1568\rangle\langle 3467\rangle - \langle 1237\rangle\langle 1678\rangle\langle 3456\rangle - \langle 1238\rangle\langle 1567\rangle\langle 3467\rangle$ $\langle 1237\rangle\langle 1568\rangle\langle 2467\rangle - \langle 1237\rangle\langle 1678\rangle\langle 2456\rangle - \langle 1238\rangle\langle 1567\rangle\langle 2467\rangle$ $\langle 1245\rangle\langle 1568\rangle\langle 3467\rangle - \langle 1245\rangle\langle 1678\rangle\langle 3456\rangle - \langle 1234\rangle\langle 1568\rangle\langle 4567\rangle$ $\langle 1256\rangle\langle 1456\rangle\langle 3478\rangle - \langle 1256\rangle\langle 1478\rangle\langle 3456\rangle - \langle 1234\rangle\langle 1456\rangle\langle 5678\rangle$ $\langle 1237\rangle\langle 1458\rangle\langle 2367\rangle - \langle 1237\rangle\langle 1678\rangle\langle 2345\rangle - \langle 1238\rangle\langle 1457\rangle\langle 2367\rangle$ $\langle 1256\rangle\langle 1267\rangle\langle 3478\rangle - \langle 1256\rangle\langle 1278\rangle\langle 3467\rangle - \langle 1234\rangle\langle 1267\rangle\langle 5678\rangle$ $\langle 1246\rangle\langle 1478\rangle\langle 3567\rangle - \langle 1278\rangle\langle 1346\rangle\langle 4567\rangle - \langle 1236\rangle\langle 1478\rangle\langle 4567\rangle$ $\langle 1246\rangle\langle 1256\rangle\langle 3478\rangle - \langle 1246\rangle\langle 1278\rangle\langle 3456\rangle - \langle 1234\rangle\langle 1256\rangle\langle 4678\rangle$ $\langle 1456\rangle\langle 2357\rangle\langle 3678\rangle - \langle 1678\rangle\langle 2357\rangle\langle 3456\rangle - \langle 1235\rangle\langle 3678\rangle\langle 4567\rangle$ $\langle 1358\rangle\langle 1456\rangle\langle 2367\rangle - \langle 1238\rangle\langle 1567\rangle\langle 3456\rangle - \langle 1236\rangle\langle 1358\rangle\langle 4567\rangle$ $\langle 1235\rangle\langle 1678\rangle\langle 2345\rangle - \langle 1238\rangle\langle 1345\rangle\langle 2567\rangle$ $+ \langle 1237\rangle\langle 1345\rangle\langle 2568\rangle - \langle 1236\rangle\langle 1578\rangle\langle 2345\rangle$ $\langle 1246\rangle\langle 1356\rangle\langle 2378\rangle - \langle 1256\rangle\langle 1378\rangle\langle 2346\rangle$ $- \langle 1236\rangle\langle 1456\rangle\langle 2378\rangle - \langle 1236\rangle\langle 1278\rangle\langle 3456\rangle$ $\langle 1246\rangle\langle 1257\rangle\langle 3458\rangle - \langle 1245\rangle\langle 1278\rangle\langle 3456\rangle$ $- \langle 1248\rangle\langle 1256\rangle\langle 3457\rangle - \langle 1245\rangle\langle 1267\rangle\langle 3458\rangle$ $\langle 1256\rangle\langle 3678\rangle\langle 4578\rangle - \langle 1236\rangle\langle 4578\rangle\langle 5678\rangle$ $+ \langle 1678\rangle\langle 2345\rangle\langle 5678\rangle - \langle 1345\rangle\langle 2678\rangle\langle 5678\rangle$	8

Table 6.2: Cyclic generators of degree 2 and 3 of the $\mathcal{A}$-variables of the cluster algebra truncated by $F_{4,8}$. In the last column, the size of the cyclic orbit of each generator is given. The generators which are not contained in the cluster algebra truncated by $pF_{4,8}$ are highlighted in blue.

Degree	Cyclic Generator	#
4	$\langle 1245\rangle\langle 1567\rangle\langle 2378\rangle\langle 3467\rangle - \langle 1278\rangle\langle 1567\rangle\langle 2345\rangle\langle 3467\rangle$ $+\langle 1234\rangle\langle 1237\rangle\langle 4567\rangle\langle 5678\rangle - \langle 1237\rangle\langle 1245\rangle\langle 3467\rangle\langle 5678\rangle$ $-\langle 1234\rangle\langle 1567\rangle\langle 2378\rangle\langle 4567\rangle$ $\langle 1234\rangle\langle 1567\rangle\langle 1678\rangle\langle 2345\rangle - \langle 1267\rangle\langle 1348\rangle\langle 1567\rangle\langle 2345\rangle$ $+\langle 1267\rangle\langle 1348\rangle\langle 1457\rangle\langle 2356\rangle - \langle 1238\rangle\langle 1267\rangle\langle 1457\rangle\langle 3456\rangle$ $-\langle 1234\rangle\langle 1457\rangle\langle 1678\rangle\langle 2356\rangle$ $\langle 1237\rangle\langle 1458\rangle\langle 1567\rangle\langle 2368\rangle - \langle 1238\rangle\langle 1567\rangle\langle 1678\rangle\langle 2345\rangle$ $+\langle 1236\rangle\langle 1238\rangle\langle 1457\rangle\langle 5678\rangle - \langle 1236\rangle\langle 1237\rangle\langle 1458\rangle\langle 5678\rangle$ $-\langle 1238\rangle\langle 1457\rangle\langle 1567\rangle\langle 2368\rangle$ $\langle 1278\rangle\langle 1678\rangle\langle 2456\rangle\langle 3456\rangle - \langle 1278\rangle\langle 1456\rangle\langle 2678\rangle\langle 3456\rangle$ $+\langle 1256\rangle\langle 1456\rangle\langle 2678\rangle\langle 3478\rangle - \langle 1256\rangle\langle 1678\rangle\langle 2456\rangle\langle 3478\rangle$ $+\langle 1234\rangle\langle 1678\rangle\langle 2456\rangle\langle 5678\rangle - \langle 1246\rangle\langle 1278\rangle\langle 3456\rangle\langle 5678\rangle$ $-\langle 1234\rangle\langle 1456\rangle\langle 2678\rangle\langle 5678\rangle$	8
5	$\langle 1345\rangle\langle 1458\rangle\langle 1567\rangle\langle 2367\rangle\langle 2378\rangle - \langle 1367\rangle\langle 1458\rangle\langle 1567\rangle\langle 2345\rangle\langle 2378\rangle$ $+\langle 1237\rangle\langle 1238\rangle\langle 1345\rangle\langle 4567\rangle\langle 5678\rangle - \langle 1238\rangle\langle 1345\rangle\langle 1567\rangle\langle 2378\rangle\langle 4567\rangle$ $+\langle 1237\rangle\langle 1367\rangle\langle 1458\rangle\langle 2345\rangle\langle 5678\rangle - \langle 1235\rangle\langle 1238\rangle\langle 1678\rangle\langle 3457\rangle\langle 4567\rangle$ $-\langle 1237\rangle\langle 1345\rangle\langle 1458\rangle\langle 2367\rangle\langle 5678\rangle$	2
	$\langle 1235\rangle\langle 1278\rangle\langle 1678\rangle\langle 2345\rangle\langle 3456\rangle - \langle 1235\rangle\langle 1245\rangle\langle 1678\rangle\langle 2378\rangle\langle 3456\rangle$ $+\langle 1235\rangle\langle 1245\rangle\langle 1568\rangle\langle 2378\rangle\langle 3467\rangle - \langle 1235\rangle\langle 1278\rangle\langle 1568\rangle\langle 2345\rangle\langle 3467\rangle$ $+\langle 1234\rangle\langle 1278\rangle\langle 1568\rangle\langle 2345\rangle\langle 3567\rangle - \langle 1234\rangle\langle 1245\rangle\langle 1568\rangle\langle 2378\rangle\langle 3567\rangle$ $+\langle 1234\rangle\langle 1238\rangle\langle 1245\rangle\langle 3567\rangle\langle 5678\rangle - \langle 1235\rangle\langle 1238\rangle\langle 1245\rangle\langle 3467\rangle\langle 5678\rangle$	8

Table 6.3: Cyclic generators of degree 4 and 5 of the $\mathcal{A}$-variables of the cluster algebra truncated by $F_{4,8}$. In the last column, the size of the cyclic orbit of each generator is given. The generators which are not contained in the cluster algebra truncated by $pF_{4,8}$ are highlighted in blue.

the Plücker variables, the x-variables are well defined coordinates on the configuration space – all cluster variables become polynomials with positive integer coefficients. Note that this phenomenon is not restricted to the variables of the truncated cluster algebra but it also holds for all further letters of the full cluster algebra that were tested.

In analogy to the seven-particle case, where the cluster algebra truncated by the fan of the partially tropicalised totally positive configuration space was sufficient to describe the MHV amplitude and its adjacency properties, it is reasonable to expect that the rational part of the eight-particle MHV alphabet will be similarly contained in the set of 272 $\widetilde{\text{pTr}}_+(4,8)$-letters mentioned above, and in fact may even be a subset thereof. Apart from the seven-particle expectations, this hypothesis is also the simplest that agrees with the available data on the two- and three-loop eight-particle symbol [187, 196], which is completely rational up to two loops.

In principle, this hypothesis could be tested by extending the amplitude bootstrap method mentioned in the introduction [28, 45–48, 50–53, 55–57], so as to construct an ansatz for the 4-loop MHV 8-particle amplitude, and fix it completely by comparing with known data in the multi-Regge [136–146] and collinear limits [147–155]. It remains to be seen whether this task is also computationally feasible in practice, as the size of linear systems that need to be solved for the construction of the ansatz crucially depends on the number of letters, which is an order of magnitude larger than e.g. the seven-particle case.

Note that both, the set of 272 and 356 $\mathcal{A}$-variables of the cluster algebra truncated by $pF_{4,8}$ and $F_{4,8}$, respectively, have been checked to be in agreement with those found by a different approach in [185]. In there, the authors also presented the f-vectors of the two fans $pF_{4,8}$ and $F_{4,8}$[4], which consist of a total of 274 and 360 rays, respectively. This indicates that the truncated cluster algebras do not capture the full fans and are missing 2 and 4 rays, respectively. Remarkably, we can recover these rays by infinite mutation sequences, as is discussed in the next section. Finally, the results presented in here are also in agreement with those obtained by a related approach in [72].

6.2.3. Non-rational octagon alphabet

The remarkable feature of the infinite mutation sequences considered in chapter 5 is that they yield quantities, the generalised cluster variables, containing square roots, see eqs. (5.53) and (5.54). The main idea of the works [72, 164, 185, 195] was that these quantities therefore provide natural candidates for the non-rational letters of amplitudes, focusing on the then-unknown frontier of multiplicity eight, related to the $\mathrm{Gr}(4,8)$ cluster algebra. Before we present the non-rational part of our proposed eight-particle alphabet, however, we first discuss why the generalised cluster variables are the correct choice of algebraic letters compared to other quantities of the infinite mutation sequences containing square-roots.

In section 3.1.4, we have discussed how the cluster rays of any cluster algebra are in a one-to-one correspondence to its cluster variables. It would therefore be a natural choice to extend this one-to-one correspondence to tropical rays and letters of the symbol alphabet, with tropical rays that are no cluster rays corresponding to square-root letters. And indeed, scanning the $\mathrm{Gr}(4,8)$ cluster algebras truncated by the full or partial tropical fan for cluster subalgebras of $A_m^{(1)}$ type, we find that it contains those with $m = 1$. Furthermore, the limiting rays of the associated infinite mutation sequences correspond to the 4 (2) tropical rays of $F_{4,8}$ ($pF_{4,8}$) that are not part of the cluster fan. Since the limits $\beta_\pm$, see eq. (5.42), of all such sequences are unique for each limiting ray, the ratio β_+/β_- is a natural choice for the algebraic letters that also respects the symmetry of the symbol alphabet.

While this construction of the algebraic letters is not in agreement with the 18 square-root letters contained in the two-loop NMHV amplitude, as calculated via the so-called $\bar{Q}$-equations in [61], one could in theory restrict the analysis to MHV amplitudes, which are technically speaking the only ones having $\widetilde{\mathrm{Gr}}(4,n)$ as their space of kinematics (beyond MHV, the analysis of the kinematic space is complicated by the existence of rational

[4] To be precise, they presented the f-vectors of the polytopes, to which these are the normal fans.

functions on top of the transcendental ones studied here). Indeed, up to the loop order $L = 2$, the eight-particle MHV amplitude only contains rational letters [187, 197], so it could be that the only additional square-root letters starting to appear at $L \geq 3$ are those uniquely associated to tropical rays. However, the recently calculated three-loop MHV symbol alphabet, which was obtained in [196] via $\bar{Q}$-bar equations, in fact also contains the 18 square-root letters previously only known to appear in NMHV amplitudes. This result demonstrates that a one-to-one correspondence between rays and algebraic letters is not possible for the eight-particle amplitude.

Nevertheless, in [72] it was further noticed that if the direction of approach to the limit ray is also taken into account, such that many square-root letters are associated to each limit ray in a particular fashion, then one in fact obtains the complete alphabet of the two-loop NMHV amplitude [61], which the unique association of letters to rays cannot account for. Along with a complementary analysis based on plabic graphs [198–200], see also [201], this seems to suggest that despite the apparent complications mentioned above for non-MHV amplitudes in $\mathcal{N} = 4$ pSYM, the symbol alphabet may be independent of the helicity configuration, at least at multiplicity $n = 8$.

Consequently, based on and extending the prescription of [72],[5] we propose that the generalised cluster variables associated to the infinite mutation sequences of $A_m^{(1)}$, which are in a many-to-one correspondence to the limiting rays, form the square-root letters of the eight-particle symbol alphabet. As it turns out, however, the generalised cluster variables obtained from sequences with $m > 1$ differ qualitatively from those with $m = 1$. For this reason, we for now restrict to $m = 1$ and turn to the other sequences in section 6.4.2 after we have also discussed applications to nine-particle scattering. For sequences of $A_1^{(1)}$ type, the corresponding formulas, eqs. (5.53) and (5.54), simplify to

$$\phi_0 \equiv \frac{C_+}{C_-} = \frac{2 - K_1 + \sqrt{K_1^2 - 4K_2}}{-2 + K_1 + \sqrt{K_1^2 - 4K_2}}\,, \qquad \tilde{\phi}_0 \equiv \frac{\tilde{C}_+}{\tilde{C}_-} = \frac{2K_2 - K_1 + \sqrt{K_1^2 - 4K_2}}{-2K_2 + K_1 + \sqrt{K_1^2 - 4K_2}}\,, \tag{6.16}$$

whereas the invariants K_1 and K_2, originally defined in eqs. (5.27) and (5.28), are given by

$$K_1 = 1 + x_{1;0} + x_{1;0}x_{2;0}\,, \qquad K_2 = x_{1;0}x_{2;0}\,. \tag{6.17}$$

The great merit of the analysis we carried out in chapter 5, and of the above formula, is that it can be directly applied to *any* such subalgebra for *any* n, not necessarily equal to eight. All we need as input is the data of a given *origin cluster*, namely the cluster containing a $A_1^{(1)}$ cluster subalgebra from which the infinite mutation sequence starts, such as for example the one depicted in figure 6.4 for $n = 8$.[6]

In this way, our results can in principle be specialized to yield predictions for the symbol alphabet of scattering amplitudes at any multiplicity n, and in section 6.3 we will indeed apply them to the $n = 9$ case. As a first cross check however, in the remainder of this

[5] More precisely, when specialized to $n = 8$ the formulas below reduce to the negative inverse of those provided in [72], with this difference being immaterial at the level of symbol letters.

[6] More concretely, to apply the above formulas in this example, we only need to evaluate eq. (6.17) with $x_{1;0} \to x_1$ and $x_{2;0} \to x_9$.

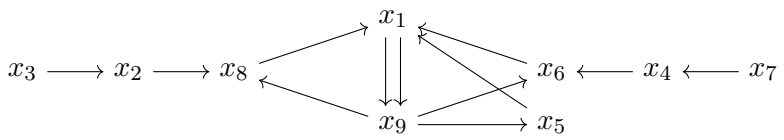

Figure 6.4: Principal part of an origin cluster in $\mathrm{Gr}(4,8)$ in terms of the cluster's $\mathcal{X}$-variables, which is utilized to find the square-root letters. From this quiver, it is also evident that $\mathrm{Gr}(4,8) \simeq E_7^{(1,1)}$ in the extended affine Dynkin diagram classification [178].

subsection we will use our method to confirm the results reported in [72] for the eight-particle alphabet. Let us also comment that while the prescription (6.16) may currently seem ad-hoc and only justified by the agreement of its symbol alphabet predictions with explicit computations, in the next subsection we will provide further evidence about its correctness by comparing it with a more recent approach based on scattering diagrams and wall-crossing [73].

Coming back to the case of eight-particle scattering, we find a total of 3,600 origin clusters with a $A_1^{(1)}$ cluster subalgebra in the 121,460 clusters of the cluster algebra of $\mathrm{Gr}(4,8)$ truncated by $\widetilde{\mathrm{pTr}}_+(4,8)$. The rays of the variables mutated in the infinite mutation sequences starting at these origin clusters converge to four different limit rays. Interestingly, only two of these limit rays are contained in $\widetilde{\mathrm{pTr}}_+(4,8)$, whereas the other two are contained only in $\widetilde{\mathrm{Tr}}_+(4,8)$ and not its partially tropicalised version. Similar to the truncation rule used to obtain a finite subset of rational cluster variables, we discard the limits of the origin quivers whose limit rays are not contained in $\widetilde{\mathrm{pTr}}_+(4,8)$. This leaves us with a truncated set of 2,800 origin clusters of which 56 for each of the two limit rays are unique,[7] since many of these clusters only differ in parts of the quiver that do not affect the $A_1^{(1)}$ cluster subalgebra and thus also not the limit of its infinite mutation sequence.

In this way, we find a total of 112 different origin clusters giving rise to 224 square-root letters via eqs. (6.16). However, these 224 letters are not multiplicatively independent. From the perspective of the alphabet – essentially the set of logarithms of these letters – this means that not all of the letters are linearly independent and hence are redundant. While the presence of square roots complicates the elimination of these redundancies, this can be done using an approach similar to that of [202], which we will describe in more detail in section 6.3.2, where it is used again. For the case at hand, we find that the aforementioned 224 letters reduce to 18 multiplicatively independent letters, which are equivalent to the square-root letters reported in [72] and previously known to appear in the two-loop NMHV and three-loop MHV eight-particle amplitudes, as computed in [61, 196].[8] The proposed non-rational alphabet for the eight-particle amplitude consisting of these 18

[7] The 800 origin clusters whose limit rays are only contained in $\widetilde{\mathrm{Tr}}_+(4,8)$ reduce to 32 different origin clusters for each of the rays.

[8] Note that the 18 square-root letters can alternatively be obtained by solving polynomial equations associated to certain plabic graphs [198, 199]. As soon as one attempts to also incorporate rational letters in this approach, however, non-plabic graphs are required as well [200]. In this case the solution space includes all cluster variables of $\mathrm{Gr}(4,8)$, that is the alphabet becomes infinite again.

multiplicatively independent square-root letters can also be found in appendix B.

To summarise, in total we obtain all 274 tropical rays of $\widetilde{\text{pTr}}_+(4,8)$ – 272 rays associated to one rational letter of the truncated cluster algebra each and 2 rays associated to 9 multiplicatively independent square-root letters obtained as the limits of infinite mutation sequences each. This 290-letter alphabet contains all letters previously known to appear in the eight-particle MHV and NMHV amplitudes, including especially those obtained from the calculations using $\bar{Q}$-equations [61, 75, 196].

6.2.4. Comparison with the scattering diagram approach

A common element of the majority of different efforts to predict the symbol alphabet of n-particle amplitudes in $\mathcal{N}=4$ pSYM, initially based on Grassmannian cluster algebras [37], and more recently on tropical Grassmannians [72, 164] or stringy canonical forms [185], is that they correspond to different compactifications of the positive part of the space of kinematics $\widetilde{\text{Gr}}(4,n)$. More recently, another such compactification refining the aforementioned works, and relying on the concepts of wall-crossing and scattering diagrams, has been proposed [73].

Having discussed the predictions of the tropical geometry approach for the eight-particle alphabet in the previous subsection, here we will compare them with those of the scattering diagram approach. In a nutshell, while the latter yields 72 letters (36 per limit ray of $\widetilde{\text{pTr}}_+(4,8)$), out of which 56 are naively non-rational, we will show that in fact *all* of these letters are contained in the 290-letter octagon alphabet of the previous subsection, *except* for the square roots of the two Gram determinants associated to the four-mass box,

$$\Delta_{1,3,5,7} = \left(1 - \frac{\langle 1234\rangle\langle 5678\rangle}{\langle 1256\rangle\langle 3478\rangle} - \frac{\langle 1278\rangle\langle 3456\rangle}{\langle 1256\rangle\langle 3478\rangle}\right)^2 - 4\frac{\langle 1278\rangle\langle 1234\rangle\langle 3456\rangle\langle 5678\rangle}{\left(\langle 1256\rangle\langle 3478\rangle\right)^2}\,, \tag{6.18}$$

$$\Delta_{2,4,6,8} = \left(1 - \frac{\langle 2345\rangle\langle 1678\rangle}{\langle 2367\rangle\langle 1458\rangle} - \frac{\langle 1238\rangle\langle 4567\rangle}{\langle 2367\rangle\langle 1458\rangle}\right)^2 - 4\frac{\langle 1238\rangle\langle 2345\rangle\langle 4567\rangle\langle 1678\rangle}{\left(\langle 2367\rangle\langle 1458\rangle\right)^2}\,, \tag{6.19}$$

whereas $\Delta_{2,4,6,8}$ is related to $\Delta_{1,3,5,7}$ by the cyclic shift $\langle ijkl\rangle \to \langle i+1\, j+1\, k+1\, l+1\rangle$.

We view the almost complete overlap of the two approaches at multiplicity $n=8$ as a strong indication of their correctness, and will further comment on the presence or absence of the extra letters, eqs. (6.18) and (6.19), from amplitudes and Feynman integrals. To provide more general backing to this conclusion, later in this section we will also show that the square-root letters obtained from the tropical geometry approach are always contained in those of the scattering diagram approach for any n. But before this, let us briefly provide some background information on scattering diagrams.

Basics of scattering diagrams

A scattering diagram can be thought of as a generalisation of the $\boldsymbol{g}$-vector fan of the cluster algebra, as defined by eq. (3.32), that also contains the limits of infinite mutation sequences. In the $\boldsymbol{g}$-vector fan of a cluster algebra, each $\mathcal{A}$-variable is associated to one of the rays in the fan. The rays of all variables in a cluster then form a cone, which intersects other cones that share some of the variables. A codimension-1 intersection, or *wall*, between cones that share all but one variable corresponds to the mutation of the variable that is not shared.

In the scattering diagram, we associate a variable x_{γ_i} to each of the rays in a cone. These *cone variables* are related to the $\mathcal{X}$-variables of the cone in the following way. Consider a wall of the cone and the $\mathcal{X}$-variable x_j that is mutated when passing through the wall. Denote the (appropriately normalized) vector perpendicular to the wall and pointing into the cone by $\gamma_j^\perp = c_i^j \gamma_i$, whereas the γ_i denote the canonical basis vectors. We then have the relation

$$x_j = \prod_i (x_{\gamma_i})^{c_i^j} \,. \tag{6.20}$$

Alternatively, we can use the inverse of eq. (6.20) to express the variables x_{γ_i} in terms of the $\mathcal{X}$-variables x_i of the cone. Note that the labelling is such that the wall denoted by j is that which is spanned by the rays associated to all $\mathcal{A}$-variables a_i except that of a_j. As we will see shortly, the advantage of using the cone variables is that they remain finite and have a well-defined limit in the relevant infinite mutation sequences.

The mutation, or *wall crossing*, of the cone variables is implemented by multiplying them with powers of a function $f(x_{\gamma_j^\perp})$ which is attached to each of the walls, whereas the argument $x_{\gamma_j^\perp}$ is equal to x_j or its inverse, depending on the side from which the wall is approached. For walls that are part of the $\boldsymbol{g}$-vector fan, this function is given by $f(x_{\gamma_j^\perp}) = 1 + x_{\gamma_j^\perp}$. Together with eq. (6.20), this reproduces the mutation rule for the x_i. Extending the cluster algebra framework, the wall crossing function for walls that are not part of the cluster algebra can be obtained by self-consistency conditions.

Eight-particle alphabet predictions and comparison with tropical geometry

Let us now review and further analyse the predictions of the scattering diagrams framework for the alphabet of the eight-particle amplitude [73], as well as compare them to the 290-letter $\widetilde{\text{pTr}}_+(4,8)$ alphabet discussed in the previous section. We will only discuss the boundary structure around one of the two limit rays of $\text{Gr}(4,8)$, since the letters associated to the other can be obtained by the cyclic shift $\langle ijkl\rangle \to \langle i+1\, j+1\, k+1\, l+1\rangle$.

In a first step, one mutates from the initial cluster to an origin cluster containing a $A_1^{(1)}$ subalgebra. Concretely, performing the mutations $\{1,2,4,1,6,8\}$ leads to the cluster depicted in figure 6.4. The parameterisation of the $\mathcal{X}$-variables x_i in this cluster in terms of Plücker variables as well as all other data required to reconstruct the non-rational alphabet can be found in appendix B.

Next, one expresses the cone variables along the $A_1^{(1)}$ sequence originating from this cluster in terms of its $\mathcal{X}$-variables x_i by using the inverse of eq. (6.20). Compared to the x_i, the cone variables do converge to a finite function when taking the limit of the infinite sequence. These limits correspond to the cone variables $x^0_{\gamma_i}$ of a cone asymptotically close to the limit ray, also known as an *asymptotic chamber*, and are given by

$$\begin{aligned}
x^0_{\gamma_i} &= x_i \quad \text{for} \quad i \in \{2,3,4,7\}\,, \\
x^0_{\gamma_i} &= \frac{x_i}{2}\left(1 + x_1\,(1+x_9) + \sqrt{\Delta'}\right) \quad \text{for} \quad i \in \{5,6,8\}\,, \\
x^0_{\gamma_1} &= \frac{4x_1\Delta'}{\left(1 + x_1 - x_1 x_9 + \sqrt{\Delta'}\right)^2}\,, \quad x^0_{\gamma_9} = \frac{x_9}{4}\left(1 + \frac{1 - x_1(1+x_9)}{\sqrt{\Delta'}}\right)^2\,,
\end{aligned} \tag{6.21}$$

where $\Delta' = (1 + x_1(1 + x_9))^2 - 4x_1x_9$. In contrast to just considering the cluster algebra itself, one can now utilise wall crossing to find other asymptotic chambers and their variables. This was carried out in [73] by means of an extensive computer search, yielding a basis of 36 multiplicatively independent polynomials of the $x^0_{\gamma_i}$, proposed to contain all non-rational letters (in the original $\mathcal{X}$- or Plücker variables) of the eight-particle amplitude. It was also noticed that 10 of these polynomials depend only on the rational $\mathcal{X}$-variables x_i for $i \in \{2, 3, 4, 7\}$, such that the set of non-rational letters is immediately reduced to (a maximum of) 26 letters.

Very interestingly, we notice that for another 6 of these letters the square roots contained in them cancel out, such that they are also secretly rational. What is more, there are 10 multiplicative combinations of the remaining 20 letters that turn out to be rational as well,[9] see appendix B for details. All in all, this implies that the scattering diagram approach in fact predicts 26 rational and 10 square-root letters for one of the two Gr(4, 8) limit rays, and more concretely the latter ones may be chosen to be

$$
\begin{aligned}
&f_1 = \left(x^0_{\gamma_1}\right)^{-1}\left(1 - x^0_{\gamma_1}x^0_{\gamma_9}\right)^2\,, \quad f_2 = x^0_{\gamma_9}\left(1 - x^0_{\gamma_1}x^0_{\gamma_9}\right)^2\,,\\
&f_3 = \frac{1 + x^0_{\gamma_5}x^0_{\gamma_1}x^0_{\gamma_9}}{1 + x^0_{\gamma_5}}\,, \qquad f_4 = \frac{1 + x^0_{\gamma_8}x^0_{\gamma_1}x^0_{\gamma_9}}{1 + x^0_{\gamma_8}}\,, \qquad f_5 = \frac{1 + x^0_{\gamma_2}\left(1 + x^0_{\gamma_8}x^0_{\gamma_1}x^0_{\gamma_9}\right)}{1 + x^0_{\gamma_2}\left(1 + x^0_{\gamma_8}\right)}\,,\\
&f_6 = \frac{1 + x_{\gamma_3}\left(1 + x^0_{\gamma_2}\left(1 + x^0_{\gamma_8}x^0_{\gamma_1}x^0_{\gamma_9}\right)\right)}{1 + x_{\gamma_3}\left(1 + x^0_{\gamma_2}\left(1 + x^0_{\gamma_8}\right)\right)}\,,\\
&f_{10} = x^0_{\gamma_5}\left(1 - x^0_{\gamma_1}x^0_{\gamma_9}\right)\,,
\end{aligned}
\tag{6.22}
$$

together with f_7, f_8, f_9 obtained from replacing $x^0_{\gamma_3} \to x^0_{\gamma_7}$, $x^0_{\gamma_2} \to x^0_{\gamma_4}$, and $x^0_{\gamma_8} \to x^0_{\gamma_6}$. As already mentioned, another 10 letters associated to the other limit ray may be obtained by a cyclic shift of the momentum twistors.

How about the relation of the scattering diagram letters to the tropical 290-letter eight-particle alphabet, discussed in the previous section? Starting with the 26 rational scattering diagram letters, we find that they are all contained in the $\widetilde{\text{pTr}}_+(4,8)$ alphabet. As far as the square-root letters are concerned, as already pointed out in [73], 9 of them (plus cyclic) are also contained in the $\widetilde{\text{pTr}}_+(4,8)$ alphabet, and we also confirm this to be the case. In the square-root letter basis (6.22), these in particular correspond to $f_1, \ldots, f_9$. So the final conclusion is that the only scattering diagram letter not contained in the $\widetilde{\text{pTr}}_+(4,8)$ alphabet is f_{10}, which remarkably can be written as (see again appendix B)

$$
f_{10} = \frac{\langle 1256\rangle\,\langle 3478\rangle}{\langle 1278\rangle\,\langle 3456\rangle}\sqrt{\Delta_{1,3,5,7}}\,,
\tag{6.23}
$$

together with its cyclic image, where the square-roots associated to the four-mass box have been defined in eqs. (6.18) and (6.19). Given that the factor in front of the square root is a monomial in the rational letters, one could equally well redefine the letter so as to remove it. For the interested reader, we provide the complete candidate eight-particle alphabet consisting of the 292 letters coming from the union of the tropical geometry and scattering

[9] We thank Dima Chicherin for pointing out the existence of these additional relations to us.

diagram approaches in the ancillary file `Gr48Alphabet.m`, which is attached to the `arXiv` submission of [195].

The fact that the two approaches overlap almost completely greatly reinforces the expectation that all singularities of eight-particle amplitudes are contained in the aforementioned candidate alphabet. In a sense, scattering diagrams provide a more systematic framework for taking infinite mutation sequences into account, and especially for taking the direction of approach to a given limit ray into account, thus justifying the particular choice of eqs. (6.16) for assigning many symbol letters (or equivalently generalisations of rational cluster variables) to it. On the other hand, while degenerate scattering diagrams have been proposed as an analog of our method for selecting a finite subset of cluster variables with the help of tropical Grassmannians, a stumbling block is currently the significant ambiguity in their construction.[10] It would be very interesting to further clarify the relation between the two approaches. While our discussion so far has been restricted to the $n = 8$ case, we will shortly show that their similarity extends to any n: In particular, that the tropical square-root letters are always a subset of the scattering diagram square-root letters.

Let us also comment on the plausibility of the additional scattering diagram letters, the square roots of the Gram determinants, eqs. (6.18) and (6.19), appearing as letters of the eight-particle amplitude. On the one hand, $\Delta_{1,3,5,7}$ and $\Delta_{2,4,6,8}$ are always positive inside the positive region [185], and so any arguments based on the expectation that amplitudes never have singularities in this region cannot exclude it. On the other hand, we observe that these letters are not present in explicit two-loop results for the (appropriately normalised) eight-particle amplitude in $\mathcal{N} = 4$ pSYM. As an additional source of information on this question, one could also consider the relation between the alphabet of the latter, and that of five-particle amplitudes in Lorentz-invariant theories, recently established in [203]. There, it was pointed out that while analogous square-root letters appear in individual integrals contributing to the two-loop five-point amplitudes, these cancel out in appropriately defined finite remainders, see also [204]. This analogy seems to suggest that at a minimum, $\Delta_{1,3,5,7}$ and $\Delta_{2,4,6,8}$ may contribute to eight-point integrals contributing to the $\mathcal{N} = 4$ pSYM amplitude. Settling whether they survive in the final expression for the latter calls for explicit higher-loop computations, however already this discussion points to scattering diagrams as an attractive tool for studying singularities of Feynman integrals. Their potential in this respect will be studied elsewhere [205].

Finally, it is interesting to note that the discrete symmetry of the eight-particle alphabet respects some of the structure of the infinite cluster algebra of $\mathrm{Gr}(4, 8)$. In particular, the group of automorphisms of the origin quiver, which can be traced back to the group of automorphisms of the initial quiver, is given by the transformation

$$x_2 \leftrightarrow x_4\,, \quad x_3 \leftrightarrow x_7\,, \quad x_6 \leftrightarrow x_8\,. \tag{6.24}$$

By the general theory [206], this quiver automorphism extends to an automorphism of the

[10] Note that the set of 26+26 rational letters that come as a byproduct of the scattering diagram analysis is too small to contain the two-loop (N)MHV eight-particle amplitude.

entire (infinite) cluster algebra. When replacing

$$x_i \to x^0_{\gamma_i}\,, \tag{6.25}$$

in the above equation, this is also a symmetry of the square-root letters. Furthermore, it can be easily verified that the rational part of the alphabet is also symmetric under the same transformation, implying that the truncation procedure as well as the procedure by which we obtained the square-root letters from the scattering diagram are compatible with this symmetry of the infinite cluster algebra. Note that this symmetry is specific to the eight-particle alphabet since this automorphism only exists for $\mathrm{Gr}(4,8)$.

Comparison of algebraic letters at any multiplicity

We now proceed to show that the tropical square-root letters of eq. (6.16) are contained in the alphabet obtained from the scattering diagram approach at any multiplicity n. In particular this adds further support to our analysis of the $n = 9$ case in the next section, which has been carried out relying on the aforementioned equation.

For simplicity, let us start by considering an $\mathrm{A}_1^{(1)}$ cluster algebra with principal coefficients. The cone variables along the infinite mutation sequence are given by

$$x_{\gamma_1;j} = (x_{1;j})^{1-j}\,(x_{2;j})^{-j}\,, \quad x_{\gamma_2;j} = (x_{1;j})^{j}\,(x_{2;j})^{1+j}\,. \tag{6.26}$$

We can now use that $x_{1;j} = a_{2;j}^{-2} y_{1;j}$ and $x_{2;j} = a_{1;j}^{2} y_{2;j}$ to express the cone variables in terms of the $\mathcal{A}$-variables and coefficients along the sequence. Due to working with principial coefficients, it can be shown that $(y_{1;j})^{1-j}(y_{2;j})^{-j} = y_{1;0}$ and $(y_{1;j})^{j}(y_{2;j})^{1+j} = y_{2;0}$ such that we can use eq. (5.50) for $m = 1$ to perform the limit $j \to \infty$, which is given by

$$x^+_{\gamma_1} \equiv x_{\gamma_1;\infty} = y_{1;0}\left(\tilde{C}_-\right)^{-2}\,, \quad x^+_{\gamma_2} \equiv x_{\gamma_2;\infty} = y_{2;0}\,(C_+)^2\,, \tag{6.27}$$

where $C_\pm$ and $\tilde{C}_\pm$ have been defined in eqs. (5.52) and (A.25), respectively. These are the variables attached to the asymptotic chamber, which is the cone asymptotically close to the limit ray that we land in when following the infinite mutation sequence in this direction. Note that from the aforementioned equations it follows that these variables are actually algebraic functions in the $\mathcal{X}$-variables $x_{1;0}, x_{2;0}$ of the initial cluster only, since $x_{1;0} = a_{2;0}^{-2} \cdot y_{1;0}$ and $x_{2;0} = a_{1;0}^{2} \cdot y_{2;0}$.

We can now use wall-crossing to obtain the variables of the asymptotic chamber accessed by following the other direction of the mutation sequence, that is by repeatedly mutating $a_{2;j}$. The function associated to the *limiting wall* of the scattering diagram that separates the two asymptotic chambers accessed by following the two directions of the mutation sequence is given by

$$f(x_{\gamma^\perp}) = y_{2;0}\frac{(C_-)^2\,\tilde{C}_-}{\tilde{C}_+} \equiv \frac{1}{y_{1;0}}\frac{\left(\tilde{C}_-\right)^2 C_-}{C_+}\,, \tag{6.28}$$

such that the variables of the other asymptotic chamber can be obtained from

$$x^+_{\gamma_1} \longrightarrow x^-_{\gamma_1} = x^+_{\gamma_1} \cdot f(x_{\gamma^\perp})^2\,, \qquad x^+_{\gamma_2} \longrightarrow x^-_{\gamma_2} = x^+_{\gamma_2} \cdot f(x_{\gamma^\perp})^{-2}\,. \tag{6.29}$$

From eqs. (6.27)–(6.29), we see that the four variables $x^{\pm}_{\gamma_i}$ associated to the two asymptotic chambers are made up of the four coefficients $C_{\pm}, \tilde{C}_{\pm}$ as well as the initial coefficients $y_{1;0}, y_{2;0}$, which are monomials in the rational cluster variables. It then follows immediately that the algebraic letters of eqs. (6.16) are given as monomials in the multiplicative basis formed by these four variables. To be precise, we have $(\phi_0)^2 = (x^+_{\gamma_1} x^-_{\gamma_1})^{-1}$ and $(\tilde{\phi}_0)^2 = x^+_{\gamma_2} x^-_{\gamma_2} (x^+_{\gamma_1} x^-_{\gamma_1})^2$. An equivalent statement also holds true when considering general coefficients, since the generalized versions of eqs. (6.27)–(6.29) only differ by a further monomial in the rational variables.

6.3. $\widetilde{\mathrm{pTr}}_+(4,9)$ and nine-particle scattering

In this section, we apply the techniques first introduced in [70, 72, 164], and further developed in the previous chapters, see also [195], in order to obtain predictions for the symbol alphabet of the nine-particle amplitude in $\mathcal{N} = 4$ pSYM. In subsection 6.3.1, we first truncate the infinite $\mathrm{Gr}(4,9)$ cluster algebra with the help of the inherently finite partially tropicalised positive configuration space $\widetilde{\mathrm{pTr}}_+(4,9)$ in order to obtain the rational part of the alphabet, which we find consists of 3,078 letters in one-to-one correspondence to tropical rays of $\widetilde{\mathrm{pTr}}_+(4,9)$. Then, in subsection 6.3.2 we study infinite mutation sequences of $A_1^{(1)}$ subalgebras of the truncated cluster algebra, and in this fashion determine an additional 324 limit rays of $\widetilde{\mathrm{pTr}}_+(4,9)$. It is especially here that our new results for such subalgebras with general coefficients, as discussed in chapter 5, allow us to associate to these rays square-root letters expected to appear in the amplitude, in particular a total of 2,349 multiplicatively independent such letters. A new feature of the nine-particle case is that the procedure we have described falls short of yielding 27 rays of $\widetilde{\mathrm{pTr}}_+(4,9)$. The discussion of alternative ways for accessing these rays, and of their possible significance for amplitudes, are presented in the next section.

6.3.1. Rational nonagon alphabet

Similarly to the eight-particle case, we start mutating from the initial cluster of $\mathrm{Gr}(4,9)$, which is depicted in figure 6.5. As before, to tame the infinity of the cluster algebra we stop mutating in a given direction whenever the result of this mutation is a cluster variable whose associated ray is redundant with respect to the totally positive (partially) tropicalised configuration space – that is, the ray does not lie on a maximal intersection of tropical hypersurfaces. By this truncation procedure, we obtain a finite subset of the infinite cluster algebra and thus a finite collection of $\mathcal{A}$-variables.

For computational purposes, we computed the truncated cluster algebra in two steps. First, we performed the aforementioned finite number of mutations only on the adjacency matrix, eq. (3.21), and cluster rays, eqs. (3.34)–(3.35). Being only matrix operations, this can be done much more efficiently than factoring the rational expressions of the variables. Having computed the truncated cluster fan, we scanned it for paths of mutations connecting the initial cluster seed with a cluster containing a given ray. Due to the one-to-one correspondence of $\mathcal{A}$-variables and rays, we finally mutated the variables along these paths to obtain all cluster variables.

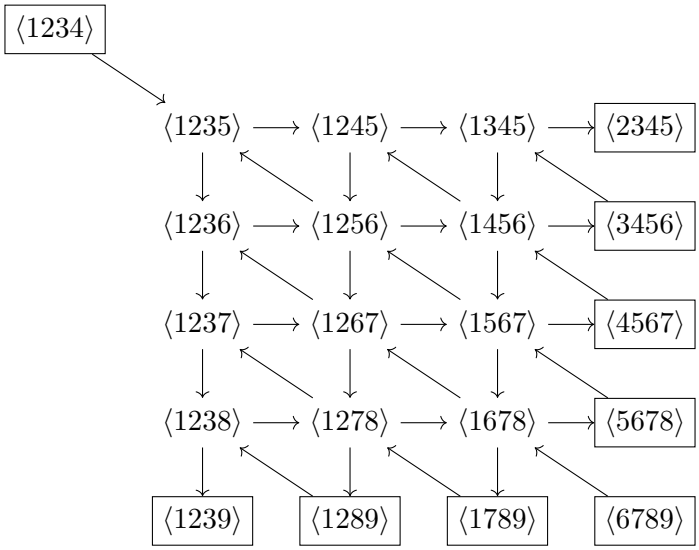

Figure 6.5: Initial seed of the cluster algebra of $\text{Gr}(4,9)$.

We find that the truncated cluster algebra obtained from the partially tropicalised totally positive configuration space $\widetilde{\text{pTr}}_+(4,9)$ contains 3,078 rational $\mathcal{A}$-variables in 24,102,954 clusters. These variables are all homogeneous polynomials in the Plücker variables of degree up to 6, see table 6.4. For comparison, we have also carried out the same truncation procedure for the full positive tropical configuration space $\widetilde{\text{Tr}}_+(4,9)$, this time finding 12,645 $\mathcal{A}$-variables distributed in 55,363,988 clusters, whose multiplicity per degree are also listed in the same table.

Degree	1	2	3	4	5	6	7	8	9	10	Total
$\widetilde{\text{pTr}}_+(4,9)$	117	576	1287	963	126	9	-	-	-	-	3078
$\widetilde{\text{Tr}}_+(4,9)$	117	576	1854	3159	2943	1926	1296	531	180	63	12645

Table 6.4: Number of $\mathcal{A}$-variables of the truncated cluster algebra of $\text{Gr}(4,9)$ grouped by their (homogeneous) polynomial degree in the Plücker variables. At degree 1, all Plücker variables appear when also including the frozen $\langle i\, i+1\, i+2\, i+3\rangle$ variables.

As discussed for the eight-particle case in section 6.2.2, existing data and symmetry reasons point to $\widetilde{\text{pTr}}_+(4,9)$ as the minimal choice relevant for scattering amplitudes, so unless otherwise stated we will be focusing on the latter. Explicitly, the $\mathcal{A}$-coordinates of degree up to three that make up the rational part of our candidate nine-particle alphabet are schematically given by[11]

[11] In this list, all types of letters are to be read as disjoint sets, such that e.g. the 8 classes of type $\langle(\bar{i})\cap(jkl)\cap(mno)\cap(pqr)\rangle$ are meant to not include those of type $\langle(\bar{i})\cap(jkl)\cap(\bar{m})\cap(nop)\rangle$, etc. We use notations where $(\bar{a})$ corresponds to the plane $(a-1\,a\,a+1)$ in momentum twistor space, the intersection of a line and a plane is given by $\langle I(ab)\cap(cde)J\rangle = \langle IaJ\rangle\langle bcde\rangle + \langle IbJ\rangle\langle cdea\rangle$, and the

- all single Plücker variables $\langle ijkl\rangle$,
- 64 cyclic (37 dihedral) classes of degree two consisting of $\langle 1i(jkl)\cap(mno)\rangle$ with $i\in\{1,2,3,5,6,7\}$,
- 143 cyclic (74 dihedral) classes of degree three consisting of
  - 8 classes of type $\langle(\bar{i})\cap(jkl)\cap(mno)\cap(pqr)\rangle$ with $i\in\{2,3,4,5,7\}$,

    35 of type $\langle(\bar{i})\cap(jkl)\cap(\bar{m})\cap(nop)\rangle$ with $2\leq i\leq 7$ and $4\leq m\leq 9$,

    20 of type $\langle(\bar{i})\cap(jkl)\cap(\bar{m})\cap(\bar{n})\rangle$ with $i\in\{1,2,4,5\}$, $4\leq m\leq 7$, $6\leq n\leq 9$,

    1 of type $\langle(\bar{2})\cap(\bar{7})\cap(\bar{5})\cap(\bar{9})\rangle$,
  - 40 classes of type $\langle i(12)\cap(jkl)(mno)\cap(pqr)\rangle$ with $3\leq i\leq 9$,

    2 of $\langle 4(13)\cap(896)(895)\cap(\bar{6})\rangle$ and $\langle 8(13)\cap(\bar{5})(549)\cap(679)\rangle$,

    2 of $\langle 3(18)\cap(\bar{8})(245)\cap(267)\rangle$ and $\langle 7(18)\cap(235)(236)\cap(\bar{5})\rangle$,
  - 30 classes of type $\langle i(12)\cap(klm)(no)\cap(pqr)s\rangle$ with $o=n+1$,

    2 of $\langle 4(12)\cap(\bar{8})(68)\cap(\bar{2})5\rangle$ and $\langle 5(79)\cap(\bar{2})(12)\cap(\bar{4})6\rangle$,

    2 of $\langle 4(13)\cap(\bar{8})(67)\cap(\bar{2})5\rangle$ and $\langle 6(89)\cap(\bar{2})(13)\cap(\bar{5})7\rangle$,

    1 of $\langle 8(14)\cap(\bar{6})(56)\cap(\bar{3})9\rangle$.

We have included these, as well as the remaining higher-degree letters, in the ancillary file `Gr49RationalAlphabet.m` attached to the `arXiv` submission of [195], where the precise ranges of the indices not stated in the text may be found as well. Note that the representation is not unique due to the many ways to equivalently express these polynomials via the Plücker identities.

In total, the rational part of our candidate nine-particle alphabet consists of 3,087 $\mathcal{A}$-coordinates forming 3,078 dual conformally invariant letters, arranged in 342 cyclic classes which always have multiplicity 9. If one also considers the dihedral flip transformation, the alphabet consists of 9, 37, 74, 57, 7, and 1 dihedral classes of rational letters of degree 1 to 6, respectively (the multiplicity of dihedral classes may be either 9 or 18, depending on whether a flip relates two cyclic classes or maps one back to itself). Consequently, the proposed rational alphabet is dihedrally invariant.

Let us conclude this section with some further comparisons and remarks on the structure of the rational part of our candidate alphabet. First of all, we can compare it with the explicit results for the symbol of the two-loop NMHV nine-particle amplitude, computed recently in [75]. The latter contains 99 square-root letters, which we will discuss in the next section, as well as 522 dual conformally invariant rational letters that are polynomials in the Plücker variables of degree up to three. We find that all of these rational letters are indeed contained in our alphabet, which serves as a first consistency check. Note that the

intersection of two planes by $\langle I(abc)\cap(def)J\rangle = \langle IabJ\rangle\langle cdef\rangle + \langle IbcJ\rangle\langle adef\rangle + \langle IcaJ\rangle\langle bdef\rangle$ for appropriate index sets $I,J\subset\{1,\ldots,9\}$. See e.g. [112] for more details.

216 nine-particle MHV letters [187] are all rational and contained in the NMHV ones, and hence our proposal trivially covers this helicity configuration as well.

To make the comparison more precise, the alphabet of [75] contains all degree one letters of the alphabet proposed here except $\langle 1357\rangle$ plus cyclic permutations. Furthermore, several cyclic classes of higher degree letters are missing compared to our alphabet. Among those are 27 cyclic classes of degree two letters, 27 cyclic classes of the type $\langle(\bar{i})\cap(jkl)\cap(\bar{m})\cap(nop)\rangle$ as well as all but one of the 30 cyclic classes of the type $\langle i(12)\cap(klm)(no)\cap(pqr)s\rangle$ our proposal includes. Letters of the type $\langle i(jk)\cap(lmn)(opq)\cap(rst)\rangle$ are not at all contained in the alphabet of the two-loop NMHV nine-particle amplitude. Additional evidence in support of our proposal for the rational part of the alphabet is that it agrees with the one obtained by other means in [207], appearing simultaneously with this article.

Finally, in search of interesting patterns, we may look at what part of the infinite $\text{Gr}(4,9)$ cluster algebra is chosen by our tropical selection rule according to the degree of the $\mathcal{A}$-variable with respect to the Plücker variables. As shown in [208], $\text{Gr}(4,9)$ contains 576 cluster variables of degree two, 2,421 of degree three, 8,622 of degree four, and 27,054 variables of degree five. A comparison with table 6.4 demonstrates that our alphabet contains all possible quadratic cluster $\mathcal{A}$-variables but only a subset of those of degree three or higher.[12] For example, the polynomials

$$\langle 4(56)\cap(\bar{8})(78)\cap(\bar{2})1\rangle\ ,\quad \langle(127)\cap(\bar{5})\cap(13i)\cap(\bar{8})\rangle\ , \tag{6.30}$$

with $i=5$ or $i=6$, are cluster $\mathcal{A}$-variables of degree three but are not associated to tropical rays of $\widetilde{\text{pTr}}_+(4,9)$, and hence are not selected by our procedure.

6.3.2. Non-rational nonagon alphabet

Having obtained a candidate for the rational part of the alphabet of nine-particle amplitudes in the previous subsection, here we will enlarge it so as to also include square-root letters. The general procedure for doing so has been presented in chapter 5, and relies on considering infinite mutation sequences starting from any origin cluster of the truncated cluster algebra, that contains an $A_m^{(1)}$ subalgebra. As with the eight-particle case, discussed in section 6.2.3, in the first instance we examine the limit of cluster rays along the sequence, and only select it, along with its associated square-root letters (or generalised cluster variables) if this limit coincides with a tropical ray of $\widetilde{\text{pTr}}_+(4,9)$. Since infinite mutation sequences for $m=1$ were sufficient in the eight-particle case to construct all previously known square-root letters, we apply the same approach in this section to nine-particle scattering and discuss sequences with $m>1$ in subsection 6.4.2.

This step therefore requires knowledge of all tropical rays. While these may be obtained with the help of dedicated software such as `polymake` [209], fortunately most of the work has already been done in [210]. There, the dual fan of the tropical configuration space

[12] The same statement for degrees two and three in fact holds also for the eight-particle rational alphabet we proposed in [164], which contains all 120 quadratic but not all 174 cubic cluster variables of $\text{Gr}(4,8)$ [200, 208]

$\widetilde{\mathrm{Tr}}_+(4,9)$ [71, 211], namely the Minkowski sum of the Newton polytopes $\mathcal{P}(4,9)$ obtained from the web-parameterisation of the Plücker variables, has been computed. Since all $\widetilde{\mathrm{pTr}}_+(4,9)$ rays are contained in $\widetilde{\mathrm{Tr}}_+(4,9)$, we may thus extract them from the provided $\mathcal{P}(4,9)$ data. As a technical remark, in this data the rays (or facets, in the language of the dual polytope) are provided in the space of $D = 126$ Plücker coordinates $\langle ijkl\rangle$, however it is easy to obtain its rays in the space of the $d = 12$ variables of the (tropicalised) web-parameterisation we reviewed in section 4.1.2: One needs to simply express the Plücker coordinates in terms of the d web-parameters, and solve for the latter after equating the former to the value of the D-dimensional rays.

In this fashion, we find that out of the 19,395 $\widetilde{\mathrm{Tr}}_+(4,9)$ rays, a total of 3,429 is contained in the partially tropicalised, totally positive configuration space $\widetilde{\mathrm{pTr}}_+(4,9)$. We have already seen that 3,078 of these rays are associated to $\mathcal{A}$-variables in the truncated cluster algebra thus corresponding to rational letters. Next, we scan the cluster algebra of $\mathrm{Gr}(4,9)$ truncated by $\widetilde{\mathrm{pTr}}_+(4,9)$ and identify a total of 549,180 origin clusters, from which we obtain the limit rays by numerically evaluating eq. (3.35) for a sufficient number of mutations along the infinite sequence. This yields another 324 rays of $\widetilde{\mathrm{pTr}}_+(4,9)$ that are not in the truncated cluster algebra.

After having obtained the limit rays, the next step is to associate two square-root letters to each origin cluster they can arise from, according to eq. (6.16). As already pointed out, the merit of the analysis of $A_1^{(1)}$ sequences with general coefficients, that we carried out for general m in chapter 5, is that we can immediately obtain the square-root letters in question by simply plugging in the $\mathcal{X}$-coordinates of the $A_1^{(1)}$ subalgebra of a given origin cluster in eq. (6.17). It is important to bear in mind, however, that many of these letters are identical, since mutating an origin cluster at a node not connected to the subalgebra will not change the data relevant for the limit. Furthermore, the resulting distinct square-root letters are not all multiplicatively independent, such that not all of them are required to describe the symbol of the amplitude.

To obtain a basis of these letters, we adopt the following approach, which is similar to that of ref. [202]. Given any set of letters, we first express them in terms of 12 independent variables, for example with the help of the web-parameterisation. We then evaluate these variables at some prime values, and find multiplicative relations of numerically evaluated letters by sampling all possible such relations with a fixed total integer power.[13] Having reduced the letters to some smaller set, say of size m, we can verify whether no more relations exist by evaluating the logarithm of the letters at m different evaluation points. In this logarithmic form, multiplicative relations among the letters correspond to integer-coefficient linear relations. Hence, if the rank of the $m\times m$ matrix formed by the evaluations of the letters is maximal, no further relations can exist.

For the case of the square-root letters obtained from $A_1^{(1)}$ sequences, we find that there is a one-to-one correspondence between the radicand of the square-root and the limit ray. This implies that there can only be multiplicative relations among letters obtained from sequences with the same limit ray. In total, we find 2,349 multiplicatively independent

[13] Note that once we find a relation in this numeric evaluation, we can also verify it symbolically.

square-root letters in 36 cyclic (21 dihedral) classes associated to the 324 limit rays. Arranged according to the number of multiplicatively independent sets of letters per ray, or equivalently per radicand, they consist of

- 6 cyclic (3 dihedral) classes of sets of 5 multiplicatively independent letters,
- 8 cyclic (4 dihedral) classes of sets of 6 independent letters,
- 8 cyclic (4 dihedral) classes of sets of 7 independent letters,
- 6 cyclic (4 dihedral) classes of sets of 8 independent letters,
- 2 cyclic (1 dihedral) classes of sets of 9 independent letters,
- 5 cyclic (4 dihedral) classes of sets of 10 independent letters, and
- 1 cyclic (1 dihedral) class of a set of 11 independent letters,

Since the explicit expressions for these letters are quite complicated, we will refrain from quoting them here, and instead provide them in the ancillary file `Gr49AlgebraicAlphabet.m` attached to the `arXiv` submission of [195]. We now briefly comment on some properties of this alphabet.

First of all, comparing the square-root letters presented in this article to those of the two-loop nine-particle NMHV amplitude reported in [75], we find that the 9×11 letters put forward in the aforementioned reference precisely correspond to the last cyclic class of 11 multiplicatively independent letters of our proposed non-rational alphabet. Together with a similar analysis we carried out in the previous section for the rational letters, this implies that we obtain the entire two-loop nine-particle (N)MHV alphabet as part of our approach, which thus passes a quite nontrivial consistency check.

Furthermore, as can be seen from the above presentation of the square-root letters, the alphabet is invariant under the dihedral transformations. The dihedral flip transformation maps a cyclic class with a given number of multiplicatively independent letters to another class of the same size, whereas the letters obtained from ϕ_0, eq. (6.16), get mapped to those obtained from $\tilde{\phi}_0$ and vice versa.

Let us also comment on the structure of square roots appearing in our algebraic letters. We can rewrite ϕ_0 and $\tilde{\phi}_0$ into the form of $(a_i \pm \sqrt{a_i^2 - 4b_i})/2$. As we saw in section 6.2, in the case of eight-particle amplitudes the radicand $\Delta = a_i^2 - 4b_i \equiv K_1^2 - 4K_2$ is always proportional to one of the square-roots of the eight-point four-mass boxes $\Delta_{1,3,5,7}$ and $\Delta_{2,4,6,8}$, see in particular eqs. (5.2) and (5.3), and e.g. [74] for more details on the four-mass boxes. However, in the non-rational alphabet for nine-particle amplitudes suggested here, we find that only the radicands of the last cyclic class of 11 independent letters each are proportional to the square-roots of the nine-point four-mass boxes, $\Delta_{1,3,5,7}$ and its cyclic permutations (a total of nine), which are the square-root singularities obtained from the Landau analysis at two loops [212]. For example, we also find square-root letters whose radicand is given by

$$\Delta \propto A^2 - 4B\,, \quad \text{with} \tag{6.31}$$

$$A = 1 - \frac{\langle 6789\rangle \langle 13\,(278)\cap(246)\rangle^2}{\langle 1235\rangle \langle 1289\rangle \langle 3567\rangle \langle 1679\rangle^2} + \frac{\langle 1267\rangle \langle 23\,(146)\cap(178)\rangle \langle 46\,(278)\cap(129)\rangle}{\langle 1235\rangle \langle 1289\rangle \langle 3567\rangle \langle 1679\rangle^2}\,, \tag{6.32}$$

$$B = \frac{\langle 1267\rangle \langle 23\,(146)\cap(178)\rangle \langle 46\,(278)\cap(129)\rangle}{\langle 1235\rangle \langle 1289\rangle \langle 3567\rangle \langle 1679\rangle^2}\,, \tag{6.33}$$

which is not proportional to one of the four-mass boxes. Attributing the additional square roots we find to particular integrals is a very interesting question we leave for future work.

As a further check of the nine-particle singularities we have obtained, the Landau equations also predict that the branch points $b_i = 0$ correspond to the zero loci of some rational letters. And indeed, we confirm that this holds for all the square-root letters of our candidate non-rational alphabet for nine-particle scattering. In fact, this is a general property for all square-root letters obtained by the prescription of eq. (6.16), independent of the particle number n, as we now show. Rewriting these in the form discussed in the previous paragraph, we obtain $b_1 = -x_{1;0}$ for ϕ_0 and $b_2 = -x_{1;0}^2 x_{2;0}$ for $\tilde{\phi}_0$, whereas $x_{1;0}, x_{2;0}$ are the $\mathcal{X}$-variables corresponding to the $A_1^{(1)}$ cluster subalgebra in the origin clusters. Since the $\mathcal{X}$-variables are monomials in the cluster $\mathcal{A}$-variables, the branch points $b_i = 0$ of all square-root letters are the zero loci of some letters from the rational alphabet.

To summarise, we have obtained 3,078 rational and 2,349 square-root letters. Whereas the rational letters are in one-to-one correspondence to tropical rays of $\widetilde{\mathrm{pTr}}_+(4,9)$, the square-root letters are associated to a total of 324 tropical rays, in sets containing between 5 and 11 letters per ray. This is very similar to the eight-particle case, where 9 square-root letters are associated to each of the two limit rays.

A great qualitative difference between the eight- and the nine-particle case is that we no longer obtain all tropical rays of $\widetilde{\mathrm{pTr}}_+(4,9)$ from the Grassmannian cluster algebra by selection or an $A_1^{(1)}$ mutation sequence: In particular we can access 3,402 out of the 3,429 such rays in this manner, so we fall short of 27 $\widetilde{\mathrm{pTr}}_+(4,9)$ rays. Given the great jump in complexity between the $\mathrm{Gr}(4,8)$ and $\mathrm{Gr}(4,9)$ cluster algebras,[14] perhaps the real surprise is not that we cannot access all rays by our method, but that the number of rays we cannot access is so small.

Nevertheless, in the next section we will explore more general infinite mutation sequences of $A_m^{(1)}$ Dynkin type as a possible means for obtaining the missing rays, as well as touch on their implications for amplitude singularities. Before concluding, it's also worth mentioning that in its current state of development, neither the scattering diagram approach [73] that we discussed in detail in subsection 6.2.4 can solve the mystery of the 27 missing rays, as it too relies on infinite mutation sequences starting from within the cluster algebra.

[14] In particular, while the cluster algebras of both $\mathrm{Gr}(4,8)$ and $\mathrm{Gr}(4,9)$ are infinite, the former one is of *finite mutation type*, implying that it consists of only a finite number of different quivers, see e.g. [159, 178].

6.4. Discussions and Outlook

Based on the observation that the symbol letters for the scattering of $n = 6, 7$ particles in planar $\mathcal{N} = 4$ super Yang-Mills theory coincide with the $\mathcal{A}$-variables of the cluster algebras of $\mathrm{Gr}(4, n)$ [118], in this work we have developed and proposed methods to extend this so-called cluster bootstrap programme to eight and more particles.

One of the major obstructions that has prevented the progress towards higher particle numbers was that the cluster algebras of $\mathrm{Gr}(4, n)$ become infinite for $n \geq 8$, whereas evidence suggests that the symbol alphabet consists of only a finite number of letters. In chapter 4, we have proposed that the tropicalisation of the kinematic space of the amplitude, the totally positive tropical configuration space $\widetilde{\mathrm{Tr}}_+(4, n)$, offers a solution. By making use of the property that the fan of $\widetilde{\mathrm{Tr}}_+(4, n)$ is triangulated by the (infinite) cluster fan, one can remove the so-called redundant rays of the latter thus obtaining a finite subset of cluster rays. Being in one-to-one correspondence to the cluster $\mathcal{A}$-variables, this results in a finite subset of these variables, the *truncated cluster algebra*.

As a first application, we have used this relation between tropical geometry and cluster algebras to study the amplitudes of generalised biadjoint scalar theory, which are related to the volume of the tropical configuration space. For the case of $\widetilde{\mathrm{Tr}}(3, 8)$, we have used the triangulation of its fan by the cluster fan to obtain the amplitude with a near-minimal amount of spurious poles.

Further to the infinity of the cluster algebras at eight and more particles, another obstruction has prevented the application of the cluster bootstrap programme. With all cluster algebras being rational functions by construction, they cannot account for the non-rational letters that are part of for example the eight-particle three-loop MHV [196] or two-loop NMHV amplitude [61]. For this reason, we studied infinite mutation sequences in chapter 5 and demonstrated that in their infinite limit, one does obtain quantities involving square-roots, the so-called *generalised cluster variables*.

Combining these two techniques, we have proposed to construct the alphabet by first removing the infinite redundant triangulations of the tropical by the cluster fan and then, in a way, adding back this infinity in terms of the limits of infinite mutation sequences. As a first check, we have verified that this is consistent with the finite cases of $n = 6, 7$ particles, where the truncated cluster algebra corresponds to the entire, finite cluster algebra of $\mathrm{Gr}(4, n)$, which correspondingly does not contain any infinite mutation sequences.

In section 6.2, we have applied this approach to the scattering of eight particles. Doing so, we were able to construct an alphabet of 290 dual conformally invariant letters, consisting of 272 rational and 18 square-root letters. All existing data from explicit calculations of eight-particle amplitudes or other, alternative approaches is consistent with this alphabet, which however contains letters beyond those already known to appear. It will be very interesting to push the explicit calculations to even higher loops to see whether these letters do actually appear in the amplitudes or whether perhaps another fan instead of the fan of the partially tropicalised totally positive configuration space $\widetilde{\mathrm{pTr}}_+(4, n)$ is more appropriate.

Similar to the eight-particle case, we have extended this approach to the scattering of

nine particles in section 6.3. There, we obtain an alphabet of 5,427 dual conformally invariant letters, 3,078 of which are rational and 2,349 contain square-roots. This jump in the count of numbers compared to the eight-particle case might be explained by the fact that, in contrast to $\mathrm{Gr}(4,8)$, the cluster algebra of $\mathrm{Gr}(4,9)$ is not of finite mutation type, that is it not only contains an infinite number of cluster variables but also an infinite number of inequivalent quivers. For the case of nine-particle scattering, however, the limit rays of the infinite mutation sequences of $A_1^{(1)}$ type did not account for all those tropical rays that are not part of the cluster rays. In fact, a total of 27 rays is missing in this way. In how far these rays are significant or have further square-root letters attached to them is an open questions.

In the remainder of this section, we discuss in how far these results could be extended to even higher particle numbers as well as some of the open questions pertaining the missing rays and further singularities from infinite mutation sequences.

6.4.1. Extrapolating to arbitrary multiplicity

As the approach we have developed in this work in principle applies to any n, let us conclude this chapter with some further general predictions. More precisely, the truncation procedure for selecting a finite subset of $\mathrm{Gr}(4,n)$ cluster variables, as predictions for the rational part of the symbol alphabet, is algorithmic (and similarly for our infinite mutation sequence analysis yielding predictions for the square-root letters). While the constructive determination of this finite subset has to be done separately for each value of n, and its computational complexity increases with n, the initial cluster of $\mathrm{Gr}(4,n)$ will always be selected. Hence the cluster variables it contains, namely the Plücker variables

$$\langle 1234\rangle\,,\langle 123i\rangle\,,\langle 12i-1\,i\rangle\,,\langle 1i-2\,i-1\,i\rangle\,,\langle i-3\,i-2\,i-1\,i\rangle \quad \text{with} \quad 5\leq i\leq n\,, \tag{6.34}$$

as well as their dihedral images (since our truncation procedure respects dihedral symmetry) will always be included in our prediction for the rational part of the symbol of the n-particle amplitude.

Furthermore, the new data point we have achieved with the nine-particle analysis affords us the possibility to also study the maximal Plücker degree of the letters as a function of the multiplicity n: Considering the cluster algebra truncated by $\widetilde{\mathrm{pTr}}_+(4,n)$, we observe that the maximum degree of letters for $n=6,7,8$, and 9 is given by $1,2,3$, and 6 for the same values of n, which interestingly matches the first few values of the sequence

$$d_{\max}(n)=\binom{n-5}{\lfloor\frac{n-5}{2}\rfloor}\,, \tag{6.35}$$

where the brackets denote the binomial coefficient and $\lfloor x\rfloor$ is the floor function. For $\widetilde{\mathrm{Tr}}_+(4,n)$, the same count is $1,2,5$, and 10, which agrees with $(n-6)^2+1$. Given that the subset of $\mathcal{A}$-variables of fixed degree in the infinite cluster algebras of $\mathrm{Gr}(4,n)$ with $n\geq 8$ can be computed by other means [208], knowing the maximal degree of those that are chosen by our tropical selection rule could thus provide a more direct means for their determination also at higher n.

6.4.2. Beyond $A_1^{(1)}$ singularities?

In the previous two sections we have discussed how generalised cluster variables associated to infinite mutation sequences of $A_1^{(1)}$ Dynkin type can be used to obtain a candidate for the square-root letters of the eight- and nine-particle alphabet. The results obtained in this way are in agreement with explicit data from alternative approaches, such as the $\bar{Q}$-equations, as well as the complementary analysis of scattering diagrams, thus lending strong support to this approach. However, in section 5.4, we introduced such generalised cluster variables for sequences of $A_m^{(1)}$ Dynkin type for any m, raising the question whether these variables are of relevance to the algebraic alphabets.

Indeed, scanning the approximately 24 million clusters of the cluster algebra of $\mathrm{Gr}(4,9)$ truncated by $\widetilde{\mathrm{pTr}}_+(4,9)$, we find that they contain cluster subalgebras of type $A_m^{(1)}$ with up to $m = 5$. The limit rays of these sequences, however, are all either part of the 324 limit rays of $A_1^{(1)}$ sequences or no tropical rays at all. Similarly, we find sequences with up to $m = 4$ in the cluster algebra of $\mathrm{Gr}(4,8)$ truncated by $\widetilde{\mathrm{pTr}}_+(4,8)$.

Remarkably, the non-rational letters obtained from the above formulas for $m > 1$ qualitatively differ from those with $m = 1$. For $m = 1$ we observe a one-to-one association of the radicand, $K_1^2 - 4K_2$, to the limit ray of the sequence. Since such non-rational letters with the same radicand can have multiplicative relations among each other, this allows the reduction of the letters associated to any such ray to a smaller, multiplicatively independent set. For $m > 1$, however, this is no longer true, as we observe that these radicands are different for every origin cluster irrespective of the limit ray, implying the multiplicative independence of all such letters. Considering for example just the letters obtained from eqs. (5.53) and (5.54) with $m = 2$ and $i = 0$, one would obtain 2912 additional, multiplicatively independent square-root letters for eight-particle scattering, where all $\widetilde{\mathrm{pTr}}_+(4,8)$ rays have already been determined.

The fact that this large number of additional letters is not encountered in the existing amplitude computations seems to suggest their irrelevance. We stress again that they arise as a generalisation of the prescription of using the generalised cluster variables as defined in 5.12 as letters, which may not be applicable to higher m. Nevertheless, we find it interesting that it is possible to obtain additional algebraic letters in this fashion.

6.4.3. Limitations of infinite mutation sequences and alternatives

Finally, let us turn to the question of the 27 tropical rays of $\widetilde{\mathrm{pTr}}_+(4,9)$ that cannot be accessed from the cluster algebra of $\mathrm{Gr}(4,9)$ truncated by that tropical configuration space. As discussed in section 6.4.2, even when including infinite mutation sequences of $A_m^{(1)}$ type for any m, we cannot access these 27 rays. In addition, we have checked all primitives of period one with rank up to 6[15] and found that they also do not account for these missing rays.

These results are in fact in line with an inherent limitation on accessing all tropical rays from within the cluster algebra, as we will now discuss. For infinite cluster algebras, e.g. for those of the Grassmannians with $k = 4, n \geq 8$, the cluster fan is not complete (see eg. [213,

[15] In the notations of [191], these correspond to the quivers labelled by $P_i^{(2)}$ for $i = 4, 5, 6$ and $P_6^{(3)}$.

Remark 3.2]). This means that the fan does not cover the entire ambient space $\mathbb{R}^d$, with d the rank of the cluster algebra, and thus also cannot triangulate the entire $\widetilde{\mathrm{pTr}}_+(k,n)$. An example for such an infinite cluster algebra of rank two, also considered in [190, 214, 215], is depicted in figure 6.6.

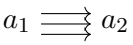

Figure 6.6: Example for an infinite cluster algebra.

The fan of this cluster algebra is two-dimensional with the rays of the initial clusters being the canonical unit vectors. In it, there are two infinite mutation sequences – repeatedly mutating at either the sink or the source of the quiver – which converge to two different rays, as depicted in fig. 6.7. The two-dimensional gap of the fan is also clearly visible in this figure. If a cluster algebra contains such an algebra as a subalgebra, its fan is expected to also be incomplete.

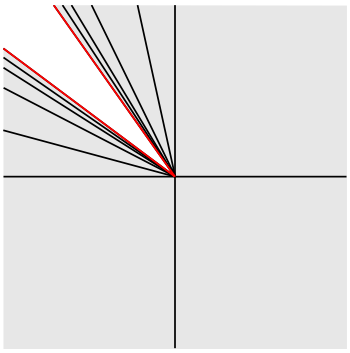

Figure 6.7: Sketch of the fan of the cluster algebra with two nodes connected by three arrows. The cluster algebra is infinite with two infinite sequences approaching the two rays highlighted in red.

In the case of eight particles, the truncated cluster algebra only contains clusters with infinite mutation sequences whose fans leave one-dimensional gaps, which could be taken care of by including the limit ray of the sequence. This is no longer the case for nine particles, since the truncated cluster algebra also contains clusters with nodes connected by three arrows, such as the one depicted in fig. 6.8.

Due to the existence of such clusters, it is expected that the cluster fan for nine particles contains higher-dimensional gaps. This might suggest that (some of) the 27 missing rays are located in the interior of such gaps, explaining why they could not be reached by any limiting procedure from within the cluster algebra. Note that the truncation of these infinite cluster algebras by the selection rule provided by the partially tropicalised positive configuration space creates further gaps in the cluster fans.

Having motivated an explanation for the inaccessibility of certain tropical rays starting from the $\mathrm{Gr}(4,n)$ cluster algebra, some the most important open questions that remain include whether there exist alternative ways for obtaining these rays, that also associate some form of generalised cluster variables to them, and whether the latter provide any

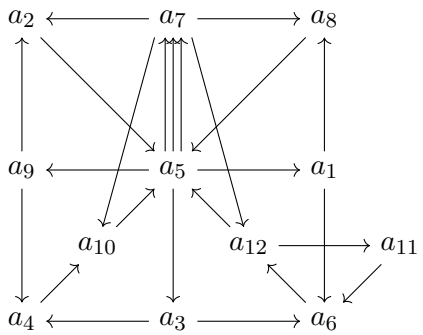

Figure 6.8: Example of a cluster in the truncated cluster algebra of $\mathrm{Gr}(4,9)$ containing nodes connected by three arrows. The $\mathcal{A}$-variables a_i correspond to certain rational nine-particle letters. The frozen variables are omitted in order to avoid clutter.

further information on the singularities of amplitudes. Perhaps the inaccessibility of the missing rays of the cluster algebra is related to the appearance of functions beyond multiple polylogarithms in $\mathcal{N}=4$ pSYM n-particle amplitudes: Indeed, while it is known that such functions certainly appear at $n=10$ [216], the possibility that these in fact also appear at lower n is currently not excluded. If this turns out to be true, then the appropriate generalisation of cluster algebras may go hand in hand with a corresponding generalisation of the notion of symbol letters along the lines of [217]. We leave these exciting questions for future work.

6.4.4. Outlook

Apart from the related articles [70, 72, 185, 186] already mentioned as well as the alternative approaches to obtain the eight- and nine-particle symbol alphabets [61, 75] that we have compared our results against, there exist many more results in the literature that are related to our work. In this final section, we briefly mention some of those other results as well as further progress that has emerged after the publication of our two articles [164, 195].

First, in [185] the authors similarly study the connection between $\mathrm{Gr}(4,n)$ cluster algebras and n-particle scattering amplitudes in planar $\mathcal{N}=4$ super Yang-Mills theory and attempt to solve the two long-standing obstructions of the cluster bootstrap for $n \geq 8$ particles by the virtue of a geometric picture. Without explicitly referring to the tropical Grassmannians $\mathrm{Tr}(4,n)$, they discuss certain compactifications of the positive part of the configuration space $\widetilde{\mathrm{Gr}}_+(4,n)$. Starting with a parameterisation of the Plücker variables in terms of the $\mathcal{X}$-variables of the initial cluster of the $\mathrm{Gr}(k,n)$ cluster algebra, they obtain the polytope $\mathcal{C}(k,n)$ as the Minkowski sum of the Newton polytopes associated to the parameterised Plücker variables. As already discussed in section 6.3.2, the resulting object is essentially combinatorially equivalent to the fan of $\widetilde{\mathrm{Tr}}_+(k,n)$ that we have used to obtain the symbol alphabet and results in an equivalent rational alphabet. Their work is one of the applications of the more general notion of *stringy canonical forms* [218], which are a generalisation of the canonical forms we discussed in section 2.2.2 and are proposed

to connect many aspects of scattering amplitudes that previously were disconnected, such as the scattering equations with tree-level string amplitudes.

In a similar way, our results are also reproduced by an analysis based on so-called *plabic graphs* [198]. These are planar bi-colored graphs that encode the combinatorial structure of the totally positive Grassmannian $\mathrm{Gr}_+(k,n)$. The 18 square-root letters of eight-particle scattering that result as the limits of infinite mutation sequences in the truncated $\mathrm{Gr}(4,8)$ cluster algebra can be shown to also correspond to the solutions of polyonomial equations associated to certain such plabic graphs. More recently, this approach has been generalised to also produce the rational letters [200] as well as the letters of nine-particle scattering [201]. However, since the solution space includes all cluster variables of $\mathrm{Gr}(4,8)$, a selection rule such as the one proposed in here is required to make proper predictions for the actual symbol alphabet.

Another, alternative geometric approach to obtain the symbol letters from the so-called *Schubert problems* has been proposed in [219]. The Schubert problem is naturally encountered in the calculation of the leading singularity of the four-mass one-loop scalar box integral in momentum twistor space [74, 220] and amounts to finding intersecting lines of momentum twistors in generic positions. Restricting to the positive Grassmannian $\mathrm{Gr}_+(k,n)$ it was found that certain cross-ratios of such intersections correspond to the symbol letters of the corresponding Feynman integrals. A noteworthy feature of this result is that it not only reproduces the 18 square-root letters of eight-particle scattering but also finds a new kind of algebraic letter for $n \geq 9$ consisting of two distinct square roots, which is expected to appear as a symbol letter of planar $\mathcal{N}=4$ super Yang-Mills amplitudes as well. It would be very interesting to compare this to the results from our predictions.

In another direction, the applicability of cluster algebras to Feynman integrals has recently been studied in [203]. Without relying on additional symmetries, such as those of $\mathcal{N}=4$ sYM, the authors discuss applications of cluster algebras to generic four-dimensional Feynman integrals in dimensional regularization and show that an important class of polylogarithms is related to the C_2 cluster algebra. Furthermore, they identify adjacency restrictions equivalent to the extended Steinmann relations we discussed in section 2.3.4. These results could potentially allow to apply bootstrap methods to a number of phenomenologically interesting scattering processes. More recent work along this line includes [221], where the authors additionally identified cluster algebras of D_4, D_5, and D_6 Dynkin type as subalgebras of the truncated cluster algebra of $\mathrm{Gr}(4,n)$ for various six-particle kinematics and $n=7,8,9$. In [222] this was further extended to planar kinematics of conformal Feynman integrals in four dimensions.

The abundance of alternative and related approaches to obtain the symbol alphabet of amplitudes in planar $\mathcal{N}=4$ super Yang-Mills theory shows that the debate is far from settled. Furthermore, the application of the methods developed in this environment to cases much more closely aligned to physically observable amplitudes demonstrates the huge potential that can be unlocked by studying this theory and its previously hidden mathematical structures.

A. Proofs for mutation sequences of type $A_m^{(1)}$

In this appendix we present the calculations and proofs required for the solution to the infinite mutation sequences of type $A_m^{(1)}$ that have been omitted in the main text. We first discuss the source direction, that is the sequence obtained by repeatedly mutating $a_{1;j}$. To avoid repetition, we often point to the relevant formulas in the main text. Finally, we turn to the sink direction, the repeated mutation of $a_{m+1;j}$.

A.1. Limit of γ_j

Having established the invariance of K_1 and K_2, we now turn to the limit of γ_j and prove that it converges to 1. In order to deal with the cluster-tropical addition, let us remind ourselves how the coefficients are related to the frozen variables. We consider the rank-$(m+1)$ cluster algebra of type $A_m^{(1)}$ with M frozen variables denoted by z_i for $i = 1, \ldots, M$. In any cluster, the coefficients are given as a monomial in the frozen variables, see eq. (3.17) and the mutation rule eq. (3.20), which demonstrates that this property holds in all clusters. We thus rewrite the coefficients as

$$y_j = \prod_{i=1}^{M} z_i^{c_j^i} . \tag{A.1}$$

Using that cluster-tropical addition, eq. (3.15), is defined on such monomials in the frozen variables, we rewrite the recursion relation of $y_{1;j}$, eqs. (5.7), in terms of the new sequences c_j^i. For this, consider first that

$$y_{1;j+1} = \frac{y_{1;j} y_{2;j}}{\left(1 \hat{\oplus} y_{1;j}\right)} = \frac{y_{1;j} y_{1;j-m+1}}{y_{1;j-m} \left(1 \hat{\oplus} y_{1;j}\right) \left(1 \hat{\oplus} y_{1;j-m+1}\right)} , \tag{A.2}$$

whereas we have used the equivalent of eq. (5.19) for the coefficients. This implies that the corresponding relation for the c_j^i is given by

$$c_{j+1}^i = c_j^i + c_{j-m+1}^i - c_{j-m}^i - \min\left(0, c_j^i\right) - \min\left(0, c_{j-m+1}^i\right) \tag{A.3}$$

Using the notation $[x]_+ = \max(0, x) = -\min(0, -x)$ and $x = [x]_+ - [-x]_+$, this results in the recursion relation

$$c_{j+1}^i + c_{j-m}^i = \left[c_j^i\right] + \left[c_{j-m+1}^i\right]_+ . \tag{A.4}$$

While the appearance of $[x]_+$ on the right hand side of this recurrence makes solving it analytically complicated, we can prove the following property of this sequence.

Lemma A.1. *Fix $m \in \mathbb{N}_{>0}$ and consider the sequence c_n for $n \geq 1$ with initial values $c_1, \ldots, c_{m+1} \in \mathbb{Z}$ and recurrence relation*

$$c_{n+1} + c_{n-m} = [c_n] + [c_{n-m+1}]_+ \,. \tag{A.5}$$

There exists a $N \in \mathbb{N}$ such that for all $n \geq N$

$$c_n \geq c_{n-m} \geq 0\,. \tag{A.6}$$

Proof. To prove the lemma, we introduce an auxiliary sequence Δ_n defined by

$$\Delta_n = c_n - c_{n-m}\,. \tag{A.7}$$

By continuing the recurrence for c_n to $n \leq 0$, we can use this definition for all $n \geq 1$. We now establish some key properties of these sequences.

Positivity/Negativity. Assume there exists a $N \in \mathbb{N}$ such that $\Delta_n \geq 1$ for all $n \geq N$. By construction, we can write $c_n = \Delta_n + c_{n-m}$ for any n and thus get for any $j \geq 0$ and $i = 0, \ldots, m-1$ that

$$c_{N+j\cdot m+i} = \sum_{l=1}^{j} \Delta_{N+l\cdot m+i} + c_{N+i} \geq j + c_{N+i}\,. \tag{A.8}$$

Note that we have included the shift by i because $N + j \cdot m + i = n$ for any $n \geq N$ and appropriate choice of i and j. Hence, for $j \geq \max(0, -c_{N+i})$ we conclude that $c_{N+j\cdot m+i} \geq 0$. To summarize, this implies that if there is a $N \in \mathbb{N}$ such that $\Delta_n \geq 1$ for all $n \geq N$, then

$$c_n \geq 0\,, \quad \forall n \geq \max_{i=0,\ldots,m-1} \{N + \max(0, -c_{N+i}) \cdot m + i\}\,. \tag{A.9}$$

If we instead assume that there exists a $N \in \mathbb{N}$ such that $\Delta_n \leq -1$ for all $n \leq N$, we get by the same reasoning as before that

$$c_n < 0\,, \quad \forall n \geq \max_{i=0,\ldots,m-1} \{N + \max(0, 1 + c_{N+i}) \cdot m + i\}\,. \tag{A.10}$$

Monotonicity. From the recursion relation of c_n, eq. (A.5), we obtain a corresponding relation for the sequence Δ_n, which is given by

$$\Delta_{n+1} = \Delta_n + [-c_n]_+ + [-c_{n-m+1}]\,, \tag{A.11}$$

whereas we used $x = [x]_+ - [-x]_+$ to arrive at this result. Since $[x]_+ \geq 0$, this relation implies that

$$\Delta_{n+1} \geq \Delta_n\,, \tag{A.12}$$

that is, Δ_n is a monotonically increasing sequence. Further to that, the relation for Δ_{n+1} also gives us the following *extended monotonicity property*

$$\Delta_{n+1} = \Delta_n \iff c_n \geq 0 \wedge c_{n-m+1} \geq 0\,, \tag{A.13}$$

which follows because $[-x]_+$ is positive and zero if and only if x is positive.

Boundedness. We now prove that Δ_n is bounded. For this, assume Δ_n to not be bounded. Since Δ_n is a monotonically increasing sequence, this implies that there exists some $N \in \mathbb{N}$ such that $\Delta_n \geq 1$ for all $n \geq N$. Hence, due to the positivity property proven above, this implies that there also exists some $N' \in \mathbb{N}$ such that $c_n \geq 0$ for all $n \geq N'$. Thus, by the extended monoticity property, eq. (A.13), this also implies that $\Delta_{n+1} = \Delta_n$ for all $n \geq N'$, which is a contradiction to the assumption of Δ_n to not be bounded.

Convergence. Since Δ_n is monotonically increasing and bounded, it converges to some constant K. Because $c_1, \ldots, c_{m+1} \in \mathbb{Z}$ we also have $c_n \in \mathbb{Z}$ and thus $\Delta_n \in \mathbb{Z}$ for all n, such that $K \in \mathbb{Z}$ and, together with monotonicity, $\Delta_n = \Delta_N \equiv K$ for all $n \geq N$ and some $N \in \mathbb{N}$. This implies that $\Delta_N \geq 0$. To see why, assume the opposite. Since $\Delta_n \in \mathbb{Z}$, this means we assume $\Delta_n \leq -1$. By the negativity property, this would imply that $c_n < 0$ for all $n \geq N'$ and some $N' \in \mathbb{N}$. However, by the extended monotonicity property, we also have $c_n \geq 0$ for all $n \geq N$, which is a contradiction.

Summary. Taking all this together, we see from the convergence property that there exists a $N \in \mathbb{N}$ such that $\Delta_n = \Delta_N \geq 0$ and thus $c_n \geq 0$ for all $n \geq N$ by the extended monotonicity property. Furthermore, since $c_n = \Delta_n + c_{n-m}$, we also see that $c_n \geq c_{n-m} \geq 0$ for all $n \geq N + m$. □

Consider now the consequence of this lemma on the sequence γ_j. Rewriting it in terms of the c_j^i, we get

$$\gamma_j = 1 \hat{\oplus} y_{1;j} \hat{\oplus} y_{1;j} \left(y_{1;j-m}\right)^{-1} = \prod_{i=1}^{M} z_i^{\min\left(0, c_j^i + \min\left(0, -c_{j-m}^i\right)\right)} . \tag{A.14}$$

From the previous lemma, we know that for some $N \in \mathbb{N}$ we have $c_n \geq c_{n-m} \geq 0$ for all $n \geq N$ and thus for $j \geq N$

$$\min\left(0, c_j^i + \min\left(0, -c_{j-m}^i\right)\right) = \min\left(0, c_j^i - c_{j-m}^i\right) = 0 , \tag{A.15}$$

proving that $\gamma_j = 1$ for $j \geq N$ for some $N \in \mathbb{N}$.

A.2. The sink direction

In the previous section and the main text, we have analysed the infinite mutation sequence obtained by repeatedly mutating $a_{1;j}$ in the $A_m^{(1)}$ cluster algebra. However, this corresponds to only one of the two possible directions. As discussed before, the mutation of the sink-variable $a_{m+1;j+1}$ is the inverse to the mutation of $a_{1;j}$ and thus takes us from cluster $j+1$ to j along the sequence, ie. the opposite direction. We now discuss its solution.

First of all, note that using the mutation relations (5.9) we can rephrase the linearised recursion relation (5.29) in terms of the sink variable as

$$\gamma_{j+m}^{-1} \gamma_{j+2m}^{-1} a_{m+1;j+2m} - \gamma_0^{-1} \beta_0 K_1 \cdot \gamma_{j+m}^{-1} a_{m+1;j+m} + \gamma_0^{-2} \beta_0^2 K_2 \cdot a_{m+1;j} = 0 . \tag{A.16}$$

Since all relations required to arrive at this equation are valid for all $j \in \mathbb{N}$, so is this recurrence. In theory, we could now go on and apply the same techniques as for the source

direction to solve this. However, we now have to consider the limit $j \to -\infty$, since the sink direction takes cluster $j+1$ to j. Accordingly, we define the new variable $\tilde{\alpha}_j$ via

$$\tilde{\alpha}_j = \gamma_{-(j \bmod m)}\gamma_{-(j \bmod m)-m} \cdots \gamma_{-j+2m}\gamma_{-j+m} \cdot a_{m+1;-j}\,, \tag{A.17}$$

such that for this variable, the limit $j \to \infty$ is the correct one to consider. In terms of this sequence, the recurrence (5.31) can be expressed as

$$\gamma_0^{-2}\beta_0^2 K_2 \cdot \tilde{\alpha}_{j+2m} - \gamma_0^{-1}\beta_0 K_1 \cdot \tilde{\alpha}_{j+m} + \tilde{\alpha}_j = 0\,, \tag{A.18}$$

with the initial values $\tilde{\alpha}_0, \ldots, \tilde{\alpha}_{2m-1}$.

Before we obtain the solution of this recurrence via its characteristic polynomial, let us first discuss γ_{-j} and its limit as j goes to infinity. This sequence is again governed by eq. (A.4), and is given in terms of the variable $d_n = c_{-n}$, which describes γ_{-j}, by

$$d_{n-1} + d_{n+m} = [d_n]_+ + [d_{n+m-1}]_+\,. \tag{A.19}$$

Since this holds for all n, we may shift the index by $n' = n+m-1$, which, due to the symmetry, reduces this equation to the original form of eq. (A.4). Hence, we may apply lemma A.1 to this case as well, proving that $\gamma_{-j} = 1$ for $j \geq J$ for some $J \in \mathbb{N}$.

The characteristic polynomial of the recurrence (A.18) is given by

$$\tilde{P}_m(t) = t^{2m} - \gamma_0\beta_0^{-1}\frac{K_1}{K_2} \cdot t^m + \gamma_0^2\beta_0^{-2}K_2^{-1}\,. \tag{A.20}$$

Its roots are given by $\tilde{\beta}_\pm^{1/m}\eta_m^i$ for $i = 0, \ldots, m-1$, with η_m again being the m-th root of unity and whereas

$$\tilde{\beta}_\pm = \gamma_0 \frac{K_1 \pm \sqrt{K_1^2 - 4K_2}}{2\beta_0 K_2}\,. \tag{A.21}$$

Note that we have $\tilde{\beta}_\pm = \beta_\mp^{-1}$. Similar to before, we may use the roots to write down the most general solution for $\tilde{\alpha}_j$ and thus get

$$\tilde{\alpha}_j = \left[\tilde{c}_0^+ + \tilde{c}_1^+\eta_m^j + \cdots + \tilde{c}_{m-1}^+\eta_m^{(m-1)j}\right](\beta_-)^{-\frac{j}{m}} + \left[\tilde{c}_0^- + \tilde{c}_1^-\eta_m^j + \cdots + \tilde{c}_{m-1}^-\eta_m^{(m-1)j}\right](\beta_+)^{-\frac{j}{m}}\,, \tag{A.22}$$

whereas we have expressed this in terms of $\beta_\pm$ but have labelled the coefficients $\tilde{c}_i^\pm$ in terms of $\tilde{\beta}_\pm$. The same analysis as before applies to the overall coefficients $\tilde{C}_\pm(j)$, which again can be obtained from the initial conditions. For this direction they are given by

$$\tilde{\alpha}_i = a_{m+1-i;0}\,, \quad \tilde{\alpha}_{m+i} = a_{m+1-i;0} \cdot \gamma_0\beta_0^{-1}\tilde{F}_i\,, \tag{A.23}$$

whereas the $\tilde{F}_i$ are now given by

$$\tilde{F}_i = K_{m+1-i}/K_{m+1}\,. \tag{A.24}$$

With these initial conditions, we again obtain a system of two linear equations from the general solution, eq. (A.22), which we can solve in terms of the $\tilde{C}_\pm(i)$, resulting in

$$\tilde{C}_\pm(i) = a_{m+1-i}\,(\beta_\mp)^{i/m}\,\frac{\pm 2K_2F_i \mp K_1 + \sqrt{K_1^2 - 4K_2}}{2\sqrt{K_1^2 - 4K_2}}\,. \tag{A.25}$$

Using the definition $\tilde{\phi} = \tilde{C}_+/\tilde{C}_-$ this proves eq. (5.54) for the non-rational expressions associated to this sequence.

Having obtained the general solution for the infinite mutation sequence of type $A_m^{(1)}$ in the sink direction, it remains to prove the initial conditions, eqs. (A.23). The first follows directly from $\tilde{\alpha}_i = a_{m+1;-i} = a_{m+1-i;0}$, as can be seen from eq. (5.9). For the other condition, we first observe that $\tilde{\alpha}_{m+i} = \gamma_{-i} a_{m+1;-i-m}$ and hence by eq. (5.9) that $\tilde{\alpha}_{m+i} = \gamma_{-i}\beta_{-i}^{-1} \cdot a_{m+1;-i} = \gamma_{-i}\beta_{-i}^{-1} \cdot a_{m+1-i;0}$. For $i = 0$ we can immediately conclude that $\tilde{F}_i = 1$. For $i \geq 1$, by again using the relation $\gamma_{j+1}^{-1}\beta_{j+1} = (1 + x_{1;j})\gamma_j^{-1}\beta_j$, we arrive at

$$\tilde{\alpha}_{m+i} = a_{m+1-i;0}\gamma_0\beta_0^{-1}\,(1 + x_{1;-i}) \cdots (1 + x_{1;-1}) \tag{A.26}$$

$$= a_{m+1-i;0}\gamma_0\beta_0^{-1}\,\frac{(1 + x_{m+1;1-i}) \cdots (1 + x_{m+1;0})}{x_{m+1;1-i} \cdots x_{m+1;0}}\,, \tag{A.27}$$

whereas we have used eq. (5.22) for the last step. This already proves eq. (A.23), with $\tilde{F}_i$ being the fraction of the $\mathcal{X}$-variables. To obtain an expression in terms of the variables of the initial cluster, we note that $x_{m+1;j-i} = x_{m+j-i;0}\,(1 + x_{m+1;j-i+1})$ such that we get

$$\tilde{F}_i = \prod_{j=0}^{i-1} (x_{m+1-j;0})^{-1} \cdot (1 + x_{m+1;1-i})\,. \tag{A.28}$$

Similar to eq. (5.25), we obtain from the mutation relations, eq. (5.22), that

$$1 + x_{m+1;1-i} = \prod_{j=i}^{m} (x_{m+1-j;0})^{-1} \cdot K_{m+1-i}\,, \tag{A.29}$$

such that we can conclude that

$$\tilde{F}_i = \frac{K_{m+1-i}}{K_{m+1}}\,, \tag{A.30}$$

completing our analysis of the infinite mutation sequences in cluster algebras of type $A_m^{(1)}$.

B. Non-rational alphabet of eight-particle scattering

In this section, for completeness, we present the entire non-rational alphabet of eight-particle scattering obtained from the perspective of scattering diagrams, see [73] or section 6.2.4. We begin with the initial cluster of the cluster algebra of $\mathrm{Gr}(4,8)$, which is depicted in figure B.1. In there, we included our convention for the unfrozen variables a_i^I of this cluster.

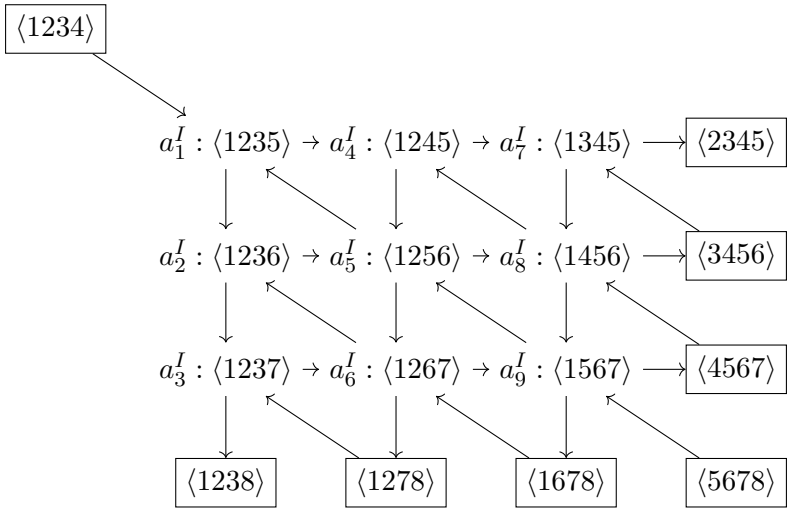

Figure B.1: Initial seed of the cluster algebra of $\mathrm{Gr}(4,8)$.

We can use eqs. (3.17) and (3.18) to immediately read off the $\mathcal{X}$-variables associated to each $\mathcal{A}$-variable. They are given by

$$x_1^I = \frac{\langle 1234\rangle\langle 1256\rangle}{\langle 1245\rangle\langle 1236\rangle}, \quad x_4^I = \frac{\langle 1235\rangle\langle 1456\rangle}{\langle 1345\rangle\langle 1256\rangle}, \quad x_7^I = \frac{\langle 1245\rangle\langle 3456\rangle}{\langle 2345\rangle\langle 1456\rangle}, \tag{B.1}$$

$$x_2^I = \frac{\langle 1235\rangle\langle 1267\rangle}{\langle 1256\rangle\langle 1237\rangle}, \quad x_5^I = \frac{\langle 1236\rangle\langle 1245\rangle\langle 1567\rangle}{\langle 1235\rangle\langle 1456\rangle\langle 1267\rangle}, \quad x_8^I = \frac{\langle 1256\rangle\langle 1345\rangle\langle 4567\rangle}{\langle 1245\rangle\langle 3456\rangle\langle 1567\rangle}, \tag{B.2}$$

$$x_3^I = \frac{\langle 1236\rangle\langle 1278\rangle}{\langle 1267\rangle\langle 1238\rangle}, \quad x_6^I = \frac{\langle 1237\rangle\langle 1256\rangle\langle 1678\rangle}{\langle 1236\rangle\langle 1567\rangle\langle 1278\rangle}, \quad x_9^I = \frac{\langle 1267\rangle\langle 1456\rangle\langle 5678\rangle}{\langle 1256\rangle\langle 4567\rangle\langle 1678\rangle}. \tag{B.3}$$

Mutating along the mutation sequence $\{1,2,4,1,6,8\}$, that is sequentially mutating the nodes with the corresponding index, we arrive at the $A_1^{(1)}$ origin quiver depicted in figure B.2. Note that since we only require the $\mathcal{X}$-coordinates for the computation of the non-rational alphabet, in the quiver we only show those, labelled by x_i in the origin quiver, and omit the (frozen and unfrozen) $\mathcal{A}$-variables.

Performing the sequence of mutations given above, we land in the origin quiver whose $\mathcal{X}$-variables x_i are rational functions in the original variables x_i^I of the initial cluster. These functions are given by

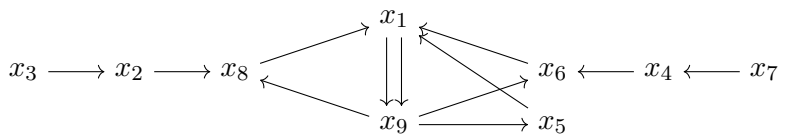

Figure B.2: Principal part of the origin cluster in $\mathrm{Gr}(4,8)$ utilized to find the square-root letters.

$$x_1 = \frac{\left(1+x_6^I+x_1^I\left(1+x_4^I\right)\left(1+x_6^I\left(1+x_2^I\right)\right)\right)\left(1+x_8^I+x_1^I\left(1+x_2^I\right)\left(1+x_8^I\left(1+x_4^I\right)\right)\right)}{x_1^I x_2^I x_4^I}\,, \tag{B.4}$$

$$x_9 = \frac{\left(1+x_1^I\left(1+x_2^I\right)\left(1+x_4^I\right)\right)x_6^I x_8^I x_9^I}{\left(1+x_6^I+x_1^I\left(1+x_4^I\right)\left(1+x_6^I\left(1+x_2^I\right)\right)\right)\left(1+x_8^I+x_1^I\left(1+x_2^I\right)\left(1+x_8^I\left(1+x_4^I\right)\right)\right)}\,, \tag{B.5}$$

$$x_5 = \frac{x_1^I x_2^I x_4^I x_5^I}{1+x_1^I\left(1+x_2^I\right)\left(1+x_4^I\right)}\,, \tag{B.6}$$

$$x_8 = \frac{1+x_1^I\left(1+x_2^I\right)}{x_8^I\left(1+x_1^I\left(1+x_2^I\right)\left(1+x_4^I\right)\right)}\,, \tag{B.7}$$

$$x_6 = \frac{1+x_1^I\left(1+x_4^I\right)}{x_6^I\left(1+x_1^I\left(1+x_2^I\right)\left(1+x_4^I\right)\right)}\,, \tag{B.8}$$

$$x_2 = \frac{x_4^I x_8^I}{1+x_8^I+x_1^I\left(1+x_2^I\right)\left(1+x_8^I\left(1+x_4^I\right)\right)}\,, \tag{B.9}$$

$$x_4 = \frac{x_2^I x_6^I}{1+x_6^I+x_1^I\left(1+x_4^I\right)\left(1+x_6^I\left(1+x_2^I\right)\right)}\,, \tag{B.10}$$

$$x_3 = \frac{x_1^I x_2^I x_3^I}{1+x_1^I\left(1+x_2^I\right)}\,, \tag{B.11}$$

$$x_7 = \frac{x_1^I x_4^I x_7^I}{1+x_1^I\left(1+x_4^I\right)}\,. \tag{B.12}$$

As is discussed in section 6.2.4 and [73], from this origin quiver we perform the limit of the infinite $A_1^{(1)}$ mutation sequence. Working within the framework of scattering diagrams, we first construct the cone variables and take their limit, which is well-defined and finite, so that we land in an asymptotic chamber around the limit ray[1]

$$r_\infty = (1,-1,0,-1,0,1,0,1,-1)\,. \tag{B.13}$$

[1]This is one of the two tropical rays of $\widetilde{\mathrm{pTr}}_+(4,8)$ that is not contained in the fan of the truncated cluster algebra, the other being $(0,1,0,1,0,-1,0,-1,0)$. Since the variables obtained from this limit ray can be obtained by a cyclic shift $\langle ijkl\rangle \to \langle i+1\, j+1\, k+1\, l+1\rangle$ we limit our analysis to the quantities around the first limit ray only.

The limits of the cone variables along the sequence, ie. the cone variables of the asymptotic chamber, can be

$$x^0_{\gamma_i} = x_i \quad \text{for} \quad i \in \{2,3,4,7\}\,, \tag{B.14}$$

$$x^0_{\gamma_i} = \frac{x_i}{2}\left(1 + x_1\,(1+x_9) + \sqrt{\Delta'}\right) \quad \text{for} \quad i \in \{5,6,8\}\,, \tag{B.15}$$

$$x^0_{\gamma_1} = \frac{4x_1\Delta'}{\left(1+x_1-x_1x_9+\sqrt{\Delta'}\right)^2}\,, \quad x^0_{\gamma_9} = \frac{x_9}{4}\left(1+\frac{1-x_1(1+x_9)}{\sqrt{\Delta'}}\right)^2\,, \tag{B.16}$$

$$\Delta' = (1+x_1(1+x_9))^2 - 4x_1x_9\,. \tag{B.17}$$

The entire non-rational alphabet is obtained from the variables of *all* asymptotic chambers around the limit ray. As is outlined in [73], a computer search yields a basis of 36 multiplicatively independent polynomials. It consists of the 20 polynomials given by

$$\tilde{f}_1 = x^0_{\gamma_1}\,, \quad \tilde{f}_2 = x^0_{\gamma_9}\,, \quad \tilde{f}_3 = 1 - x^0_{\gamma_1}x^0_{\gamma_9}\,, \tag{B.18}$$

$$\tilde{f}_4 = x^0_{\gamma_5}\,, \quad \tilde{f}_5 = 1 + x^0_{\gamma_5}\,, \quad \tilde{f}_6 = 1 + x^0_{\gamma_5}x^0_{\gamma_1}x^0_{\gamma_9}\,, \tag{B.19}$$

$$\tilde{f}_7 = x^0_{\gamma_8}\,, \tag{B.20}$$

$$\tilde{f}_8 = 1 + x^0_{\gamma_8}\,, \quad \tilde{f}_9 = 1 + x^0_{\gamma_2}\tilde{f}_8\,, \quad \tilde{f}_{10} = 1 + x^0_{\gamma_3}\tilde{f}_9\,, \tag{B.21}$$

$$\tilde{f}_{11} = 1 + x^0_{\gamma_8}x^0_{\gamma_1}x^0_{\gamma_9}\,, \quad \tilde{f}_{12} = 1 + x^0_{\gamma_2}\tilde{f}_{11}\,, \quad \tilde{f}_{13} = 1 + x^0_{\gamma_3}\tilde{f}_{12}\,, \tag{B.22}$$

$$\tilde{f}_{14} = x^0_{\gamma_6}\,, \tag{B.23}$$

$$\tilde{f}_{15} = 1 + x^0_{\gamma_6}\,, \quad \tilde{f}_{16} = 1 + x^0_{\gamma_4}\tilde{f}_{15}\,, \quad \tilde{f}_{17} = 1 + x^0_{\gamma_7}\tilde{f}_{16}\,, \tag{B.24}$$

$$\tilde{f}_{18} = 1 + x^0_{\gamma_6}x^0_{\gamma_1}x^0_{\gamma_9}\,, \quad \tilde{f}_{19} = 1 + x^0_{\gamma_4}\tilde{f}_{18}\,, \quad \tilde{f}_{20} = 1 + x^0_{\gamma_7}\tilde{f}_{19}\,. \tag{B.25}$$

as well as 16 more polynomials given by

$$\tilde{f}_{21} = x^0_{\gamma_2}\,, \quad \tilde{f}_{22} = x^0_{\gamma_3}\,, \tag{B.26}$$

$$\tilde{f}_{23} = 1 + x^0_{\gamma_2}\,, \quad \tilde{f}_{24} = 1 + x^0_{\gamma_3}\,, \tag{B.27}$$

$$\tilde{f}_{25} = 1 + x^0_{\gamma_3}\tilde{f}_{23}\,, \quad \tilde{f}_{26} = 1 + x^0_{\gamma_2}\tilde{f}_8\tilde{f}_{11}\,, \quad \tilde{f}_{27} = 1 + x^0_{\gamma_3}\tilde{f}_{26}\,, \tag{B.28}$$

$$\tilde{f}_{28} = 1 + x^0_{\gamma_2}\tilde{f}_{27} + x^0_{\gamma_3}\left(1 + x^0_{\gamma_2}\left(\tilde{f}_7 + \tilde{f}_{11}\right)\right)\,, \tag{B.29}$$

$$\tilde{f}_{29} = x^0_{\gamma_4}\,, \quad \tilde{f}_{30} = x^0_{\gamma_7}\,, \tag{B.30}$$

$$\tilde{f}_{31} = 1 + x^0_{\gamma_4}\,, \quad \tilde{f}_{32} = 1 + x^0_{\gamma_7}\,, \tag{B.31}$$

$$\tilde{f}_{33} = 1 + x^0_{\gamma_7}\tilde{f}_{31}\,, \quad \tilde{f}_{34} = 1 + x^0_{\gamma_4}\tilde{f}_{15}\tilde{f}_{18}\,, \quad \tilde{f}_{35} = 1 + x^0_{\gamma_7}\tilde{f}_{34}\,, \tag{B.32}$$

$$\tilde{f}_{36} = 1 + x^0_{\gamma_4}\tilde{f}_{35} + x^0_{\gamma_7}\left(1 + x^0_{\gamma_4}\left(\tilde{f}_{14} + \tilde{f}_{18}\right)\right)\,. \tag{B.33}$$

As can be seen from eq. (B.14) and eqs. (B.4)–(B.12), the variables $x^0_{\gamma_i}$ are rational for $i \in \{2,3,4,7\}$ and hence so are 10 of the polynomials of the above basis. In fact, by parameterising the Plücker variables in terms of the web-parameterisation and evaluating the web-variables with prime values, it is easy to see that the polynomials $\tilde{f}_{21}$ to $\tilde{f}_{36}$ are rational, that is the square-roots cancel. Even more than that, these 16 polynomials are

actually contained in the 272-letter rational alphabet of [72, 164, 185] and can be expressed as

$$\tilde{f}_{21} = \frac{R_{157}}{R_{163}}\,, \qquad \tilde{f}_{22} = \frac{R_9}{R_2}\,, \qquad \tilde{f}_{23} = \frac{R_2 R_{143}}{R_{163}}\,, \qquad \tilde{f}_{24} = \frac{R_3}{R_2}\,, \tag{B.34}$$

$$\tilde{f}_{25} = \frac{R_{164}}{R_{163}}\,, \qquad \tilde{f}_{26} = \frac{R_2 R_{194}}{R_9 R_{157}}\,, \qquad \tilde{f}_{27} = \frac{R_{192}}{R_{157}}\,, \qquad \tilde{f}_{28} = \frac{R_2 R_{146}}{R_{163}}\,, \tag{B.35}$$

$$\tilde{f}_{29} = \frac{R_{36}}{R_{42}}\,, \qquad \tilde{f}_{30} = \frac{R_{97}}{R_{10}}\,, \qquad \tilde{f}_{31} = \frac{R_{10} R_{34}}{R_{42}}\,, \qquad \tilde{f}_{32} = \frac{R_{43}}{R_{10}}\,, \tag{B.36}$$

$$\tilde{f}_{33} = \frac{R_{44}}{R_{42}}\,, \qquad \tilde{f}_{34} = \frac{R_{10} R_{93}}{R_{36} R_{97}}\,, \qquad \tilde{f}_{35} = \frac{R_{91}}{R_{36}}\,, \qquad \tilde{f}_{36} = \frac{R_{10} R_{89}}{R_{42}}\,, \tag{B.37}$$

whereas R_i refers to the i-th rational letter in the alphabet provided in the attached file `Gr48Alphabet.m` of [195].

Since 16 of these polynomials are contained in the 272-letter rational alphabet, we are left with the 20 letters given by $\tilde{f}_1$ to $\tilde{f}_{20}$. While these 20 letters can be numerically checked to actually contain square-roots, we find 10 multiplicative combinations that are contained in the rational alphabet. They are given by

$$\tilde{f}_1 \tilde{f}_2 \tilde{f}_4^2 = \frac{R_{222}}{R_9 R_{97}}\,, \qquad \frac{\tilde{f}_7}{\tilde{f}_4} = \frac{R_2 R_{97}}{R_{157}}\,, \qquad \frac{\tilde{f}_{14}}{\tilde{f}_4} = \frac{R_9 R_{10}}{R_{36}}\,, \tag{B.38}$$

$$\tilde{f}_5 \tilde{f}_6 = \frac{R_4 R_{131}}{R_9 R_{97}}\,, \qquad \tilde{f}_8 \tilde{f}_{11} = \frac{R_{163} R_{197}}{R_9 (R_{157})^2}\,, \qquad \tilde{f}_{15} \tilde{f}_{18} = \frac{R_{42} R_{94}}{(R_{36})^2 R_{97}}\,, \tag{B.39}$$

$$\tilde{f}_9 \tilde{f}_{12} = \frac{(R_2)^2 R_{147}}{R_9 R_{163}}\,, \qquad \tilde{f}_{16} \tilde{f}_{19} = \frac{(R_{10})^2 R_{90}}{R_{42} R_{97}}\,, \tag{B.40}$$

$$\tilde{f}_{10} \tilde{f}_{13} = \frac{R_{196}}{R_{163}}\,, \qquad \tilde{f}_{17} \tilde{f}_{20} = \frac{R_{96}}{R_{42}}\,, \tag{B.41}$$

whereas again R_i corresponds to the i-th rational letter in the rational alphabet. Using these 10 relations, we can further reduce the square-root letters to the basis of 10 multiplicatively independent letters given by

$$\begin{aligned}
f_1 &= \left(x^0_{\gamma_1}\right)^{-1} \left(1 - x^0_{\gamma_1} x^0_{\gamma_9}\right)^2\,, \quad f_2 = x^0_{\gamma_9} \left(1 - x^0_{\gamma_1} x^0_{\gamma_9}\right)^2\,, \qquad f_3 = \frac{1 + x^0_{\gamma_5} x^0_{\gamma_1} x^0_{\gamma_9}}{1 + x^0_{\gamma_5}}\,, \\
f_4 &= \frac{1 + x^0_{\gamma_8} x^0_{\gamma_1} x^0_{\gamma_9}}{1 + x^0_{\gamma_8}}\,, \qquad f_5 = \frac{1 + x^0_{\gamma_2} \left(1 + x^0_{\gamma_8} x^0_{\gamma_1} x^0_{\gamma_9}\right)}{1 + x^0_{\gamma_2} \left(1 + x^0_{\gamma_8}\right)}\,, \\
f_6 &= \frac{1 + x_{\gamma_3} \left(1 + x^0_{\gamma_2} \left(1 + x^0_{\gamma_8} x^0_{\gamma_1} x^0_{\gamma_9}\right)\right)}{1 + x_{\gamma_3} \left(1 + x^0_{\gamma_2} \left(1 + x^0_{\gamma_8}\right)\right)}\,, \\
f_7 &= \frac{1 + x^0_{\gamma_6} x^0_{\gamma_1} x^0_{\gamma_9}}{1 + x^0_{\gamma_6}}\,, \qquad f_8 = \frac{1 + x^0_{\gamma_4} \left(1 + x^0_{\gamma_6} x^0_{\gamma_1} x^0_{\gamma_9}\right)}{1 + x^0_{\gamma_4} \left(1 + x^0_{\gamma_6}\right)}\,, \\
f_9 &= \frac{1 + x_{\gamma_7} \left(1 + x^0_{\gamma_4} \left(1 + x^0_{\gamma_6} x^0_{\gamma_1} x^0_{\gamma_9}\right)\right)}{1 + x_{\gamma_7} \left(1 + x^0_{\gamma_4} \left(1 + x^0_{\gamma_6}\right)\right)}\,, \\
f_{10} &= x^0_{\gamma_5} \left(1 - x^0_{\gamma_1} x^0_{\gamma_9}\right)\,.
\end{aligned} \tag{B.42}$$

It can be easily demonstrated that the set of 112 $A_1^{(1)}$-letters obtained in section 6.2.3 for the limit ray r_∞, eq. (B.13), is equivalently described by the basis of the 9 multiplicatively independent square-root letters given by f_1 to f_9 of eqs. (B.42).

In summary, we see that the non-rational alphabet obtained from the scattering diagram adds one further letter $f_{10} = x^0_{\gamma_5}\left(1 - x^0_{\gamma_1} x^0_{\gamma_9}\right)$ per limit ray compared to the previously known 9 letters, see section 6.2 or [61, 72]. Using eqs. (B.14) and (B.16), we can simplify this letter and find that

$$f_{10} = x_5 \sqrt{\Delta'}\,. \tag{B.43}$$

With x_5 being one of the $\mathcal{X}$-variables of the origin quiver, this already demonstrates that f_1 corresponds to the square-root up to a monomial in the rational alphabet. In fact, this square-root is proportional to the square-root $\Delta_{1,3,5,7}$ of one of the two eight-particle four-mass boxes. In terms of the four-mass box, we can write the additional letter as

$$f_{10} = \frac{\langle 1256\rangle \langle 3478\rangle}{\langle 1278\rangle \langle 3456\rangle} \sqrt{\Delta_{1,3,5,7}}\,, \tag{B.44}$$

whereas we have

$$\Delta_{1,3,5,7} = \left(1 - \frac{\langle 1234\rangle \langle 5678\rangle}{\langle 1256\rangle \langle 3478\rangle} - \frac{\langle 1278\rangle \langle 3456\rangle}{\langle 1256\rangle \langle 3478\rangle}\right)^2 - 4\frac{\langle 1278\rangle \langle 1234\rangle \langle 3456\rangle \langle 5678\rangle}{\left(\langle 1256\rangle \langle 3478\rangle\right)^2}\,. \tag{B.45}$$

The square-root $\Delta_{2,4,6,8}$ of the other eight-particle four-mass box appears in a similar way in the non-rational alphabet of the other limit ray, which is obtained by the cyclic shift $i \to i+1$ on the indices of the Plücker variables.

References

[1] C. Duhr, *Mathematical aspects of scattering amplitudes*, in *Theoretical Advanced Study Institute in Elementary Particle Physics: Journeys Through the Precision Frontier: Amplitudes for Colliders*, pp. 419–476, 2015, 1411.7538, DOI.

[2] N. Arkani-Hamed and J. Trnka, *The Amplituhedron*, *Journal of High Energy Physics* **1410** (2014) 30, [1312.2007].

[3] ATLAS collaboration, G. Aad et al., *Observation of a new particle in the search for the Standard Model Higgs boson with the ATLAS detector at the LHC*, *Phys. Lett. B* **716** (2012) 1–29, [1207.7214].

[4] CMS collaboration, S. Chatrchyan et al., *Observation of a New Boson at a Mass of 125 GeV with the CMS Experiment at the LHC*, *Phys. Lett. B* **716** (2012) 30–61, [1207.7235].

[5] F. Englert and R. Brout, *Broken symmetry and the mass of gauge vector mesons*, *Phys. Rev. Lett.* **13** (Aug, 1964) 321–323.

[6] P. W. Higgs, *Broken symmetries and the masses of gauge bosons*, *Phys. Rev. Lett.* **13** (Oct, 1964) 508–509.

[7] G. S. Guralnik, C. R. Hagen and T. W. B. Kibble, *Global conservation laws and massless particles*, *Phys. Rev. Lett.* **13** (Nov, 1964) 585–587.

[8] J. M. Henn, *What can we learn about QCD and collider physics from N=4 super Yang-Mills?*, 2006.00361.

[9] C. Duhr, *Hopf algebras, coproducts and symbols: an application to Higgs boson amplitudes*, *Journal of High Energy Physics* **2012** (Aug., 2012) 43, [1203.0454].

[10] J. M. Henn and J. C. Plefka, *Scattering Amplitudes in Gauge Theories*, vol. 883. Springer, Berlin, 2014, 10.1007/978-3-642-54022-6.

[11] H. Lehmann, K. Symanzik and W. Zimmermann, *Zur Formulierung quantisierter Feldtheorien*, *Il Nuovo Cimento (1955-1965)* **1** (1955) 205–225.

[12] M. L. Mangano and S. J. Parke, *Multiparton amplitudes in gauge theories*, *Phys. Rept.* **200** (1991) 301–367, [hep-th/0509223].

[13] S. J. Parke and T. R. Taylor, *An Amplitude for n Gluon Scattering*, *Phys. Rev. Lett.* **56** (June, 1986) 2459.

[14] R. Eden, P. Landshoff, D. Olive and J. Polkinghorne, *The Analytic S-Matrix*. Cambridge University Press, 1966.

[15] R. Britto, F. Cachazo and B. Feng, *New recursion relations for tree amplitudes of gluons*, *Nucl. Phys. B* **715** (2005) 499–522, [hep-th/0412308].

[16] R. Britto, F. Cachazo, B. Feng and E. Witten, *Direct proof of tree-level recursion relation in Yang-Mills theory*, *Phys. Rev. Lett.* **94** (2005) 181602, [hep-th/0501052].

[17] J. Bedford, A. Brandhuber, B. J. Spence and G. Travaglini, *A Recursion relation for gravity amplitudes*, *Nucl. Phys. B* **721** (2005) 98–110, [hep-th/0502146].

[18] F. Cachazo and P. Svrcek, *Tree level recursion relations in general relativity*, hep-th/0502160.

[19] Z. Bern, L. J. Dixon, D. C. Dunbar and D. A. Kosower, *One loop n point gauge theory amplitudes, unitarity and collinear limits*, *Nucl. Phys. B* **425** (1994) 217–260, [hep-ph/9403226].

[20] F. Cachazo, S. He and E. Y. Yuan, *Scattering equations and Kawai-Lewellen-Tye orthogonality*, *Phys. Rev. D* **90** (2014) 065001, [1306.6575].

[21] F. Cachazo, S. He and E. Y. Yuan, *Scattering of Massless Particles in Arbitrary Dimensions*, *Phys. Rev. Lett.* **113** (Oct., 2014) 171601, [1307.2199].

[22] F. Cachazo, S. He and E. Y. Yuan, *Scattering of Massless Particles: Scalars, Gluons and Gravitons*, *Journal of High Energy Physics* **2014** (July, 2014) 33, [1309.0885].

[23] N. Arkani-Hamed, J. L. Bourjaily, F. Cachazo, A. B. Goncharov, A. Postnikov et al., *Scattering Amplitudes and the Positive Grassmannian*, 1212.5605.

[24] F. Brown and C. Duhr, *A double integral of dlog forms which is not polylogarithmic*, 6, 2020, 2006.09413.

[25] Z. Bern, L. J. Dixon and V. A. Smirnov, *Iteration of planar amplitudes in maximally supersymmetric Yang-Mills theory at three loops and beyond*, *Phys. Rev.* **D72** (Oct., 2005) 085001, [hep-th/0505205].

[26] L. F. Alday, D. Gaiotto and J. Maldacena, *Thermodynamic Bubble Ansatz*, *JHEP* **09** (2011) 032, [0911.4708].

[27] G. Yang, *A simple collinear limit of scattering amplitudes at strong coupling*, *JHEP* **03** (2011) 087, [1006.3306].

[28] L. J. Dixon and M. von Hippel, *Bootstrapping an NMHV amplitude through three loops*, *Journal of High Energy Physics* **2014** (Oct., 2014) 65, [1408.1505].

[29] A. Goncharov, *Multiple polylogarithms and mixed Tate motives*, math/0103059.

[30] A. B. Goncharov, *Galois symmetries of fundamental groupoids and noncommutative geometry*, *Duke Math. J.* **128** (June, 2005) 209–284, [math/0208144].

[31] F. Brown, *On the decomposition of motivic multiple zeta values*, 1102.1310.

[32] A. B. Goncharov, M. Spradlin, C. Vergu and A. Volovich, *Classical Polylogarithms for Amplitudes and Wilson Loops*, *Phys.Rev.Lett.* **105** (Oct., 2010) 151605, [1006.5703].

[33] S. Caron-Huot, L. J. Dixon, J. M. Drummond, F. Dulat, J. Foster, O. Gürdoğan et al., *The Steinmann Cluster Bootstrap for $N = 4$ Super Yang-Mills Amplitudes*, *PoS* **CORFU2019** (2020) 003, [2005.06735].

[34] G. Papathanasiou, *The SAGEX Review on Scattering Amplitudes, Chapter 5: Analytic Bootstraps for Scattering Amplitudes and Beyond*, 2203.13016.

[35] V. Del Duca, C. Duhr and V. A. Smirnov, *An Analytic Result for the Two-Loop Hexagon Wilson Loop in $\mathcal{N} = 4$ SYM*, *Journal of High Energy Physics* **2010** (Mar., 2010) 99, [0911.5332].

[36] V. Del Duca, C. Duhr and V. A. Smirnov, *The Two-Loop Hexagon Wilson Loop in $\mathcal{N} = 4$ SYM*, *Journal of High Energy Physics* **2010** (May, 2010) 84, [1003.1702].

[37] J. Golden, A. B. Goncharov, M. Spradlin, C. Vergu and A. Volovich, *Motivic Amplitudes and Cluster Coordinates*, *JHEP* **01** (2014) 091, [1305.1617].

[38] N. Arkani-Hamed, F. Cachazo, C. Cheung and J. Kaplan, *A Duality For The S Matrix*, *JHEP* **03** (2010) 020, [0907.5418].

[39] J. M. Drummond, J. Henn, G. P. Korchemsky and E. Sokatchev, *Conformal Ward identities for Wilson loops and a test of the duality with gluon amplitudes*, *Nucl. Phys. B* **826** (2010) 337–364, [0712.1223].

[40] J. M. Drummond, J. Henn, V. A. Smirnov and E. Sokatchev, *Magic identities for conformal four-point integrals*, *JHEP* **01** (2007) 064, [hep-th/0607160].

[41] Z. Bern, M. Czakon, L. J. Dixon, D. A. Kosower and V. A. Smirnov, *The Four-Loop Planar Amplitude and Cusp Anomalous Dimension in Maximally Supersymmetric Yang-Mills Theory*, *Phys. Rev.* **D75** (Apr., 2007) 085010, [hep-th/0610248].

[42] Z. Bern, J. Carrasco, H. Johansson and D. Kosower, *Maximally supersymmetric planar Yang-Mills amplitudes at five loops*, *Phys. Rev.* **D76** (Dec., 2007) 125020, [0705.1864].

[43] L. F. Alday and J. Maldacena, *Comments on gluon scattering amplitudes via AdS/CFT*, *Journal of High Energy Physics* **2007** (Nov., 2007) 68, [0710.1060].

[44] A. Hodges, *Eliminating spurious poles from gauge-theoretic amplitudes*, *JHEP* **05** (2013) 135, [0905.1473].

[45] L. J. Dixon, J. M. Drummond and J. M. Henn, *Bootstrapping the three-loop hexagon*, *Journal of High Energy Physics* **2011** (Nov., 2011) 23, [1108.4461].

[46] L. J. Dixon, J. M. Drummond and J. M. Henn, *Analytic result for the two-loop six-point NMHV amplitude in $\mathcal{N} = 4$ super Yang-Mills theory*, *Journal of High Energy Physics* **2012** (Jan., 2012) 24, [1111.1704].

[47] L. J. Dixon, J. M. Drummond, M. von Hippel and J. Pennington, *Hexagon functions and the three-loop remainder function*, *Journal of High Energy Physics* **2013** (Dec., 2013) 49, [1308.2276].

[48] L. J. Dixon, J. M. Drummond, C. Duhr and J. Pennington, *The four-loop remainder function and multi-Regge behavior at NNLLA in planar $\mathcal{N} = 4$ super-Yang-Mills theory*, *Journal of High Energy Physics* **2014** (June, 2014) 116, [1402.3300].

[49] L. J. Dixon, J. M. Drummond, C. Duhr, M. von Hippel and J. Pennington, *Bootstrapping six-gluon scattering in planar $\mathcal{N} = 4$ super-Yang-Mills theory*, *PoS* **LL2014** (Aug., 2014) 077, [1407.4724].

[50] L. J. Dixon, M. von Hippel and A. J. McLeod, *The four-loop six-gluon NMHV ratio function*, *Journal of High Energy Physics* **2016** (Jan., 2016) 53, [1509.08127].

[51] S. Caron-Huot, L. J. Dixon, A. McLeod and M. von Hippel, *Bootstrapping a Five-Loop Amplitude Using Steinmann Relations*, *Phys. Rev. Lett.* **117** (2016) 241601, [1609.00669].

[52] S. Caron-Huot, L. J. Dixon, F. Dulat, M. von Hippel, A. J. McLeod and G. Papathanasiou, *Six-Gluon amplitudes in planar $\mathcal{N} = 4$ super-Yang-Mills theory at six and seven loops*, *Journal of High Energy Physics* **2019** (Aug., 2019) 16, [1903.10890].

[53] S. Caron-Huot, L. J. Dixon, F. Dulat, M. Von Hippel, A. J. McLeod and G. Papathanasiou, *The Cosmic Galois Group and Extended Steinmann Relations for Planar $\mathcal{N} = 4$ SYM Amplitudes*, *JHEP* **09** (2019) 061, [1906.07116].

[54] V. Chestnov and G. Papathanasiou, *Hexagon Bootstrap in the Double Scaling Limit*, 2012.15855.

[55] J. M. Drummond, G. Papathanasiou and M. Spradlin, *A symbol of uniqueness: the cluster bootstrap for the 3-loop MHV heptagon*, *Journal of High Energy Physics* **2015** (Mar., 2015) 72, [1412.3763].

[56] L. J. Dixon, J. Drummond, T. Harrington, A. J. McLeod, G. Papathanasiou and M. Spradlin, *Heptagons from the Steinmann Cluster Bootstrap*, *JHEP* **02** (2017) 137, [1612.08976].

[57] J. Drummond, J. Foster, Ö. Gürdoğan and G. Papathanasiou, *Cluster adjacency and the four-loop NMHV heptagon*, *Journal of High Energy Physics* **2019** (Mar., 2019) 87, [1812.04640].

[58] L. J. Dixon and Y.-T. Liu, *Lifting Heptagon Symbols to Functions*, *JHEP* **10** (2020) 031, [2007.12966].

[59] I. Prlina, M. Spradlin and S. Stanojevic, *All-loop singularities of scattering amplitudes in massless planar theories*, *Phys. Rev. Lett.* **121** (2018) 081601, [1805.11617].

[60] N. Arkani-Hamed, H. Thomas and J. Trnka, *Unwinding the Amplituhedron in Binary*, *JHEP* **01** (2018) 016, [1704.05069].

[61] S. He, Z. Li and C. Zhang, *Two-loop octagons, algebraic letters and $\bar{Q}$ equations*, *Phys. Rev. D* **101** (2020) 061701, [1911.01290].

[62] D. Speyer and B. Sturmfels, *The Tropical Grassmannian*, *Advances in Geometry* **4** (May, 2003) 389–411, [math/0304218].

[63] F. Cachazo, N. Early, A. Guevara and S. Mizera, *Scattering Equations: From Projective Spaces to Tropical Grassmannians*, *JHEP* **06** (2019) 039, [1903.08904].

[64] F. Cachazo and J. M. Rojas, *Notes on Biadjoint Amplitudes,* $\mathrm{Trop}\, G(3,7)$ *and* $X(3,7)$ *Scattering Equations*, 1906.05979.

[65] D. García Sepúlveda and A. Guevara, *A Soft Theorem for the Tropical Grassmannian*, 1909.05291.

[66] F. Borges and F. Cachazo, *Generalized Planar Feynman Diagrams: Collections*, 1910.10674.

[67] F. Cachazo, B. Umbert and Y. Zhang, *Singular Solutions in Soft Limits*, 1911.02594.

[68] N. Early, *From weakly separated collections to matroid subdivisions*, 1910.11522.

[69] N. Arkani-Hamed, Y. Bai, S. He and G. Yan, *Scattering Forms and the Positive Geometry of Kinematics, Color and the Worldsheet*, *Journal of High Energy Physics* **05** (May, 2018) 096, [1711.09102].

[70] J. Drummond, J. Foster, Ö. Gürdoğan and C. Kalousios, *Tropical Grassmannians, cluster algebras and scattering amplitudes*, 1907.01053.

[71] D. Speyer and L. Williams, *The Tropical Totally Positive Grassmannian*, *Journal of Algebraic Combinatorics* **22** (Sept., 2005) 189–210, [math/0312297].

[72] J.M. Drummond, J. Foster, Ö. Gürdoğan, C. Kalousios, *Algebraic singularities of scattering amplitudes from tropical geometry*, 1912.08217.

[73] A. Herderschee, *Algebraic branch points at all loop orders from positive kinematics and wall crossing*, *JHEP* **07** (2021) 049, [2102.03611].

[74] J. L. Bourjaily, S. Caron-Huot and J. Trnka, *Dual-Conformal Regularization of Infrared Loop Divergences and the Chiral Box Expansion*, *JHEP* **01** (2015) 001, [1303.4734].

[75] S. He, Z. Li and C. Zhang, *The symbol and alphabet of two-loop NMHV amplitudes from $\bar{Q}$ equations*, 2009.11471.

[76] M. Kontsevich and D. Zagier, *Periods*, *Mathematics unlimited–2001 and beyond* (2001) 771–808.

[77] C. Bogner and S. Weinzierl, *Periods and Feynman integrals*, *J. Math. Phys.* **50** (2009) 042302, [0711.4863].

[78] G. 't Hooft and M. Veltman, *Scalar one-loop integrals*, *Nuclear Physics B* **153** (1979) 365–401.

[79] A. B. Goncharov, *Multiple polylogarithms, cyclotomy and modular complexes*, *Math. Res. Lett.* **5** (1998) 497–516, [1105.2076].

[80] D. Zagier, *The Dilogarithm Function*, pp. 3–65. Springer Berlin Heidelberg, Berlin, Heidelberg, 2007. 10.1007/978-3-540-30308-4.

[81] C. Duhr, H. Gangl and J. R. Rhodes, *From polygons and symbols to polylogarithmic functions*, *Journal of High Energy Physics* **1210** (2012) 075, [1110.0458].

[82] K.-T. Chen, *Iterated path integrals*, *Bull. Amer. Math. Soc.* **83** (Sept., 1977) 831–879.

[83] N. Arkani-Hamed, Y. Bai and T. Lam, *Positive Geometries and Canonical Forms*, *JHEP* **11** (2017) 039, [1703.04541].

[84] L. Brink, J. H. Schwarz and J. Scherk, *Supersymmetric Yang-Mills Theories*, *Nucl. Phys. B* **121** (1977) 77–92.

[85] F. Gliozzi, J. Scherk and D. I. Olive, *Supersymmetry, Supergravity Theories and the Dual Spinor Model*, *Nucl. Phys. B* **122** (1977) 253–290.

[86] J. Fokken, *A hitchhiker's guide to quantum field theoretic aspects of $\mathcal{N} = 4$ SYM theory and its deformations*, PhD thesis, 1, 2017.

[87] N. Beisert, *Review of AdS/CFT Integrability, Chapter VI.1: Superconformal Symmetry*, *Lett. Math. Phys.* **99** (2012) 529–545, [1012.4004].

[88] L. Eberhardt, *Superconformal symmetry and representations*, *J. Phys. A* **54** (2021) 063002, [2006.13280].

[89] R. Blumenhagen, D. Lüst and S. Theisen, *Conformal field theory III: Superconformal field theory*, pp. 355–390. Springer Berlin Heidelberg, 2012. DOI.

[90] P. Francesco, P. Mathieu and D. Sénéchal, *Conformal Field Theory*. Springer, 1997.

[91] S. R. Coleman and J. Mandula, *All Possible Symmetries of the S Matrix*, *Phys. Rev.* **159** (1967) 1251–1256.

[92] R. Haag, J. T. Lopuszanski and M. Sohnius, *All possible generators of supersymmetries of the S-matrix*, *Nucl. Phys. B* **88** (1975) 257.

[93] J. M. Maldacena, *The Large N limit of superconformal field theories and supergravity*, *Adv. Theor. Math. Phys.* **2** (1998) 231–252, [hep-th/9711200].

[94] E. Witten, *Anti-de Sitter space and holography*, *Adv. Theor. Math. Phys.* **2** (1998) 253–291, [hep-th/9802150].

[95] G. 't Hooft, *A Planar Diagram Theory for Strong Interactions*, *Nucl. Phys. B* **72** (1974) 461.

[96] N. Beisert, C. Ahn, L. F. Alday, Z. Bajnok, J. M. Drummond et al., *Review of AdS/CFT Integrability: An Overview*, *Lett.Math.Phys.* **99** (2012) 3–32, [1012.3982].

[97] L. J. Dixon, *Calculating scattering amplitudes efficiently*, in *Theoretical Advanced Study Institute in Elementary Particle Physics (TASI 95): QCD and Beyond*, pp. 539–584, 1, 1996, hep-ph/9601359.

[98] L. J. Dixon, *Scattering amplitudes: the most perfect microscopic structures in the universe*, *J. Phys. A* **44** (2011) 454001, [1105.0771].

[99] Z. Bern and D. A. Kosower, *Color decomposition of one loop amplitudes in gauge theories*, *Nucl. Phys. B* **362** (1991) 389–448.

[100] V. P. Nair, *A Current Algebra for Some Gauge Theory Amplitudes*, *Phys. Lett. B* **214** (1988) 215–218.

[101] H. Elvang, D. Z. Freedman and M. Kiermaier, *Solution to the Ward Identities for Superamplitudes*, *JHEP* **10** (2010) 103, [0911.3169].

[102] H. Elvang, D. Z. Freedman and M. Kiermaier, *SUSY Ward identities, Superamplitudes, and Counterterms*, *J. Phys. A* **44** (2011) 454009, [1012.3401].

[103] P. De Causmaecker, R. Gastmans, W. Troost and T. T. Wu, *Multiple Bremsstrahlung in Gauge Theories at High-Energies. 1. General Formalism for Quantum Electrodynamics*, *Nucl. Phys. B* **206** (1982) 53–60.

[104] Z. Xu, D.-H. Zhang and L. Chang, *Helicity Amplitudes for Multiple Bremsstrahlung in Massless Nonabelian Gauge Theories*, *Nucl. Phys. B* **291** (1987) 392–428.

[105] R. Gastmans and T. T. Wu, *The Ubiquitous photon: Helicity method for QED and QCD*, vol. 80. 1990.

[106] L. J. Dixon, *A brief introduction to modern amplitude methods*, in *Theoretical Advanced Study Institute in Elementary Particle Physics: Particle Physics: The Higgs Boson and Beyond*, pp. 31–67, 2014, 1310.5353, DOI.

[107] L. F. Alday and J. M. Maldacena, *Gluon scattering amplitudes at strong coupling*, *JHEP* **06** (2007) 064, [0705.0303].

[108] J. M. Drummond, G. P. Korchemsky and E. Sokatchev, *Conformal properties of four-gluon planar amplitudes and Wilson loops*, *Nucl. Phys. B* **795** (2008) 385–408, [0707.0243].

[109] J. M. Drummond, J. Henn, G. P. Korchemsky and E. Sokatchev, *Dual superconformal symmetry of scattering amplitudes in N=4 super-Yang-Mills theory*, *Nucl. Phys. B* **828** (2010) 317–374, [0807.1095].

[110] A. Brandhuber, P. Heslop and G. Travaglini, *A Note on dual superconformal symmetry of the N=4 super Yang-Mills S-matrix*, *Phys. Rev. D* **78** (2008) 125005, [0807.4097].

[111] J. M. Drummond, *Review of AdS/CFT Integrability, Chapter V.2: Dual Superconformal Symmetry*, *Lett. Math. Phys.* **99** (2012) 481–505, [1012.4002].

[112] N. Arkani-Hamed, J. L. Bourjaily, F. Cachazo and J. Trnka, *Local Integrals for Planar Scattering Amplitudes*, *JHEP* **06** (2012) 125, [1012.6032].

[113] R. Penrose, *Twistor algebra*, *J. Math. Phys.* **8** (1967) 345.

[114] G. P. Korchemsky and E. Sokatchev, *Superconformal invariants for scattering amplitudes in N=4 SYM theory*, *Nucl. Phys. B* **839** (2010) 377–419, [1002.4625].

[115] T. Adamo, M. Bullimore, L. Mason and D. Skinner, *Scattering Amplitudes and Wilson Loops in Twistor Space*, *J. Phys. A* **44** (2011) 454008, [1104.2890].

[116] T. Adamo, *Twistor actions for gauge theory and gravity*, master's thesis, 8, 2013.

[117] T. Adamo, *Lectures on twistor theory*, *PoS* **Modave2017** (2018) 003, [1712.02196].

[118] J. Golden, A. B. Goncharov, M. Spradlin, C. Vergu and A. Volovich, *Motivic Amplitudes and Cluster Coordinates*, *Journal of High Energy Physics* **2014** (Jan., 2014) 91, [1305.1617].

[119] J. Golden, A. J. McLeod, M. Spradlin and A. Volovich, *The Sklyanin Bracket and Cluster Adjacency at All Multiplicity*, *JHEP* **03** (2019) 195, [1902.11286].

[120] N. Beisert, B. Eden and M. Staudacher, *Transcendentality and Crossing*, *J. Stat. Mech.* **0701** (2007) P01021, [hep-th/0610251].

[121] J. M. Henn, S. G. Naculich, H. J. Schnitzer and M. Spradlin, *Higgs-regularized three-loop four-gluon amplitude in N=4 SYM: exponentiation and Regge limits*, *JHEP* **04** (2010) 038, [1001.1358].

[122] Z. Bern, J. J. M. Carrasco, L. J. Dixon, H. Johansson and R. Roiban, *The Complete Four-Loop Four-Point Amplitude in N=4 Super-Yang-Mills Theory*, *Phys. Rev. D* **82** (2010) 125040, [1008.3327].

[123] Z. Bern, J. J. M. Carrasco, H. Johansson and R. Roiban, *The Five-Loop Four-Point Amplitude of N=4 super-Yang-Mills Theory*, *Phys. Rev. Lett.* **109** (2012) 241602, [1207.6666].

[124] Z. Bern, M. Czakon, D. A. Kosower, R. Roiban and V. A. Smirnov, *Two-loop iteration of five-point N=4 super-Yang-Mills amplitudes*, *Phys. Rev. Lett.* **97** (2006) 181601, [hep-th/0604074].

[125] F. Cachazo, M. Spradlin and A. Volovich, *Iterative structure within the five-particle two-loop amplitude*, *Phys. Rev. D* **74** (2006) 045020, [hep-th/0602228].

[126] Z. Bern, L. J. Dixon, D. A. Kosower, R. Roiban, M. Spradlin, C. Vergu et al., *The Two-Loop Six-Gluon MHV Amplitude in Maximally Supersymmetric Yang-Mills Theory*, *Phys. Rev. D* **78** (2008) 045007, [0803.1465].

[127] J. M. Drummond, J. Henn, G. P. Korchemsky and E. Sokatchev, *Hexagon Wilson loop = six-gluon MHV amplitude*, *Nucl. Phys. B* **815** (2009) 142–173, [0803.1466].

[128] O. Steinmann, *Über den Zusammenhang zwischen den Wightmanfunktionen und der retardierten Kommutatoren*, *Helv. Physica Acta* **33** (1960) 257.

[129] O. Steinmann, *Wightman-Funktionen und retardierten Kommutatoren. II*, *Helv. Physica Acta* **33** (1960) 347.

[130] K. E. Cahill and H. P. Stapp, *Optical Theorems and Steinmann Relations*, *Annals Phys.* **90** (1975) 438.

[131] A. Sabry, *Fourth order spectral functions for the electron propagator*, *Nuclear Physics* **33** (May, 1962) 401–430.

[132] N. Arkani-Hamed, J. L. Bourjaily, F. Cachazo, A. B. Goncharov, A. Postnikov and J. Trnka, *Grassmannian Geometry of Scattering Amplitudes*. Cambridge University Press, 4, 2016, 10.1017/CBO9781316091548.

[133] S. Caron-Huot, *Superconformal symmetry and two-loop amplitudes in planar N=4 super Yang-Mills*, *JHEP* **12** (2011) 066, [1105.5606].

[134] J. Golden and M. Spradlin, *An analytic result for the two-loop seven-point MHV amplitude in $\mathcal{N} = 4$ SYM*, *Journal of High Energy Physics* **2014** (Aug., 2014) 154, [1406.2055].

[135] D. Gaiotto, J. Maldacena, A. Sever and P. Vieira, *Pulling the straps of polygons*, *Journal of High Energy Physics* **1112** (2011) 011, [1102.0062].

[136] J. Bartels, L. Lipatov and A. Sabio Vera, *$\mathcal{N} = 4$ supersymmetric Yang Mills scattering amplitudes at high energies: The Regge cut contribution*, *Eur. Phys. J.* **C65** (Dec., 2010) 587–605, [0807.0894].

[137] V. Fadin and L. Lipatov, *BFKL equation for the adjoint representation of the gauge group in the next-to-leading approximation at $\mathcal{N} = 4$ SUSY*, *Phys.Lett.* **B706** (Jan., 2012) 470–476, [1111.0782].

[138] J. Bartels, A. Kormilitzin, L. Lipatov and A. Prygarin, *BFKL approach and $2 \to 5$ maximally helicity violating amplitude in $\mathcal{N} = 4$ super-Yang-Mills theory*, *Phys. Rev.* **D86** (Sept., 2012) 065026, [1112.6366].

[139] L. Lipatov, A. Prygarin and H. J. Schnitzer, *The Multi-Regge limit of NMHV Amplitudes in $\mathcal{N} = 4$ SYM Theory*, *Journal of High Energy Physics* **2013** (Jan., 2013) 68, [1205.0186].

[140] L. J. Dixon, C. Duhr and J. Pennington, *Single-valued harmonic polylogarithms and the multi-Regge limit*, *Journal of High Energy Physics* **2012** (Oct., 2012) 74, [1207.0186].

[141] J. Bartels, A. Kormilitzin and L. Lipatov, *Analytic structure of the $n = 7$ scattering amplitude in $\mathcal{N} = 4$ SYM theory at multi-Regge kinematics: Conformal Regge pole contribution*, *Phys.Rev.* **D89** (Mar., 2014) 065002, [1311.2061].

[142] B. Basso, S. Caron-Huot and A. Sever, *Adjoint BFKL at finite coupling: a short-cut from the collinear limit*, *Journal of High Energy Physics* **2015** (Jan., 2015) 27, [1407.3766].

[143] J. M. Drummond and G. Papathanasiou, *Hexagon OPE Resummation and Multi-Regge Kinematics*, *Journal of High Energy Physics* **2016** (Feb., 2016) 185, [1507.08982].

[144] V. Del Duca, S. Druc, J. Drummond, C. Duhr, F. Dulat, R. Marzucca et al., *Multi-Regge kinematics and the moduli space of Riemann spheres with marked points*, *Journal of High Energy Physics* **2016** (Aug., 2016) 152, [1606.08807].

[145] V. Del Duca, S. Druc, J. Drummond, C. Duhr, F. Dulat, R. Marzucca et al., *The seven-gluon amplitude in multi-Regge kinematics beyond leading logarithmic accuracy*, *Journal of High Energy Physics* **2018** (June, 2018) 116, [1801.10605].

[146] V. Del Duca, S. Druc, J. M. Drummond, C. Duhr, F. Dulat, R. Marzucca et al., *All-order amplitudes at any multiplicity in the multi-Regge limit*, 1912.00188.

[147] L. F. Alday, D. Gaiotto, J. Maldacena, A. Sever and P. Vieira, *An Operator Product Expansion for Polygonal null Wilson Loops*, *Journal of High Energy Physics* **2011** (Apr., 2011) 88, [1006.2788].

[148] B. Basso, A. Sever and P. Vieira, *Spacetime and Flux Tube S-Matrices at Finite Coupling*

for $\mathcal{N} = 4$ Supersymmetric Yang-Mills Theory, *Phys.Rev.Lett.* **111** (Aug., 2013) 091602, [1303.1396].

[149] B. Basso, A. Sever and P. Vieira, *Space-time S-matrix and Flux tube S-matrix II. Extracting and Matching Data*, *Journal of High Energy Physics* **2014** (Jan., 2014) 8, [1306.2058].

[150] G. Papathanasiou, *Hexagon Wilson Loop OPE and Harmonic Polylogarithms*, *Journal of High Energy Physics* **2013** (Nov., 2013) 150, [1310.5735].

[151] B. Basso, A. Sever and P. Vieira, *Space-time S-matrix and Flux-tube S-matrix III. The two-particle contributions*, *Journal of High Energy Physics* **2014** (Aug., 2014) 85, [1402.3307].

[152] G. Papathanasiou, *Evaluating the six-point remainder function near the collinear limit*, *Int. J. Mod. Phys.* **A29** (2014) 1450154, [1406.1123].

[153] B. Basso, A. Sever and P. Vieira, *Space-time S-matrix and Flux-tube S-matrix IV. Gluons and Fusion*, *Journal of High Energy Physics* **2014** (Sept., 2014) 149, [1407.1736].

[154] A. Belitsky, *Nonsinglet pentagons and NHMV amplitudes*, 1407.2853.

[155] A. Belitsky, *Fermionic pentagons and NMHV hexagon*, 1410.2534.

[156] S. Fomin and A. Zelevinsky, *Cluster Algebras I: Foundations*, *Journal of the American Mathematical Society* **15** (Apr., 2002) 497–529, [math/0104151].

[157] S. Fomin and A. Zelevinsky, *Cluster algebras II: Finite type classification*, *Inventiones mathematicae* **154** (Oct., 2003) 63–121, [math/0208229].

[158] A. Berenstein, S. Fomin and A. Zelevinsky, *Cluster algebras III: Upper bounds and double Bruhat cells*, *Duke Mathematical Journal* **126** (June, 2003) 1–52, [math/0305434].

[159] S. Fomin and A. Zelevinsky, *Cluster algebras IV: Coefficients*, *Compositio Mathematica* **143** (Jan., 2007) 112–164, [math/0602259].

[160] J. S. Scott, *GRASSMANNIANS AND CLUSTER ALGEBRAS*, *Proceedings of the London Mathematical Society* **92** (Mar., 2006) 345–380, [math/0311148].

[161] B. Keller, *Cluster algebras and derived categories*, 2012.

[162] V. V. Fock and A. B. Goncharov, *Cluster ensembles, quantization and the dilogarithm*, *Ann. Sci. Éc. Norm. Supér. (4)* **42** (2009) 865–930, [math/0311245].

[163] S. Fomin and P. Pylyavskyy, *Tensor diagrams and cluster algebras*, 2015.

[164] N. Henke and G. Papathanasiou, *How tropical are seven- and eight-particle amplitudes?*, *JHEP* **08** (2020) 005, [1912.08254].

[165] T. Nakanishi and A. Zelevinsky, *On tropical dualities in cluster algebras*, 2011.

[166] G. Ziegler, *Lectures on Polytopes*. Graduate texts in Mathematics. Springer-Verlag, 1995.

[167] M.-L. P. Blind, Roswitha, *Puzzles and polytope isomorphisms.*, *Aequationes mathematicae* **34** (1987) 287–297.

[168] G. Kalai, *A simple way to tell a simple polytope from its graph*, *Journal of Combinatorial Theory, Series A* **49** (1988) 381–383.

[169] S. Fomin and A. Zelevinsky, *Y-systems and generalized associahedra*, *Annals of Mathematics* **158** (Nov., 2003) 977–1018, [hep-th/0111053].

[170] F. Chapoton, S. Fomin and A. Zelevinsky, *Polytopal Realizations of Generalized Associahedra*, *Canadian Mathematical Bulletin* **45** (Dec., 2002) 537–566, [math/0202004].

[171] L. K. Williams, *Cluster algebras: an introduction*, 2013.

[172] J. D. Stasheff, *Homotopy associativity of H-spaces. I*, *Transactions of the Ammerican Mathematical Society* **108** (1963) 275–292.

[173] J. D. Stasheff, *Homotopy associativity of H-spaces. II*, *Transactions of the Ammerican Mathematical Society* **108** (1963) 293–312.

[174] I. M. Gelfand, M. M. Kapranov and A. V. Zelevinsky, *Discriminants, resultants, and multidimensional determinants*, 1994.

[175] C. W. Lee, *The associahedron and triangulations of the n-gon*, *Eur. J. Comb.* **10** (1989) 551–560.

[176] J. Drummond, J. Foster and O. Gürdoğan, *Cluster Adjacency Properties of Scattering Amplitudes in $N = 4$ Supersymmetric Yang-Mills Theory*, *Phys. Rev. Lett.* **120** (2018) 161601, [1710.10953].

[177] J. Drummond, J. Foster and O. Gürdoğan, *Cluster adjacency beyond MHV*, *JHEP* **03** (2019) 086, [1810.08149].

[178] S. Fomin, M. Shapiro and D. Thurston, *Cluster algebras and triangulated surfaces. Part I: Cluster complexes*, *arXiv Mathematics e-prints* (Aug., 2006) math/0608367, [math/0608367].

[179] D. Maclagan, *Introduction to tropical algebraic geometry*, 1207.1925.

[180] E. Katz, *What is... Tropical Geometry?*, *Notices of the AMS* **64** 380–384.

[181] G. Mikhalkin, *Tropical geometry and its applications*, *International Congress of Mathematicians* **2** (Feb, 2006) 827–852, [math/0601041].

[182] E. Brugallé, I. Itenberg, G. Mikhalkin and K. Shaw, *Brief introduction to tropical geometry*, 1502.05950.

[183] T. Bogart, A. Jensen, D. Speyer, B. Sturmfels and R. Thomas, *Computing tropical varieties*, *Journal of Symbolic Computation* **42** (Jan, 2007) 5473.

[184] S. B. Brodsky, C. Ceballos and J.-P. Labbé, *Cluster Algebras of Type D_4, Tropical Planes, and the Positive Tropical Grassmannian*, 1511.02699.

[185] N. Arkani-Hamed, T. Lam and M. Spradlin, *Non-perturbative geometries for planar $\mathcal{N} = 4$ SYM amplitudes*, 1912.08222.

[186] J. Drummond, J. Foster, Ö. Gürdoğan and C. Kalousios, *Tropical fans, scattering equations and amplitudes*, 2002.04624.

[187] S. Caron-Huot, *Superconformal symmetry and two-loop amplitudes in planar $\mathcal{N} = 4$ super Yang-Mills*, *Journal of High Energy Physics* **2011** (Dec., 2011) 66, [1105.5606].

[188] J. Henn, E. Herrmann and J. Parra-Martinez, *Bootstrapping two-loop Feynman integrals for planar $\mathcal{N} = 4$ sYM*, *JHEP* **10** (2018) 059, [1806.06072].

[189] I. Canakci and R. Schiffler, *Cluster algebras and continued fractions*, *Compositio Mathematica* **154** (Mar., 2018) 565–593, [1608.06568].

[190] N. Reading, *A combinatorial approach to scattering diagrams*, 1806.05094.

[191] A. P. Fordy and R. J. Marsh, *Cluster mutation-periodic quivers and associated Laurent sequences*, *J. Algebr. Comb.* **34** (2011) 19–66, [0904.0200].

[192] N. Arkani-Hamed, *Space-Time and Quantum Mechanics, Positive Geometries + Cluster Algebras*, in *Cluster Algebras and the Geometry of Scattering Amplitudes*, Mar., 2020.

[193] N. Arkani-Hamed, *Scattering Amplitudes and Clusterhedra in Kinematic Space*, in *Amplitudes 2020*, May, 2020.

[194] S. Hermann, M. Joswig and D. E. Speyer, *Dressians, tropical Grassmannians, and their rays*, *Forum Mathematicum* **26** (Nov., 2014) 1853–1881, [1112.1278].

[195] N. Henke and G. Papathanasiou, *Singularities of eight- and nine-particle amplitudes from cluster algebras and tropical geometry*, *JHEP* **10** (2021) 007, [2106.01392].

[196] Z. Li and C. Zhang, *The three-loop MHV octagon from $\overline{Q}$ equations*, *JHEP* **12** (2021) 113, [2110.00350].

[197] J. Golden and A. J. Mcleod, *The Two-Loop Remainder Function for Eight and Nine Particles*, 2104.14194.

[198] J. Mago, A. Schreiber, M. Spradlin and A. Volovich, *Symbol alphabets from plabic graphs*, *JHEP* **10** (2020) 128, [2007.00646].

[199] S. He and Z. Li, *A note on letters of Yangian invariants*, *JHEP* **02** (2021) 155, [2007.01574].

[200] J. Mago, A. Schreiber, M. Spradlin, A. Yelleshpur Srikant and A. Volovich, *Symbol Alphabets from Plabic Graphs II: Rational Letters*, 2012.15812.

[201] J. Mago, A. Schreiber, M. Spradlin, A. Yelleshpur Srikant and A. Volovich, *Symbol Alphabets from Plabic Graphs III: n=9*, 2106.01406.

[202] V. Mitev and Y. Zhang, *SymBuild: a package for the computation of integrable symbols in scattering amplitudes*, 1809.05101.

[203] D. Chicherin, J. M. Henn and G. Papathanasiou, *Cluster algebras for Feynman integrals*, *Phys. Rev. Lett.* **126** (2021) 091603, [2012.12285].

[204] S. Badger, H. B. Hartanto and S. Zoia, *Two-loop QCD corrections to $Wb\bar{b}$ production at hadron colliders*, 2102.02516.

[205] D. Chicherin, N. Henke, J. M. Henn, G. Papathanasiou and S. Zoia. Work in progress.

[206] I. Assem, R. Schiffler and V. Shramchenko, *Cluster automorphisms*, *Proceedings of the London Mathematical Society* **104** (2012) 1271–1302, [1009.0742].

[207] L. Ren, M. Spradlin and A. Volovich, *Symbol Alphabets from Tensor Diagrams*, 2106.01405.

[208] J. Li, private communication. See also W. Chang, B. Duan, C. Fraser and J. Li, *Quantum affine algebras and Grassmannians*, 1907.13575.

[209] E. Gawrilow and M. Joswig, ***polymake**: a framework for analyzing convex polytopes*, in *Polytopes—combinatorics and computation (Oberwolfach, 1997)*, vol. 29 of *DMV Sem.*, pp. 43–73. Birkhäuser, Basel, 2000.

[210] S. He, L. Ren and Y. Zhang, *Notes on polytopes, amplitudes and boundary configurations for Grassmannian string integrals*, *JHEP* **04** (2020) 140, [2001.09603].

[211] L. Williams, *The positive tropical Grassmannian, the hypersimplex, and the $m = 2$ amplituhedron*, in *Amplitudes 2020*, May, 2020.

[212] I. Prlina, M. Spradlin, J. Stankowicz and S. Stanojevic, *Boundaries of Amplituhedra and NMHV Symbol Alphabets at Two Loops*, *JHEP* **04** (2018) 049, [1712.08049].

[213] N. Reading, *Scattering Fans*, *International Mathematics Research Notices* **00** (Nov., 2018) 1–34, [1712.06968].

[214] C. Córdova and A. Neitzke, *Line Defects, Tropicalization, and Multi-Centered Quiver Quantum Mechanics*, *JHEP* **09** (2014) 099, [1308.6829].

[215] T. Bridgeland, *Scattering diagrams, Hall algebras and stability conditions*, *arXiv e-prints* (Mar., 2016) arXiv:1603.00416, [1603.00416].

[216] S. Caron-Huot and K. J. Larsen, *Uniqueness of two-loop master contours*, *JHEP* **10** (2012) 026, [1205.0801].

[217] J. Broedel, C. Duhr, F. Dulat, B. Penante and L. Tancredi, *Elliptic symbol calculus: from elliptic polylogarithms to iterated integrals of Eisenstein series*, *JHEP* **08** (2018) 014, [1803.10256].

[218] N. Arkani-Hamed, S. He and T. Lam, *Stringy canonical forms*, *JHEP* **02** (2021) 069, [1912.08707].

[219] Q. Yang, *Schubert Problems, Positivity and Symbol Letters*, 2203.16112.

[220] N. Arkani-Hamed, J. L. Bourjaily, F. Cachazo and J. Trnka, *Local Integrals for Planar Scattering Amplitudes*, *JHEP* **06** (2012) 125, [1012.6032].

[221] S. He, Z. Li and Q. Yang, *Truncated cluster algebras and Feynman integrals with algebraic letters*, *JHEP* **12** (2021) 110, [2106.09314].

[222] S. He, Z. Li and Q. Yang, *Kinematics, cluster algebras and Feynman integrals*, 2112.11842.

Erklärung

Ich versichere, dass dieses gebundene Exemplar der Dissertation und das in elektronischer Form eingereichte Dissertationsexemplar (über den Docata-Upload) und das bei der Fakultät (zuständiges Studienbüro bzw. Promotionsbüro Physik) zur Archivierung eingereichte gedruckte gebundene Exemplar der Dissertationsschrift identisch sind.

Hamburg, 31.05.2022

Niklas Henke